Connecting Offshore Wind and Hydrogen:

The Role of Energy Islands in a Meshed North Sea Energy System

J.S. (Janne) Nelisse

TU Delft

For this thesis, ChatGPT was used during various stages of the research process as a supportive tool. It was used to generate the cover image, to help write Python code, to summarize literature and to structure and to refine texts. The ChatGPT output has always been critically reviewed and was adapted to guarantee the academic and analytical level of this thesis. The author remains fully responsible of this thesis' content.

The cover image is inspired by Gottlieb Paludan Architects (2021).

Connecting Offshore Wind and Hydrogen: The Role of Energy Islands in a Meshed North Sea Energy System

by

J.S. (Janne) Nelisse
Student ID: 4993454

A thesis submitted to the Delft University of Technology
to obtain the degree of Master of Science
in Complex Systems Engineering and Management,
to be defended publicly on September 25, 2025, at 15:00.

Track: Energy.

February 2025 – September 2025

Graduation committee: Dr. ir. P.W. (Petra) Heijnen, TU Delft, chair & first supervisor
Prof. dr. M.E. (Martijn) Warnier, TU Delft, second supervisor
Dr. D. (Daniel) Scholten, WUR, external supervisor

An electronic version of this thesis is available at http://repository.tudelft.nl/

Faculty of Technology, Policy and Management
Delft University of Technology

This page is intentionally left blank.

Preface

Dear reader,

The report in front of you is my master thesis. For the last couple of months, I have been working on this project. This thesis is the final leg in fulfilling a master in Complex Systems Engineering and Management. Doing so, my time at the Delft University of Technology is coming to an end. Coming to Delft in 2019, I was not entirely sure what it would bring me. Looking back, time flew by, but it gave me the opportunity to discover where my true interests lie and what gives me energy. Being able to explore the integration of offshore wind and hydrogen via the conceptual idea of energy islands in this project, has been the highlight of my time at the TU Delft.

My thesis would not have been the same without the support of my thesis committee. First, I would like to thank Petra Heijnen, my first supervisor. After your guidance during my bachelor's thesis, I knew you would once again be an outstanding mentor. Your eye for detail and critical perspective during our weekly meetings helped me to make this research as complete as possible. Beyond your academic support, I valued the personal support, as I could always confide in you when needed. I am truly grateful for how you have helped me throughout this process.

Second, I would like to thank Martijn Warnier, my second supervisor. Your excellent feedback pushed the quality of this project to the next level. I also greatly appreciated your advice on balancing this thesis with other things in life, which often proved invaluable. Your reminder that the goal is to look back after a few months and feel proud of the work, helped me to keep perspective throughout this process.

Finally, I would like to thank Daniel Scholten, my external supervisor. Although the part on energy security is not highlighted as much as initially expected, your perspective and expertise on this topic added an invaluable dimension. I also greatly enjoyed our conversations on politics, and I hope that future research will succeed in combining geopolitical considerations with techno-economic optimization.

These last few months, and all my time in Delft, would not have been the same without my dear family and friends. Whether it was to get something off my chest, or to get my mind off things, I am so grateful for the support and laughter you gave me when I need it the most. A special thanks goes out to my former roommates, who provided distraction, advice and many delicious meals and great walks.

I am especially grateful to the person who is still my roommate. Moving during this thesis was not always easy, but you made it fun and enjoyable. Your endless advice, coffees and treats, and your steady support made all the difference.

Also, I would like to thank my mom. Your patience and understanding gave me the peace of mind I needed throughout this process and guided me through the difficult times. I am deeply grateful for the unconditional support you have always given me.

Finally, I am especially grateful for my boyfriend. Thank you for listening to me, for giving me the reassurance that I sometimes need, for always believing in me and for helping me with the smallest things. These last months would have been much harder if you were not there with me.

There were many ups and downs during this project, but I look back on it with a sense of pride. I gave it my all for the entire period and enjoyed doing the research. Thank you for allowing me to.

Janne Nelisse

Executive Summary

The Ostend Declaration (2023) sets out the ambition to transform the North Sea into Europe's green power plant by increasing electricity generation from offshore wind significantly. Although this is crucial to meet in Europe's growing energy demand and to meet sustainability targets (North Sea Energy, 2020), it also raises major challenges. The transmittance of electricity of such large amounts faces technical bottlenecks, including grid congestion and limited storage options, as well as economic barriers due to high costs for offshore electricity cables (Beaubouef, 2024; North Sea Energy, 2020). Hydrogen offers a promising pathway to address these challenges. It is a flexible and storable energy carrier that facilitates energy system balancing and reduces reliance on costly electricity grid expansions (Dute et al., 2024; Farahmand et al., 2024). Offshore electrolysis is feasible within wind turbines, in offshore hubs or at energy islands reduces pressure on onshore grids and land use (Ramboll, 2025; Janssen et al., 2025). However, large-scale offshore electrolysis is still underdeveloped as no full-scale projects exist, optimal locations are undefined and effective deployment requires cross-border coordination (European Commission, 2025a; Van Wingerden et al., 2023).

Realizing the full potential of offshore hydrogen requires cross-border collaboration among North Sea countries (Van Wingerden et al., 2023). This not only implies connecting the offshore systems of individual countries but also connecting electricity and hydrogen infrastructures into one supranational, integrated North Sea energy system (North Sea Energy, 2020; One North Sea, 2021). Within this vision, energy islands can be a strategic asset by connecting offshore wind farms to an offshore hydrogen backbone. This enables economies of scale and facilitates cross-border energy flows (Arteaga et al., 2024). At the same time, system design is complicated by multiple uncertainties and external pressures. The hydrogen economy is still developing, making investment conditions uncertain. Moreover, national governments and transmission system operators continue to plan mainly within their own borders, limiting system-wide efficiency (North SEE, n.d.). Additionally, the presence of ecological areas, military zones and shipping routes in the North Sea pose spatial constraints, demanding a careful multi-use spatial planning for the region (Staeb, 2025). Against this background, there is a need for system-level research that explores how offshore wind, hydrogen and energy island infrastructures can be integrated into one energy system. This thesis therefore addresses that need by developing a conceptual system design for 2050 that minimizes overall system costs while accounting for spatial constraints and infrastructure reuse.

This research societally relevant as it shows that energy islands can enable large-scale offshore wind and hydrogen production, while it highlights the importance of a multinational approach for achieving Europe's climate goals. Academically, it is relevant because it contributes to the still limited literature on multi-energy, multinational offshore systems. To guide this research, the following research question is formulated:

What is a system design with minimal overall system costs for the North Sea, in which energy islands enable the integration of electricity from offshore wind farms in an offshore hydrogen network, while accounting for other North Sea uses?

To answer this main research question, three sub-questions are assessed. The first concerns how many energy islands are needed to balance efficiency and costs, given the expected offshore wind farms in 2050. For this, wind farms are grouped by the distance between them. The cost implications of these groups are analysed to identify the group with minimal costs. The second focuses on the locations of these islands, while considering other North Sea uses that pose spatial constraints. Alternative network layouts are constructed and compared to identify energy island locations that are technically feasible and economically attractive. The third examines the design of a cost-efficient hydrogen backbone, in which the identified island locations are connected to land so that cross-border energy flows and system integration is enabled. This is done by constructing a potential network layout for an offshore hydrogen backbone.

The results show that a cost-efficient system design can be achieved by developing eight energy islands. With this number, the high construction costs of energy islands are balanced against the costs of offshore cabling, leading to an initial cost estimation of €36.4 billion. Island locations are strongly dependent on the spatial constraints posed for ecological areas, military zones and shipping routes. Accounting for these constraints in the network design reduces the electricity cabling costs for connecting offshore wind farms to energy islands significantly: from €14 billion to €0.3 billion. This estimation is more realistic because it accounts for technical factors and results from fewer and shorter connections. The analysis further shows that the total electrical capacity connected to energy islands is a key driver of costs. This emphasizes the need to integrate energy islands in a way that electricity capacity flows are balanced across islands.

Building on the resulting energy island locations, a potential offshore hydrogen backbone is designed in which islands serve as hubs connecting offshore wind to hydrogen production. The results show that such backbone could integrate around 93 GW of hydrogen capacity, requiring 186 GW of electricity, at a cost of €8.9 billion. Part of the existing natural pipeline network can be reused to reduce costs. However, their predefined capacity and fixed location mean that new hydrogen pipelines are still needed.

The combined system consists of energy islands, electricity cables connecting offshore wind farms to these islands and an offshore hydrogen backbone connecting them to shore. The overall investment amount to €31.7 billion, which reflects a coordinated multinational approach. An integrated system would enable large-scale offshore wind development, offshore hydrogen production and cross-border transport in the North Sea. If countries plan separately, costs are likely to be higher and integration weaker.

Taken together, this thesis demonstrates that integration offshore wind, hydrogen and energy islands into one North Sea energy system is technically plausible and can be achieved at substantial but necessary investment costs. These investments should, however, not be seen as burdens but as strategic opportunities: without them, climate targets will not be reached, Europe's energy supply is likely less secure, and dependence on unstable regions may persist. While this thesis has findings that are rather indicative than definitive due to methodological, empirical and computational limitations, it provides a conceptual framework for planning an integrated, cross-border offshore energy system that ultimately contributes to Europe's goal of achieving climate neutrality by 2050.

This page is intentionally left blank.

Table Of Contents

List of Figures

List of Tables

Acronyms

ABM	Agent-Based Modelling
AC	Alternating Current
CAPEX	capital expenditures
DBSCAN	Density Based Spatial Clustering of Applications
DC	Direct Current
EEZ	Exclusive Economic Zone
EHB	European Hydrogen Backbone
ESS	error sum of squares
EU	European Union
GHG	greenhouse gas
GGT	Geometric Graph Theory
HVAC	High Voltage Alternating Current
HVDC	High Voltage Direct Current
IMO	International Marine Organization
MI(N)LP	Mixed Integer (Non-) Linear Programming
MPA	Marine Protection Area
MSP	Marine Spatial Plan
NSWPH	North Sea Wind Power Hub
OEH	offshore energy hub
OFTO	offshore transmission owner
ONLT	Optimal Network Layout Tool
OPEX	operational expenditures
OTC	offshore transmission system operator collaboration
OWF	offshore wind farm
ROW	right-of-way
TSO	transmission system operator
UK	United Kingdom
UNCLOS	United Nations Convention on Law of the Sea
US	United States

Nomenclature

Prefix

k	Kilo
M	Mega
G	Giga

Symbols

g	gram
J	Joule
K	Kelvin
m	meter
mol	mole
Pa	Pascal
s	second
W	Watt
€	euro
$	US dollar

1 Introduction

Human activities, such as industry, transportation and agriculture, are responsible for an increase of 11.4% in greenhouse gas (GHG) concentration from 2003 to 2023 (WMO, 2024). This led to an average global temperature increase of 1.22°C within this period, posing extreme risks to global biodiversity, health, and economy (EEA, 2024). Mitigation strategies and climate action are needed to reduce these risks and their impacts (CCAC, n.d.). Consequently, 194 states and the European Union (EU) signed the Paris Agreement and are therefore legally bounded to limit the increase in global temperature to +1.5°C in reference to 1900 (UN, 2024). The EU contributed to the Paris Agreement by launching the European Green Deal in December 2019 (European Council, 2024). It is the EU strategy to realize a green transition by achieving climate neutrality by 2050 (European Commission, 2021b).

Figure 1. Map of the North Sea (Wikipedia contributors, 2010).

The North Sea, of which a map is shown in Figure 1, has a high potential for low carbon energy, especially for offshore wind energy as it has shallow waters (New Energy Coalition, 2024). Consequently, offshore wind energy in the North Sea area is crucial for the success of the European transition (North Sea Energy, 2020). In 2023, seven EU Member States[1], Norway, and the United Kingdom (UK) signed the *Ostend Declaration on the North Seas as Europe's Green Power Plant* (2023). Though Ireland and Luxembourg cannot be labeled as North Sea countries, they aim to contribute by cooperating on renewable energy projects in the North Sea (*Ostend Declaration*, 2023). The other seven countries border the North Sea, see Figure 2, and are therefore referred to as the North Sea countries.

[1] Belgium, Denmark, Germany, the Netherlands, France, Ireland and Luxembourg.

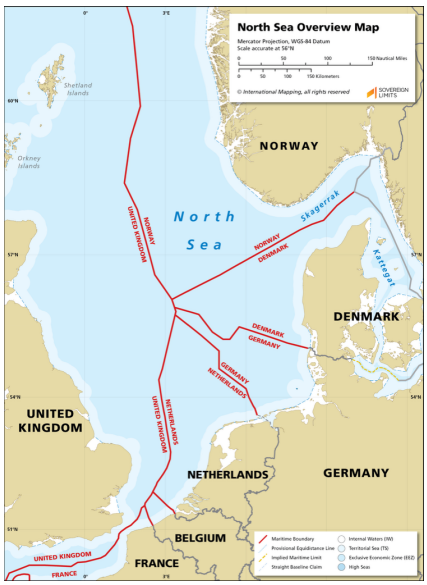

Figure 2. Offshore regions of the North Sea countries (Marsh, 2023).

1.1 Problem Formulation

The aim of the *Ostend Declaration* (2023) is to increase electricity generation from offshore wind to meet Europe's growing energy demand. The increase in electricity, however, is expected to cause supply risks due to congestion and large-scale storage difficulties (North Sea Energy, 2020). Consequently, scaling electricity from offshore wind can become technically challenging. Moreover, a great extension of offshore electricity infrastructure is needed to facilitate new offshore wind farms (OWFs). As the costs for offshore electricity cables are extremely high, extending electricity infrastructures is also economically challenging (Beaubouef, 2024).

An efficient way to cope with these challenges is via hydrogen (Dowling & Jansen, 2023). If produced from offshore wind energy or other renewable energy sources, hydrogen is referred to as 'green' because no GHGs are emitted during the production process (TNO, n.d.). The production process of green hydrogen is called electrolysis. In this process, electricity is used to split water into hydrogen and oxygen molecules (US DOE, n.d.). Electrolysis is feasible either on- and offshore (NSWPH, 2022b). Onshore electrolysis requires the transportation of electricity from OWFs to shore, thus extending offshore electricity infrastructures is still needed. On top of that, space for electrolyzers is required, which is limited available in certain regions (NSWPH, 2024b). Offshore electrolysis, on the other hand, takes place within a wind turbine or at an offshore energy hub (OEH) (Ramboll, 2025), hence not requiring space on land. Janssen et al. (2025) shows that offshore electrolysis maximizes the potential of offshore wind. The North Sea countries have acknowledged offshore electrolysis by explicitly including it in the *Ostend Declaration* (2023) as it could have technical, spatial and economic benefits over onshore electrolysis. Offshore electrolysis is, however, in early stages of development, and large-scale production locations have not yet been determined (European Commission, 2025a; Venugopalan et al., 2024). Additionally, Van Wingerden et al. (2023) points out that: "the potential of offshore hydrogen production can only be fully exploited through network effects." This entails that cross-border collaboration among the North Sea countries is required to effectively develop the full potential of offshore electrolysis. For that reason, cross-border projects form the basis of the *Ostend Declaration* (2023).

According to One North Sea (2021), effective collaboration can be achieved by integrating the national offshore energy systems into one international offshore system. Doing so, the offshore energy systems of the North Sea countries are linked, and the electricity and hydrogen energy systems are integrated into one (North Sea Energy, 2020). North Sea Energy (2020) highlights that this approach allows for emission and cost reductions and improves an efficient use of space, hence accelerating the European energy transition. The North Sea Wind Power Hub (NSWPH) (2024a) concludes that offshore energy hubs (OEHs) play a key role in the realization of an integrated North Sea energy system. An OEH consists of one or more physical, offshore facilities where multiple energy carriers are generated, converted, distributed and/or stored (Aleem et al., 2022; Rettig et al., 2023). In other words, it is an offshore location where offshore electrolysis is powered by electricity from offshore wind. It thereby connects the offshore wind and hydrogen energy systems. Additionally, OEHs allow electrolysis close to the electricity source which reduces transmission losses and infrastructure costs (NSWPH, 2024a). A specific type of OEH is an energy island, which is an artificial island where all OEH assets are located at one physical location, rather than in several hubs or platforms (Dutch Marine Energy Centre, 2024).

With the *Ostend Declaration* (2023), North Sea countries outline a vision to transform the North Sea into Europe's green power plant using offshore wind energy. Energy islands can play a role in this as it is found to enhance offshore energy production and cross-border transport of green hydrogen (NSWPH, 2022a; Wang et al., 2020). In conclusion, electricity from OWFs can be transported to an energy island where it is used to produce hydrogen from. From there, hydrogen is transported to shore. The specific implications of the system's assets, however, are still unclear.

The aim of this thesis is therefore to explore an integrated energy system design in which energy islands connect offshore wind generation to an offshore hydrogen network. In line with the EU's target for climate neutrality, a time horizon for the year 2050 is considered throughout this research. The research objective and a detailed formulation of the research question is discussed in *3.4 Research Objective*.

1.2 Reading Guide

To understand how the identified problem is researched, the thesis is structured as follows. In *Chapter 2. Stakeholder Analysis,* the points of view of relevant stakeholders are analyzed which underpin the societal relevance of the research. Then, in *Chapter 3. Literature Review*, the scientific relevance of the research is determined by indicating core concepts, identifying a knowledge gap and formulating a main research question. Three sub-questions are determined to answer the main research question is in a structured way. In *Chapter 4. Research Methodology*, the approach to answer these questions is provided. In *Chapter 5. Data Preparation,* the data required to execute the research is discussed and prepared. The results of are shown in *Chapter 6. Results*. These results are interpreted in *Chapter 7. Discussion*, including the limitations of the research. Finally, the answers to the research questions, the academic and societal contribution of the research and suggests future research are concluded in *Chapter 8. Conclusion*.

2 Stakeholder Analysis

The North Sea is the busiest marine area in the world. There are large-scale technological projects that involve many stakeholders. The stakeholders have a great variety of opinions, values, needs and roles that must be considered to understand the complexity of the playing field. Doing so, their interests in integrating electricity and hydrogen into one energy system in the North Sea can be identified. Incorporating these interests into the design finally not only contributes to enhancing the social acceptance of such offshore system, but it also ensures a successful implementation.

This Chapter presents a stakeholder analysis that is conducted in a structured approach. First, the key stakeholders are identified and analysed in *2.1 Identification of Stakeholders*. For each stakeholder, its role, needs and values are determined. Then, in *2.2 System Implications*, the system implications of their requirements are analysed to understand the impacts of social considerations on the system design. Lastly, these implications are used to conclude the societal relevance of this research in *2.3 Societal Relevance*.

2.1 Identification of Stakeholders

In this system, seven types of stakeholders can be identified: governmental entities, transmission operators and energy island developers, offshore wind operators, hydrogen operators, energy consumers, nature conservation organizations and other North Sea users. Each group is analyzed in this section.

2.1.1 Governmental Entities

Governmental entities are crucial for enabling offshore electricity and hydrogen networks by providing regulatory frameworks that ensure economic and environmental stability (Gluzman, 2025). Each North Sea country manages its Exclusive Economic Zone (EEZ). This area extends up to 370 km offshore from a country's coast, wherein it has the exclusive rights to explore and exploit natural resources (UNCLOS, 1982, Part V). The national governments of France, Belgium, the Netherlands, Germany, Denmark, Norway and the UK regulate energy network developments in their EEZ by granting permits, managing spatial and network planning, and providing subsidies (British Chambers of Commerce, 2025; De Klerk et al., 2021; TenneT, 2025). In view of Europe's climate, energy, geopolitical and security challenges, national governments aim for energy system that are reliable, environmentally sustainable, and cost-minimizing (British Chambers of Commerce, 2025; De Klerk et al., 2021; Ministry of Foreign Affairs Denmark, n.d.).

At the supranational level, the European Commission has a regulating role as it aligns EU energy markets by providing multiple acts, including the *2019/944 EU Electricity Directive* (2019), *2024/1788 Gas Directive* (2024) and *2019/942 ACER Regulation* (2019). It gives incentive for cross-border renewable energy projects to achieve climate neutrality by 2050 and to secure the energy supply (Babiker & Ciucci, 2025). For this, the European Commission launched the Connecting Europe Facility for Energy (European Commission, 2025b), which provides economic funding. For example, it granted 1.25 billion euros for cross-border offshore wind and energy island projects (Santaella, 2025). Hence, the European Commission supports economically efficient development of

offshore energy projects and values an energy system that is secure, affordable and environmentally sustainable. The *Ostend Declaration* (2023), signed by all relevant governmental bodies, shows that collaboration is essential to unluck the North Sea's renewable energy potential.

2.1.2 Transmission Operators

The offshore electricity and hydrogen networks are developed and coordinated by transmission operators. Belgium, Denmark, France, Germany, the Netherlands and Norway follow the Transmission System Operator (TSO) model, whereas the UK applies the Offshore Transmission Owner (OFTO) model (WindEurope, 2019). In the TSO model, a TSO, which is oftentimes a publicly owned entity, manages and supervises infrastructure planning, operation, and expansion (ECC, n.d.; GridX, 2025). TSOs facilitate the infrastructure connections between suppliers and consumers and regulate cross-border energy flows (GridX, 2025; WindEurope, 2019). In the OFTO model, developers of energy projects decide where infrastructure is needed, after which the British Office of Gas and Electricity Markets (Ofgem) sells transmission infrastructures via a competitive tender process (Evans, 2014; Ofgem, n.d.). The OFTO, which is an independent entity, guarantees efficient infrastructure, also for cross-border projects (HSF, 2021). The National Grid then regulates, and coordinates flows across the system (National Grid, n.d.). The difference is how responsibilities are spread: grid connections are financed and secured by the TSO, whereas the responsibility in the OFTO model lies with the project developer (Vattenfall, 2024).

Twelve transmission operators, including TenneT, Gasunie, Energinet, National Grid, Stattnet and Elia, collaborate in the Offshore TSO Collaboration (OTC). Their aim is to advance offshore network infrastructure by coordinating grid planning and maximize benefits (TenneT, n.d.), in line with the *Ostend Declaration* (2023). Their main interest is to ensure secure, efficient and affordable energy supply (Van de Weijer, 2025). Historically, the OTC mainly focused on electricity, but its 2025 pilot analysis suggested that incorporating hydrogen infrastructures could further maximize the benefits for Europe's energy security, independence and competitiveness (OTC, 2025).

In some cases, the transmission operators also initiate and develop energy islands with national governments. There is no energy island realized yet, but there are several energy islands under development. The *Princess Elisabeth Energy* project is under construction, but commissioning is likely to be delayed as result of increase electricity cable costs (Elia, 2025; De Leener, 2025; Tractebel, 2024). The *Energiø Nordsø Energy Island* and NSWPH projects have been postponed because of financial and political setbacks (Buljan, 2022; Jacobsen, 2024; Jenkinson, 2024; M. Dubbelboer, personal communication, April 4, 2025; Tang, 2022). These delays show the importance for cost-reliable and politically stable project developments.

2.1.3 Offshore Wind Operators

Offshore wind operators design, construct and operate OWFs after they are granted a permit by a national government. They manage electricity production and sales (Benn, 2025; Vattenfall, n.d.-a). Operators include Vattenfall, Ørsted, Equinor, E.ON, RWE and Eneco (De Klerk et al., 2021). They aim to deliver affordable and reliable fossil-free

electricity to ensure a sustainable future for everyone (Eneco, n.d.; Ørsted, n.d.; Vattenfall, n.d.-b). To do so, they need a stable, long-term investment climate (De Klerk et al., 2021).

Areas suitable for offshore wind are already identified (4C Offshore, n.d.), yet investment conditions are volatile. Supply chain costs and interest rates have increased, while electricity prices are lower than expected, reducing project profitability (Gualthérie Van Weezel, 2025; Roland Berger, 2024). Consequently, some OWF auctions have no bids (WindEurope, 2024), or developers withdraw before construction (York, 2025). Because of this, governments have postponed auctions (Belga, 2025; Reuters, 2025). This undermines the realization of a reliable fossil-free energy system.

Furthermore, the regulatory frameworks for tendering vary across North Sea countries, complicating the investment climate strongly (Vattenfall, 2024). The permitting process is lengthy and complex, often taking longer than construction itself (Dickson & Wesche, 2022). Consequently, offshore wind operators would therefore benefit the alignment of a simplified tendering and permitting process across the region.

2.1.4 Hydrogen Operators

Hydrogen operators design, construct, and operate offshore electrolyzers under permits granted via a tendering process similar as for OWFs. The operators also manage the hydrogen production and sales. The offshore hydrogen production is still market, with projects largely in pilot phase and dependent on offshore wind developments. Delays of OWF projects have therefore also delayed some hydrogen pilot projects (RVO, 2025).

Most operators, including Gasunie, Neptune Energy, NAM, RWE and Equinor, originate from the natural gas sector and are transitioning to (Equinor, n.d.; Gasunie, n.d.; RWE, n.d.). They often collaborate in consortia with governments and research institutions to develop and scale the market (PosHYdon, n.d.). For these companies, strong business cases are essential: profitability and stability are key to investment decisions, while they aim to deliver an affordable and reliable hydrogen supply (De Klerk et al., 2021).

Hydrogen can be transported in multiple forms: as high-pressure gas via pipelines, as a low-temperature liquid in special tanks or in solid form blended in other materials (Alsaba et al., 2023). The transportation mode influences the operator's business case strongly. According to the European Commission (2021a), pipelines are the most cost-effective option for offshore transport, enabling transport of large capacities at relatively low cost. Importantly, the extensive offshore natural gas network in the North Sea can, with few modifications, be repurposed for hydrogen (Gasunie, 2025; Van de Weijer, 2024). This makes infrastructure reuse advantageous for hydrogen operators.

2.1.5 Energy Consumers

Energy consumers are the end users of electricity and hydrogen (Tooki & Popoola, 2024). They can be divided into domestic consumers, which are households and bulk consumers such as factories, hospitals and datacenters with high energy demand (Energie Nederland, n.d.; Lévy & Belaïd, 2017). Consumers are the fundament of the energy system: without demand, no energy system would be developed (Dupont, 2023).

Energy is vital for daily life, making consumers highly dependent on a reliable and continuous supply (Eurostat, 2025). Through energy payments, they indirectly finance the system assets and developments. Accordingly, consumers value energy security and affordability (Swallow, 2024). Moreover, the location and volume of demand strongly influence system design, making consumer profiles an essential factor in spatial planning (Gertler et al., 2016).

2.1.6 Nature Conservation Organizations

Human activities drive both rising global GHG concentration (see *Chapter 1. Introduction*) and biodiversity loss (Keck et al., 2025). According to EEA (2008), the North Sea has one of the richest ecosystems in the world due to its shallow waters and rich ecosystems (Álvarez et al., 2019). Nature conservation organizations such as Greenpeace, the WWF, the North Sea Foundation and BirdLife International, are crucial in protecting these ecosystems by preserving and restoring marine habitats and the variety of sea life (Greenpeace UK, 2025; WWF, n.d.).

While energy islands and offshore renewable energy projects contribute to decarbonization, their construction and operation disturb marine habitats (Calamaio, 2024). Ecological impacts therefore need to be carefully assessed (De Klerk et al., 2021). Marine Protection Areas (MPAs) exist to conserve biodiversity and prevent extinction and destruction of habitats, sea life and natural resources by regulating human activity (EEA, 2019; National Geographic, 2024). Conservation organizations emphasize that ecological preservation must be balanced with the energy transition, ensuring environmental sustainability is integrated into spatial planning (Stichting De Noordzee, 2022).

2.1.7 Other North Sea Users

Next to ecological preservation and energy exploitation, the North Sea also supports shipping, military activity, fishing, sand extraction and tourism (Noordzeeloket, n.d.). These activities compete for valuable space and therefore depend on efficient spatial planning (De Klerk et al., 2021). Some users require exclusive areas to ensure safety. The International Marine Organization (IMO) defines specific shipping routes, under the *United Nations Convention on Law of the Sea* (UNCLOS) (1982, Art. 261), to ensure safe shipping (IMO, n.d.). Additionally, national military defence forces require specific zones for missile testing and other defence training (Van Dyke, 1991). Profitability and secure access to designated areas are therefore key values for these stakeholders.

2.2 System Implications

The identified stakeholder perspectives form the social requirements of the system design. Collaboration is required to develop a reliable, cost-minimizing, environmentally sustainable, profitable and stable system, that ensures energy security and supplies affordable energy. Four implications for the system design are discussed in this section.

First, hydrogen operators face uncertainty in the emerging hydrogen market. Repurposing natural gas infrastructures can strengthen their business cases. The European Hydrogen Backbone (EHB) initiative envisions a pan-European hydrogen network, connecting production and demand regions via pipelines (EHB, n.d.; Van Rossum et al., 2022). An offshore hydrogen backbone in the North Seam though not realized yet, is considered

essential to reinforce the investment climate for hydrogen operators (North Sea Energy, 2024). Hydrogen pipelines require lower investment costs compared to electricity grids (Hydrogen Europe, 2024; Van Wingerden et al., 2023) and can make offshore production cost-competitive with hydrogen imports, enhancing energy independence (Hydrogen Europe, 2024; T&E, 2024; Van Wingerden et al., 2023). Although an offshore backbone is of strategic importance, no exact design has been defined (Slowinski et al., 2023).

Second, offshore project development is currently primarily organized at the national EEZ level (North SEE, n.d.), but supranational planning is lacking. Experience from the EU Green Deal shows that long-term collective strategies enhance system reliability and stability (Signorelli & Leonardi, 2025). Such planning could benefit the offshore developments as economies of scale results in cost reductions, and it improves the energy security (Buljan, 2025; North Sea Energy, n.d.). Without supranational coordination, the optimal number and location of energy islands, and the integration of hydrogen into the system remain unclear (NSWPH, 2024a).

Third, geopolitical tensions between Europe and other regions in the world have increased in 2024 due to the Ukrainian war, the tension between Russia and NATO and the wars in the Middle East (DNV, n.d.; Erlanger, 2025; S&P Global, n.d.). Europe is largely dependent on the United States (US), Russia and the Middle East for most of its energy supply (Tobback, 2025). As outlined in the *World Energy Outlook 2024* (IEA, 2024), these tensions, in combination with the US' tariffs put on European goods (Erlanger, 2025; Steinberg & Anderson, 2025), create risks for energy security and might interfere with realizing sustainability targets (Alvik, 2022). In this context, energy islands and a hydrogen backbone can mitigate these risks by enabling large-scale renewable energy production, efficient cross-border transport and reduced dependency on international suppliers. Doing so, these developments contribute to European energy independence and thus are important for strengthening Europe's autonomy in a geopolitical tensed landscape.

Fourth, the North Sea is a small, intensively used area, requiring careful spatial planning (Staeb, 2025). The Dogger Bank area illustrates the challenge as the area spans four countries and is simultaneously a MPA while attractive for offshore wind development (Albert, 2025; BFN, 2024; SSE Renewables, n.d.). Without cross-border coordination, legal conflicts, project delays and deterioration of ecological areas are highly likely. Spatial planning must account for ecological areas, shipping routes and military zones.

In conclusion, a coordinated supranational approach is required to balance spatial, economic and geopolitical considerations. Energy islands emerge as a strategic asset for system efficiency and European energy independence by connecting offshore wind to hydrogen. An offshore hydrogen backbone enables efficient integration of hydrogen in the system. As Giles Dickson, CEO of WindEurope, stated: "Energy islands will become a reality soon. And they will be incredibly useful in helping integrated offshore wind in the energy system and improving energy flows between countries" (Tang, 2022). Realizing this vision requires political ambition, technological developments and economic commitment.

2.3 Societal Relevance

For this thesis, a technological understanding of the possibilities, limitations, and consequences of an integrated North Sea energy system is required. The integration of the electricity and hydrogen markets into one offshore energy system, involves many complex interactions between technological systems, institutional frameworks and stakeholder values. The North Sea is located within seven different countries which have their own policy, governance, and legal structures. Aligning these countries and other multifaceted stakeholders, is essential for the success of the system design. It is a typical example of a socio-technical system with interdependencies, uncertainty and multi-actor complexity.

A realistic system design requires the understanding of regulatory frameworks, ecological concerns, geopolitical relations, supranational coordination and the economic impact of an integrated North Sea system. This makes the research highly relevant in a societal context. At the same time, the need for multi-disciplinary thinking and designing within an uncertain and complex system also makes this research directly relevant for the Complex Systems Engineering and Management program. North Sea Energy (2020) emphasizes this as: “unlocking the low-carbon energy potential of the North Sea requires integrated system thinking rather than merely sectoral optimization.”

3 Literature Review

In *Chapter 1. Introduction*, it is brought forward that the EU aims to achieve climate neutrality by 2050. To achieve this target, offshore wind energy in the North Sea should be used to produce hydrogen at energy islands. Thereby, the offshore electricity and hydrogen systems are connected. The societal relevance of integrating these systems is outlined in *Chapter 2. Stakeholder Analysis*. It concluded that this can be achieved by a supranational planning approach, which includes the considerations of other North Sea uses. Moreover, the economic benefit of an offshore hydrogen backbone and strategic implications of energy islands to realize European energy independence were highlighted in the second chapter.

In this Chapter, the academic relevance of integrating energy islands in the North Sea energy system is analysed by reviewing literature. First, the literature review focuses on system design relating to offshore energy in *3.1 Offshore Energy System Design*. Next, in *3.2 North Sea Energy Assets*, it focuses on literature regarding the infrastructures requierd in the system design: electricity cables, hydrogen pipelines and energy islands. Relevant research methodologies are reviewed in *3.3 Research Approach*. Lastly, the research objective is formulated in *3.4 Research Objective*, discussing the research questions and concluding the academic relevance of this thesis in *3.5. Academic Relevance*.

3.1 Offshore Energy System Design

Energy is delivered to consumers via networks (Chen et al., 2017). Their network structure is defined by the network's topology. Dedecca & Hakvoort (2016) define network topology as the combination of grid structure and technology components. Network topologies are traditionally divided into two groups: *radial* and *integrated*. Kristiansen et al. (2018) define radial topology as point-to-point connections, while integrated topology allows multiple offshore assets to interconnect at shared joints. For offshore networks, Lüth & Keles (2024) and Glaum et al. (2024) identified several topology designs:

- *Farm-to-owner-country,* also referred to as *radial*: the traditional connection that directly connects offshore projects to shore of the owner country.
- *Country-to-country*, also referred to as *interconnector*: a direct connection between two countries.
- *Hybrid interconnector*: a connection between two offshore energy projects in different countries facilitating inter-country transmission.
- *Meshed*, also referred to as *integrated*: the connection between multiple offshore energy projects in various countries facilitating multi-country transmission.

These topologies are visualized in Figure 3.

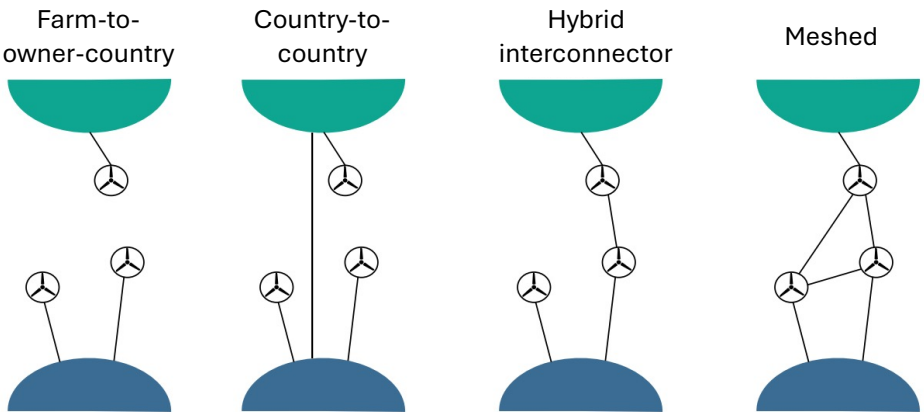

Figure 3. Schematic illustration of four offshore network designs: farm-to-owner-country, country-to-country, hybrid interconnector and meshed. Based on Glaum et al. (2024).

Konstantelos et al. (2016), Traber et al. (2017) and Wiegner et al. (2023) conclude a meshed network is most beneficial: it stimulates cross-border trade enhancing energy price stability and increasing energy security. Economies of scale thereby allow an increase in energy extraction from offshore assets and reduction of connection costs. Ultimately, this results in a more value energy supply. According to Martínez-Gordón et al. (2022), meshed energy system topology enables the integration of multiple energy networks. Glaum et al. (2024), Guşatu et al. (2024), Peters et al. (2020), Quirk et al. (2021) and Wiegner et al. (2023) emphasize the importance of a meshed energy system in the North Sea region. However, a specific system design for such meshed network in this region remains undefined. Designing a meshed network for the North Sea is thus relevant. This research aims to assess such system design. In the following sections, several aspects for a meshed system design are discussed.

3.1.1 Market Design

The economic definition of a network is equally crucially as the technical system design. Energy markets are defined by a bidding zone, in which market participants submit bids and offers for energy (Dobos et al., 2025). Most bidding zones are defined by national borders, but this might limit the efficiency of meshed networks extending multiple countries. By introducing offshore bidding zones, a separate price zone for each energy production location is created (Tosatto et al., 2022). It ensures that the market price for offshore energy is not influenced by market prices in other countries. Doing so, the cross-border trade in meshed networks can be efficient (Lüth et al., 2023b). Lüth et al. (2023b) also discuss other energy market designs. However, the focus of this research remains on technical system design. Since offshore bidding zone enable efficient use of meshed networks, it is assumed as energy market design.

3.1.2 Hydrogen

Ekoue et al. (2025) highlight that the intermittency of renewables is challenging for the operation of electricity networks. Dute et al. (2024) underscore this, as a potential mismatch between supply and demand is balanced if hydrogen is produced from renewable electricity. Hydrogen is thus a relevant source to use to deal with these intermittency challenges. According to Farahmand et al. (2024), hydrogen production from offshore wind improves wind asset utilization by reducing curtailment, thereby increasing overall system efficiency. Moreover, Glaum et al. (2024) stress that hydrogen

from offshore wind contributes to fulfilling the future electricity and hydrogen demand in Europe. Consequently, offshore electricity is considered simultaneously with hydrogen.

Hydrogen can be produced both offshore and onshore. Gea-Bermúdez et al. (2023) find that offshore hydrogen production results in higher overall energy system costs compared to onshore production. Hydrogen transmission infrastructures offshore are namely more expensive than onshore infrastructures. However, this study purely focuses on cost optimization, thereby excluding the consideration of other aspects, such as use of space, required network reinforcements and public acceptance. These aspects should be included as realistic offshore energy system design is not purely based on economic efficiency (Gea-Bermúdez et al., 2023). Besides, Durakovic et al. (2022) find that the development of the offshore hydrogen system depends on a significant development required of the electricity grid. Though, the costs for offshore hydrogen transmission infrastructure are lower than for offshore electricity transmission infrastructure. This advantage increases when hydrogen is produced further at sea (Durakovic et al., 2022). Moreover, according to Travaglini et al. (2025), centralized offshore hydrogen production results in the lowest levelized cost of hydrogen, compared to onshore and decentralized offshore production. Centralized offshore hydrogen production is therefore considered for the system design in this thesis.

3.1.3 Offshore Energy Hubs

According to Dute et al. (2024), OEHs accommodate centralized offshore hydrogen production. Furthermore, OEHs are crucial to unlock offshore wind in the North Sea. Xu (2024) highlights that OEHs allow for the integration of electricity and hydrogen networks, which ultimately improves overall system efficiency and sustainability. More importantly, OEHs are important elements in meshed networks for efficient system design (Kristiansen et al., 2018). Consequently, OEHs are included in the system design for a meshed North Sea system as it enables a connection between the offshore electricity and hydrogen systems.

3.2 North Sea Energy Assets

A meshed system connecting electricity and hydrogen system, includes electricity cables, hydrogen pipelines and energy islands. To design such system, each asset should be understood. In this section, relevant literature is reviewed.

3.2.1 Electricity Cables

Electrical energy is transmitted via direct current (DC) or alternating current (AC) cables. Von Meier (2006) explains the difference: in DC cables, electrical energy always flows in one way, whereas in AC cables, the electrical energy flow periodically changes direction. The electrical losses for AC are generally lower than for DC. Initially, AC cables were preferred for long distance transmission, because it was easier to increase the voltage. It resulted in lower transmission losses, leading to the development of High Voltage AC (HVAC) (Pillay et al., 2020). More recently, however, technological advancements made High Voltage DC (HVDC) cables technically more advantageous for longer distances (Alassi et al., 2019). These studies show that the choice between HVAC and HVDC depends on cable length and capacity. Accordingly, both cable technologies are considered in the offshore system design.

All cable types can be applied offshore. However, so-called submarine cables have other mechanical implications compared to onshore cables (Gulski et al., 2021). Relating to offshore wind, the cable length and capacity determine which technology is technically and economically the most suitable. The electrical losses of all cable technologies, however, increase with distance and size (Apostolaki-Iosifidou et al., 2019). Machado et al. (2015) provide an extensive analysis on which technology is optimal considering these metrics. The costs of submarine cables are already high, and the further increase when cables are longer and larger (Gulski et al., 2021). As OWFs are gradually located further offshore and production capacity increases (Soares-Ramos et al., 2020), cable costs will only increase further. The distance from OWFs to shore thus influences cable technology and length. Besides distance, the electrical capacity of OWFs affects the required cable capacity. Consequently, the distance and electrical capacity are essential to determine the system costs of the network design.

3.2.2 Hydrogen Pipelines

Alsaba et al. (2023) discuss multiple forms of offshore hydrogen transmission. Among these forms, pipelines are identified as the most efficient and cost-effective option (Zhang et al., 2024a). Additionally, Jacquemin et al. (2024) conclude that a hydrogen pipeline network reduces the total costs for the European energy transition. Accordingly, hydrogen pipelines are exclusively considered in the system design of this thesis.

An important aspect of pipelines is the reuse of existing infrastructure. McKenna et al. (2021) identify that the many existing natural gas pipelines in the North Sea can be repurposed for hydrogen transmission to reduce system costs. This is supported by Terenzi et al. (2024), Wang et al. (2023), Koo et al. (2023) and Wen et al. (2023), which elaborate on the technical modifications that are required. These studies underscore that both new and repurposed pipelines should be considered to develop a hydrogen network. Accordingly, existing natural gas infrastructure in the North Sea are included in the design.

3.2.3 Energy Islands

Energy islands enable the connection between offshore electricity and hydrogen systems. Ibrahim et al. (2022) show that offshore hydrogen production is economically attractive located further at sea. Similarly, Lüth et al. (2023a) highlight that the value of offshore wind is enhanced when hydrogen is produced at energy islands. Thommessen et al. (2021) emphasize that energy islands enable the optimal integration of offshore electricity and hydrogen systems. Additionally, Arteaga et al. (2024) find that energy islands provide interconnections between multiple countries and allow for centralized power-to-X technologies. Taken together, these studies confirm that energy islands are not stand-alone projects but are crucial assets for a meshed North Sea energy system. A conceptual illustration is shown in Figure 4.

Wu et al. (2025) offer practical guidelines for the configuration and operation of energy islands. The guidelines are based on the integration of offshore wind power, hydrogen production and hydrogen storage. A configuration concept for energy islands is outlined in Dadkhah et al (2022). However, Lüth & Keles (2024) highlight that there is still no consensus on the optimal number of and location for energy islands. A minimal distance from energy islands to OWFs is particularly relevant as longer transmission distances

increase costs and power losses (Apostolaki-Iosifidou et al., 2019; Ibrahim et al., 2022). The distribution of OWFs can thus be used to specify an optimal number of energy islands. Moreover, the OWF locations can also be used to define potential energy island locations. Although Bengtsson (2024) applies multicriteria decision analysis to define potential energy island locations in the North Sea, it does not include the distance from islands to OWFs. It thereby remains unknown how incorporating OWF locations would affect the overall system design. Consequently, OWFs are used to define an optimal number of and potential locations for energy islands.

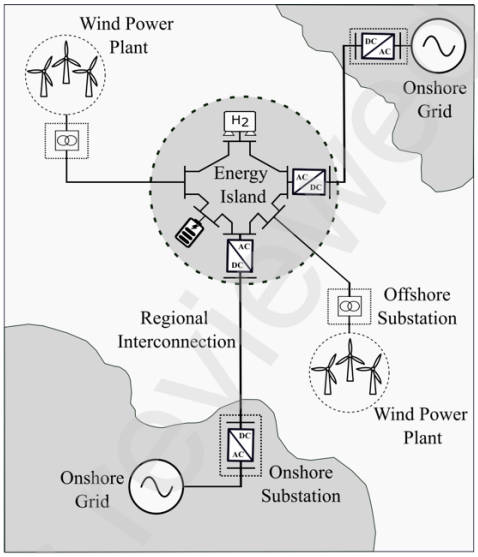

Figure 4. Possible schematic concept of an energy island (Arteaga et al., 2024).

The societal dimensions of energy islands are also emphasized in literature. Dadkhah et al. (2022) underscore that: “energy islands offer many advantages, including energy independence, environmental awareness, economic development, durability, efficiency, reliability, and social sustainability.” In contrast, Gusatu et al. (2020) point out political and societal barriers, such as conflicting national interests in energy policy. Nieuwenhout & Andreasson (2022) discuss the legal framework required to develop energy islands in the North Sea. Finally, Lüth & Keles (2024) emphasize that the social acceptance of energy islands is a condition for the success of its implementation. These aspects are not directly modelled in this thesis but acknowledging them highlights the broader challenges of energy island development.

3.3 Research Approach

Literature is reviewed to explore an appropriate research approach for designing meshed energy systems. In this section, several methodologies are discussed.

3.3.1 Clustering

OWFs in the North Sea are distributed throughout the whole system. Some farms are located near shore, others far out at sea. As discussed in *3.2.3 Energy Islands*, a minimal distance between OWFs and energy islands is preferred. Since multiple OWFs are connected to one energy island, the challenge is to determine which OWFs should be connected to the same energy island. Clustering is a technique that can be used to group OWFs that are spatially close to each other.

Ismail et al. (2015) defines clustering as: “a division of data into groups (clusters) of similar objects.” For spatial problems such as this, distance is used to define which objects belong to the same cluster (Han et al., 2012). Each cluster has a centroid which identifies the geometric center of the OWFs in one cluster (Deakin et al., 2002). Clustering can be used to indicate potential location(s) of energy islands in the North Sea.

There is not one specific definition for what a “cluster” is, because there are various clustering methods applying different principles (Rokach & Maimon, 2006). Fraley & Raftery (1998) and Han et al. (2012) categorize the clustering methods into density-based, hierarchical and partitioning. Density-based methods group data points using specific probability distributions, partitioning methods iteratively relocate data points between clusters until specific criteria are satisfied, and hierarchical methods partition data via divisive or agglomerative approaches (Rokach & Maimon, 2006). Divisive approaches are top-down approach, while agglomerative approaches are bottom-up (Halkidi, 2009). Each clustering technique has advantages, but its relevance for this research depends on how OWFs are grouped based on the distance between them. By clustering OWFs, their locations are used to determine potential energy island locations.

3.3.2 Network Optimization Models

The importance of minimal system costs has come forward multiple times in previous sections. Designing a meshed offshore system hence requires minimizing costs while ensuring connectivity between infrastructures. Network optimization models provide mathematical tools to address this challenge in system design. Heijnen et al. (2019), identifies three approaches: Geometric Graph Theory (GGT), Mixed Integer (Non-)Linear Programming (MI(N)LP) and Agent-Based Modeling (ABM).

GGT includes heuristics and algorithms from graph theory and geometry that are applied to find the optimal topology and location of certain points in a network (Heijnen et al., 2019). Sharma & Kumar (2021) explain GGT as: “a mathematical tool that is broadly used to model pairwise interactions.” It relates to physical and figurative networks. GGT has been used in several contexts, from sensor networks (Ghosh & Das, 2008) and communication networks (Karyotis & Khouzani, 2016), to visualizing pipeline layouts (Zhou et al., 2019). Ultimately, Heijnen (2025) makes use of GGT in a tool to show the layout of networks. GGT is relevant for system design as it can be used to spatially represent OWFs, hydrogen pipelines, electricity cables and energy islands. Doing so, it enables the visualization of potential meshed network layouts.

MI(N)LP is a mathematical modelling approach that uses an objective function to optimize specific variables. The aim of the objective function is to optimize within certain boundaries (Romeo, 2020). MI(N)LP has been used for several network optimization problems, such as battery integration in micro-grids (Lipu et al., 2022) or renewable energy planning in electricity grids (Ehsan & Yang, 2017). With MI(N)LP, trade-offs between different system aspects can be captured (Lipu et al., 2022). It thereby complements GGT in optimizing a meshed energy system in the North Sea.

By contrast, ABM is a modelling approach representing systems as a collection of autonomous agents that interact with each other and their environment (Öttl & Termansen, 2025). It is useful for exploring the emergent behavior of existing systems.

ABM is used to understand water distribution networks (Rezaei et al., 2014), pipeline systems on ships (Wang et al., 2025) and renewable energy systems (Abera et al., 2025; Zhang et al., 2024b). The focus of this research is on designing a new system, considering system efficiency rather than system behavior. ABM is thus not further applied.

3.4 Research Objective

In *3.1 Offshore Energy System Design*, it comes forward that a meshed network topology is most beneficial, but that specific design for the North Sea is lacking. In such design, offshore hydrogen production from offshore wind energy should take place at energy islands. The infrastructures required are discussed in *3.2 North Sea Energy Assets*. It shows that submarine cables require a trade-off between HVAC and HVDC cabling and that hydrogen transmission is most efficient via pipelines, especially by repurposing existing natural gas pipelines. Furthermore, the distance between OWFs, to energy islands and to shore are key variables that influence overall system costs. Research that explicitly incorporates OWFs as the basis for offshore system design is lacking.

It is shown in *3.3 Research Approach*, that clustering and network optimization models are relevant methodologies for this research. The combination of these approaches has not been applied in previous research to design a meshed energy system design for the North Sea. Clustering uses OWF locations to find potential island locations, while network optimization models allow for techno-economic optimization and visualization of network layouts of all assets in a meshed system.

Considering this, in combination with the requirements identified in *Chapter 1. Introduction* and *Chapter 2. Stakeholder Analysis,* the research objectives for this thesis are formulated as follows:

- Determine the required number of energy islands and their locations based on the geographic distribution of OWFs,
- Include the distance between OWFs, to shore and to energy islands as key cost parameter in the system design,
- Envision the North Sea as a single integrated system, disregarding national borders to enable supranational planning,
- Account for the spatial constraints of ecological areas, military zones and shipping routes within the network optimization model,
- Assess the feasibility of repurposing existing offshore natural gas pipelines to design an offshore hydrogen backbone.

Following these objectives, a meshed offshore system design is explored. Energy islands are crucial as they are used for connecting the electricity and hydrogen systems in the North Sea. Consequently, the research aims to answer the following research question:

What is a system design with minimal overall system costs for the North Sea, in which energy islands enable the integration of electricity from offshore wind farms in an offshore hydrogen network, while accounting for other North Sea uses?

The overall system costs include the investment costs of all system assets: energy island construction, electricity cabling and hydrogen pipelines. To answer the main research

question in a structured approach, three sub-questions are assessed. In all three sub-questions, optimality and efficiency refer to configurations in which the investment costs within the boundaries of that system component are minimal. The following three sub-questions are assessed:

1. *What is the cost-optimal number of energy islands in the North Sea by 2050, based on operational and planned offshore wind farms?*
   The operational and planned OWFs in the North Sea are the starting point for the system design. By clustering OWFs, potential island locations are identified via the cluster centroids. The clustering results are then used to determine a cost-optimal number of energy islands by minimizing the combined costs for energy island construction and electricity cabling. Additionally, the hydrogen production capacity of each energy island can be derived from this configuration.

2. *What are the optimal locations for energy islands in the North Sea considering other North Sea uses?*
   The spatial constraints of other North Sea uses are not considered in the clustering process, which makes the initial island locations only indicative. To obtain realistic results, these constraints are applied to adjust potential island locations. In addition, the electricity transmission network for each cluster, which connects the OWFs to an island, is determined with minimal network costs.

3. *What is the most cost-efficient system design for an offshore hydrogen backbone, given the locations of energy islands?*
   Based on the location and hydrogen production capacity of energy islands, and the existing natural gas transmission infrastructures, a cost-efficient hydrogen backbone can be derived using the network optimisation model. This includes the reuse of existing infrastructure where feasible.

3.4 Academic Relevance

This thesis contributes to the academic field of integrated offshore energy system by addressing a gap in existing research. Previous studies have assessed offshore wind, offshore hydrogen production and energy island separately, but few have combined these aspects into one meshed system design. Moreover, most research adopts a national design perspective, whereas this research considers the North Sea as one supranational energy system.

The academic relevance of this thesis can also be found in the research approach. by combining clustering with network optimization models, this bridges asset-level decision-making for localization and system-level optimization. This framework has not been applied before to such meshed system design. It offers a new perspective on how energy islands can function as strategic assets in connecting two offshore systems while enhancing overall system efficiency and European energy independence.

4 Research Methodology

The research objectives outlined in *Chapter 3. Literature Review* are used to define several research questions that address specific aspects of a meshed system design. To answer each question in a structured approach, this chapter presents the research methodology.

First, the overall research strategy is introduced in *4.1 Research Strategy*, outlining the general approach for this thesis. This is followed by *4.2 Offshore Wind Farm Distance Range*, in which it is described how OWFs are classified based on their distance from shore. In *4.3 Number of Energy Islands*, an approach for determining a cost-optimal number of energy islands is presented, which includes clustering and an economic assessment. Finally, it is described in in *4.4 Network Optimization Modelling* how optimal energy island locations and an offshore hydrogen backbone design are determined. This includes an introduction to the relevant models, which are applied in both design steps.

4.1 Research Strategy

Designing an integrated offshore electricity and hydrogen system via energy islands requires a systematic approach accounting for technical, economic and spatial considerations. Multiple designs are possible, but the aim is to identify the most feasible and cost-effective design (Dagdia & Mirchev, 2020; Valencia-Rivera et al., 2023). This section presents the overall research strategy. It begins by explaining the research approach in *4.4.1 Modelling Approach*, followed by an overview of the research process in *4.4.2 Research Flow Diagram*.

4.1.1 Modelling Approach

To represent and evaluate this in the design of offshore energy systems, a mathematical modelling approach is applied. A mathematical model allows for the understanding of the functional characteristics and limitation of real-life situations using mathematical expressions (Jordaan & Lategan, 2010).

In this research, models are used to represent the North Sea's OWF distribution, potential energy locations, and associated electricity and hydrogen infrastructure. These models include technical and economic parameters, and spatial restrictions to enable a consistent evaluation across different design phases. The specific modelling methodologies and tools applied are introduced in the following sections.

4.1.2 Research Flow Diagram

An overview of the research approach is presented in a research flow diagram shown in Figure 5. In the diagram, color coding is used to indicate which methodology is applied to determine each parameter. To illustrate the research flow and the coherence between the research questions, the in- and output parameters are also highlighted, indicating how they are used.

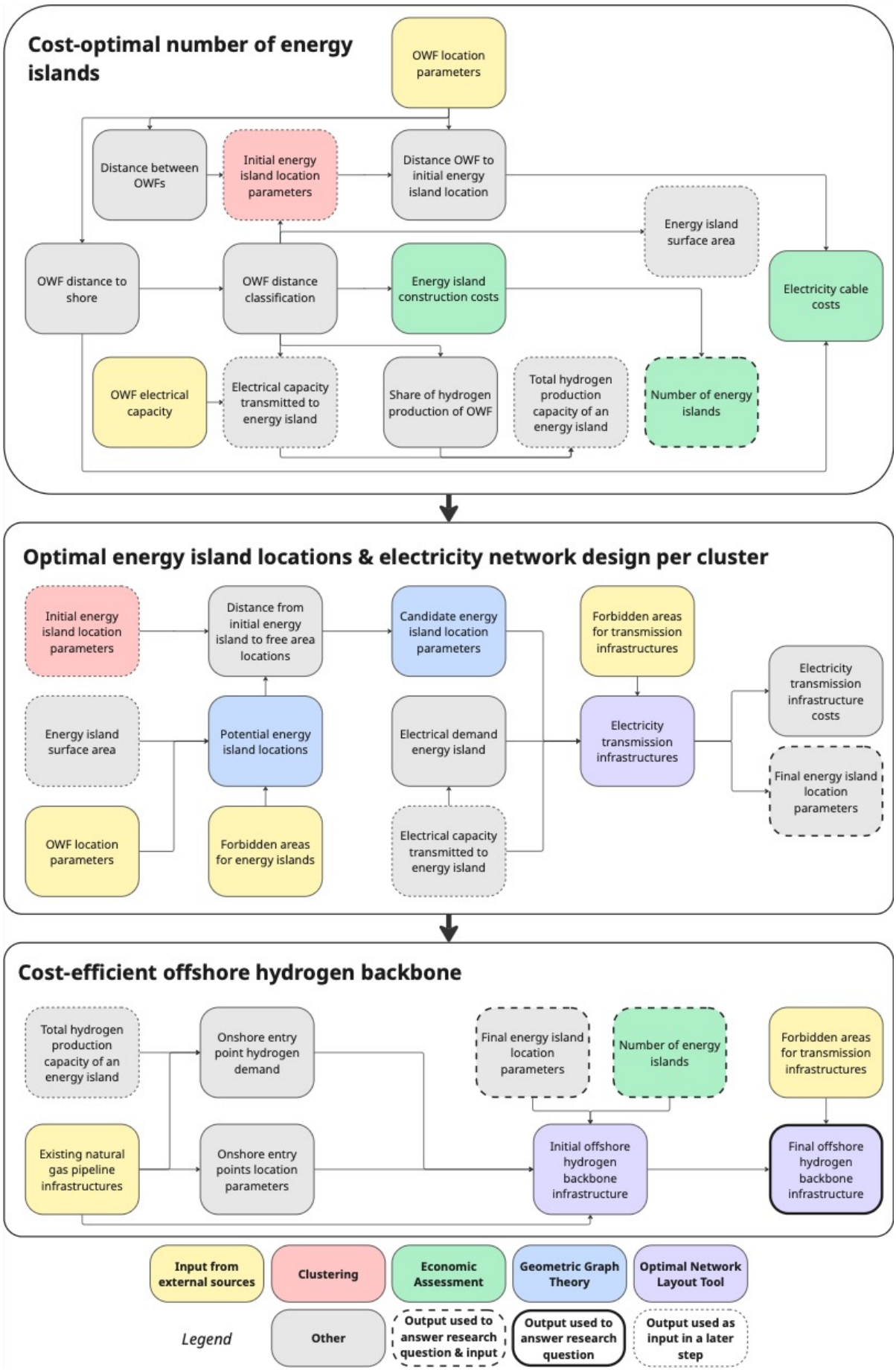

Figure 5. Research flow diagram.

4.2 Offshore Wind Farm Distance Range

The operational and planned OWF areas in the North Sea are known and form the basis for modelling. These locations determine where electricity production takes place, and thus where the energy enters the system. Consequently, they shape system design choices such as where energy islands should be built and indirectly affect where hydrogen is produced from electricity. As discussed in *3.2.1 Electricity Cables*, the decision to transmit energy in the form of electricity or hydrogen depends on electricity cable length and associated system costs. To ensure a technically and economically efficient system, OWFs are therefore categorized based on their distance from shore.

The categorization reflects the current reality, in which all OWFs are directly connected to shore. It is a pragmatic and relevant starting point, as it improves the likelihood of implementing the design in practice. The approach is also chosen to systematically account for differences in transmission costs and technologies.

The categorization is based on several studies. NSWPH (2024b) identify that for OWFs close to shore, low-voltage AC cables with minimal power losses and transmission costs make direct electricity transmission favorable. Conversely, Sall (2023) found that for OWFs far out at sea, hydrogen transport via pipelines becomes more economical. Then, pipeline system costs are lower than electricity cable costs. Although literature does not provide a comprehensive framework with specific thresholds, Ibrahim et al. (2022) refer to OWFs within 60 km from shore as “near shore sites.” Literature, see *3.2.1 Electricity Cables* and *3.2.2 Hydrogen Pipelines*, suggests that transmission preferences change with increasing distance from shore. Together, these sources support the assumption that distance to shore is a key metric in determining the form of energy transmission.

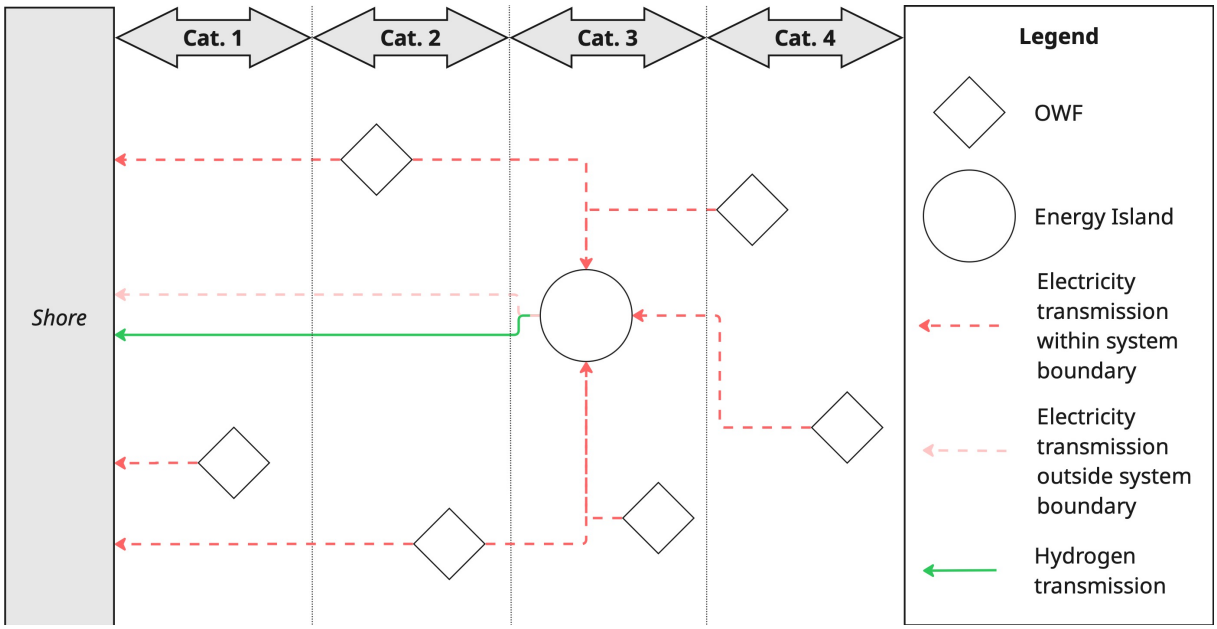

Figure 6. Conceptual illustration of energy transmission choice per OWF category, based on distance to shore.

To operationalize this logic, OWFs are grouped in four distance-based categories, each having a specific routing strategy for electricity and hydrogen. This strategy is defined by two parameters:

1) The share of electricity produced at an OWF that is transported to an island,
2) The share of OWF electrical capacity used for hydrogen production at an island.

The conceptual logic is illustrated in Figure 6. It shows how electricity from OWFs is transmitted directly to shore and/or aggregated at an energy island. There, it is partly or fully used for hydrogen production which is transmitted to shore via pipelines. The OWF and island locations in Figure 6 are schematic and intended to illustrate how the system design is influenced by OWF locations, rather than to reflect actual distances or data.

4.3 Number of Energy Islands

In this section, the methodology used applied to define a cost-optimal number of energy islands is presented. First, OWFs are clustered as discussed in *4.3.1 Offshore Wind Farm Clustering*. To ensure a cost-optimal outcome, the clustering results are then economically assessed, as presented in *4.3.2 Economic Assessment*. The configuration with the lowest overall cost defines the number of energy islands.

4.3.1 Offshore Wind Farm Clustering

By using clustering, OWFs are grouped based on their geographic location. This is done to identify which OWFs should be connected to the same energy island. As outlined in *3.3.1 Clustering*, there are various clustering methods. The focus of this thesis is to explore a system design rather than evaluating thos methods. A selection of commonly used methods is therefore considered in *4.3.1.1 Clustering Algorithms*. The Ward clustering method is selected as most appropriate algorithm. How this method is applied in the context of this thesis, is discussed in *4.3.1.2 Ward Clustering*. The clustering results are then prepared for the economic assessment, as presented in *4.3.1.3 Post-Clustering*.

4.3.1.1 Clustering Algorithms

Clustering of OWFs in the North Sea must ensure that the distance between each OWF and a potential energy island location is minimized, resulting in minimal cable length. Moreover, all relevant OWFs need to be assigned to a cluster, as the clustering output forms the basis for a complete system design. The OWF dataset is therefore defined in advance, with exclusions already applied where appropriate. This way, the full set of OWFs are clustered. Finally, because uncertainties in future OWF developments may introduce unrealistic data points, the chosen clustering method should be robust to noise, which is “mislabeled examples or errors in the values of attributes” of data points (Salgado et al., 2016). Relevant data is thereby not discarded.

The basis for density-based clustering is Density Based Spatial Clustering of Applications with Noise (DBSCAN) (Ankerst et al., 1999). DBSCAN is effective at identifying clusters using two parameters: *Eps*, defining the radius of a data point neighborhood, and *MinPts*, defining the minimal number of cluster data points (Ester et al., 1996). However, determining correct values for these parameters is highly complex (Starczewski et al., 2020). Moreover, DBSCAN excludes data points that do not satisfy the parameter thresholds, treating them as outliers (Gaonkar & Sawant, 2013; Salgado et al., 2016). Because the system design requires that all relevant OWFs are included, DBSCAN is not selected for clustering as its result can contain outliers.

Two agglomerative hierarchical clustering methods, single linkage and Ward linkage, are also considered (Murtagh & Contreras, 2017). Both methods assign all data points to clusters, but their merging processes are based on different principles. In single linkage, clusters are merged when the distance between data points is minimal (Gower & Ross, 1969; Vijaya et al., 2019). This can lead to the chaining effect: an undesirable merging of clusters due to two isolated data points that have minimum distance between them (Jarman, 2020). As a result, single linkage is sensitive to noise (Salgado et al., 2016), making single linkage unsuitable for the system design.

Ward linkage method merges data points incrementally into clusters by minimizing the increase in within-cluster variance at each step (Vijaya et al., 2019). Variance reflects how data points are dispersed around the cluster mean. For a cluster, it is calculated as the difference between each data point and the average of all points in that cluster. It therefore shows the loss of information when a cluster is represented by its mean (James, 2003). Low variance reflects high compactness, and thus meaningful clustering.

The most used partitioning method is the K-Means algorithm (Rokach & Maimon, 2006). Like Ward's method, it aims to minimize the within-cluster variance (Jain, 2010), but its approach is different. K-Means starts by randomly selecting k initial centroids. The remaining data points are assigned to the nearest centroid. Then, the centroid is updated to the geometric cluster center. The steps are repeated until the centroid locations stabilize (Lloyd, 1982; MacQueen, 1967; Salih & Jacksi, 2020). Although K-Means appears similar in objective to Ward's method, there is a fundamental difference: Ward's method uses a bottom-up merging process, whereas K-Means is a top-down iterative reallocation process of data points.

Both Ward linkage and K-Means are suitable for the system design. Studies that compare both methods are inconclusive: Melnykov & Michael (2019) and Młodak (2020) conclude that K-Means is generally faster, while Gupta et al. (2021) report that Ward's method performs better on smaller data sets. In this context, 'small' typically refers to datasets below a few thousand data points. In 2022, 41 OWFs were operational in the North Sea (Chirosca et al., 2022). Even with the expected increase in OWFs, the total number of OWFs will not exceed more than a few hundred due to spatial limitations. Given the relatively small number of OWFs in the North Sea, Ward's method is suitable. It performs best on small datasets and ensures compact clusters and is thus selected for clustering.

4.3.1.2 Ward Clustering

In Ward's method (Ward, 1963), each data point initially forms its own cluster. Given n OWFs, there are n initial clusters. Then, two clusters are merged incrementally if it results in the smallest increase in within-cluster variance. This process continues until the predefined number of clusters k are formed. Ward's method is a greedy algorithm: the locally optimal choice at each step is made, without considering the effect on the clustering outcome in a later step (Joshi & Verma, 2021).

In Figure 7, Ward's merging process is illustrated. Each plot shows the result after one additional merging step, corresponding to a decreasing value of k. The red dashed line indicates the pair of clusters that are merged to obtain the next configuration. This Figure is for illustrative purposes only and does not represent real-world information.

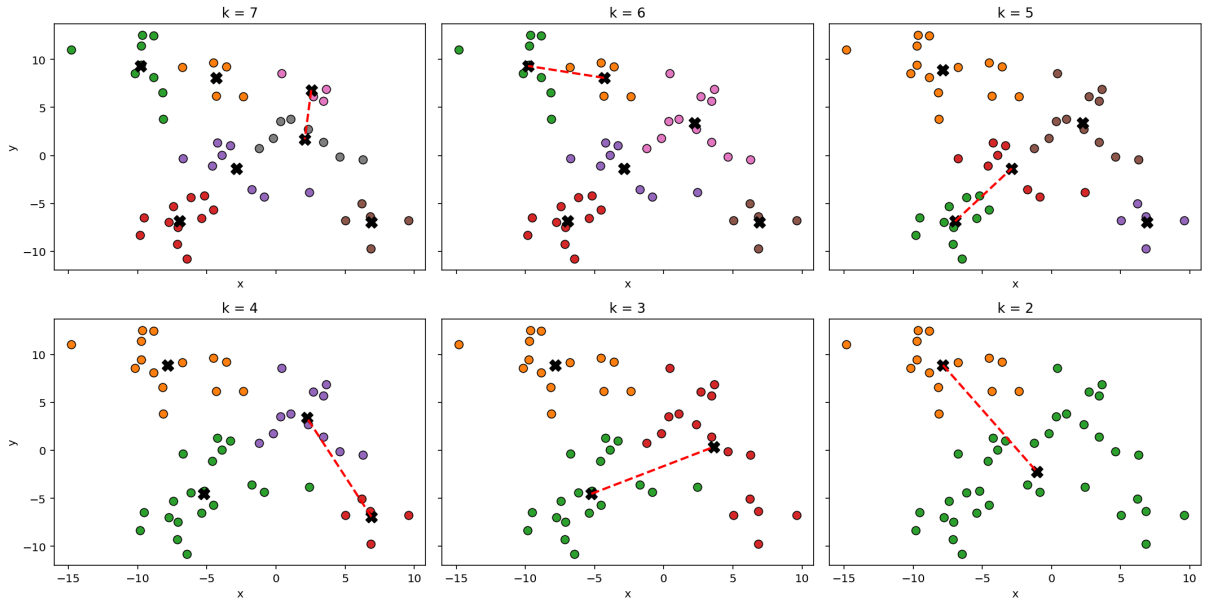

Figure 7. . Illustration of the merging process in Ward's clustering for different values of k. The application of these plots is for illustrative purposes only; the data thus does not represent real-world information about OWFs or any other asset.

The increase in variance is formally expressed using the error sum of squares (ESS). This is the sum of the squared distance from any OWF to a cluster centroid for any pair in a cluster. The centroid is the average position of all OWFs in a cluster. A detailed explanation of how ESS is calculated, is presented in *Appendix A1. Mathematical Explanation of Ward's Clustering*.

ESS is calculated for an individual cluster. The total ESS of all clusters in reflects the compactness of the clustering. At each clustering step, the cluster pair resulting in the smallest increase in total ESS are merged.

In the context of this thesis, compact clusters directly translate to shorter average cable lengths between OWFs and the island they are connected to. Minimizing ESS therefore contributes to minimizing electricity cabling, and thus to cost minimization.

Ward's method is applied to cluster OWFs into k clusters. All OWFs in a cluster are connected to one similar island. The aim is to find a cost-optimal number of energy islands by minimizing the distance between OWFs and the energy island their connected to. Thereby, k represents the number of energy islands. Ward's method is repeated for $k \in [3,20]$. In *4.3.2 Economic Assessment*, it is discussed how these configurations are evaluated based on their contribution to the total system costs.

4.3.1.3 Post-Clustering

The centroids defined by Ward's method represent initial, theoretical island locations. A minimal average distance between OWFs and centroids is favorable. However, the differences in electrical capacity of OWFs are not considered. Energy islands are likely to be positioned closer to OWFs with a larger electrical output to reduce infrastructure costs and increase technical efficiency. Accordingly, the centroid of each cluster is recalculated after clustering is applied.

Let a cluster consist of $n \in \mathbb{N}$ OWFs, indexed by $i \in \{1, \dots, n\}$. Each OWF i has lat_i, the latitude of OWF i in degrees, lon_i, the longitude of OWF i in degrees, and $q_{i,e}$, the electrical capacity of OWF i that is transmitted to the energy island in MW. The weighted average centroid $(lat_{centroid}, lon_{centroid})$ is then calculated as follows:

$$lat_{centroid} = \frac{\sum_{i=1}^{n} q_{i,e} \cdot lat_i}{\sum_{i=1}^{n} q_{i,e}}, \qquad lon_{centroid} = \frac{\sum_{i=1}^{n} q_{i,e} \cdot lon_i}{\sum_{i=1}^{n} q_{i,e}}$$

Here the value of q_i depends on the share of total electricity production of the OWF is transmitted to the island, as determined by the distance-based categories explained in *4.2 Offshore Wind Farm Distance Range*.

The recalculated centroid is used in the economic assessment, as it can be used to define cable distances and costs. While clustering is purely based on distance, no spatial constraints are yet considered. To include these constraints, a more specific methodology is applied, which is outlined in *4.4.3 Energy Island Location*.

Energy islands are interesting if they add economic or technical value to the system. They do so by facilitating offshore hydrogen production and reducing electricity transmission distances. Therefore, if an OWF is closer to shore than to an island, it is illogical to transmit the electricity to the island. Nevertheless, offshore hydrogen production should be incentivized. To reflect this trade-off, the following filtering criterion is applied:

Distance criterion: $d_{OWF \rightarrow shore} < 0.5 \cdot d_{OWF \rightarrow centroid}$

Filtered OWFs are then assumed to connect directly to shore and are excluded from the clusters. It ensures OWFs are only clustered when their connection to the island is value.

After these post-clustering adjustments, the clustering results for each number of islands k provide a more realistic basis for economic assessment and comparison.

4.3.2 Economic Assessment

The output of the clustering steps described in *4.3.1 Offshore Wind Farm Clustering* is the basis for the cost calculations. For each $k \in [3,20]$ the total infrastructure costs are calculated. These costs are split up into two components: 1) energy island construction costs, and 2) electricity cable costs.

First, both the cost components are discussed in *4.3.2.1 Energy Island Construction Costs* and *4.3.2.2 Electricity Cable Costs*. Then, it is outlined how a cost-optimal number of energy islands is determined in *4.3.2.3 Selection of Cost-Optimal Number of Energy Islands*.

4.3.2.1 Energy Island Construction Costs

The energy island construction costs are calculated per cluster configuration k. These costs are determined by the total amount of electricity that is transmitted to each energy island and the extent to which this electricity is used for hydrogen production.

The total construction cost for a given configuration k is the sum of all individual energy island construction costs:

$$C_{island} = \sum_{j=1}^{k} c_j$$

where c_j is the construction cost of energy island j, and k the number of energy islands in a configuration.

The construction cost c_j of energy island j depends on the required assets for both electricity transmission and hydrogen production on the island (Van Der Veer et al., 2020). The size of the electrical transmission system is determined by the total electrical capacity that is transmitted to an energy island: a higher capacity requires more space and system components. Similarly, the size of the hydrogen production system depends on the expected hydrogen output on the island, which is determined by the level of hydrogen conversion. For the economic picture, Van Der Veer et al. (2020) only focuses on the actual capital expenditures (CAPEX) for construction of the energy islands and the assets on that island. The CAPEX of electricity cables and hydrogen pipelines from and to the island are excluded. Therefore, these are calculated separately.

Categories are used to account for various infrastructure requirements, depending on the scale of electricity transmission and hydrogen production (Van Der Veer et al., 2020). This categorization is applied to realistically capture economies of scale: large islands require proportionally more infrastructure but also benefit from lower cost per capacity due to economies of scale. Accordingly, the construction costs of an energy island j are calculated as:

$$c_j = f_{island} \cdot P_{j,e}, \quad \forall\, j \in J$$

where f_{island} is the construction cost factor in €/MW, $P_{j,e}$ the total electrical capacity that is transmitted from all OWFs to energy island j in MW, and $j \in J$ representing each energy island j in the set of all island J.

The cost factor f_{island} is determined using a classification based on two variables: 1) the total electrical capacity that is transmitted to an energy island $P_{j,e}$, and 2) the average hydrogen conversion rate of $n \in \mathbb{N}$ OWFs connected to energy island j, denoted in X_{j,H_2}. These variables are dependent on the distance-based categories of each OWF, as discussed in *4.2 Offshore Wind Farm Distance Range*. Accordingly, distance to shore is used as a variable for conversion choice to reflect the economic benefit of hydrogen production for OWFs further offshore compared to direct transmission to shore. Using the average conversion rate ensures that a difference in system design is captured realistic by avoiding that either the energy is fully transmitted as electricity or fully as hydrogen.

The structure of categorization is visualized in Figure 8. First, each energy island is categorized as *Small*, *Middle* or *Grand*, depending on the total electrical capacity it receives. Then, within each capacity category, there are two subcategories based on the average hydrogen conversion rate: *Low* and *High*. This results in six category combinations. Each of these energy island categories subsequently corresponds to a

different cost factor f_{island}, in €/MW. Additionally, each energy island category also refers to a specific surface area A_j that is required for energy island j. This thereby reflects the various infrastructure requirements on energy islands. This is important because it influences technical and spatial feasibility of islands.

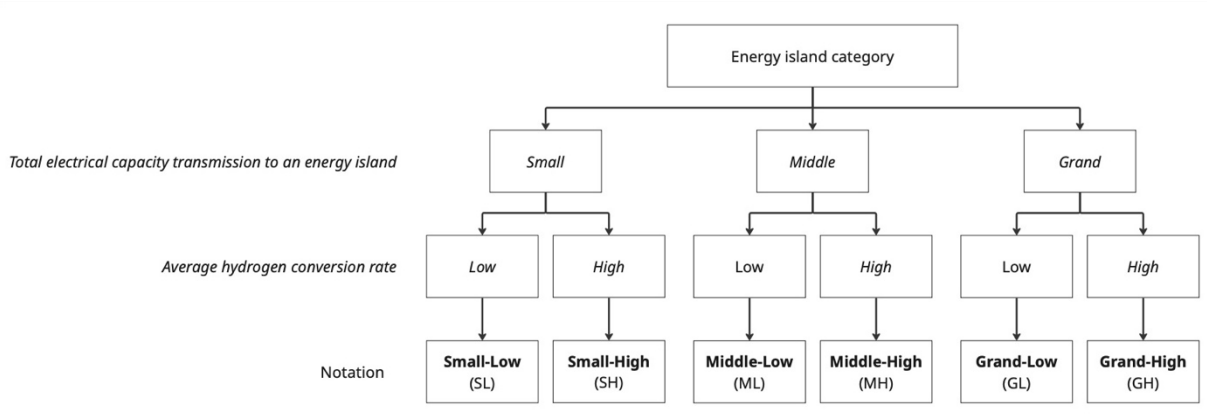

Figure 8. Classification of energy island infrastructure requirements, based on Van Der Veer et al. (2020).

To calculate $P_{j,e}$, the total electricity capacity transmitted to energy island j, the effective contribution of each OWF i in the cluster is summed:

$$P_{j,e} = \sum_{i=1}^{n} q_{i,e} \;\; with \;\; q_{i,e} = \; x_{i,e} \cdot p_{i,e}$$

Here, $p_{i,e}$ denotes the electrical capacity of OWF i, in MW, and $x_{i,e}$ is the share of electricity that is transmitted from OWF i to energy island j. The value of $x_{i,e}$ is based on the relative distance of OWF i to shore and is thus dependent on the distance-based category of OWF i, as introduced in *4.2 Offshore Wind Farm Distance Range*.

In addition to the amount of electricity transmitted, the level of hydrogen production on each energy island j is considered. Each OWF i has an associated hydrogen conversion rate x_{i,H_2}, which indicates the share of electricity that is converted into hydrogen. This rate is also determined based on the OWF's distance to shore. The total hydrogen production q_{i,H_2} from OWF i is given by:

$$q_{i,H_2} = p_{i,e} \cdot \; x_{i,H_2}$$

The total hydrogen production for an energy island j is then obtained by summing over all OWFs in that cluster calculated:

$$Q_{j,H_2} = \eta_{H_2} \cdot \sum_{i=1}^{n} q_{i,H_2}$$

Here, η_{H_2} is the production efficiency of the electrolyzer. Additionally, the average hydrogen conversion rate for energy island j is calculated as:

$$X_{j,H_2} = \frac{\sum_{i=1}^{n} \sum_{i=1}^{n} p_{i,e} \cdot \; x_{i,H_2}}{P_{j,e}}$$

This combined approach ensures that both the scale of electricity transmission and hydrogen production are quantitatively captured and ultimately used to define the total energy island construction costs C_{island} for each cluster configuration k.

4.3.2.2 Electricity Cable Costs

All OWFs are categorized as outlined in *4.2 Offshore Wind Farm Distance Range*. OWFs whose category implies that they are not connected to an energy island are placed outside the system boundary before clustering takes place. Excluding them at this stage ensures consistency with reality, as offshore hydrogen production is not attractive for these OWFs. By excluding these OWFs, it prevents that they could influence the clustering output in an unrealistic way.

The clustering process is therefore only applied to the full set of OWFs within the system boundary. However, during later modelling steps, certain OWFs are reassigned from an island connection to a direct shore connection, based on the distance criterion defined in *4.3.1.3 Post-Clustering*. These OWFs remain inside the system boundary, as they were included in the clustering but filtered as result of modelling results. For these OWFs, the alternative cost of a direct connection to shore must therefore still be accounted for.

This distinction ensures that all relevant OWFs are consistently represented in the system design. OWFs excluded before clustering therefore do not contribute to costs, while OWFs reassigned after clustering continue to contribute through their shore connection. Ultimately, for each cluster configuration k, two types of cable connections are considered:

1) *OWF-to-island* cable connections: cables between OWFs and energy islands,
2) *OWF-to-shore* cable connections: cables between OWFs and shore. These are excluded from a cluster k after clustering, as outlined in *4.3.1.3 Post-Clustering*.

For each OWF within the system boundary, exactly one connection type is considered. If an OWF is eligible for both shore and island connections based on its distance-based category, only the cable cost for the island connection is included. The cable cost for the shore connection is then outside the system boundary as it is not a modelling result.

The total electricity cable cost for a given configuration k is the sum of the costs for both connection types:

$$C_{electricity\ cables} = C_{cable,island} + C_{cable,shore}$$

Where $C_{electricity\ cables}$ denotes the total electricity costs, $C_{cable,island}$ represents the total costs for all OWF-to-island connections, and $C_{cable,shore}$ represents the costs of all OWF-to-shore connections in configuration k.

As outlined in *3.2.1 Electricity Cables*, multiple cable types are considered. The cost for each cable type is determined using a cable cost factor f_{cable}, which is expressed in €/km/MW. An appropriate cable type is selected based on the cable length and the electrical capacity that it must transmit. Cable length is derived from the clustering output, while the electrical capacity to the island is influenced by an OWF's distance-based category, as discussed in *4.2 Offshore Wind Farm Distance Range*.

Machado et al. (2015) studied the break-even point between HVDC and HVAC cables. This point is necessary to include because HVDC is more economically beneficial for longer cables and higher cable capacities, while HVAC is preferable for shorter cables. Based on their findings, the appropriate cable type is chosen through a selection logic. This logic is visualized in Figure 9.

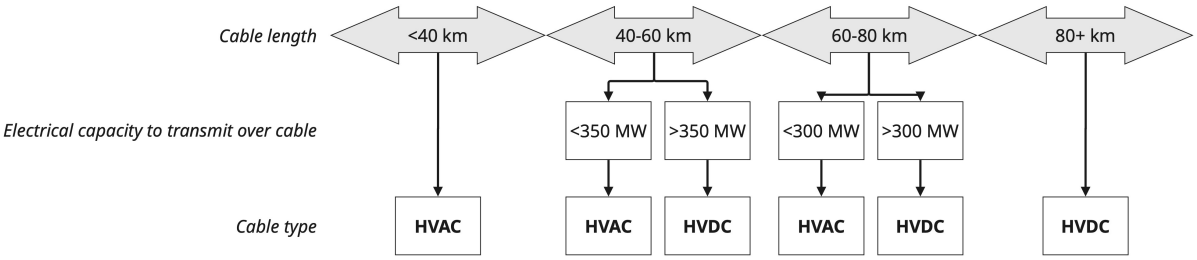

Figure 9. Selection logic for appropriate cable type, which are used to determine the cable cost factor. Based on Machado et al. (2015).

The electricity cable costs for OWF-to-island connections are calculated as:

$$C_{cable,island} = \sum_{s \in S} \left(f_{cable} \cdot d_s \cdot P_{s,e} \right)$$

where f_{cable} denotes the cable cost factor in €/km/MW, d_s is the length of cable s in km, $P_{s,e}$ the electrical capacity transmitted over cable s in MW, and S the set of OWF-to-island connections.

Similarly, the electricity cable costs for the OWF-to-shore connections are calculated as:

$$C_{cable,shore} = \sum_{r \in R} \left(f_{cable} \cdot d_r \cdot P_{r,e} \right)$$

where d_r is the length of cable r in km, $P_{r,e}$ the electrical capacity transmitted over cable r in MW, and R is the set of OWF-to-shore connections.

The cable lengths d_s and d_r are determined using the haversine distance (see *Appendix A2. Haversine Formula*), which provides an accurate estimate of the shortest distance over the Earth's surface between two geographic coordinates (Veness, n.d.). This ensures that cable costs are not underestimated by using simplified distance projections.

4.3.2.3 Cost-Optimal Number of Energy Islands

The objective is to find the number of energy islands k for which the total infrastructure costs are minimized. This is denoted as:

$$MIN(C_{total})$$

The total infrastructure costs C_{total} for each cluster configuration k can be calculated as:

$$C_{total} = C_{island} + C_{electricity\ cables}$$

As discussed in *4.3.1.3 Post-Clustering*, some OWFs are reassigned to shore post-clustering based on the distance criterion. This filtering step reduces the set of OWFs that are connected to energy islands. if the original clustering result is used directly, centroid locations and cluster compositions would be influenced by OWFs that are no longer directly connected to islands. The resulting costs do not reflect the costs of the actual modelling output. To avoid this inconsistency, a second clustering round is performed.

In the first round, clustering configurations are generated for $k \in [3,20]$. To keep the approach computationally tractable, the second clustering round is limited to the three configurations with lowest C_{total}. Re-clustering all configurations in $k \in [3,20]$ would increase model run time without a significant change in modelling results.

For each of the re-clustered configuration $u \in \{u_1, u_2, u_3\}$, the total costs C_{total} is recalculated using the same equations presented in *4.3.2.1 Energy Island Construction Costs* and *4.3.2.2 Electricity Cable Costs*. A redistribution of OWFs over clusters may shift cluster centroids and reassign OWFs to other clusters. This directly affects cable lengths and the total electrical capacity aggregated at an island. As a result, the energy island cost factor f_{island} may be change, which changes of overall system cost.

Finally, the configuration with the lowest total cost is selected as cost-optimal number of energy islands. Formally, this can be expressed as:

$$u^* = \underset{u \in \{u_1, u_2, u_3\}}{\arg min} \; C_{total}(u)$$

where u^*denotes the configuration with the lowest infrastructure costs among the three re-clustered options. The results reflect the technical constraints imposed by the filtering criterion and the economic objective of minimizing infrastructure, reflecting a realistic system design.

4.4 Network Optimization Modelling

Following the selection of a cost-optimal number of energy islands, this section presents the network optimization modelling approach that identifies optimal energy island energy islands and generates cost-efficient electricity and hydrogen network layouts.

The Optimal Network Layout Tool (ONLT), developed by Heijnen (2025), is used to determine a techno-economically efficient offshore network configuration for both electricity and hydrogen. The model builds upon GGT. Accordingly, *4.4.1 Geometric Graph Theory* provides a brief explanation of GGT, followed by an introduction of the ONLT in *4.4.2 Optimal Network Layout Tool*. Then, in *4.4.3 Energy Island Location*, it is described how GGT and the ONLT are applied to determine an optimal energy island location and electricity networks. Finally, it is outlined in *4.4.4 Offshore Hydrogen Backbone* how these are applied to define a cost-efficient offshore hydrogen network.

4.4.1 Geometric Graph Theory

The GGT is a mathematical method concerned with defining graphs (Carlson, 2024). A graph consists of two elements: *nodes* and *edges*. Nodes are shown in the form of circles or dots and can have multiple functions. Edges represent the connections between

nodes and are shown in the form of lines (Fornito et al., 2016). A graph is denoted by $G = (N, E)$, while an edge between two nodes u and v is denoted by $e = (u, v)$ (Rahman, 2017). The *degree* of a node u in a graph G is the number of edges that are connected to that node, denoted by $\deg(u)$ (Rahman, 2017). An example of a simple graph G is shown in Figure 10. In this example the degree of each node is $\deg(u) = 2$.

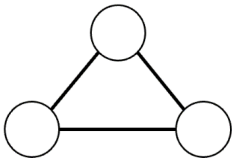

Figure 10. Illustration of a simple graph with three nodes and three edges.

There are various types of nodes, which are described in Table 1.

Node type	Description
Source	*Source* nodes represent the location of an energy production location. This is either an OWF, representing the position of electricity production, or an energy island, representing the position of hydrogen production. There is always at least one edge that leaves this node.
Sink	*Sink* nodes represent the location where there is energy demand. This is either an energy island, representing the position of electricity demand, or an onshore entry point, representing the position of hydrogen demand. There is always at least one edge that is going into this node.
Connection	Connection nodes represent the connections between cables or between pipelines in the networks.

Table 1. Description of source, sink and connection node types.

In Figure 11, a *directed graph* and an *undirected graph* are illustrated. When energy over edges flows both ways, a graph G is *undirected*, and a connection between nodes is indicated with a line. When the flow goes only one specific way, a graph G is *directed*, and a connection is indicated with an arrow pointing in the flow direction (Heijnen, n.d.-a).

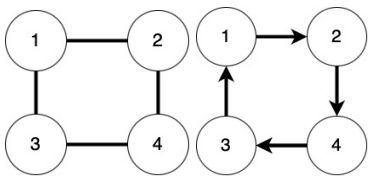

Figure 11. Illustration of an undirected graph (left) and a directed graph (right).

In Figure 12, the difference between a *connected graph* and a *disconnected graph* is presented. A graph G is connected when there is a path from each node to each other node in G. If a path is not present in graph G, it is disconnected (Rahman, 2017).

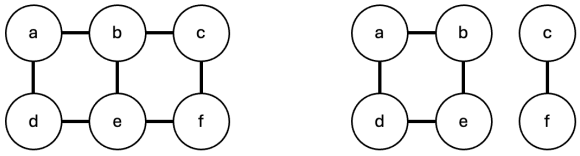

Figure 12. Illustration of a connected graph (left) and a disconnected graph (right).

In Figure 13, a graph G is presented with *tree topology*. A tree is a connected graph that has no cycles and has exactly one path going from each node to each other node (Heijnen, n.d.-a). A cycle is a closed path (Rahman, 2017).

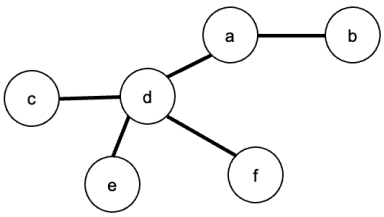

Figure 13. Illustration of a graph with tree topology.

A complete graph, see Figure 14, is a graph G where all nodes have a connection with each other node in the graph and, in comparison to the tree topology, there are cycles present in the graph (Rahman, 2017).

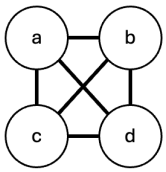

Figure 14. Illustration of a complete graph.

Ultimately, graph G can be a *weighted graph*. It entails that the edges have certain weights assigned to them (Rahman, 2017). This weight can represent many things, but usually it represents either the length, costs or flow capacity of an edge.

A graph structure enables modelling of energy systems and including directionality and weighted edges. The electricity and hydrogen flows will only go one way; electricity flows from an OWF to an energy island, and hydrogen flows from an energy island to shore. The graphs in the research are thus directed. A simplified representation of a network with *source* nodes, *sink* nodes, and connection nodes is shown in Figure 15.

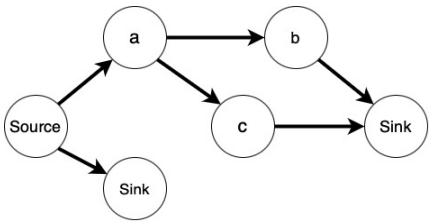

Figure 15. Illustration of a directed graph with sources and sinks.

GGT is used in this research because it provides a structured way to model offshore energy systems by presenting nodes for OWFs, islands and shore, and by presenting edges for cables and pipelines. It thereby represents a directionality of the energy flows from OWFs to islands and from islands to shore. At the same time, weighted edges allow the inclusion of connection costs and capacities. GGT is therefore suited for connecting spatial layouts to techno-economic optimization.

4.4.2 Optimal Network Layout Tool

Building on the mathematical foundation of the GGT, the ONLT includes optimization algorithms to generate techno-economic efficient network designs. The ONLT is a model

from Heijnen (2025) in Python to construct a network layout with minimal total network costs. The ONLT follows a few steps. For this research, only Steps 0 to 3 are implemented to Before the algorithms are implemented to limit computational time, to avoid incomplete cost calculations and to prevent complexity in result interpretation. The modellingcase is prepared by reading the input data in *Step 0* and supply and demand data are analyzed in *Step 1*. After these preparation steps, first a minimum spanning tree is constructed in *Step 2*. Then, in *Step 3*, a minimum-cost-spanning tree is constructed. Existing connections and obstacles can be included, and costs are minimized using a cost function. These aspects are discussed after the discussion of the three modelling steps.

Step 0: Preparation

The ONLT reads data from an Excel file containing multiple worksheets. Firstly, there is an obligatory worksheet called 'terminals.' A terminal is a node that must be included within the network and is known beforehand. In this thesis, it refers to the nodes representing OWFs (electricity source-node), energy islands (electricity sink-node and hydrogen source-node) and hydrogen shore entry points (hydrogen sink-nodes). This worksheet includes the geographic coordinates of each terminal node. Additionally, the demand and supply of each terminal is indicated for a given timestep. Source-nodes have a positive demand as they supply a certain flow to the network, whereas sink-nodes consume from the network, having a negative demand. The second worksheet represents the obstacles. Obstacles are defined in the form of a polygon and indicate the restricted areas for new connections. Thirdly, it includes a worksheet for existing connections in which the existing infrastructures to consider in the network design are defined. The start and end point of an existing connection, with the capacity that can flow through it, are defined.

Step 1: Supply and demand analysis

The ONLT constructs a network in which supply meets demand. To do so, the tool analyses the supply and demand per terminal and per timestep. The outcomes of both analyses are shown using a bar chart. The supply and demand profiles per terminal over all time steps are then analyzed and shown in a plot. In this thesis, there is only one timestep: 2050, thus only the distribution of supply and demand per terminal is relevant.

Step 2: Determine minimum spanning tree

After all relevant input data is prepared, read and analyzed, the minimum spanning tree is determined. A minimum spanning tree is a network with tree topology with the sum of the weight or length of all edges being minimized. Kruskal's algorithm is applied to determine the minimum spanning tree. An example of the ONLT output for a minimum spanning tree is shown in Figure 16 in the left plot.

Step 3: Determine minimum-cost-spanning tree

In Step 2, the costs of the edges are excluded from optimization. Therefore, the total costs of adding new edges, reusing existing edges or expanding the capacity of existing edges is calculated and minimized. This is achieved by iteratively evaluating replacements for ach edge of the minimum spanning tree with other edges to find a tree with the lowest costs possible. As a result, the minimum-cost-spanning tree is found which has minimal cost, which is calculated via the cost function as explained in the next section. The right plot in Figure 16 illustrates the ONLT output for a minimum-cost-spanning tree.

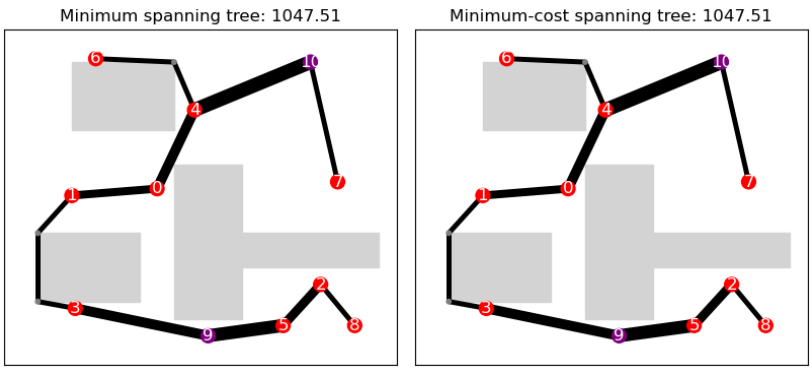

Figure 16. Illustration of the ONLT (Heijnen, 2025) output for a minimum spanning tree and minimum-cost spanning tree, considering obstacles as grey polygons and presenting the network costs in the plot title.

Cost function

The ONLT determines the quality of each possible network topology based on calculating the costs using the following equation (Heijnen, 2025):

$$C(G) = \sum_{e \in E_n(G)} l_e q_e^{\beta} + spc \cdot s(G) + \sum_{e \in E_0(G)} l_e (upc \cdot \min(q_e, rq_e))^{\beta} + cpc \cdot \max(0, q_e - rq_e)^{\beta})$$

The equation consists of multiple parts. The first part calculates the costs of adding new edges based on: $E_n(G)$ indicates the set of all new edges in network G; l_e is the total length of an edge e; q_e indicates the capacity of an edge e; β is the capacity-cost exponent, indicating the scaling of the costs if the capacity of an edge e is increased. The second part calculates the costs for splitting points as spc indicates the additional costs of splitting points $s(G)$. Lastly, the costs of reusing existing infrastructures are calculated using the following: $E_0(G)$ indicates the set of all existing connections; rq_e is the current capacity of an (existing) edge e; upc is the relative cost of reusing an edge e in comparison to constructing a new edge e; cpc is the relative cost of extending the capacity of the current capacity of an existing edge e. The outcomes of this cost function are expressed in monetary units. Using this formulation, different network topologies can be directly compared in terms of their relative cost implications.

The capacity-cost exponent β determines the rate at which the cost of an edge increases when its capacity is scaled up. In the simplest for, the cost-capacity relationship is expressed as:

$$costs = \alpha \cdot capacity^{\beta}$$

where α is a proportionality factor. β is a value between 0 and 1. A higher β indicates that the costs increase more strongly with capacity, whereas a lower β indicates a weaker sensitivity of costs to an increase in capacity.

Existing connections

The use of existing infrastructure in network construction can lower the total costs. The same steps are followed to find an optimal topology as the cost function includes reusing them in the optimization. The capacity of an existing connection can be partially reused; the entire edge must then however be reused. In a minimum spanning tree and minimum-cost-spanning tree, an existing edge, as indicated in the input file, cannot be split. The

capacity of a connection, however, can for all trees partially be reused. For example, if the existing connection has a capacity of 5 units, it is possible that only 3 units are reused. Moreover, the ONLT also allows reinforcement of a connection when this is required. For the example, it entails that if a capacity of 8 units is required, the connection can be reinforced with 3 units. The influence of including existing connection is illustrated in Figure 17. A minimum spanning tree is shown on the left and a minimum-cost-spanning tree on the right. Comparing Figures 16 and 17, it shows the influence of existing connections on the network design. The existing connections are indicated with light blue lines, and reuse of such connection also indicated with a dark blue line.

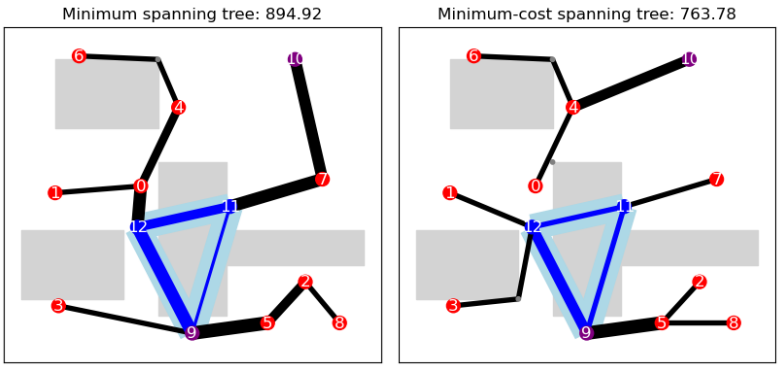

Figure 17. Illustration of the ONLT (Heijnen, 2025) output for a minimum spanning tree and a minimum-cost spanning tree considering existing connections, indicated by blue lines.

4.4.3 Energy Island Location

Based on the results of the clustering and economic assessment described in *4.3 Number of Energy Islands*, an optimal number of clusters k is determined. The assignment of OWFs to each cluster is thereby known, providing the basis for designing electricity networks for each cluster that connect OWFs to a shared energy island. The initial location of each energy island is defined as the centroid of the cluster, calculated as the weighted average location of the OWF coordinates in a cluster. However, this centroid does not account for spatial constraints. Therefore, a method is introduced to identify spatially feasible locations for energy islands.

It includes an analysis of the cluster areas to identify candidate locations for energy islands, as described in *4.4.3.1 Candidate Energy Island Locations*. For each of the candidate locations, the ONLT is used to compute the corresponding electricity networks for each cluster, which is outlined in *4.4.3.2 Electricity Networks*. Finally, the most cost-efficient location is determined after several iteration rounds, which is discussed in *4.4.3.3 Energy Island Location Selection*.

4.4.3.1 Candidate Energy Island Locations

To determine feasible candidate island locations, the cluster area must be analysed. To do so, first, a raster grid is applied. Then, geospatial constraints are discussed, and a node classification is provided. Finally, the candidate locations are identified in a four-step approach. Figure 18 shows an example which is used to illustrate these steps. For this example, data are randomized.

Raster grid

A raster grid is used to divide the continuous search space into manageable units, ensuring that potential island locations can be systematically compared across a cluster. Each grid cell corresponds to the required surface area of the energy island A_j for that cluster. This required area, expressed in m^2, is based on the classification of infrastructure needs described in *4.3.2.1 Energy Island Construction Costs*. As a result, the cell size is cluster specific. The raster is aligned such that the initial island location lies at the center of one the grid cells. See the example shown in Figure 18 (left plot).

Geospatial constraints

The raster grid is overlaid with geospatial data to ensure that spatial restrictions are respected when defining candidate locations to avoid unrealistic results. Therefore, each raster cell is evaluated against the following constraint: if a cell overlaps, even partially, with a forbidden area, the cell is marked as infeasible and coloured red. The cell containing the cluster centroid, is highlighted in blue. OWF locations are indicated with black nodes at its specific position. All remaining white and empty cells ultimately represent candidate locations. See the example shown in Figure 18 (middle plot).

Node classification

Once the grid is finalized, a spatial node is placed at the centre of each cell to enable a graph-based analysis. Each node is classified based on its contents:

1) An *Island* node is placed if the cell contains the initial island location,
2) An *OWF* node is placed if the cell contains an OWF,
3) An *Empty* node is placed in all remaining unconstrained cells. These are the candidate locations for energy islands.

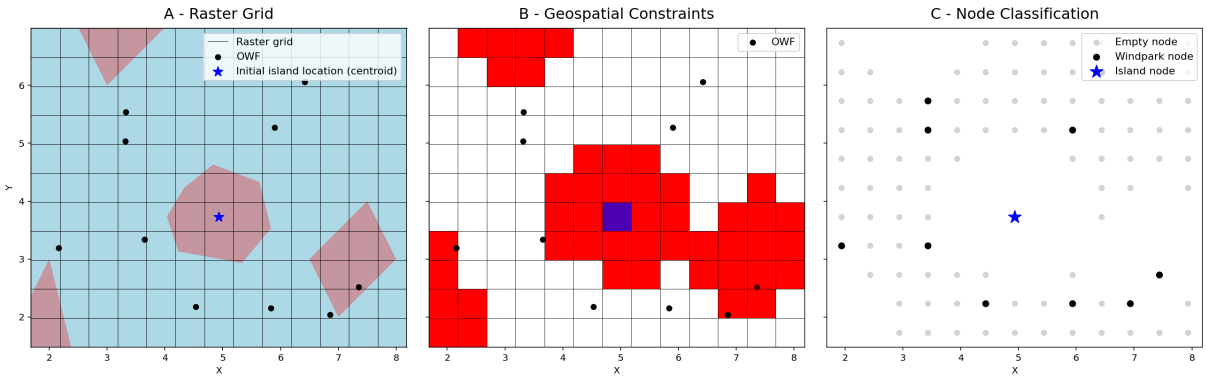

Figure 18. The output of an example cluster for the raster grid, geospatial constraints and node classification steps.

While *OWF* nodes represent fixed infrastructure, the *Empty* nodes are considered as potential new island locations. Nevertheless, the *Island* node could also be a potential location, if it is not located in a forbidden area. This structure forms the basis for the spatial optimization described in *4.4.3.2 Electricity Networks*. The node classification for the cluster example is presented in Figure 18 (right).

Candidate location selection

To reduce the computational complexity only nine candidate island locations are selected for further analysis. Limiting the candidate set to nine ensures computational

tractability in the next step. Simultaneously, it captures the most realistic alternatives for cost-efficient network designs. The selection is based on the proximity to the *Island* node, and follows a four-step process, which are visualised in Figure 19:

1. A circular buffer with a radius r equal to 1000 m is drawn around the *Island* node. All *Empty* nodes that fall within this radius are selected, along with the *Island* node itself. If fewer than 20 nodes are found, the radius r is incrementally increased by 1000 m. Hence, it follows $r := r + 1000$, until a set of 20 nodes is found. These nodes are then put in a list. All distances are Euclidean.
2. The Euclidean distance from each node to the *Island* node is calculated. The list is then sorted in ascending order of distance. Additionally, it is checked whether the *Island* node is in a forbidden area. If so, the *Island* node does not represent a feasible potential island location and is thus removed from the candidate list.
3. A filtering step is applied to ensure model validity. Duplicate nodes that have a (near-)identical position are deleted.
4. From the final list, the nine nodes with the shortest distance to the *Island* node are considered as candidate energy island location.

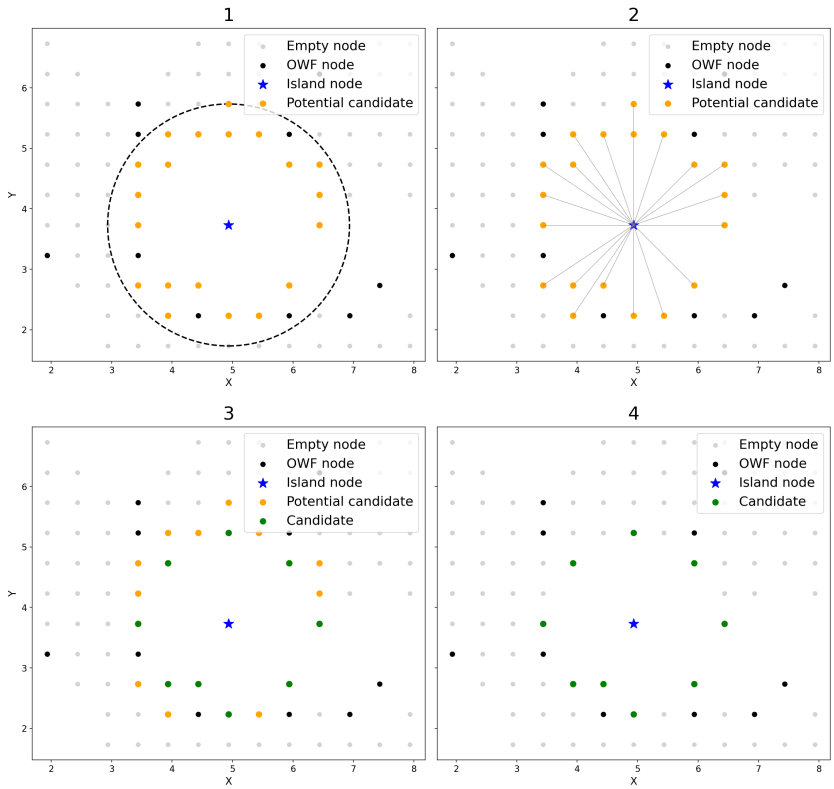

Figure 19. Illustration of the selection process for identifying 9 candidate location. In the example, the initial island location is located within a forbidden area, radius is 4 grid cell sizes.

A second example is included in Figure 20, where the initial island location is not within a forbidden area: a radius r with the size of 3 grid cells was needed to identify 20 potential candidates. Consequently, the initial island location is included in the final 9 candidate locations. Moreover, the other candidate locations are closer to this initial location.

Ultimately, the nine candidate nodes are analysed further using the ONLT to determine which location results in the most cost-efficient electricity network for that cluster.

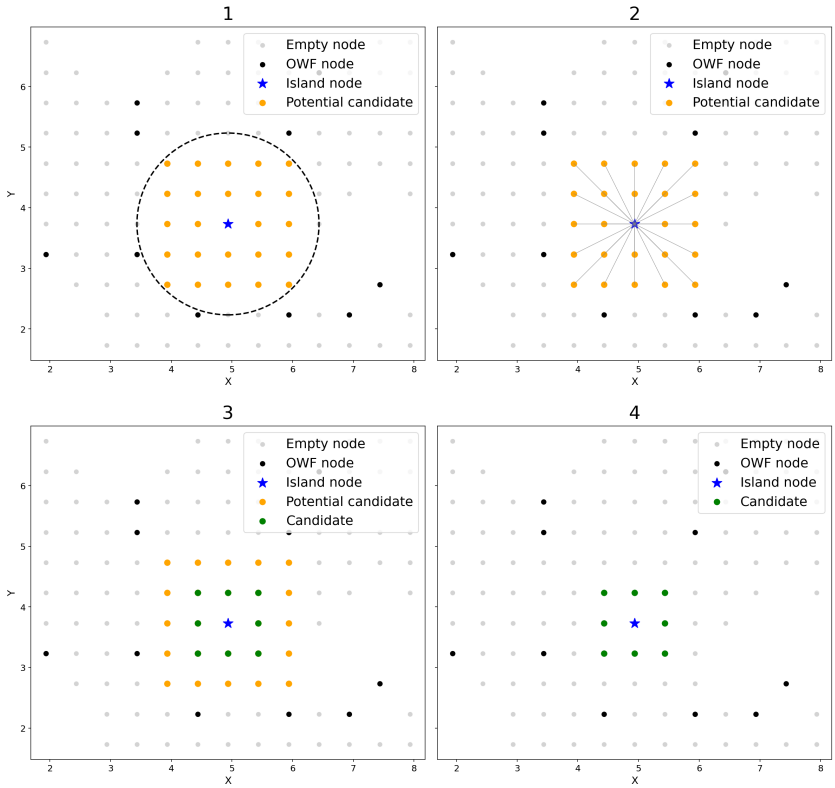

Figure 20. Illustration of the selection process for identifying 9 candidate location. The initial island location is not located within a forbidden area, radius is 3 grid cell sizes.

4.4.3.2 Electricity Networks

For each of the nine candidate locations identified in *4.4.3.1 Candidate Energy Island Locations,* an electricity network is generated using the ONLT because it ensures that each candidate location is assessed with a cost-minimal network design. An introduction to this tool is provided in *4.4.2. Optimal Network Layout Tool*. The objective here is to evaluate the network implications of each candidate island location. Finally, the total costs associated with these locations are calculated.

The network is constructed such that the electricity generated by an OWF is transmitted to the energy island within that cluster. The OWFs supply electrical capacity, which is consumed by the energy island. The electrical capacity from an OWF to energy island j, denoted as $P_{j,e}$ and expressed in MW, is calculated using the same equation defined in *4.3.2.1 Energy Island Construction Costs*. In the ONLT, demand is represented as negative figure, whereas the supply is positive. Accordingly, the electricity demand for energy island j is calculated as:

$$Q_j = -P_{j,e}$$

where Q_j is the electricity demand of energy island j.

Forbidden areas within the cluster area are included in the input for the ONLT to guarantee the feasibility of the resulting network layouts. Existing electricity cables, however, are excluded because they only exist for direct connections between OWFs and countries. Including them would have an unrealistic influence on results.

The cost function, as outlined in *4.3 Optimal Network Layout Tool,* is used to calculate the total electricity network costs for a given cluster n. These costs are denoted by $C_{e,network_n}(z)$ and expressed in monetary units. Since the standard functionality of the ONLT is sufficient for this application, no model modifications are required. It must be noted, however, that to obtain the actual costs, the outcomes should be multiplied by an appropriate scaling factor based on real-world cost data.

Finally, for each candidate island location, the output of the minimum-cost-spanning tree is used to define its corresponding cluster electricity network. In this context, no additional step is applied because the minimum-cost-spanning tree already provides a realistic and cost-minimal approximation for the network design. Considering the results of additional steps would increase computational complexity. The costs associated with the networks are compared across all candidate locations to identify the most cost-efficient network. Ultimately, an optimal location for each cluster can be determined.

4.4.3.3 Energy Island Location Selection

Once the minimum-cost-spanning tree is generated for each of the nine candidate island locations within every cluster, the location that facilitates the lowest total electricity network cost is selected as the optimal location. Formally, the optimal energy island location z_n^* for each cluster n is selected by minimizing the total electricity network cost across the set of candidate locations $z \in \{z_1, \dots, z_9\}$. This is defined as:

$$z_n^* = \underset{z \in \{z_1, \dots, z_9\}}{\arg min}\ C_{e,network_n}(z)$$

where $C_{e,network_n}(z)$ the total electricity network costs for island location z in cluster n.

An iterative improvement process is applied because the first set of centroid candidates may overlook possible cost-efficient candidate locations that are outside the first search radius as defined in *4.4.3.1 Candidate Energy Island Locations*. Repeating the process reduces the dependency on the starting point and increases the likelihood of approaching a true optimal solution. The selected optimal location z_n^* replaces the initial cluster centroid as the new *Island* node in this process.

To balance accuracy with computational tractability, the steps are repeated three times. The island location with the lowest value for $C_{e,network_n}$ after the third iteration round is considered the final optimal location for the energy island in cluster n. The influence of the iteration rounds is thereby reflected in the results. The total network cost across all clusters $C_{e,total}$ is calculated as:

$$C_{e,total} = \sum_{n=1}^{N} C_{e,network_n}(z)$$

The cost function of the ONLT generates costs in relative measures, rather than in absolute values as $C_{e,total}$ is in monetary units. To ensure comparability with other cost components, the results of the ONLT should be converted into euros. The cost c_i of each individual edge i is then calculated as:

$$c_i = f_{cable} \cdot d_i \cdot {q_i}^{\beta}$$

Here, f_{cable} is the cable cost factor (*4.3.2.2 Electricity Cable Costs*), expressed in €/km/MW, d_i is the length of edge i in km, q_i the capacity that flows over edge i in MW, and β the capacity-cost exponent. f_{cable} and β are dependent on the cable technology.

Since the model input is in latitude/longitude coordinates, the length of an edge is not given directly in km, but in degrees. Therefore, d_i is calculated using the haversine formula (Heckman, 2024), which is detailed in *Appendix A2. Haversine Formula*.

Ultimately, the total network cable costs are then obtained by summing over all edges:

$$C_{E,total} = \sum_{i \in E} c_i$$

$C_{E,total}$ is now expressed in euros and can be compared with the results for OWF-to-island cable costs as outlined in 4.*3.2.2 Electricity Cable Costs*.

4.4.4 Offshore Hydrogen Backbone

The offshore hydrogen backbone connects the optimally located energy islands, as described in *4.4.3 Energy Island Location*, to designated onshore entry points, creating a spatially feasible and cost-efficient offshore pipeline network. The network design is optimized using the ONLT. Existing natural gas pipelines are used where possible and spatially infeasible segments are routed around forbidden areas. The design process proceeds in four stages.

It is discussed in 4.*4.4.1 Hydrogen Network Optimization* how the ONLT is applied to compute an initial offshore hydrogen backbone. Then, the edges in this initial backbone are classified, and spatially infeasible edges are identified, which is outlined in *4.4.4.2 Edge Classification*. In, *4.4.4.3 Spatial Rerouting Procedure*, an approach to analyze spatially infeasible edges is provided. This is de basis for a local redesign of segments that should be rerouted. Finally, the rerouted segments following from the local redesign are merged into the final network as described in *4.4.4.4 Hydrogen Backbone Integration*.

4.4.4.1 Hydrogen Network Optimization

To ensure the ONLT is compatible for the offshore hydrogen network, the hydrogen supply and demand, the network setup and required modifications for the cost function are discussed in this section.

Hydrogen supply

In the offshore hydrogen network, each energy island acts as a supply node. Hydrogen is produced on the island and transported to the onshore network via designated entry points. The production capacity of an energy island j, denoted as Q_{j,H_2} and expressed in MW, is calculated as defined in *4.3.2.1 Energy Island Construction Costs*. The total hydrogen production of all energy islands is therefore calculated as:

$$Q_{total,H_2} = \sum_{j \in J(G)} Q_{j,H_2}$$

Here, $J(G)$ is the set of all energy islands in network G.

Hydrogen demand

North Sea countries have not yet specified offshore hydrogen demand targets for 2050. To make the ONLT operational, demand must be allocated to specific locations. Existing entry points, where offshore natural gas pipelines connect to the onshore gas grid, are used as demand nodes. Accordingly, it stimulates reuse of natural gas pipeline to reduce the investments required for new infrastructure. The demand at each entry point Q_{h,H_2} is allocated proportionally to its share of the total offshore-onshore pipeline capacity:

$$Q_{h,H_2} = Q_{total,H_2} \cdot \frac{x_{cap,h}}{X_{cap,total}}$$

Where $x_{cap,h}$ is the current total capacity of natural gas pipelines at entry point h; $X_{cap,total}$ is the sum of capacities across all entry points H.

This proportional allocation is a simplification, but it ensures that the modeled hydrogen flows are consistent with existing infrastructure capacities rather than based on random demand distribution over entry points.

Cost function

The default cost function, see *4.4.2 Optimal Network Layout Tool*, expresses relative rather than absolute costs. The hydrogen backbone is a single configuration rather than multiple competing designs, so an absolute model is appropriate. For this purpose, the ONLT cost function is replaced by the pipeline cost model of Brown et al. (2022).

Brown et al. (2022) split pipeline costs into four components: material, labor, right-of-way (ROW) and miscellaneous (includes surveying, engineering, direct labor supervision and interest during construction). For a new pipeline, the costs c_{new} are calculated as:

$$c_{new} = c_{material} + c_{labor} + c_{ROW} + c_{miscellaneous}$$

Each component depends on pipeline diameter D and length L, with a cost factor a_c. Consequently, the cost c_c for a pipeline are calculated per component as:

$$c_c = a_c \cdot D \cdot L$$

Brown et al. (2022) conducted its study in the US, thus pipeline cost c_c is expressed in $, diameter D in inches, length L in miles, and cost factor a_c in $/inch·mile.

The cost factor a_c is region-specific. It is therefore required to determine what a_c implies for the North Sea region. There is, however, no North Sea data set, and deriving appropriate values is out of this thesis' scope. Consequently, the average values for a_c derived by Brown et al. (2022) are used, see Table 2.

Cost component	Cost-factor a_c in $/inch·mile
Material	24,198
Labor	55,313
ROW	7,119
Miscellaneous	26,396

Table 2. Cost factors for specific cost component in US regions in $/inch·mile, according to Brown et al. (2022).

To reuse an existing natural gas pipeline, physical modifications to the pipelines are required. The repurposing costs $c_{repurpose}$ of pipelines are different from the costs of new pipelines. To account for this difference, a repurposing factor upc is included, which is the same as in the default cost function. $c_{repurpose}$ is calculated as:

$$c_{repurpose} = upc \cdot c_{new}$$

If any part of a pipeline is reused, the entire pipeline is repurposed because it cannot be partially repurposed. These costs are thus calculated for a pipeline's full capacity, although its full capacity is not used.

Additionally, the ONLT assumes that existing infrastructures can be reinforced if a greater capacity is required, which adds costs. A reinforcing factor cpc is included which is the same as in the default cost function. As extra pipeline area is required, the scale of the reinforcement depend on the difference in initial and final diameters of the reused pipeline. Ultimately, $c_{reinforce}$ is calculated as:

$$c_{reinforce} = cpc \cdot c_{new} \cdot \frac{D_{final} - D_{initial}}{D_{initial}}$$

Brown et al. (2022) considers onshore pipelines, thus an offshore cost factor α is included to account for potential cost differences.

In conclusion, the total cost of a network G is calculated as:

$$C(G) = \alpha \cdot \sum_{p \in P_n(G)} (c_{new}) + \sum_{p \in P_0(G)} (c_{repurpose} + c_{reinforce})$$

Where $P_n(G)$ indicates the set of new pipelines and $P_0(G)$ indicates the set of existing pipelines in network G.

The absolute cost function is applied during ONLT optimization to ensure that resulting layouts are directly cost-optimal in monetary terms. Since Brown et al. (2022) report costs for US regions, however, the total network costs $C(G)$ are expressed in US dollars. The other system costs in this research are in euros. To maintain consistency throughout the research, an exchange rate $X_{exchange}$ is applied to calculate network costs in euros:

$$C(G) = C(G) \cdot X_{exchange}$$

The data of all parameter values for repurposing, reinforcement, the offshore multiplier and exchange rate are detailed in *5.7.2 Hydrogen Network*.

4.4.4.2 Edge Classification

The initial hydrogen backbone is determined by the output of the resulting minimum-cost-spanning tree. In this context, no additional step is applied to avoid incomplete cost calculations and complexity in result interpretation.

Since forbidden areas are not included in the ONLT yet to reduce computational complexity, the spatial feasibility of the resulting network must be checked afterward. To

do so, each edge is categorized according to its role within the network. This classification is essential because they differ in technical feasibility. There are four categories distinguished based on its initial and final diameter and edge costs as shown in Table 3.

Edge type	$D_{initial}$	D_{final}	c_e
New	$= 0$	$\neq 0$	> 0
Repurposed	$\neq 0$	$\leq D_{initial}$	> 0
Reinforced	$\neq 0$	$> D_{initial}$	> 0
Not used, existing	$\neq 0$	$= 0$	$= 0$

Table 3. Edge classification for pipelines in the initial hydrogen backbone.

New, repurposed and reinforced edges form the initial offshore hydrogen backbone. Each edge is checked for two feasibility criteria: 1) location within the North Sea boundary, and 2) no intersection with forbidden areas. Edges that fail either one of these two criteria are spatially infeasible hence selected for rerouting.

4.4.4.3 Spatial Rerouting Procedure

Each infeasible edge is rerouted using the ONLT to design an alternative route that avoids obstacles. In contrast to the initial optimization (*4.4.4.1 Hydrogen Network Optimization*), forbidden areas are included to generate feasible paths. The rerouting process is constrained to a segment's local area to reduce computational time. The minimum-cost-spanning tree is used to avoid incomplete cost calculations and complexity in result interpretation. The rerouting procedure consists of five steps. A detailed description is provided in *Appendix A3. Hydrogen Backbone Rerouting Procedure*.

Step 1: Supply and demand nodes

The two end nodes of the infeasible edge are assigned as supply and demand. Fixed roles are applied where possible to preserve their physical meaning: energy islands are supply nodes; entry points are demand nodes. If neither of the nodes have fixed roles, they are assigned randomly. End nodes that are located inside forbidden areas are moved to the nearest feasible node using a shortest-path logic, ensuring that rerouted edges extend realistically from the initial backbone.

Additionally, there is a special case. If both end nodes are onshore entry points, and one these nodes has a degree equal to 1, that entry point is removed. The hydrogen demand of that point is added to the total demand of the resulting entry point. If an entry point is connected only to one other entry point, this connection could also be part of the onshore network instead.

Step 2: Rerouting area

The area between the supply and demand nodes is expanded with a buffer zone. This zone provides the ONLT a sufficient flexibility to find alternative paths that avoid obstacles.

Step 3: Supply and demand capacity

Capacities for the end nodes are based on the original edge. For segments with multiple edges, the maximum capacity is taken to avoid underestimation of flow requirements.

Step 4: Obstacles
All forbidden areas within the rerouting area are identified and treated as closed polygons, preventing the ONLT from generating paths that

Step 5: Existing connections
Available infrastructure in the rerouting area is identified using the edge classification. Not used and partially repurposed pipelines are included. For the partially repurposed pipelines their remaining capacity is considered. This enables a realistic reuse of infrastructure.

4.4.4.4 Hydrogen Backbone Integration

After rerouting, the original infeasible segments are removed from the backbone and replaced by the newly generated feasible alternatives. This replacement ensures that the final network contains only spatially valid connections. A new output list is then compiled with updated edge capacities, diameters and cost, which allow the recalculation of the total network costs for the final backbone.

The purpose of this step is to integrated local rerouting results into a consistent system-wide backbone. In doing so, the final configuration achieves three objectives: 1) it provides a cost-efficient and spatially feasible offshore hydrogen backbone that connects all energy islands and entry points, 2) it maximizes reuse of existing natural gas infrastructures where possible, and 3) it accounts for competing uses of the North Sea by ensuring that pipelines avoid ecological and military areas.

5 Data Preparation

This chapter presents the data used to design an integrated offshore energy system. It outlines how the data is sourced and prepared for modelling. First, in *5.1 North Sea*, the spatial boundaries of the system are described. The OWF dataset is then filtered and prepared for modelling, as discussed in *5.2 Offshore Wind Farms*. How the energy island construction cost factor and required surface area are determined is then explained in *5.3 Energy Islands*. In *5.4 Existing Gas Pipelines*, it is presented how the existing gas infrastructure dataset is prepared to be used in the ONLT. The required data for the entry points of the hydrogen backbone are then defined in *5.5 Onshore Entry Points*. The restricted areas for energy infrastructures are then identified in *5.6 Forbidden Areas*. Finally, the data for the cost functions in the ONLT are discussed in *5.7 Techno-Economic Data*.

5.1 North Sea

This thesis focuses on the North Sea. The spatial boundaries of the study area are defined by the dataset from Flanders Marine Institute (2021), shown in Figure 21. These boundaries are used consistently throughout the research to set the system boundaries.

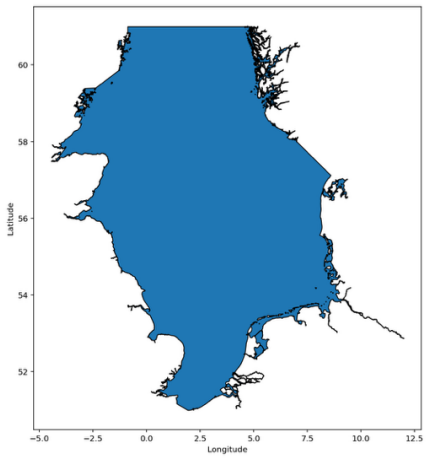

Figure 21. North Sea (Flanders Marine Institute, 2021).

5.2 Offshore Wind Farms

OWFs are the primary energy input points in the offshore system design, as they are the only offshore infrastructure asset that are predefined. Their distance to shore, location installed electrical capacity and distance to shore directly influence the modelling steps. Location and capacity data for all decommissioned, operational and planned OWFs in the North Sea are obtained from 4C Offshore (2025) and EMODnet (2025). In addition to existing and planned sites, the dataset also includes search areas. These are areas designated for future offshore wind development. The indicative location and capacity data are provided by the same sources.

This thesis focuses on a system design for 2050. Therefore, decommissioned OWFs are excluded from the initial dataset. Each OWF covers a surface area of multiple km^2. For modelling purposes, the coordinates of a specific position are selected to represent an OWF. When the dataset provides a single location, these coordinates are used directly. If

an OWF is represented as a polygon, the center of the OWF is calculated and used as reference point. Figure 22 shows all operational and planned OWFs included in the initial dataset using green nodes.

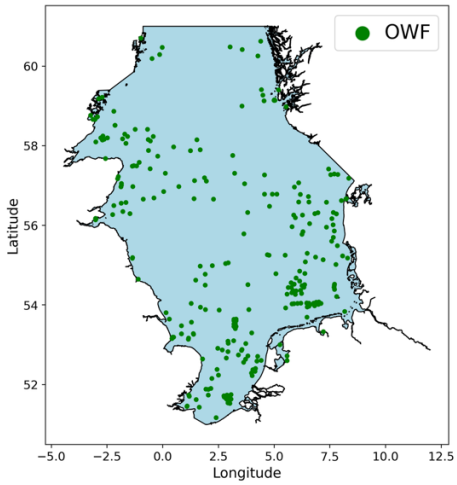

Figure 22. Operational and planned OWFs in the North Sea (4C Offshore, 2025; EMODnet, 2025).

The function of OWFs in the system is to supply electricity to energy islands, where it is used for offshore hydrogen production. As outlined in *4.2 Offshore Wind Farm Distance Range*, OWFs are classified into four distance-based categories. Each category determines:

1) The share of electricity transmitted from the OWF to an energy island.
2) The share of that electricity that is used for hydrogen production at the island.

For OWFs located within 20 km from shore, NSWPH (2024b) finds that a direct connection to shore is technically and economically favorable. These OWFs are therefore assumed to not connect to energy islands.

For OWFs more than 100 km from shore, Sall (2023) shows that hydrogen transport via pipelines is more cost-effective than long-distance electricity transmission. These OWFs are therefore assumed to connect to an energy island, with all generated electricity used for hydrogen production at an energy island.

No explicit requirements or percentage values are provided in literature for the two intermediate distance ranges (20-60 km and 60-100 km). the values for these categories are therefore estimated in a way that it represents plausible system configurations. Moreover, these estimations are used to illustrate the potential multifunctionality of energy islands.

For OWFs located 20 to 60 km from shore, 50% of their capacity is assumed to connect directly to shore, and 50% to an energy island. All capacity reaching the island is converted for hydrogen. This way, the system features of a meshed energy system are represented, as it connects OWFs to various assets in the system.

Then, for OWFs located 60 to 100 km from shore, 100% of their capacity is assumed to connect to an energy island, but only 50% of that electricity is used for hydrogen production. The remaining 50% is aggregated and transmitted as electricity or potentially

used for other purposes. This way, other possible design features of energy islands are considered in the system design.

In conclusion, energy islands serve both as hydrogen production hubs as electricity aggregation locations. The values for each category are presented in Table 4.

Distance of OWF from shore	*Electrical capacity transmitted to island*	*Electrical capacity used for hydrogen production*
< 20 km	0%	0%
20 – 60 km	50%	50%
60 – 100 km	100%	50%
> 100 km	100%	100%

Table 4. Specification of electrical capacity transmission of OWFs per distance category

From these parameters, the share of OWF capacity that is transmitted as electricity or converted into hydrogen at an island can be derived, as shown in Table 5. This allocation is a key parameter for calculating the total hydrogen production at each energy island.

Distance of OWF from shore	*Transmitted as electricity*	*Transmitted as hydrogen*
< 20 km	0%	0%
20 – 60 km	0%	100%
60 – 100 km	50%	50%
> 100 km	0%	100%

Table 5. Transmission strategy per OWF distance category.

Based on the values for the distance-based categories, the dataset must be filtered:

Data Filtering Step 1. OWFs that are within 20 km from shore according to the dataset, are excluded pre-modelling, as they do not connect to islands. In Figure 23, these OWFs are indicated with red nodes, and the remaining OWFs are indicated with green nodes. For this step, the distance that is provided in the source dataset are used. The distances from an OWF to shore are not recalculated, so results may look counter intuitive.

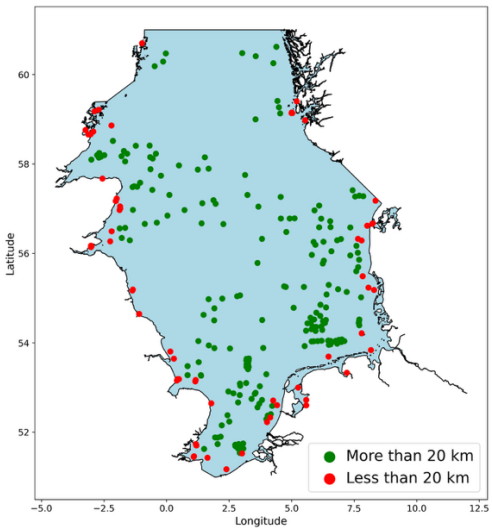

Figure 23. OWFs within 20 km from shore are indicated in red, OWFs further than 20 km from shore are indicated in green. Red nodes are excluded from the dataset, while green nodes remain in the dataset. Apparent cases reflect source data distance values as distances are not recomputed.

For example, a red node in the north-western North Sea near Scotland appears farther offshore than some green nodes, such as the north-eastern node close to Norway. Similarly, in a group of OWFs in the southern North Sea, one OWF is red while its neighbours are green. These cases reflect the distance in the source data relative to the 20 km threshold.

After the first filtering step is applied, a set of relevant OWFs remains which are used for clustering as described in *4.3.1 Offshore Wind Farm Clustering*. To avoid outliers influencing the clustering results, a second data filtering step must be applied:

Data Filtering Step 2. OWFs that are excessively distant from all other OWFs, are removed prior to clustering. The average geodesic distance from each OWF to all others are used for this. In Figure 24, the average distance per OWF is shown.

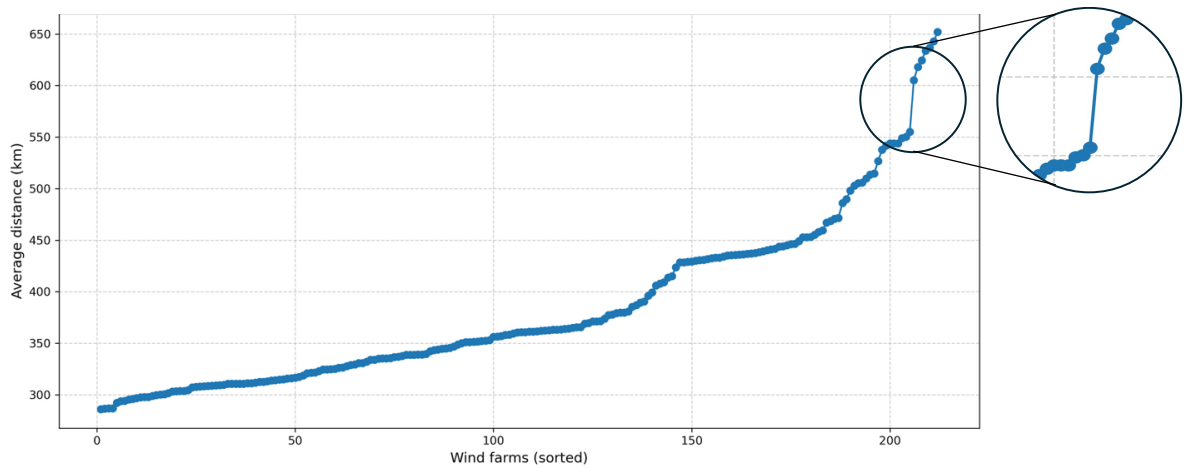

Figure 24. Average geodesic distance of each OWF to all other OWFs. The distribution shows a marked increase around 600 km, which is used as filtering threshold.

In Figure 24, a clear 'elbow' can be seen around the average distance of 600 km. Therefore, OWFs with an average distance to all other OWFs higher than 600 km are considered too distant and are excluded from the dataset.

As can be seen in Figure 25, the OWFs in the southern North Sea are more densely concentrated. Consequently, the northern OWFs naturally have a higher average distance to all OWFs than southern OWFs. Ultimately, some of these OWFs are excluded and indicated in red in Figure 25 as their average distance to other OWFs exceeds 600 km.

The final set of OWF, which is used as input for clustering, contains only relevant and spatially compatible OWFs. In total, it includes 205 OWFs. In Figure 26, the remaining OWFs are shown, with a color to indicate their distance-based category. Detailed information of each OWF, including name, coordinates, installed capacity and category properties, is provided in *Appendix A1. Dataset Offshore Wind Farms*.

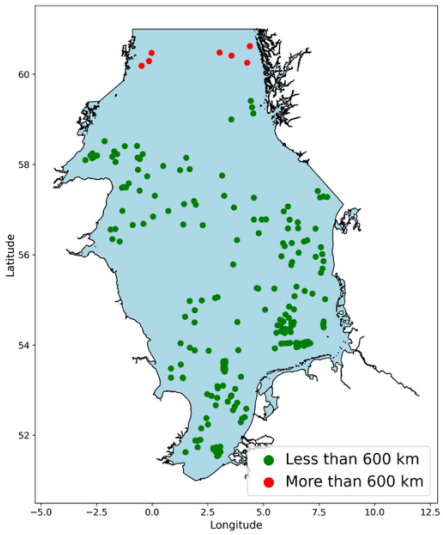

Figure 25. OWFs with more than 600 km average distance to all other OWFs are indicated in red and excluded from further analysis, other OWFs are indicated in green and remain in the dataset. The concentration of OWFs is higher in the southern than in the northern OWFs.

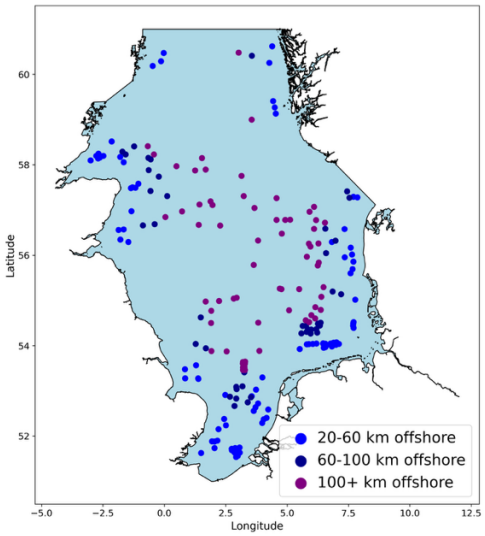

Figure 26. Final dataset of OWFs with distance-based categories.

Lastly, the OWFs are connected to energy islands via electricity cables. As outlined in *4.3.2.2 Electicity Cable Costs*, the HVAC and HVDC have different cost implications. EU ACER (2023) estimate a cost factor f_{cable} for both HVAC as HVDC submarine cables:

$$f_{HVAC} = 2{,}000\ €/km/MW$$

$$f_{HVDC} = 1{,}100\ €/km/MW$$

These cable cost factors are applied for the economic assessment to calculate initial cable costs to determine a cost-optimal number of energy islands, and to calculate the electricity cable costs for the cost-optimal electrical cluster networks.

5.3 Energy Islands

In *4.3.2.1 Energy Island Construction Costs*, the energy island construction cost factor f_{island} and surface area A_j for each energy island category are introduced. These values are derived from six energy island categories in Van Der Veer et al. (2020), which provide

the required surface area and total CAPEX for islands at fixed combinations of the total electrical capacity and hydrogen conversion rate. Each of these categories represents a different combination of island size and production system requirements. The CAPEX includes all costs for constructing the energy island itself, and the assets on the island. The costs for electricity cables and hydrogen pipelines coming to and going away from an island are excluded. They are therefore calculated separately in this thesis.

The categories in Van Der Veer et al. (2020) use fixed electrical capacities: 2, 5 and 20 GW. The total electrical capacity of energy island j, however, depends on the clustering outcomes of the OWFs as the sum of their individual electrical capacities determines the value for $P_{j,e}$. It is unlikely that it will match these exact values. To allow more flexible modelling, the three fixed capacities are generalized into categories, which are presented in Table 6.

Category notation	**Fixed capacity *(Van Der Veer et al., 2020)***	**Electrical capacity $P_{j,e}$**
Small (S)	2 GW	$P_{j,e} < 3.5\ GW$
Middle (M)	5 GW	$3.5\ GW < P_{j,e} < 10\ GW$
Grand (G)	20 GW	$P_{j,e} > 10\ GW$

Table 6. Thresholds for the electrical capacity $P_{j,e}$ per energy island category.

To provide a balanced split between small and middle islands, a lower threshold of 3.5 GW is chosen as it is between 2 and 5 GW. The upper threshold of 10 GW is chosen in a way that a too large of a jump from middle to grand capacities are avoided, while the largest size islands are still considered in a similar way. Additionally, the hydrogen conversion rates are generalized into categories, which are presented in Table 7.

Category notation	**Hydrogen conversion rate X_{j,H_2}**
Low (L)	$X_{j,H_2} < 75\%$
High (H)	$X_{j,H_2} \geq 75\%$

Table 7. Thresholds for the hydrogen conversion rate X_{j,H_2} per energy island category.

In this thesis, offshore hydrogen production on energy islands is more emphasized than in Van Der Veer et al. (2020). To reflect this, a stronger threshold is applied than the values considered by Van der Veer et al. (2020). With a threshold of 75%, the consideration of other design configurations is included.

Ultimately, these thresholds form the six energy island categories identified in *4.3.2.1 Energy Island Construction Costs* as shown in Table 8.

	Low hydrogen conversion $X_{j,H_2} < 75\%$	**High** hydrogen conversion $X_{j,H_2} \geq 75\%$
Small electrical capacity $P_{j,e} < 3.5\ GW$	**Small-Low (SL)**	**Small-High (SH)**
Middle electrical capacity $3.5\ GW < P_{j,e} < 10\ GW$	**Middle-Low (ML)**	**Middle-High (MH)**
Grand electrical capacity $P_{j,e} > 10\ GW$	**Grand-Low (GL)**	**Grand-High (GH)**

Table 8. Overview of thresholds per energy island category.

For each of these categories, the values for the required surface area A_j and construction cost factor f_{island} are derived from the results of Van Der Veer et al. (2020). The reference categories in that study provide the surface area and CAPEX for islands at 30% and 70% hydrogen conversion rates for each of the fixed capacities 2, 5 and 20 GW. The categories in this thesis use capacity and conversion thresholds, rather than exact fixed values. Therefore, first interpolation takes place based on the hydrogen conversion rate, and then the values are scaled for the electrical capacity.

For each of the three fixed capacities in Van Der Veer et al. (2020), two data points are available at the hydrogen conversion rates $X_l = 30\%$ and $X_h = 70\%$. The values at these points are the starting points for the surface area A_x and CAPEX K_x for each fixed capacity. The first step is to calculate how much the value for surface area and total CAPEX change per percentage point of the hydrogen conversion. This is calculated as:

$$m_A = \frac{A_h - A_l}{X_h - X_l}$$
$$m_K = \frac{K_h - K_l}{X_h - X_l}$$

Here, m_A and m_K indicate the slope for the change per % for, respectively, the surface area A_x and CAPEX K_x. A_l and K_l indicate, respectively, the surface area and CAPEX at 30%, while A_l and K_l indicate those at 70%. With that, it is described how the surface area and costs change with the hydrogen conversion rate at the reference capacity.

In the second step, the appropriate values for A_x and K_x are calculated for a specific hydrogen rate. For the *Low* category, a hydrogen conversion rate of 50% is used to calculate the values, while for the *High* category, a rate of 100% is used. These rates are referred to as representative rate, which is denoted by $\hat{X}$. The slopes m_A and m_K are thereby used to find what values for A_x and K_x are found at the corresponding representative conversion rate $\hat{X}$, which is calculated as:

$$A_x(\hat{X}) = A_l + m_A \cdot (\hat{X} - X_l)$$

$$K_x(\hat{X}) = K_l + m_K \cdot (\hat{X} - X_l)$$

In case of the *Low* category, $\hat{X}$ has a value between 30% and 70%, namely 50%. Then, this approach is called interpolation. In case of the *High* category, however, $\hat{X}$ has a value outside 30% and 70%, namely 100%. This approach is then called linear extrapolation.

Ultimately, this step calculates the required energy island surface area A_j per category. Thus: $A_j = A_x(\hat{X})$. The construction cost factor f_{island} can be derived using $K_x(\hat{X})$ and P_{fixed} that corresponds to each category as:

$$f_{island} = \frac{K_x(\hat{X})}{P_{fixed}}$$

Finally, the A_j and f_{island} values for each category are derived and presented in Table 9.

Category	Surface area A_j (km²)	Cost factor f_{island} (euros per MW_e)
SL	0.25	€365,000
ML	0.44	€210,000
GL	1.16	€80,000
SH	0.31	€400,000
MH	0.56	€240,000
GH	1.81	€100,000

Table 9. Input data for energy island surface area A_j and cost factor f_{island}. Derived from categories of Van Der Meer et al. (2020).

Additionally, an electrolyzer on an energy islands have a production efficiency η_{H_2}. According to Younas et al. (2022), the energy efficiency of electrolysis is about 50%, which is therefore assumed for the hydrogen production on the energy islands.

5.4 Existing Gas Pipelines

Existing natural gas pipelines are used as primary infrastructure candidates for reuse in an offshore hydrogen backbone. Their reuse could significantly reduce the total investment required, compared to constructing a completely new network. To ensure that the infrastructure data are fitted for the ONLT, these data are accurately and efficiently prepared so that the relevant information is preserved while unnecessary complexity is removed.

The dataset for existing pipelines is retrieved from EMODnet (2025) and includes data from various sources. The pipeline geometries are stored as MultiLineString, which is a set of LineStrings, which are data points forming a one-dimensional geometric object (Cockroach Labs, n.d.). The coordinates are listed in a consecutive order, in the form:

$$\text{MultiLineString}((x_1, y_1), (x_2, y_2), \dots, (x_n, y_n))$$

The complete dataset contains 3,146 pipelines, including the pipelines for different mediums, such as oil, and states of use. Therefore, only active or pre-commissioned natural gas pipelines are selected. This reduces the dataset to 765 pipelines. Moreover, Since EMODnet includes, there are duplicate pipelines. The dataset is therefore cleaned, resulting with 757 unique pipelines, as shown in Figure 27 (left).

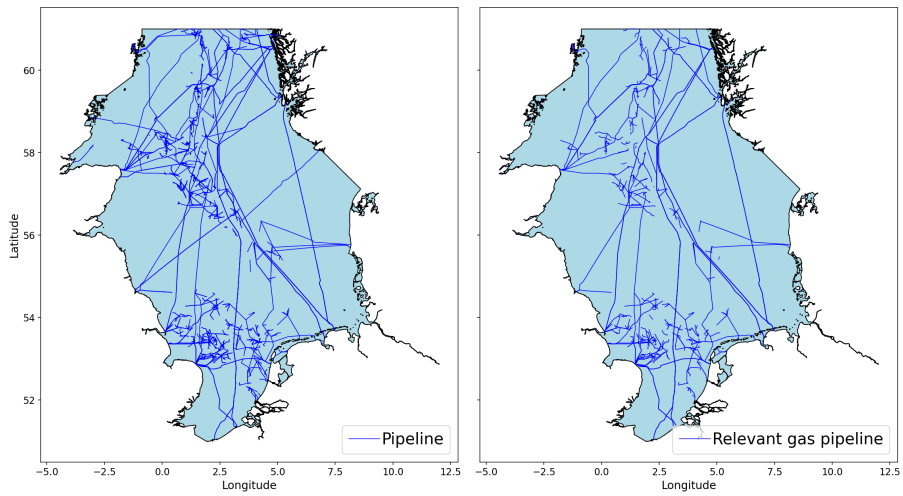

Figure 27. Unfiltered active and pre-commissioning pipelines (left), and natural gas pipelines in the North Sea (right). Based on EMODnet (2025).

A threshold for minimal pipeline diameter is to be part of the backbone but is not specified in academic literature. A minimum diameter of 20 inch reoccurs in reports from the EHB initiative (Van Rossum et al., 2022; Wang et al., 2020). Consequently, all pipelines with a diameter smaller than 20 inches are considered irrelevant for an offshore backbone and excluded from the dataset. 182 pipelines remain relevant for the backbone, which are shown in Figure 27 (right).

Each pipeline is defined in a MultiLineString, containing a high number of coordinates describing its path. These coordinates need to be extracted from the MultiLineString to be able to use as input for the ONLT. In total, the 182 pipelines consist of 307,751 different coordinates, which are shown by the black nodes in Figure 28. Including this number of coordinates in the ONLT, significantly increases its computational time. Moreover, the accuracy of the network will not be improved proportionally since each intermediate coordinate rarely represents an intersection but is used to specify a pipelines' path.

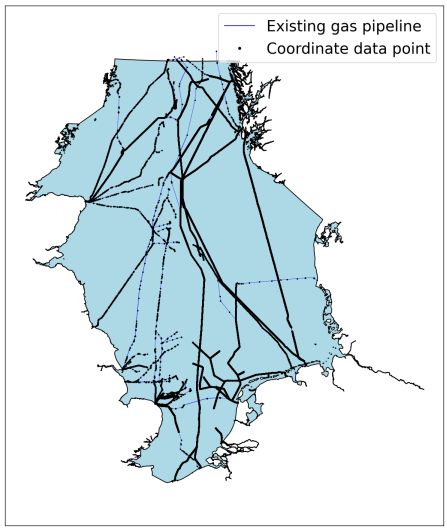

Figure 28. Relevant gas pipelines for an offshore backbone in the North Sea.

Data simplification is required to reduce computational complexity. The dataset is simplified in three steps: 1) contracting nearby nodes, 2) removing small deviations, and 3) merging short paths. In each step, a different form of redundancy is approached. Because all three steps rely on actual distances between coordinates, the data are first converted from geographic coordinates (Latitude/Longitude) into Universal Transverse Mercator (UTM) projection to preserve network accuracy. UTM ensures that the distance between points is consistent across the map, unlike Latitude/Longitude where the actual distance varies based on the points' proximity to the poles and Equator (Maptools, n.d.).

The implementation details for the data simplification are provided in *Appendix C1. Pipeline Data Simplification Steps*. In Figure 29, the results per step are presented for the complete network. Black nodes represent coordinate points. The results of contracting nearby nodes (Figure 29, left), show that the remaining point density is still so high that the pipelines, indicated by the blue edges, are barely distinguishable. Following the results for removing small deviations (Figure 29, middle), the connections become clearly visible while the overall network layout remains accurate. After merging short paths (Figure 29, right), the connections are further straightened with no apparent change in the overall layout. Ultimately, the complete pipeline network visually resembles the pre-

simplification network presented in Figure 28, indicating that the geometry is preserved during data simplification.

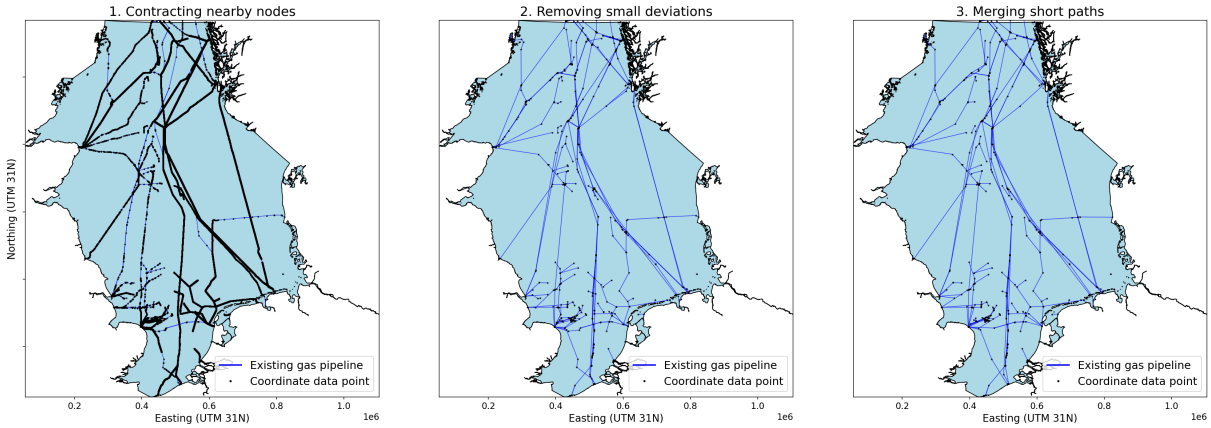

Figure 29. Results for the three data simplification steps for all natural gas pipelines in the dataset: 1) contracting nearby nodes (left), 2) removing small deviations (middle), and 3) merging short paths (right). Black nodes indicate coordinate points.

Overall, these three steps reduce the number of nodes and edges, which lowers the computational time of the ONLT without sacrificing spatial fidelity. The results of the third data simplification step conclude the final dataset of existing gas pipeline infrastructure used in the ONLT.

After the spatial layout is prepared, the next step is to process the technical properties for each pipeline so that they can be used in the ONLT. In the EMODnet dataset, the pipeline diameter of each pipeline is included in inches. The ONLT, however, requires the potential capacity for each segment to be expressed in MW. It is detailed in *Appendix C2. Hydrogen Pipeline Capacity* how the appropriate pipeline capacity is derived.

The final dataset of existing pipelines that is used for the hydrogen backbone can be found in *Appendix C3. Final Dataset Existing Gas Pipelines*.

5.5 Onshore Entry Points

The onshore entry points in the hydrogen network are defined as the locations where existing natural gas pipelines connect to the onshore transmission system. These locations are identified from the final dataset of existing pipelines as described in 5.*4 Existing Gas Pipelines*, which is based in EMODnet (2025). In addition to the entry points derived from EMODnet (2025), IJmuiden is added as an extra location, because it is repeatedly referenced as potential entry in Van Wingerden et al. (2023). The complete set of entry points are shown in Figure 30. The specific coordinates can be found in *Appendix D. Dataset Onshore Entry Points*.

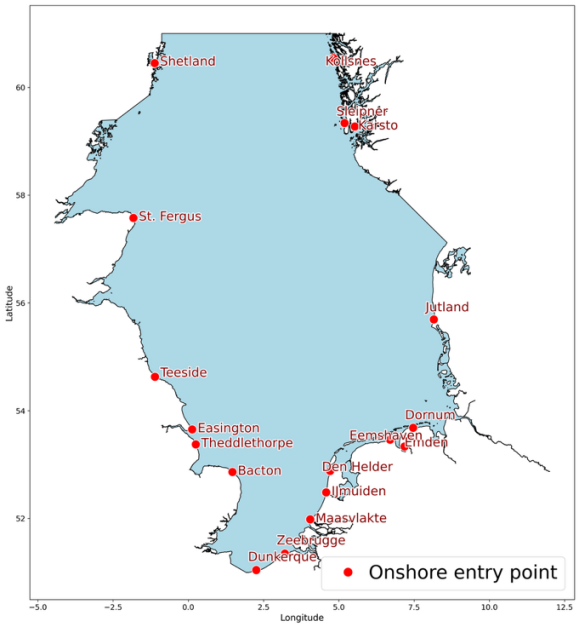

Figure 30. Identification of onshore entry point locations in the North Sea.

In the hydrogen network, entry points are the demand locations. As North Sea countries have not set offshore hydrogen targets yet, supply is assumed to meet demand. The total hydrogen demand equals the total hydrogen production across all energy islands:

$$Q_{J,H_2} = \sum_{j=1}^{n} Q_{j,H_2}$$

Where Q_{j,H_2} is the hydrogen production at energy island j, as outlined in *4.3.2.1 Energy Island Construction Costs,* and Q_{J,H_2} is the total hydrogen production across all energy islands J.

The hydrogen demand per entry point is allocated in proportion to the aggregate pipeline diameter at each location. Pipeline connections in the EMODnet dataset were reviewed and the combined diameter, expressed in inches, per entry point are manually summed with the following rule: for all EMODnet entry points, only pipelines with a diameter $\geq 20\ inches$ are included in the sum. IJmuiden is an exception: it does not appear as an offshore entry point in the EMODnet dataset, because it has no incoming onshore pipelines with a diameter $\geq 20\ inches$. Since IJmuiden is added as extra point, the sum of all pipelines that have diameter $< 20\ inches$ at that location.

Formally, for entry point m with total pipeline diameter d_m, the share of hydrogen demand x_m is proportional to the total pipeline diameter d_M across all energy points M:

$$x_m = \frac{d_m}{d_M}$$

The results are reported in *Appendix D. Dataset Onshore Entry Points*. It can be concluded that $d_M = 1670\ inch$ is the total pipeline diameter across all energy points M. Ultimately, the specific hydrogen demand at entry point m is calculated as:

$$D_m = x_m \cdot Q_{J,H_2}$$

This approach ensures that entry points with larger pipelines are assigned a higher share of the total hydrogen demand.

5.6 Forbidden Areas

As outlined in *3.4 Research Objectives*, ecological areas, shipping routes and military zones are considered forbidden areas for energy infrastructure construction in the North Sea. Each North Sea country determines the spatial planning of its EEZ, resulting in variation in the size and location of these areas. No single database contains all constraints, so multiple datasets are combined. For integration, shapefiles are used as they allow spatial dataset to be easily merged. A shapefile is a vector data storage format in which geographical data is stored (GIS Resources, 2020).

Shipping routes are based on each country's Marine Spatial Plan (MSP), which includes the IMO shipping routes and, in many cases, additional areas (North SEE, n.d.-a). MSP data from EMODnet (2025) and North Sea Energy (2025) are used for all countries except for the UK, where IMO data (UK Hydrographic Office, 2025) is applied. Shipping routes are shown in grey in Figure 31 (left). Ecological areas are based on OSPAR MPAs (OSPAR Commission, 2021), complemented with Natura 2000 data (EEA, 2025) to account for recent updates. Ecological areas are shown in green in Figure 31 (middle). Military zones are derived from EMODnet (2025) and North Sea Energy (2025) datasets and are shown in red in Figure 31 (right).

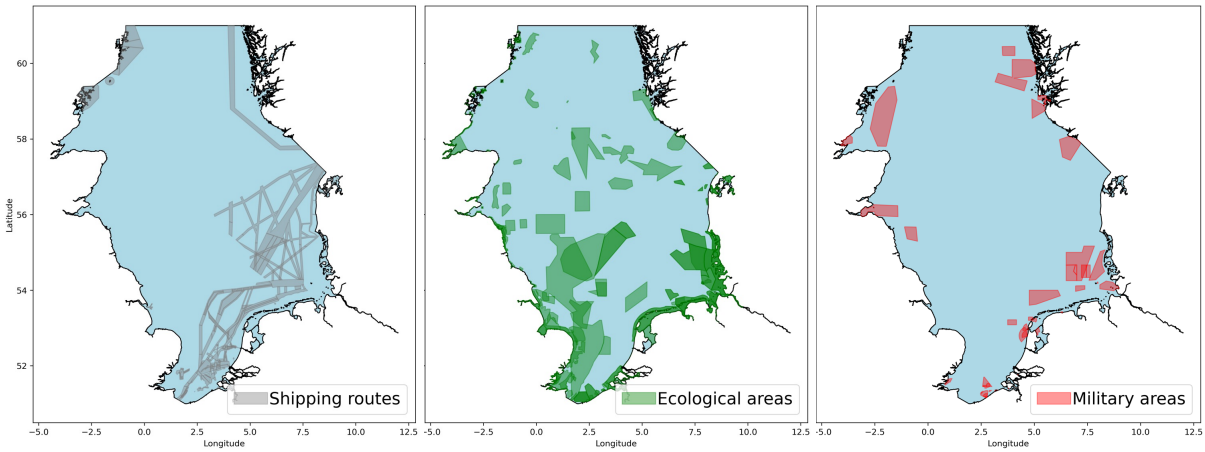

Figure 31. Forbidden areas in the North Sea: shipping routes (left), ecological areas (middle) and military zones (right).

The combination of these three area types, as shown in Figure 32 (left), are the forbidden areas for energy island construction. These data are considered when determining potential energy island locations, as outlined in *4.4.3.1 Candidate Energy Island Locations*.

For the electricity and hydrogen networks, however, only the ecological and military areas are considered forbidden, as shown in Figure 32 (right). Electricity cables and hydrogen pipelines are namely located at the bottom of the sea, so they do not interfere with shipping.

Forbidden areas are included in the ONLT as obstacles. The areas are extracted from a shapefile as polygons. If multiple areas overlap, the outer boundary of the combined area

is used. Additionally, OWFs can be located within a forbidden area. Then, that polygon is excluded from the forbidden area set: the network must be able to connect the OWF to an energy island via the cluster network.

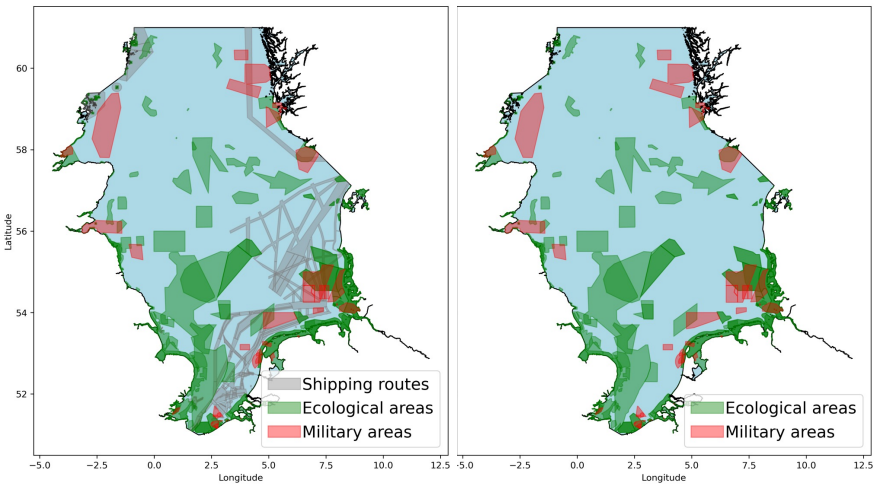

Figure 32. Forbidden areas for energy island construction (left) and for electricity cables and hydrogen pipelines placement (right). Ecological areas are in green, military zones in red and shipping routes in grey.

The offshore hydrogen backbone is based on existing natural gas pipelines. If these pipelines intersect with forbidden areas, they may still be reused. Prohibiting their reuse would require construction of new pipelines elsewhere. This could increase costs and potentially have a higher environmental impact. Repurposing pipelines has minimal environmental impact, is legally allowed and is generally more sustainable (Hammes, 2023). The construction of new infrastructures, however, is strictly forbidden in these areas. In practice, reinforcing pipelines requires construction of a new pipeline, as capacity is added with a parallel pipeline at the same location. Therefore, reinforcement is also not allowed in forbidden areas. Given that some modelling steps do not directly account for forbidden areas due to the dataset size, reinforcement of any existing pipeline is excluded entirely to ensure spatial constraints are respected in all modelling steps.

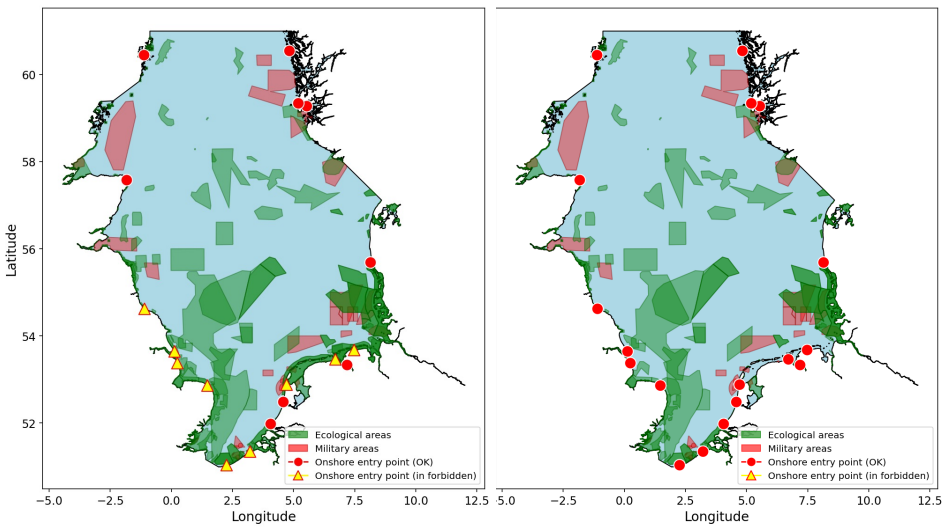

Figure 33. Identification of entry points located within ecological or military areas (left), and the filtered set of forbidden areas (right).

For the ONLT to function properly, supply and demand nodes cannot be located within forbidden areas. Some of the onshore entry points may fall within forbidden areas. In this thesis, the system boundary for a pipeline is set at the onshore entry point, although in practice it is not the physical end of the gas pipeline. To ensure the model operates on valid inputs, a data filtering step is applied for the hydrogen backbone: any entry point located within a forbidden area is identified, as shown in Figure 33 (left), and the corresponding area is removed from the dataset. This filtering step is only applied to the hydrogen network. The filtered set of forbidden areas is shown in Figure 33 (right).

Although some entry points still appear to be within forbidden areas, validation confirms that none remain inside these areas, as all entry point nodes are red. Additionally, some entry points appear enclosed by forbidden areas, such as Emden and Dunkerque, but they are still reachable: entry points define the system boundary of existing pipelines, and these pipelines may pass through forbidden areas. These entry points thus connect to the existing natural gas infrastructure.

5.7 Techno-Economic Data

The ONLT is applied for two distinct purposes. Firstly, it is used to design electricity networks that connect OWFs to energy islands within clusters. In these networks, the edges represent electricity cables of which their costs are calculated using the capacity-cost exponent β. An appropriate value for β is defined in *5.7.1 Electricity Network*. Secondly, the ONLT is used to design an offshore hydrogen backbone connecting the energy islands to onshore entry points. Then, the edges represent hydrogen pipelines of which their costs are calculated using the offshore cost factor α, a repurposing factor upc and reinforcement factor cpc. Appropriate values for these parameters are defined in *5.7.2 Hydrogen Network*.

5.7.1 Electricity Network

The capacity-cost exponent β for electricity cables is derived from cable cost data provided by Xiang et al. (2016). This dataset lists unit cable costs in £/km for two cable technologies (HVAC and HVDC) with different voltage levels (kV) and conductor cross-sections (mm^2). Although β is not directly defined in Xiang et al. (2016), the data set can still be used to estimate appropriate values for β.

At a fixed voltage level, the electrical power capacity of a cable is proportional to its allowable current. The allowable current depends on the scale of the conductor cross-section. Therefore, the allowable current is scaled approximately with the conductor cross-section of cables of the same technology (Xiang et al., 2016) and ultimately be used for deriving β. The equation for the capacity-cost exponent β is introduced in *4.4.2 Optimal Network Layout Tool*. Taking the logarithm of both sides linearises this equation, which brings:

$$\log costs = \log \alpha + \beta \log capacity$$

For each cable technology, the cost-capacity data points are transformed to this logarithmic form and fitted with a simple linear regression. β then represents the slope of the best-fit line. The dataset contains multiple voltage levels per cable type. Determining

the most appropriate voltage level for a given cable in the network is beyond the scope of this thesis. The difference between HVAC and HVDC, however, remains within scope. Therefore, the analysis considers the lowest voltage levels available for each technology when calculating β. The outcomes are presented in Table 10.

Type	Voltage (kV)	β
HVAC	132	0.494
HVDC	150	0.434

Table 10. β per cable type.

5.7.2 Hydrogen Network

For the hydrogen backbone, a cost function for the ONLT is applied as outlined in *4.4.4.1 Hydrogen Network Optimization*. The offshore cost factor α, a repurposing factor upc and reinforcement factor cpc need to be defined. However, as outlined in *5.5 Forbidden Areas*, existing pipelines cannot be reinforced thus it is no need to define a value for cpc.

Offshore hydrogen cost factor

An appropriate value for α is based on a cost factor for onshore hydrogen infrastructure $c_{onshore}$, and on offshore infrastructures $c_{offshore}$:

$$\alpha = \frac{c_{offshore}}{c_{onshore}}$$

Travaglini et al. (2025) provides the economic specifications of all assets in an offshore hydrogen system, including values for $c_{onshore}$ and $c_{offshore}$. The costs for newly build onshore hydrogen infrastructures $c_{onshore}$ is equal to 3.2 million €/km, while $c_{offshore}$ equals 3.6 million €/km. Finally, the offshore hydrogen backbone is $\alpha = 1.47$ times more expensive than onshore infrastructure.

Repurposing factor

An appropriate value for upc is determined based on comparing the costs of repurposed pipelines with newly build pipelines:

$$upc = \frac{c_{repurpose}}{c_{new}}$$

Slowinski et al. (2023) indicate that c_{new} for offshore hydrogen pipelines with a 36-inch diameter equals 5.4 million €/km. For that same pipeline type, $c_{repurpose}$ is equal to 1.1 million €/km. For a 36-inch pipeline $upc = 0.20$. Additionally, Slowinski et al. (2023) also indicate the costs for a 48-inch pipeline. c_{new} is then equal to 7.5 million €/km, and $c_{repurpose}$ to 1.5 million €/km. For a 48-inch pipeline $upc = 0.20$. Therefore, the diameter of the pipeline should not be considered, hence the value for upc is 0.20 for all repurposed pipelines.

Exchange rate

According to XE Currency (2025), 1 US dollar is equal to 0.86 euros on August 14, 2025. This exchange rate is therefore used throughout this thesis.

6 Results

In this chapter, the main results are presented without interpretation or discussion. First, the clustering results and associated economic assessment are reported in *6.1 Number of Energy Islands*. In *6.2 Energy Island Locations*, the results of the spatial analysis and electrical cluster optimizations are presented. Then, in *6.3 Offshore Hydrogen Backbone*, the results for a cost-efficient and spatially feasible offshore hydrogen backbone are shown. Intermediate and more detailed results are provided in Appendices E, F and G.

6.1 Number of Energy Islands

The results for subtotal costs, total electrical capacity aggregated and total hydrogen production at the energy islands for $k = [3,20]$ are presented in Table 11. The subtotal costs include costs for island construction, OWF-to-shore cabling and OWF-to-island cabling, which are detailed in *Appendix E3. Techno-Economic Details Post-Filtering*.

For $k = \{6, 7, 8\}$, the total costs are below €38 billion euros and are thereby the lowest among all configurations. The set of OWFs that result after filtering and used for the second clustering round is specific per configuration.

k	Subtotal costs (billion euros)	Total electrical capacity to energy island (GW)	Total hydrogen production capacity (GW)
3	€43.6	191	87
4	€40.4	191	87
5	€38.5	200	91
6	€37.0	200	91
7	€37.5	204	93
8	€37.5	204	93
9	€38.3	208	95
10	€38.7	209	95
11	€39.8	209	95
12	€40.3	209	95
13	€40.8	210	95
14	€41.6	212	96
15	€41.1	212	96
16	€40.8	212	96
17	€41.1	214	97
18	€42.3	214	97
19	€43.6	217	99
20	€45.1	217	99

Table 11. Results for $k = [3,20]$ after the first clustering round: the subtotal system costs post-filtering as result of the economic assessment in billion euros; the aggregated electrical capacity to all energy islands in GW and the total hydrogen production capacity across all energy islands.

The second clustering round is only applied for the three configurations of k with lowest total costs due to this research' time limitations, which is discussed in *7.10.1 Scope and Computational Feasibility*. The second round is only executed for $k = \{6, 7, 8\}$. The output is shown in Figure 34. The results for all configurations $k = [3,20]$ are presented in *Appendix E1. Result Specification of First Clustering Round*.

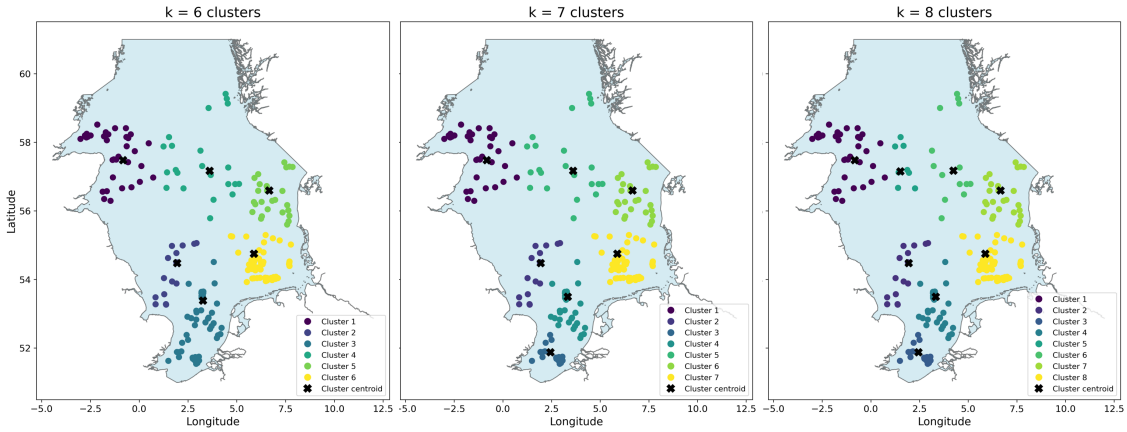

Figure 34. Results for Ward's clustering in the first round for $k = \{6,7,8\}$.

OWFs located more than twice times closer to shore than to the centroid are removed after applying the distance criterion (see *4.3.1.3 Post-Clustering*). The filtering results for $k = \{6, 7, 8\}$ are shown in Figure 35. The filtering results of all clusters in $k = [3,20]$ are presented in *Appendix E2. Specification of Filtering Results*.

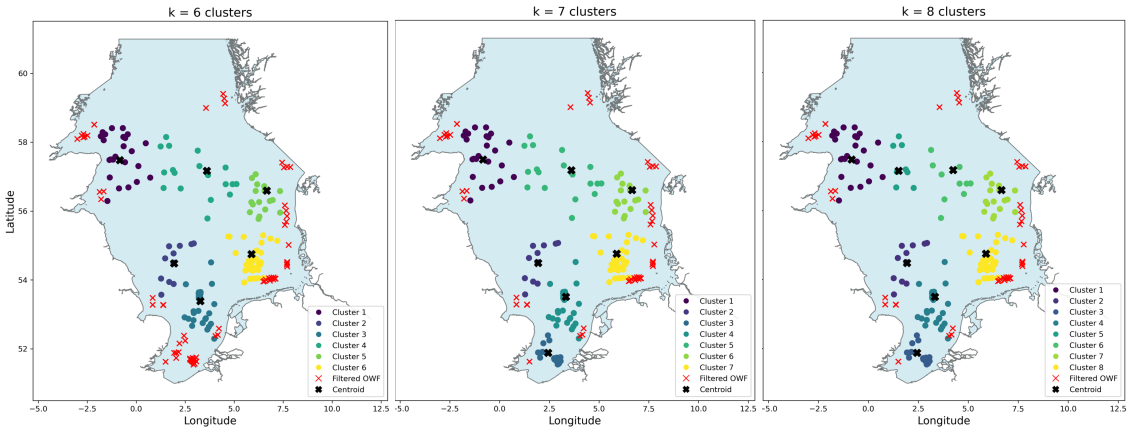

Figure 35. Results for filtering the output of the first clustering round based on the distance criterion for $k = \{6,7,8\}$.

There is a difference between OWF-to-shore and OWF-to-island cabling, as defined in *4.3.2.2 Electricity Cable Costs*. The OWF-to-shore cabling connections indicate how many OWFs are filtered according to the distance criterion. The number of OWF-to-shore and OWF-to-island cable connections for $k = \{6, 7, 8\}$ is shown in Table 12. For $k = 7$ and $k = 8$, the number of connections is the same. For $k = 6$, the number of OWF-to-shore connections is higher than for $k = 7$ and $k = 8$, indicating that more OWFs are filtered.

k	OWF-to-shore connections	OWF-to-island connections
6	72	133
7	49	156
8	49	156

Table 12. Number of connection types for OWF-to-shore and OWF-to-island cabling for $k = \{6,7,8\}$. The results for $k = 7$ and $k = 8$ are similar, and the number of OWF-to-shore connections is higher for $k = 6$ than for $k = 7$ and $k = 8$.

After filtering, Ward's clustering is applied a second time to $k = \{6, 7, 8\}$. The set of OWFs that are included in this round depend on the filtering results: all OWFs that have an OWF-

to-island cabling connection are included. For $k = 6$, this set is different than for $k = 7$ and $k = 8$. The results are presented in Figure 36.

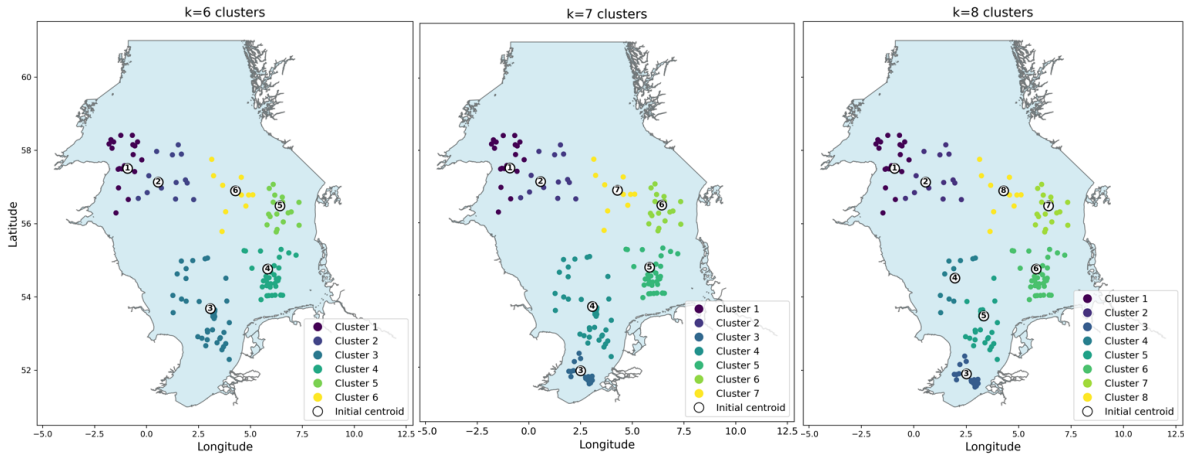

Figure 36. Results for Ward's clustering in the second round for $k = \{6,7,8\}$.

The technical properties for configurations $k = \{6, 7, 8\}$ are shown in Table 13. It shows the total electrical capacity aggregated across all energy islands, from which part of the capacity is used for hydrogen production. Considering the hydrogen conversion rates at the energy islands and the electrolyzer efficiency, the total potential hydrogen production is defined. Additionally, the total required surface area across all energy islands is presented. The results for $k = 7$ and $k = 8$ are the same, except for the required surface area: this is higher for $k = 8$. The results for $k = 6$ is lower for all parameters.

k	Total potential electrical capacity (GW)	Total electrical capacity for hydrogen production (GW)	Total potential hydrogen production (GW)	Total required island surface area (km²)
6	200	181	91	10.2
7	204	186	93	10.8
8	204	186	93	12.6

Table 13. Technical properties for $k = \{6,7,8\}$ after the second clustering round, including total electrical capacity, total electrical capacity used for hydrogen, total hydrogen production potential and required island surface area across all islands.

The results of the economic assessment for $k = \{6, 7, 8\}$ are specified in Table 14. It shows the island construction, OWF-to-island cabling and OWF-to-shore cabling costs. Comparing the subtotal costs across the three configurations, $k = 8$ has the lowest overall costs, amounting to €36.4 billion. $k = 6$ amount to €37.5 billion and $k = 7$ to €38.3 billion for $k = 7$. Comparing the results of the first and second round, it shows that the subtotal costs for $k = 6$ and $k = 7$ have increased, while the costs for $k = 8$ are lower.

k	Island construction cost (billion euros)	OWF-to-island cable cost (billion euros)	OWF-to-shore cable cost (billion euros)	Subtotal (billion euros)
6	€19.7	€15.5	€2.3	€37.5
7	€20.7	€15.8	€1.8	€38.3
8	€20.7	€14.0	€1.8	€36.4

Table 14. Cost specification for $k = \{6,7,8\}$, in billion euros. Including island construction, OWF-to-island cabling and OWF-to-shore cabling costs.

Overall, the costs are minimal for $k = 8$, so this configuration is taken for further analysis.

The final clustering results for $k = 8$ clusters are shown in Figure 36 (right). with the corresponding coordinates for the initial island location presented in *Appendix G1. Specifications for Island Location Results*.

The technical and economic details per cluster for $k = 8$ are specified in *Appendix F. Specification per Cluster for* $k = 8$. Clusters 5 and 6 have significantly more aggregated electricity than the other clusters, resulting in significantly higher costs.

6.2 Energy Island Locations

The forbidden areas (ecological areas, military zones and shipping routes) are included to determine a feasible location for energy islands. The initial cluster centroid locations found in the previous step (see *6.1 Number of Energy Islands*) are used as starting point. The required surface area per energy island, as specified in Table F.2, are used in a spatial analysis to identify candidate island locations. The candidate locations across each round for Cluster 3 are shown in Figure 37. The result for the remaining clusters is shown in *Appendix G1. Identification Steps of Energy Island Locations*.

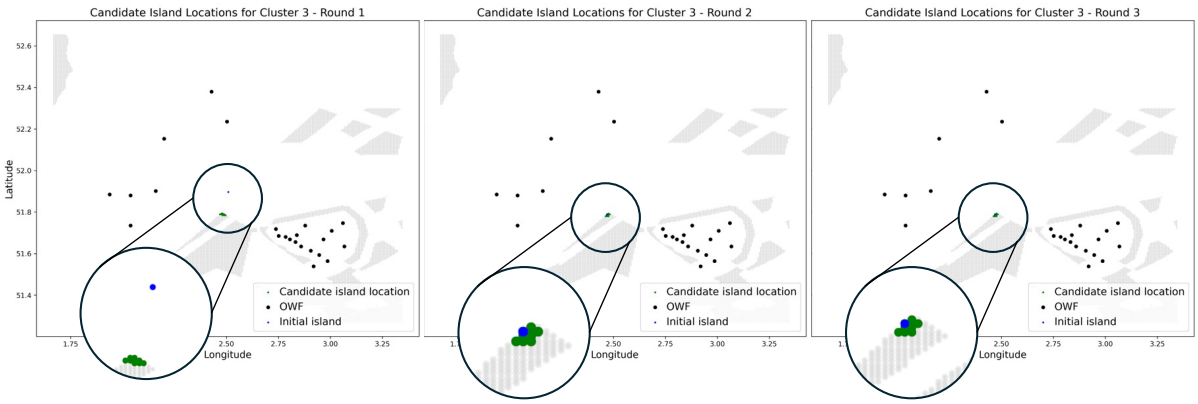

Figure 37. Identification of candidate island locations for Cluster 3, in Round 1 to 3.

In Round 1, the initial island location of Cluster 3 is within a forbidden area. As a result, the distance from this initial location to candidate island locations is higher than for initial locations that are outside forbidden areas. This is also visible in Round 2 and 3 as the initial island is relocated outside the forbidden area, as shown in the middle and right plot of Figure 37. A similar effect is observed for Clusters 4, 6 and 8, of which the initial island location in Round 1 is also within a forbidden area.

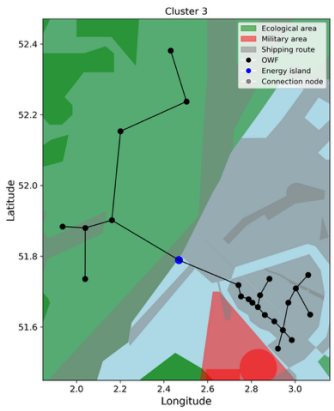

Figure 38. Result for the Cluster 3 electricity network of the cost-optimal candidate island location after Round 3. It represents the final cluster network this cluster.

An electricity network corresponds to each candidate island location. Since the candidate island locations are close to each other, these networks appear similar. Therefore, only the resulting network for Cluster 3 in Round 3 is shown in Figure 38. The final networks of the other clusters are presented in *Appendix G2. Specifications of Optimal Island Locations per Round*. It also includes cost and island location details.

Appendix G2. Specifications of Optimal Island Locations per Round includes a cost and island location details per cluster. These results are used to determine the total network costs across all clusters per round, which are shown in Table 15. It stands out that the total network cost in euros is lowest after Round 1, while the total cost in monetary units is highest for Round 1. This result is discussed in *7.7 Electricity Network Costs*.

Round	***Network costs (monetary unit)***	***Network costs (million euros)***
1	2275	€295.9
2	2261	€297.6
3	2255	€296.9

Table 15. Total electrical network costs across all clusters, per round.

In this research, the cost-optimal energy island location is concluded after Round 3. Its corresponding network has the lowest total costs. The networks across all clusters are shown in Figure 39. Technical and economic details of the nodes and edges of the final network are shown in *Appendix G3. Final Network Details per Cluster.*

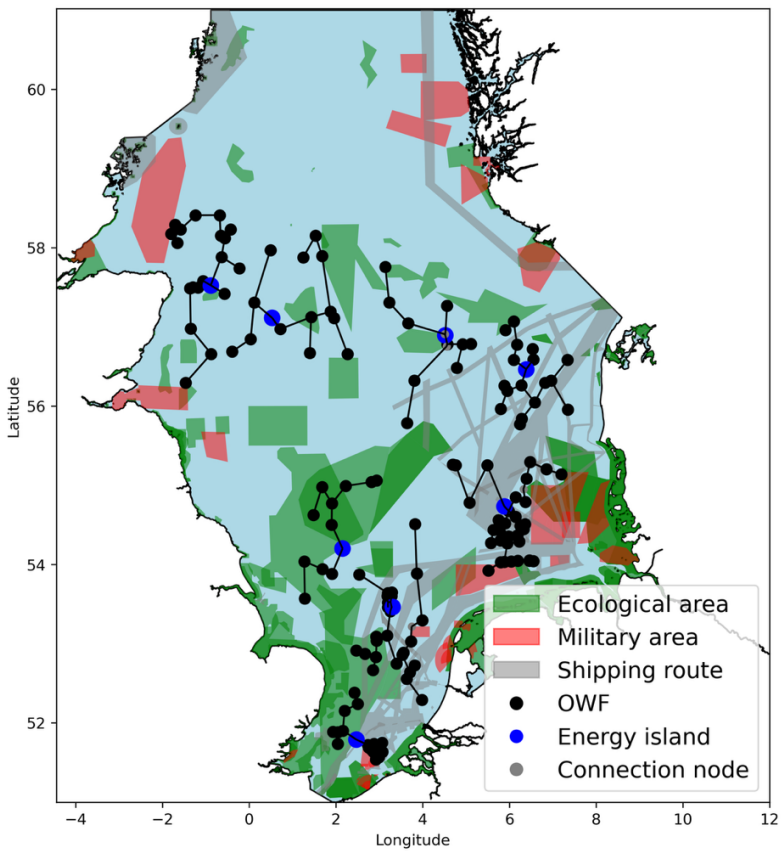

Figure 39. Final cost-optimal cluster network results across all clusters (Round 3).

6.3 Offshore Hydrogen Network

The total hydrogen production capacity on energy islands is equal to 93 GW. This potential is used to define the hydrogen demand per entry point, which is discussed in *Appendix H. Hydrogen Demand*. An initial offshore hydrogen backbone is seen in Figure 40 (left). The total costs of this network are €9.3 billion. This backbone is based on the energy islands (see *6.2 Energy Island Locations*), the hydrogen production per island (specified in Table F.1) and the hydrogen demand per entry point (specified in Table H.1).

In Figure 40 (middle and right), the forbidden areas for hydrogen pipelines are held under the initial backbone. The pipeline segments that are infeasible must be rerouted.

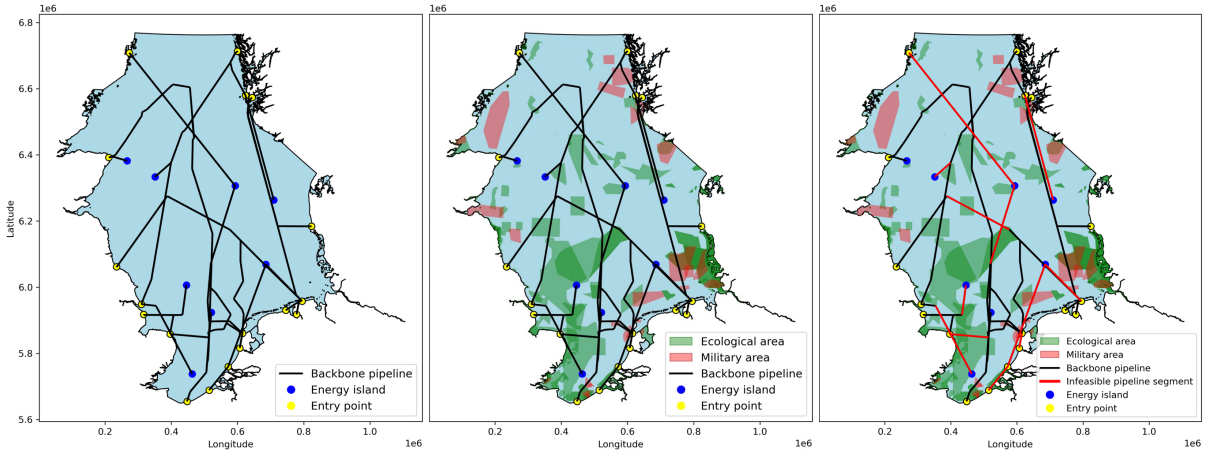

Figure 40. Initial hydrogen backbone results (left), and identification of infeasible pipeline segments in this initial backbone by adding forbidden areas (middle, right).

A total of 12 infeasible segments is identified. The capacity per segment that must be rerouted is detailed in *Appendix I1. Rerouting Details of Infeasible Segments*.

The result of the rerouting process for Segment 4 is shown in Figure 41. For the remaining segments, their results of the rerouting process are shown in *Appendix I2. Rerouting Results per Infeasible Segment*.

Segments 9 and 10, as shown in Figure 42, are excluded from the final backbone as they connect two entry points with one having a node degree equal to 1 (see *4.4.4.3 Spatial Rerouting Procedure*). Segment 9 connects Den Helder to IJmuiden and Segment 10 connects Maasvlakte to Zeebrugge. As these are the only connections for IJmuiden and Zeebrugge to the rest of the backbone, these segments comply with this special case. The segments are removed from the network as these points can also be connected onshore.

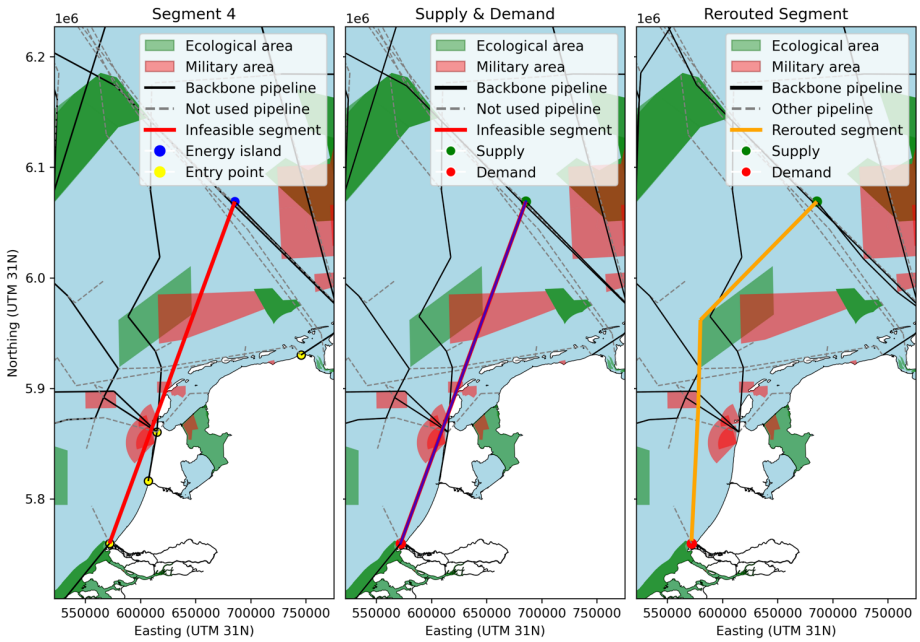

Figure 41. Rerouting steps for infeasible pipeline Segment 4.

Segments 9 and 10, as shown in Figure 42, are excluded from the final backbone as they connect two entry points with one having a node degree equal to 1 (see *4.4.4.3 Spatial Rerouting Procedure*). Segment 9 connects Den Helder to IJmuiden and Segment 10 connects Maasvlakte to Zeebrugge. As these are the only connections for IJmuiden and Zeebrugge to the rest of the backbone, these segments comply with this special case. The segments are removed from the network as these points can also be connected onshore.

The hydrogen demand at IJmuiden and Zeebrugge is added to the demand at Den Helder and Maasvlakte, respectively. The demand at IJmuiden and Zeebrugge become zero, while the demand for Den Helder and Maasvlakte increase to, respectively 7,783 MW (8.4% of the total) and 8,116 MW (8.8% of the total).

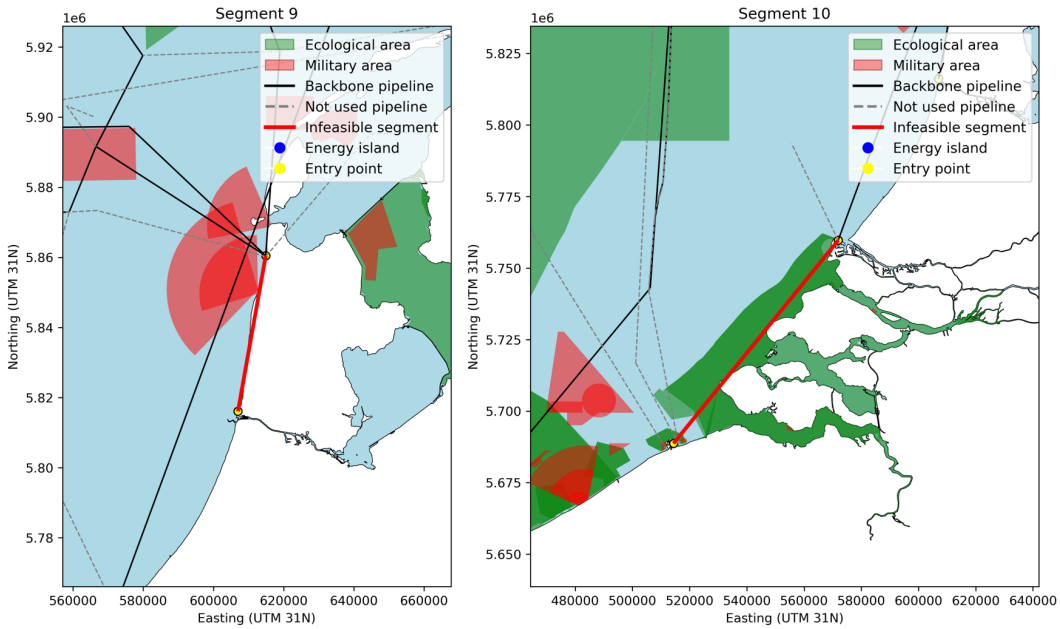

Figure 42. Segments 9 and 10 connecting two entry points with one entry point having a node degree equal to 1.

After the replacement of infeasible segments, the final offshore hydrogen backbone is determined, see Figure 43. It includes similar details as for the initial backbone, but the hydrogen demand at Zeebrugge, Maasvlakte, IJmuiden and Den Helder differ (Table H.2), and the infeasible segments are rerouted. The total cost for this backbone is €8.9 billion.

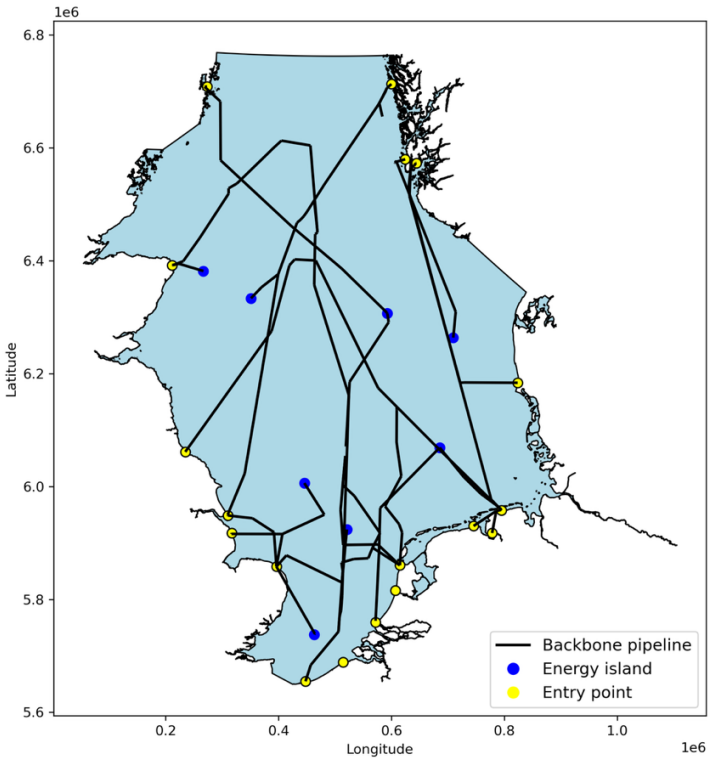

Figure 43. Final offshore hydrogen backbone

However, this final backbone cannot be validated since there are still segments intersecting forbidden areas, see (Figure 44). This is discussed in *7.9 Hydrogen Network*.

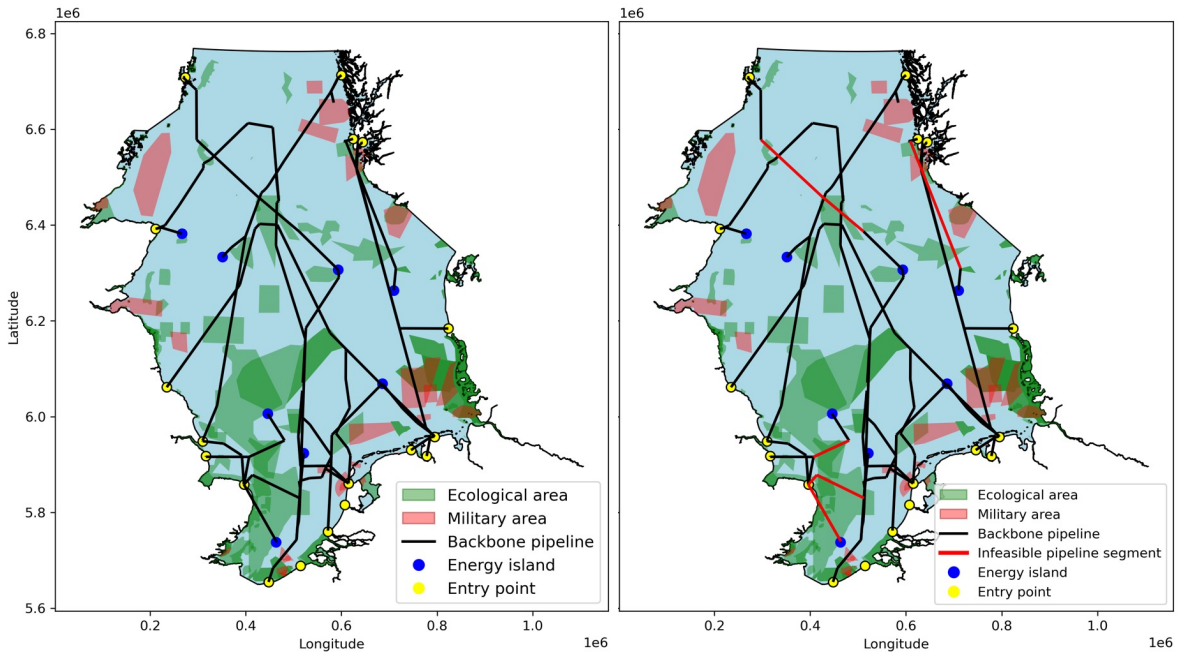

Figure 44. Validation if infeasible pipeline segments are rerouted correctly by including forbidden areas.

7 Discussion

The aim of this thesis is to explore if an offshore energy system can be designed such that the North Sea electricity and hydrogen systems are connected via energy islands. OWFs, energy islands and hydrogen pipelines are considered simultaneously. By combining the clustering with network optimization models, it is assessed how OWF distribution, spatial constraints and cost considerations influence such design.

In this chapter, the results that are presented in *Chapter 6. Results* are interpreted in a broader academic and societal context. It is structured per topic from *7.1 Clustering* to *7.9 Hydrogen Network*, following with a discussion of limitations in *7.10 Limitations*.

7.1 Clustering

The clustering results, as presented in *6.1 Number of Energy Islands*, show that the OWF distribution across clusters is relatively stable for $k = \{6,7,8\}$. For $k = 6$, a large southern cluster is split into two when moving to $k = 7$. All other clusters remain stable. At $k = 7$, the largest cluster, in the central North Sea, is divided into two clusters when moving to $k = 8$, while all other compositions remain unchanged. This reflects Ward's method: clusters with highest internal variance are split first to reduce total within-cluster variance, while smaller and more isolated clusters remain stable across configurations.

Filtering mainly excludes OWFs at the cluster edge near the shore. The more centrally located OWFs and those towards the centre of the North Sea remain. This leads to more compact clusters. For example, the OWFs filtered out in $k = 6$ reappear as a seventh cluster at $k = 7$. This shows that filtering affects which OWFs connect to energy islands, and that a higher k can reduce exclusion by providing more OWFs for aggregation.

Thus, filtering interacts with the choice for k. Fewer clusters increase the chance of OWFs being filtered, while more clusters limit exclusion. The design choice therefore concerns not only the number of islands, but also which OWFs are connected to them. These dynamics directly influence cost trade-offs discussed in *7.2 Economic Assessment*.

7.2 Economic Assessment

The results in *6.1 Number of Energy Islands* indicate a trade-off between island construction and cabling costs, which is split into OWF-to-island and OWF-to-shore cabling. With fewer islands, construction costs are lower, but OWF-to-island connections are longer and more OWFs are filtered. This increases both the costs for OWF-to-island and OWF-to-shore cabling. With more energy islands, overall construction costs are higher, but average distance to OWFs decrease. Also, less OWFs are filtered. OWF-to-island and OWF-to-shore cabling costs are therefore lower.

This trade-off is seen in the results of the first round (Table E3.1). At $k = 3$, island construction costs are €19.1 billion, OWF-to-island cabling is €21.2 billion, and OWF-to-shore cabling is €3.2 billion. In total, the system costs are €43.6 billion, which is among the highest observed. At $k = 6$, island construction costs increase to €20 billion, while OWF-to-island cabling costs fall to €14.7 billion and OWF-to-shore cabling costs fall to €2.3 billion. In total, the costs are €37 billion, which is minimal across configurations. At

$k = 7$ and $k = 8$, the total costs are €37.5 billion. Compared to $k = 6$, the cabling costs are lower, but island construction costs are higher. When k further increases, the total system costs increase overall as result of a marginally decrease of cabling costs. The economic optimum is therefore achieved at $k = \{6,7,8\}$, because cabling costs are balanced against island construction costs instead of maximizing k.

In the second clustering, the minimum costs are at $k = 8$, amounting to €36.4 billion. The cost reduction compared to the first round is a result of the filtering. Less OWFs are included and OWFs are redistributed across clusters which result in lower OWF-to-island cabling length and costs. In this case, a redefinition of cluster composition leads to lower overall costs. However, the total costs for $k = 6$ and $k = 7$ have increased because of higher OWF-to-island cabling costs. This is counterintuitive, since re-clustering reduces cable lengths, but overall costs increase due to a shift from HVDC to HVAC cabling. HVDC is appropriate for longer cables than for HVAC, but its costs are lower: $1{,}100\ €/km/MW$ for HVDC, compared to $2{,}000\ €/km/MW$ for HVAC. Despite shorter cable lengths, the overall OWF-to-island cabling costs therefore lead to an increase in overall costs.

Finally, the cabling costs resulting from the economic assessment are only indicative: straight-line distances are assumed from OWFs to islands. It does not consider obstacles or potential efficiencies resulting from network optimization. A more realistic assessment is therefore discussed in *7.6 Electricity Network Costs*.

7.3 Energy Island Categories

The results in *6.1 Number of Energy Islands* show that island construction costs are identical for several configurations, despite an increase in number of islands. In the first round, this occurs for: $k = 3$ and $k = 4$; $k = 5$ and $k = 6$; and $k = 14$, $k = 15$ and $k = 16$ (Table E3.1). In the second round, this occurs for $k = 7$ and $k = 8$ (Table 14). This seems counterintuitive, but it follows directly from the cost function: island construction costs are calculated as a linear function of aggregated electrical capacity per island, multiplied by a cost factor f_{island}. The cost factor only changes when certain category thresholds are crossed. If islands remain within the same category, costs scale with the aggregated capacity and do not increase with the number of islands.

For example, Cluster 4 in $k = 7$ aggregates 77.6 GW. In $k = 8$, it is split into two islands of 15.1 GW and 62.5 GW (Table E4.2). Both islands remain above the 10 GW threshold, so the cost factor does not change. As a result, the total construction costs remain the same (Table E4.1), even though overall surface area requirements increase (Table E4.3). This effect explains why island size across clusters are generally identical in $k = 8$. It highlights the impact of threshold-based categories and absence of base cost components, which is further discussed in *7.10.2 Cost Assumptions*.

7.4 Spatial Analysis

The results are presented in *6.2 Energy Island Locations*. The analysis identifies candidate island locations, assessed across three optimization rounds. If the initial centroid lies within a forbidden area, nine candidates are found along its border. If it is already spatially feasible, the initial centroid is included as candidate. If the initial centroid is feasible, Candidate 1 in Round 1 corresponds to that centroid and indicates the lowest network

costs (Table G1.1). For infeasible centroids, however, Candidate 1 does not represent the initial centroid. In Round 2 and 3 (Tables G1.2 and G1.3), Candidate 1 is always feasible, thus represents the optimal result in previous rounds.

Cluster 8 illustrates this principle. Its initial centroid was infeasible, so Candidate 1 in Round 1 referred to another location providing minimal cost. In Round 2, Candidate 8 yielded lower network costs and reappeared in Round 3 as Candidate 1. It confirms that this location is the final optimal within this approach.

The initial centroid location strongly influences the efficiency of the search. Feasible centroids limit candidates directly next to the initial centroids. Infeasible centroids generate candidates along the nearest border of a forbidden area. This ensures spatial feasibility but biased results towards one side of a forbidden area or the immediate surroundings of the initial centroid. This leaves other potential lower-cost locations unexplored. Across all clusters, optimal locations for initially infeasible centroids (Cluster 3, 4, 6 and 8), were consistently found within three rounds. In contrast, feasible initial centroids could still be improved in Round 3. This suggests that both the limited candidate set, and the fixed number of rounds constrained their optimization.

7.5 Cluster Networks

The cluster network results, as shown in *6.2 Energy Island Locations*, highlight the difference in spatial constraints for energy islands and electricity networks. Energy islands are excluded from the ecological areas, military zones and shipping routes, while electricity cables may cross shipping routes but not ecological or military areas. Some cables, however, cross these areas. This reflects the need for OWF connections located in these areas rather than a methodological error. The distinction between islands and cables, together with the simplified restrictions, is needed to produce realistic results.

When visualizing all clusters together (Figure 39), only minor differences appear between rounds. This is expected, as candidate island locations change position very subtle relative to the North Sea scale. At cluster level, the layouts also remain largely stable. Although these layouts appear nearly identical at both levels, the specific location of the island node affects total cable length and costs of the networks. These cost implications are further discussed in *7.6 Electricity Network Costs*.

7.6 Electricity Network Costs

The total network costs across all clusters, as presented in *6.2 Energy Island Locations*, are shown in Table 15. In monetary units, the costs decrease steadily from 2275 in Round 1, to 2255 in Round 3. It indicates that the optimization converges to more efficient networks. Expressed in euros, however, the lowest costs are in Round 1 (€295.9 million), while the costs in Round 2 (€297.6 million) and 3 (€296.9 million) are slightly higher. This results because the absolute costs after calculated after optimization. The ONLT minimizes relative costs, which result in shorter connections that yield higher electrical capacities. In Round 3, most connections are shorter than 40 km, requiring HVAC cabling instead of HVDC cabling (Tables G3.5 and G3.6). Since HVAC has a higher cost factor, the change in cabling technology increases costs. Absolute costs therefore increase, even when relative efficiency improves.

Compared to the OWF-to-island cabling costs resulting from the economic assessment (€14 billion), the ONLT results far lower network costs. The tool designs efficient network layouts instead of straight-line OWF-to-island cable connections. The optimized layouts require fewer and shorter cables, while spatial constraints are respected. After three optimization rounds, the cost-optimal island locations are identified based on minimal network costs. The corresponding networks as presented in Figure 39, can therefore be considered a more realistic and stable system representation.

Cluster-level results further illustrate these dynamics. In Clusters 5 and 6, more OWFs are connected to its island than in other clusters (Table F.3). This results in more electricity cables compared to other clusters. About 62 GW of electricity is aggregated to these islands, which is more than other islands (Table F.2), resulting in higher required cable capacities. As only few connections are longer than 40 km, the more expensive HVAC cabling is used often (Tables G3.5 and G3.6). The use of HVAC technology for cables with higher capacity, in combination with a higher number of cables, result in significantly higher network costs: €71.1 million for Cluster 5, and €62.3 million for Cluster 6. Moreover, the high electrical capacity at the islands results in significantly higher island construction costs, compared to other clusters (Table F.4): €6.25 billion for Cluster 5 and €6.21 billion for Cluster 6.

When looking at Cluster 3, however, a high number of OWFs in a cluster does not directly relate to high costs. Its network cost is €11.8 million, which is the lowest observed (Table G2.3). Similarly, its island construction costs are, with €1.03 billion, also the lowest observed (Table F.4). This is explained by the aggregated electricity to the island, which is 4.3 GW (Table F.2). The OWFs in this cluster are located relatively close to shore (Figure 39), which reduces the aggregated electrical load as result of the distance-based categories. This results in low network costs. The aggregate capacity thus strongly influences costs, and cluster size predominantly influence network design.

7.7 Hydrogen Production

The hydrogen production potential, presented in *6.3 Offshore Hydrogen Backbone*, highlights the scale and distribution of offshore electrolysis. In total, 93 GW of hydrogen can be produced from 186 GW of offshore wind (Table 13). This reflects that the 50% electrolyser efficiency is applied correctly.

The distribution across islands varies with OWF distance categories. Cluster 3, for example, functions as a hydrogen hub: all aggregated electricity is converted to hydrogen production. This occurs because its OWFs are located 20 to 60 km from shore. For each of these OWFs, half of its capacity is directed to the island and then fully used for hydrogen production. This example illustrates how OWF locations, combined with cluster composition, influence the allocation of electricity and hydrogen in the North Sea system.

7.8 Onshore Entry Points

The hydrogen production potential is distributed across 18 entry points in proportion to existing pipeline diameters (Table 15). This allocates nearly half of all hydrogen to the UK as Bacton accounts for 17.5%, St. Fergus for 12.6% and Easington for 10.2%. Together, with the three other points, it accounts for 49.7%. In contrast, the four Dutch entry points

combined receive 12.2% of the total demand, and Denmark only receives 1.8%. The distribution is therefore strongly uneven since it reflects existing infrastructure rather than future demand. This introduces a bias, illustrating that using current pipelines to forecast demand risks the design networks that misalign with eventual hydrogen strategies.

The exclusion of IJmuiden and Zeebrugge further demonstrates the gap between technical feasibility and strategic priorities. Both are removed from the backbone because they connect only to other entry points: IJmuiden to Den Helder, Zeebrugge to Maasvlakte. Their connections could also be constructed onshore as they intersect with areas outside the North Sea. Onshore pipelines are cheaper than offshore pipelines, so the demand at IJmuiden and Zeebrugge is reassigned to Den Helder and Maasvlakte. They are thus no longer supplied directly from the offshore system. Although IJmuiden features prominently in the Dutch hydrogen development strategy (Van Wingerden et al., 2023), it does not appear in the optimized offshore system.

Finally, the structure of existing natural gas pipelines helps explain the results. Most were built to connect natural gas fields directly to national networks, with a few larger interconnections between countries. To integrate them into the ONLT, three simplification steps are applied. This leads to results that can be visually confusing. For example, Eemshaven and Emden each appear connected only to Bornum, seeming to cross the area outside the North Sea. It illustrates that the natural gas pipeline dataset is simplified and the visualizations in Figures 40, 43 and 44 are indicative.

7.9 Hydrogen Network

The initial offshore hydrogen backbone costs €9.3 billion. Several new, direct connections appear between energy islands and entry points, crossing areas outside the North Sea. These direct connections appear because repurposing existing pipelines is constrained by its current capacities. Although the ONLT assumes that reinforcement is allowed, it does not apply in this analysis because it requires the construction of parallel pipelines. For the initial backbone, no obstacles were included yet to reduce computational complexity. Allowing reinforcement would therefore conflict with the restriction to construct in forbidden areas. As a result, the limited capacity of existing pipelines prevents the effective reuse of some existing infrastructures, leading to spatially unrealistic connections between some energy islands and entry points.

The final backbone costs are €8.9 billion, which is lower that the initial backbone design. This is counterintuitive because infeasible segments in the initial backbone are rerouted for the final backbone, expecting to have higher costs. The infeasible segments are mainly rerouted via existing infrastructures. Since most of the infeasible segments are direct connections between islands and entry points, as discussed above, newly constructed pipelines are replaced by repurposed pipelines. Consequently, the total costs are reduced. Moreover, the two infeasible pipeline segments between IJmuiden and Den Helder, and Zeebrugge and Maasvlakte are removed, which further reduces costs.

In total, twelve pipeline segments are found infeasible. The pipeline capacities that must be rerouted range from 1.1 GW to 20.4 GW. After rerouting, two segments are removed (Figure 42), five are successfully rerouted and five remained infeasible (Figure 44). It is explained in *7.10.1 Scope and Computational Feasibility* why these segments remain

infeasible. Their capacity, however, ranges from 1.7 GW to 14.1 GW. It shows that the infeasibility is not associated with pipeline capacity, but by geometric complexity and presence of forbidden areas. This highlights that spatial and geometric constraints should be assessed simultaneously with limited pipeline capacities of existing connections.

As a result, not all hydrogen demand could be met. Islands could not be connected to Bacton (UK), Theddlethorpe (UK), Shetland (UK) and Sleipner (Norway). The inclusion of Bacton, which has the highest demand of all entry points, shows that the existing natural gas layout does not align with offshore hydrogen system needs. Relying solely on existing infrastructure therefore limits the ability to meet demand at designated entry points.

7.10 Limitations

This research provides insights into a cost-optimal integration of energy islands, OWFs and a hydrogen backbone in one energy system. There are, however, several limitations to consider when interpreting the results. In this section, these are discussed per topic.

7.10.1 Scope and Computational Feasibility

Due to time constraints, clustering iterations were restricted to $k = \{6,7,8\}$. In principle, the approach could have been extended to $k = [3,20]$, or multiple iteration steps. The aim of this thesis, however, is to explore whether a system-level cost optimum exists, not to analyze all possible cluster configurations in-depth.

For the offshore hydrogen backbone, the initial goal was to compute a cost-optimal network integrating existing pipelines forbidden areas. The scale of the North Sea and the size of the datasets made this computationally infeasible. Instead, a two-step approach was used: first, a backbone with only existing connections and no obstacles is constructed; second, infeasible pipeline segments intersecting with forbidden areas are identified and locally rerouted. This reduced the computation time, but the backbone is therefore rather indicative than realistic.

Data simplification was applied to the dataset of existing connection, but not to obstacles. This is impossible as their geometric precision is crucial to ensure feasible island locations. The large obstacle dataset therefore further increased computational time. The overall feasibility of this approach is therefore limited by the trade-off between data simplification and geometric accuracy.

A further limitation lies in the ONLT assumption that existing connections can be reinforced. In practice, this requires the construction of new, additional pipelines parallel to the existing connections. This conflicts with the restriction to construct infrastructure in forbidden areas. An extremely high value for the reinforcement factor cpc is used to prevent reinforcement. Nevertheless, the assumption remained deeply rooted within the tool. As a result, five segments remain infeasible in the final hydrogen backbone. This highlights that the reinforcement assumption can be a structural limitation of the ONLT.

Additionally, these segments are often in areas dense with forbidden areas. Therefore, it shows the geometric complexity of the North Sea, which might limit certain system

designs. It also shows how spatial constraints can fundamentally restrict optimization results in such large system.

Finally, to reduce average cable lengths, cluster centroid locations are recalculated after clustering using capacity-weighted averages. This adjustment generally shifts centroids further offshore, where larger OWFs are located. Because the clustering was not capacity weighted, this can create uneven capacity distributions across clusters. Since the consideration of capacity was introduced only after clustering, this methodological choice introduces a structural limitation of the approach.

7.10.2 Cost Assumptions

Reliable cost data for energy island construction is scarce, as energy islands are still conceptual. Thresholds are therefore applied to approximate economies of scale. This approach has clear limitations. No base cost component is included, so adding an island does not necessarily increase costs if its capacity falls within the same category. In practice, islands larger than 10 GW are treated equally, whether they represent 11 GW or 70 GW. This simplification results from the limited differentiation of thresholds. A more detailed categorization could improve cost scaling. This is, however, impossible due to scarce cost data in academic and technical literature. Only Van Der Veer et al. (2020) specifies costs for various island types. As a result, certain financial, technical and social dimensions of energy island construction are not captured.

In this thesis, categories were defined to capture economies of scale indirectly. Smaller islands are assigned higher cost per MW than larger islands. Yet these differences are not reflected in the results because nearly all energy islands fall into the largest category. Nonetheless, the categories make optimization of the integrated electricity-hydrogen system possible. Still, they do not capture fixed or nonlinear costs, nor financial, technical or social uncertainties. Accordingly, these results should be interpreted with care: the current formulation is useful to compare trade-offs between island construction and cabling costs, rather than a precise prediction of investment needs.

The specification of cabling technologies and its corresponding voltages are similarly simplified: it is solely based on distance thresholds. All HVAC cables are assumed at 132 kV, and all HVDC at 150 kV (Machado et al., 2015). In practice, other factors also determine voltage and appropriate cabling technology.

Both island and cable cost factors are treated as fixed values without a temporal dimension. This thesis focuses on a system finalized in 2050, which is still 25 years from now. The North Sea energy system will be developed over decades. Also, the capital costs may change over the years as result from technological progress, inflation or market conditions. The cost results should therefore be seen as indicative rather than predictive.

Finally, there are two limitations regarding the ONLT application for the electricity networks. The capacity-cost relationship is based on a small dataset from 2016. The exponent is therefore useful for scaling but does not reflect developments such as inflation or technological innovation. Moreover, the tool is designed for UTM coordinates, while this analysis used latitude and longitude coordinates. As the results are converted afterwards, it may introduce distortions between distance and cost calculations.

7.10.3 Spatial and Geographical Assumptions

This research assumes that all current operational, planned and search areas for OWFs are available by 2050. In practice, policy changes, spatial conflicts, ecological restrictions or other uncertainties may limit this. Moreover, only CAPEX is considered, while the operational expenditures (OPEX) of OWFs, islands and infrastructures are excluded. Including it could alter the relative attractiveness of island configurations.

All forbidden areas are treated the same across the North Sea. Although in practice governance of these areas differs, no distinction is made between countries. Its actual implications may therefore be different, affecting the network layout and overall costs.

Finally, the scope of this thesis is geographically limited to the North Sea. Potential connections to OWFs in the seas on the north, east, and south are excluded. However, the scope is already very systematic, so an extension of the research area could possibly further decrease the chance for realistic results.

7.10.4 System-Level Assumptions

This research assumes that the North Sea is treated as one integrated system. This reflects a best-case scenario because it assumes a supranational coordination of offshore energy development and infrastructure. Such integration could reduce costs, improve infrastructure use and enhance energy security. Although the Ostend Declaration (2023) illustrates political intent, offshore cooperation remains fragmented as most projects are regional, bilateral or trilateral. It is unlikely that a full system integration will develop in the short term. This underscores, however, the relevance of this thesis' scope for 2050 as it is the timespan in which such integration can be realized.

A second assumption is that energy islands are modeled only in relation to OWFs to facilitate electricity aggregation for hydrogen production. In practice, islands may serve broader functions, such as port functions, connections to salt caverns for hydrogen storage or to carbon capture utilization storage (Wu et al., 2025). Including these features would significantly increase the model complexity. This thesis therefore provides starting point for future assessment that integrate such additional features.

7.10.5 Energy Security

This thesis has a techno-economic focus. Energy security is, however, increasingly recognized as an important part of the European energy transition but is rarely incorporated into system optimization. Winzer (2012) defines it as "the continuity of energy supplies relative to demand." Defining appropriate optimization indicators for energy security is challenging, as it covers multiple dimensions, including economic, political and technical sides. Ang et al. (2015), Sovacool & Mukherjee (2011) and Winzer (2012) points out indicators such as the diversity of supply, redundancy of critical infrastructure and reliability of cross-border interconnections to substantiate energy security. This research does not account for such indicators, which limits the ability to evaluate system robustness and the design's vulnerability to geopolitical shocks.

8 Conclusion

In this final chapter, the main findings are brought together, and their implications are put into scientific and societal perspective. In *8.1 Research Questions*, the sub-questions are answered before the main research question is addressed. The academic relevance of this research is concluded in *8.2 Scientific Contribution*, and the societal relevance in *8.3 Societal Contribution*. Suggestions for future research are in *8.4 Future Research*.

8.1 Research Questions

To answer the main research question, first the sub-questions are answered. The first sub-question is:

> *What is the cost-optimal number of energy islands in the North Sea by 2050, based on operational and planned offshore wind farms?*

The research concludes 8 energy islands to be cost-optimal within the system description. This is determined based on the minimization of capital costs of energy island construction and costs for required cabling. There are two types of electricity cabling connecting offshore wind farms (OWFs): OWF-to-island cabling connects them to islands, while OWF-to-shore cabling connects excluded OWFs after filtering to shore.

The initial cost estimation amounts to €36.4 billion. A clear trade-off between these costs is found: less energy island results in lower island construction costs but requires higher investments for cabling. Conversely, more energy islands result in higher island construction costs and a marginal reduction of cabling costs. This thesis therefore suggests that the economic optimum lies at an intermediate number of energy islands. Note that cost functions are simplified: the island construction cost function should include a base cost or representable thresholds; for the OWF-to-island cabling, straight-line connections are assumed. A more realistic assessment for OWF-to-island cabling costs is conducted for the second research question. The second sub-question is:

> *What are the optimal locations for energy islands in the North Sea considering other North Sea uses?*

The research shows that including ecological areas, military zones and shipping routes strongly influence the feasibility of energy island locations. In turn, the specific island location determines electricity network layouts and OWF-to-island cabling costs. Compared to the initial estimation, which was used to answer the first research question, these cabling costs have significantly been reduced: from €14 billion to €0.3 billion (€296.9 million). This is explained as technical aspects of the system are included, leading to more realistic network layouts than assuming straight-line connections.

The research further show that the differences in cost are mainly driven by the electrical capacity aggregated to an island, rather than by the number of connected OWFs. Energy islands with a high capacity are associated with much higher costs, while islands with lower capacity are relatively low-cost. A more even distribution of capacity across islands could potentially reduce overall costs, but this has not been assessed in this research.

The optimal island locations identified here are therefore those that are spatially feasible while yielding the lowest observed network costs. These locations play a role for the third sub-question, which is:

> *What is the most cost-efficient system design for an offshore hydrogen backbone, given the locations of energy islands?*

Given the system description of this research, an offshore backbone can integrate 93 GW of hydrogen capacity at an estimated cost of €8.9 billion. The reuse of existing natural gas pipelines helps to reduce costs but is limited by their capacity and location. The resulting backbone, however, could not meet the demand at several locations, such as Bacton in the UK, due to model limitations and busy areas in the North Sea. It shows that an offshore hydrogen backbone is technically plausible but should be assessed differently.

From this, the main research question can be answered. The main research question is:

> *What is a system design with minimal overall system costs for the North Sea, in which energy islands enable the integration of electricity from offshore wind farms in an offshore hydrogen network, while accounting for other North Sea uses?*

Taken together, a cost-efficient integrated North Sea energy system can be achieved by developing 8 energy islands that are strategically located. This number of islands balances the costs for island construction and electricity cabling, while it provides a basis for an offshore hydrogen production and transmission system. The overall system costs amount to €31.7 billion: €20.7 billion for energy island construction, €1.8 billion for OWF-to-shore cabling, €0.3 billion for OWF-to-island cabling and €8.9 billion for the hydrogen backbone.

Spatial constraints, the distribution of electrical capacity and technical performance of infrastructures strongly influence the economic and technical performance of an integrated energy system. Ultimately, the research shows that energy islands can potentially act as hubs connecting the offshore grid to offshore electrolysis.

As result of methodological and computational limitations, this research is rather indicative than definitive. Nevertheless, this research provides a basis for a conceptual framework that can be applied to integrate energy islands into offshore energy systems in a spatially and techno-economic efficient approach.

8.2 Scientific Contribution

This research contributes to academic literature on offshore energy system design in four ways.

Firstly, this research contributes to system design theory by integrating offshore wind, hydrogen and energy islands into one single design framework. Previous studies mainly considered these assets separately: the benefits of meshed networks and cross-border system integration for offshore electricity in the North Sea region (Lüth & Keles, 2024; Quirk et al., 2021), the benefits of hydrogen for balancing intermittency, reducing curtailment and fulfilling future European energy demand (Dute et al., 2024; Farahmand

et al., 2024; Glaum et al., 2024), or the strategic potential of energy islands (Arteaga et al., 2024). There is little research that combines offshore electricity and hydrogen networks into one integrated design. By introducing energy islands as shared nodes between offshore electricity and hydrogen networks, this thesis shows how these systems can be co-optimized. The results show that an integrated approach changes the network layout compared to single-energy designs (Glaum et al., 2024; Konstantelos et al., 2016). This thesis thus provides insights into how energy islands function as system integrators. Moreover, the supranational approach of this research, provides a framework that is consistent with arguments in existing literature that European-level system planning is necessary for efficient offshore development (Buljan, 2025; North Sea Energy, n.d.).

Secondly, this research highlights the decisive role of spatial constraints in offshore system design. Most optimization studies emphasize asset costs (Glaum et al., 2024; Kristiansen et al., 2018; Konstantelos et al., 2016), while only few explicitly include spatial constrained areas (Guşatu et al. (2024). The results show that forbidden areas affect the feasibility of the hydrogen backbone layout and results in redirection of transmission infrastructures leading to higher costs. The research demonstrates that the spatial feasibility of energy infrastructures is not optional but fundamental for a realistic design. This shows that techno-economic designs without spatial considerations are incomplete and potentially also misleading.

Thirdly, this thesis introduces a methodological framework that combines clustering with network optimization modelling. While clustering has been used to group OWFs (Svendsen, 2013), and network optimization models have been applied to energy networks (Ehsan & Yang, 2017; Zhou et al., 2019), these methods have not yet been combined in the context of multi-energy offshore system design. The results show how OWF clustering decisions at micro-level directly influence system-level network layouts and costs. This methodological link adds a new perspective to literature by showing how asset localization choices affect the supranational system design.

Fourthly, this research contributes methodologically by identifying bottlenecks in the application of the ONLT to large-scale hydrogen networks. In previous studies, the ONLT has been successfully applied (Van Den Assum, 2022; Van Tongeren, 2022). In this research, the ONLT functioned well for electricity cluster networks, but the application for the scope of the entire North Sea turned out computationally infeasible. Moreover, the integration of existing pipelines revealed that assumptions embedded in the tool are unrealistic: in reality, it is impossible to reinforce existing pipelines to develop an offshore hydrogen backbone. The identification of these bottlenecks is relevant as it gives reason for future model developments.

Taken together, this thesis contributes by 1) demonstrating the system-level design implications of integrating offshore electricity and hydrogen networks via energy islands; 2) demonstrating that spatial constraints as a crucial design parameter; 3) combining clustering with network optimization models to bridge local and system-level perspectives; and 4) identifying methodological limitations that are the basis for future research. This research thus builds on existing literature on offshore system design, energy islands, and infrastructure reuse. Importantly, it provides new insights into a supranational, multi-energy North Sea energy system.

8.3 Societal Contribution

This thesis contributes in several ways to society by providing a conceptual framework that assesses the role of energy islands in a North Sea energy system.

Energy islands can act as hubs that connect offshore wind to hydrogen production. The development of energy islands brings transmission infrastructure and electrolyzers offshore and alleviate spatial scarcity on land. As offshore wind moves further offshore, OWF-to-shore cabling becomes increasingly expensive. Energy islands enable the exploitation of offshore wind further at sea (Jansen et al. 2022), which will become increasingly important to meeting future offshore wind targets. In this sense, they are not a means to reduce costs by themselves, but rather an enabler that makes large-scale offshore wind development technically and economically feasible.

The research also highlights the strategic importance of energy islands for the future of hydrogen in Europe. The estimated levels of offshore hydrogen production could make a significant contribution to European demand by 2050. Currently, the EU aims to install 40 GW of electrolysers by 2030 both on- and offshore. Also, hydrogen should supply approximately 10% of the EU's total energy demand by 2050 (Norton Rose Fulbright, 2025). Although there are no specific targets for offshore hydrogen in 2050 yet, the results underscore the role of the North Sea in achieving climate neutrality and the potential for energy islands to increase overall system efficiency.

The analysis further shows the societal value of approaching the North Sea as one integrated energy system, rather than as separate national systems. A coordinated, multinational approach enables more efficient use of infrastructure, avoids inefficiencies at borders, and allows for reuse of existing pipelines. At the same time, such integration faces political and institutional challenges. Cross-border projects are more vulnerable to shifting political projects, while single-country projects are more stable.

Relating this to real-world projects illustrates this point: the Danish Belgian *Energiø Nordsø Energy Island* project is delayed because the project cost amounted €7 billion more than expected and political commitments changed (Jacobsen, 2024; Jenkinson, 2024; Reuters, 2023). Similarly, the NSWPH, initiated by the Dutch, German and Danish TSOs and planned for development in the Dutch area of the Dogger Bank, has been canceled after financial and political setbacks (M. Dubbelboer, personal communication, April 4, 2025). In contrast, the Belgian *Princess Elisabeth Energy Island* project, which has started construction in April 2025 (Memija, 2025), reflecting a stronger national alignment and political support. These projects show how the cross-border system integration can be challenging as it directly affects decision-making and project feasibility. The Ostend Declaration is therefore an important step towards aligning national ambitions into a coordinated vision for the North Sea.

Taken together, this thesis shows that energy islands can play a central role in enabling offshore wind expansion, supporting offshore hydrogen production and contributing to Europe's long-term energy transition. At the same time, political coordination and fair distribution of costs and benefits across countries remain critical challenges. The energy transition is unavoidable and will require very large investments. These costs, however, should be seen in perspective: without them, climate targets will not be achieved,

Europe's energy supply is likely less secure, and dependence on unstable regions may persist. In this light, the investments identified in this thesis should be interpreted not as financial burdens but as strategic opportunities for a more efficient energy future. The integrated approach presented offers an efficient pathway compared to fragmented national solutions. By integrating energy islands in a coordinated multinational framework, Europe can reduce overall costs while meeting future renewable energy demands and potentially strengthening energy security and independence.

8.4 Future Research

This thesis has presented a system-level exploration of how energy islands can be cost-efficient enables for integrating the North Sea offshore electricity and hydrogen systems into one. However, it highlights areas for future research. These areas can be put into three categories: empirical refinement of cost functions, methodological improvements to system modelling and the expansion of research towards energy security considerations. Each of these categories are discussed in the sections below.

8.4.1 Empirical Refinement of Cost Functions

One of the main limitations in this research is brought with the assumptions made for the energy island cost functions. As energy islands remain conceptual, their construction costs, configuration and the scaling of costs are uncertain and not well understood. Future research should therefore substantiate these functions through empirical data on technical design, cost-optimal island sizes and configurations, and their cost developments. In particular, the thresholds for very large islands, specifically exceeding 10 GW, should then be developed instead of assuming energy island categories. Similarly, future research should systematically assess the relation between island size and configuration, as this would allow for more realistic results that can give reason for investment decisions. Lastly, refining the empirical basis for cable and pipeline cost functions, including more recent datasets, differentiation between HVAC and HVDC voltages and applications, and specifically viewed on the North Sea, would strengthen technical accuracy of system-level cost estimations.

Furthermore, future research could incorporate the hydrogen pipeline costs explicitly into the cost assessment with cable and island construction costs. This would provide a more comprehensive assessment of the integrated offshore system and allows a more realistic evaluation of the integration of electricity and hydrogen infrastructures.

Next to the refinements of the cost functions and assessment in this thesis, future research could focus on the levelized cost of electricity and the levelized cost of hydrogen as result of such integrated system. This would provide a clearer picture of the economic competitiveness of these energy sources.

8.4.2 Methodological Improvements

In this thesis, clustering is used to group the OWFs based on distance. Although this approach is suitable for exploring system layouts, alternative approaches can be of added value. For example, clustering based on electrical capacity and specified for a selected set of OWFs can identify different trade-offs between cable length, island construction costs and system efficiency. Also, developing a method to include of forbidden areas

within the clustering process, avoids spatially infeasible clusters. This would specifically be relevant in regions where forbidden areas lay between OWFs and energy islands. Such spatially aware clustering approach, however, would be highly complex to develop as it would entail combining clustering with another mathematical method that includes spatial constraints. Additionally, the closeness of energy islands to ecological areas, miliary zones or shipping routes would be an interesting topic for future research to understand its impact. It should also be noted that several OWFs were excluded from the clustering and were no longer assessed. This choice reflects the system-level focus of the research. The excluded OWFs could be reconsidered in future research to better understand how their integration would affect the system design.

The spatial analysis conducted that is used to determine energy island locations in this research could also by further refined by increasing the number of candidate locations can be a valuable improvement. This allows the testing of candidate locations on multiple sides of a forbidden area, and it might reduce the number of iterations required to find optimal locations.

This thesis highlights that further refinements can also be made to the ONLT regarding the reinforcement of existing connections. For this, the procedures in the ONLT should be changed in a way that reinforcement is rather a choice than a given option. Without such refinements directly to the tool, there are also methodological extensions that can be assessed in future research. First, an additional iteration step can be included where local optimization is done excluding existing connections while including obstacles. This would exclude the potential for reinforcement and is solely based on new connections. This would possibly, however increase overall costs. Second, the reinforcement of existing infrastructures would be allowed for these few segments that cannot be optimized. It gives an idea of how the system can be developed, based on which policymakers can make well-considered decisions. Third, the hydrogen flows across existing pipelines can be split up and only the excess capacity is rerouted. This allows reuse of existing infrastructure through forbidden areas but is methodologically complex. The implications of the first two strategies can be seen in Figure 45.

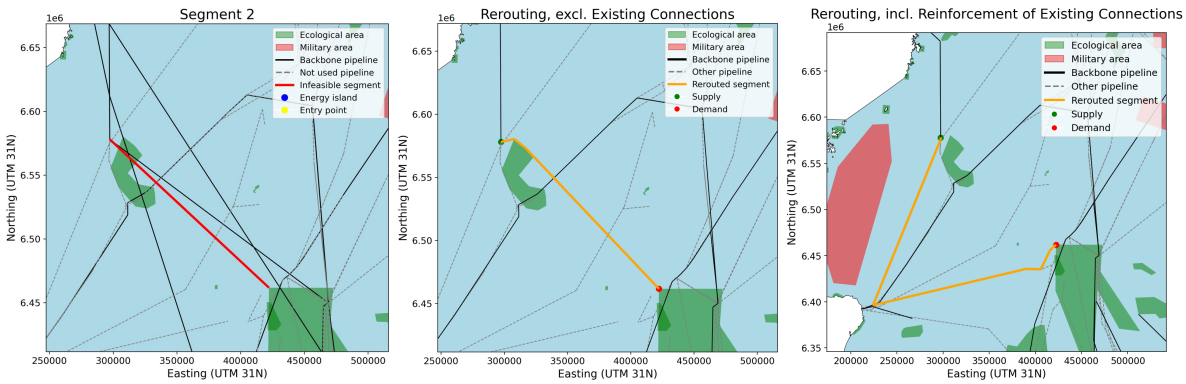

Figure 45. Potential rerouting strategies applied to infeasible Segment 2.

However, as can be seen in Figure 46, excluding existing connections would not always ensure feasible results. It therefore shows that these strategies need refinement before a final design can be concluded. Ultimately, each of these strategies has distinct implications for costs, system feasibility and compliance with spatial constraints, thus should be systematically explored in future research.

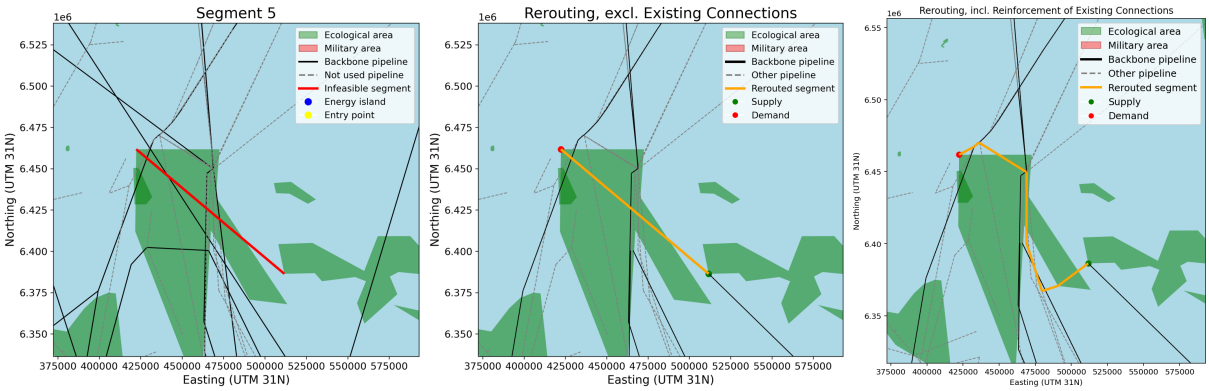

Figure 46. Potential rerouting strategies applied to infeasible Segment 5.

Moreover, applying the ONLT directly with UTM coordinates instead of using the haversine formula post-optimizations could eliminate potential distance distortions for the electricity networks. This would strengthen the validity of the results of this thesis.

8.4.3 Inclusion of Energy Security Considerations

As discussed, the focus of this thesis is on techno-economic optimization and excludes addressing energy security. There are few optimization models that explicitly include energy security factors. A systematic methodology to integrate such factors into system design thus remains underdeveloped. Developing these methods is therefore an important field of research for future work. Future work should assess metrics for redundancy, resilience and reliability alongside merely techno-economic optimization. Such an approach would allow for a more comprehensive evaluation of trade-offs.

At the same time, the results of this research provide useful starting points for such research. Meshed offshore networks lead to an increase in system redundancy by facilitating multiple connections between supply and demand. In turn, redundancy improves the system resilience in times of outages or disruptions resulting from geopolitical conflict (Levalle & Nof, 2017). Future work could develop a way to quantify redundancy and test how different network topologies perform under disruption scenarios.

Similarly, this research concludes an offshore hydrogen production potential of 93 GW. Such capacity may reduce the reliance on hydrogen imports and thus potentially presents an opportunity for European energy independence and might strengthen European autonomy. This is something to desire given the increase in geopolitical tensions with other regions in the world (Kaya, 2024). Future research could therefore analyse how this offshore hydrogen potential would affect Europe's reliance on imports under different policy and market conditions.

Another promising direction lies in the geopolitical dimension. The results show that two energy islands located in the UK's EEZ are exclusively linked to UK entry points. This points to a potential tension between national and European energy security as result of certain design choices. Therefore, future studies could analyse how potential geopolitical tensions arise as result from specific cross-border governance frameworks and institutional arrangements. It could also include an analysis on how this influences the integration and coordination of supranational, multi-energy system design.

This page is intentionally left blank.

References

2019/942 Agency fort he Cooperation of Energy Regulators (ACER) Regulation. (2019). https://eur-lex.europa.eu/legal-content/EN/TXT/?uri=CELEX%3A02019R0942-20220623

2019/944 Electricity Directive. (2019). https://eur-lex.europa.eu/legal-content/EN/TXT/?uri=CELEX%3A02019L0944-20240716

2024/1788 Gas Directive. (2024). https://eur-lex.europa.eu/legal-content/en/TXT/?uri=CELEX%3A32024L1788

4C Offshore. (n.d.). *Global Offshore Renewables Map*. map.4coffshore.com. https://map.4coffshore.com/offshorewind/

Abera, A. G., Yetayew, T. T., & Alyu, A. B. (2025). Optimized solar PV integration for voltage enhancement and loss reduction in the Kombolcha distribution system using hybrid Grey Wolf-Particle swarm optimization. *Results in Engineering*, *26*, 105484. https://doi.org/10.1016/j.rineng.2025.105484

Alassi, A., Bañales, S., Ellabban, O., Adam, G., & MacIver, C. (2019). HVDC Transmission: Technology review, market trends and future outlook. *Renewable and Sustainable Energy Reviews*, *112*, 530–554. https://doi.org/10.1016/j.rser.2019.04.062

Albert, M. (2025, June 11). *Dogger Bank | Map, depth, & Facts*. Encyclopedia Britannica. https://www.britannica.com/place/Dogger-Bank

Aleem, S. H. E. A., Ali, Z. M., Zobaa, A. F., Ćalasan, M., & Rawa, M. (2022). Editorial: Energy hubs in modern energy systems with renewables and energy storage. *Frontiers in Energy Research*, *10*. https://doi.org/10.3389/fenrg.2022.1014252

Alsaba, W., Al-Sobhi, S. A., & Qyyum, M. A. (2023). Recent advancements in the hydrogen value chain: Opportunities, challenges, and the way Forward–Middle East perspectives. *International Journal of Hydrogen Energy*, *48*(68), 26408–26435. https://doi.org/10.1016/j.ijhydene.2023.05.160

Álvarez, H., Perry, A. L., Blanco, J., García, S., & Aguilar, R. (2019). *PROTECTING THE NORTH SEA: NEW RESEARCH FOR BIODIVERSITY RECOVERY* (p. 20). Oceana, Madrid. https://europe.oceana.org/wp-content/uploads/sites/26/d_files/north_sea_overview_report_web.pdf

Alvik, S. (2022). *The Ukraine war will not derail Europe's energy transition*. DNV. https://www.dnv.com/feature/the-ukraine-war-will-not-derail-europes-energy-transition/

Ankerst, M., Breunig, M. M., Kriegel, H., & Sander, J. (1999). OPTICS. *ACM SIGMOD Record*, *28*(2), 49–60. https://doi.org/10.1145/304181.304187

Ang, B., Choong, W., & Ng, T. (2014). Energy security: Definitions, dimensions and indexes. *Renewable and Sustainable Energy Reviews*, *42*, 1077–1093. https://doi.org/10.1016/j.rser.2014.10.064

Apostolaki-Iosifidou, E., Mccormack, R., Kempton, W., Mccoy, P., & Ozkan, D. (2019). Transmission Design and Analysis for Large-Scale Offshore Wind Energy Development. *IEEE Power and Energy Technology Systems Journal*, *6*(1), 22–31. https://doi.org/10.1109/jpets.2019.2898688

Arteaga, M., Gomis-Bellmunt, O., Lacerda, V., Cheah, M., Castro, B., & Gebraad, P. (2024). Energy Islands: Opportunities, Challenges and Topologies. *Elsevier*.

Babiker, D., & Ciucci, M. (2025, April). *Internal energy market | Fact Sheets on the European Union | European Parliament*. European Parliament. https://www.europarl.europa.eu/factsheets/en/sheet/45/internal-energy-market

Beaubouef, B. (2024, November 4). *Shortage of submarine power cables poses threat to offshore wind market*. Offshore. https://www.offshore-mag.com/renewable-energy/article/55240474/shortage-of-submarine-power-cables-poses-threat-to-offshore-wind-market

Belga. (2025, June 27). Uitstel voor aanbesteding eerste kavel nieuw offshorewindpark | VRT NWS: nieuws. *VRTNWS*. https://www.vrt.be/vrtnws/nl/2025/06/27/aanbesteding-offshore-windpark/

Bengtsson, M. (2024). A site selection of an energy island in the North Sea: optimal location in an ecological and an economic scenario using a Multicriteria Decision Analysis (MCDA) [Master Thesis]. In *Master in Geographical Information Science* (Vol. 30). Lund University.

Benn, T. (2025, June 10). *Wind energy developers: Choosing the right one to work with*. Lumify Energy. https://lumifyenergy.com/blog/wind-energy-developers/

BFN. (2024, November 27). *Dogger Bank NCA*. https://www.bfn.de/en/dogger-bank-nca#anchor-13603

British Chambers of Commerce. (2025). Securing the future of the energy transition in the North Sea. In *britishchambers.org.uk*. https://www.britishchambers.org.uk/wp-content/uploads/2025/03/North-Sea-Transition-Taskforce-Securing-The-Future-Of-The-Energy-Transition-In-The-North-Sea-Report-1.pdf

Brown, D., Reddi, K., & Elgowainy, A. (2022). The development of natural gas and hydrogen pipeline capital cost estimating equations. *International Journal of Hydrogen Energy*, *47*(79), 33813–33826. https://doi.org/10.1016/j.ijhydene.2022.07.270

Buljan, A. (2022, July 5). *Denmark pushes North Sea Energy Island Tender back by one year | Offshore wind*. Offshore Wind. https://www.offshorewind.biz/2022/07/05/denmark-pushes-north-sea-energy-island-tender-back-by-one-year/

Buljan, A. (2025, April 16). *European TSOs: "Energy independence must begin at sea" | Offshore wind*. Offshore Wind. https://www.offshorewind.biz/2025/04/16/european-tsos-energy-independence-must-begin-at-sea/

Calamaio, M. (2024, September 13). *The North Sea Gamble: Energy vs. Ecology?* Green European Journal. https://www.greeneuropeanjournal.eu/energy-vs-ecology-the-north-sea-gamble/

Carlson, S. C. (2024, December 20). *Graph theory | Problems & Applications*. Encyclopedia Britannica. https://www.britannica.com/topic/graph-theory

Chen, H., Ge, H., Wen, J., Qiu, M., & Ngan, H. (2017). Energy network: towards an interconnected energy infrastructure for the future. *arXiv (Cornell University)*. https://doi.org/10.48550/arxiv.1704.04842

Climate & Clean Air Coalition (CCAC). (n.d.). *Why we need to act now*. Climate & Clean Air Coalition. https://www.ccacoalition.org/content/why-we-need-act-now#:~:text=to%202010%20levels).-,Climate%20benefits,C%20of%20warming%20by%202050.&text=Cutting%20emissions%20of%20carbon%20dioxide,set%20by%20the%20Paris%20Agreement

Cockroach Labs. (n.d.). *LINESTRING*. CockroachDB Docs. https://www.cockroachlabs.com/docs/stable/linestring

Dadkhah, A., Van Eetvelde, G., & Vandevelde, L. (2022). Optimal investment and flexible operation of Power-to-Hydrogen systems increasing wind power utilisation. *2022 IEEE International Conference on Environment and Electrical Engineering and 2022 IEEE Industrial and Commercial Power Systems Europe (EEEIC / I&Amp;CPS Europe)*. https://doi.org/10.1109/eeeic/icpseurope54979.2022.9854674

Dagdia, Z. C., & Mirchev, M. (2020). When evolutionary computing meets astro- and geoinformatics. In *Elsevier eBooks* (pp. 283–306). https://doi.org/10.1016/b978-0-12-819154-5.00026-6

Deakin, R. E., Bird, S. C., & Grenfell, R. I. (2002). The Centroid? Where would you like it to be be? *Cartography*, *31*(2), 153–167. https://doi.org/10.1080/00690805.2002.9714213

Dedecca, J. G., & Hakvoort, R. A. (2016). A review of the North Seas offshore grid modeling: Current and future research. *Renewable and Sustainable Energy Reviews*, *60*, 129–143. https://doi.org/10.1016/j.rser.2016.01.112

De Klerk, I., Reijmers, N., Wurpel, G., & Jørgensen, A.-M. (2021). *Social embedding of North Sea energy system integration: A stakeholder analysis* (TNO, Ed.; pp. 1–39) [Report].

De Leener, M. (2025, April 30). *First building blocks of Belgian energy island successfully placed in the North Sea*. Jan De Nul. https://www.jandenul.com/news/first-building-blocks-belgian-energy-island-successfully-placed-north-sea

Dickson, G., & Wesche, J. (2022, March 10). *#14 Wind Power in Europe (with Giles Dickson - CEO of WindEurope)* (episode 14). https://open.spotify.com/episode/3cokRwCOny8086k7BgexwQ?si=y5dpC_wPSlquUgmact9wMw

DNV. (n.d.). *Offshore energy islands*. https://www.dnv.com/energy-transition/offshore-energy-islands/

Dobos, T., Bichler, M., & Knörr, J. (2025). Challenges in finding stable price zones in European electricity markets: Aiming to square the circle? *Applied Energy*, *382*, 125315. https://doi.org/10.1016/j.apenergy.2025.125315

Dowling, R., & Jansen, N. (2023). Potential cases for electrolysis as solution for grid congestion. In *TNO* (TNO 2023 R10556; pp. 6–24). https://publications.tno.nl/publication/34640797/IeFY7I/TNO-2023-R10556.pdf

Dupont, F. (2023, December 4). *Understanding Stakeholders in the Energy and Public Utilities sector*. Borealis Stakeholder Management Software. https://www.boreal-is.com/blog/stakeholders-in-energy-and-utilities-sector/

Durakovic, G., Del Granado, P. C., & Tomasgard, A. (2022). Powering Europe with North Sea offshore wind: The impact of hydrogen investments on grid infrastructure and power prices. *Energy*, *263*, 125654. https://doi.org/10.1016/j.energy.2022.125654

Dute, E., Fokkema, J., Land, M., Wortmann, J., & Douwes, M. (2024). Determining onshore or offshore hydrogen storage for large offshore wind parks: The North Sea Wind Power Hub case. *Journal of Cleaner Production*, *472*, 143395. https://doi.org/10.1016/j.jclepro.2024.143395

Dutch Marine Energy Centre. (2024, November 18). *Energy Hubs & Islands | Dutch Marine Energy Centre*. https://www.dutchmarineenergy.com/use-cases/energy-hubs-and-islands#:~:text=In%20energy%20islands%20all%20assets,without%20one%20large%20island%20structure.

Ehsan, A., & Yang, Q. (2017). Optimal integration and planning of renewable distributed generation in the power distribution networks: A review of analytical techniques. *Applied Energy*, *210*, 44–59. https://doi.org/10.1016/j.apenergy.2017.10.106

Ekoue, M. K., Woerman, M., & Clastres, C. (2025). Intermittency and uncertainty in wind and solar energy: Impacts on the French electricity market. *Energy Economics*, *142*, 108176. https://doi.org/10.1016/j.eneco.2024.108176

Elia. (2025, February 4). *Elia temporarily postpones signing HVDC contracts for Princess Elisabeth Island to weigh multiple options with government in changing market context*. Elia Group. https://www.elia.be/en/press/2025/02/20250204_elia-temporarily-postpones-signing-hvdc-contracts-for-princess-elisabeth-island

EMODnet. (2025). *EMODnet Map Viewer*. emodnet.ec.europa.eu. https://emodnet.ec.europa.eu/geoviewer/

Eneco. (n.d.). *Mission: sustainable energy for everyone | Eneco*. https://www.eneco.nl/en/about-us/who-we-are/mission/

Energie Nederland. (n.d.). *Bulk consumers - Energie Nederland*. https://www.energie-nederland.nl/en/topics/bulk-consumers/

Engati. (n.d.). *Euclidean distance | Engati*. https://www.engati.ai/glossary/euclidean-distance

Erlanger, S. (2025, April 5). The predatory friend: Trump treats Europe as anything but an ally. *The New York Times*. https://www.nytimes.com/2025/04/05/world/europe/trump-europe-tariffs-defense.html

Ester, M., Kriegel, H., Sander, J., & Xu, X. (1996). A density-based algorithm for discovering clusters in large spatial Databases with Noise. *Knowledge Discovery and Data Mining*, 226–231. https://www.aaai.org/Papers/KDD/1996/KDD96-037.pdf

European Commission. (2021a). Assessment of Hydrogen Delivery Options. In *joint-research-centre.ec.europa.eu* (No. JRC124206). https://joint-research-centre.ec.europa.eu/document/download/5cdbd6f7-7ab4-447b-be0a-dde0a25198ab_en

European Commission. (2021b, July 14). *The European Green Deal*. Europese Commission. https://commission.europa.eu/strategy-and-policy/priorities-2019-2024/european-green-deal_nl

European Commission. (2025a). *Hydrogen and decarbonised gas market*. energy.ec.europa.eu. https://energy.ec.europa.eu/topics/markets-and-consumers/hydrogen-and-decarbonised-gas-market_en

European Commission. (2025b, July 10). *Energy Infrastructure (Connecting Europe Facility)*. European Climate, Infrastructure and Environment Executive Agency. https://cinea.ec.europa.eu/programmes/connecting-europe-facility/energy-infrastructure-connecting-europe-facility-0_en

European Council. (2024, November 15). *European Green Deal*. Council of the European Union. https://www.consilium.europa.eu/en/policies/green-deal/

European Commodity Clearing (ECC). (n.d.). *Transmission system operators*. Ecc. https://www.ecc.de/en/about-ecc/partners/transmission-system-operators

European Environment Agency (EEA). (2019, October 29). *Marine protected areas - European Environment Agency (EEA)*. https://www.eea.europa.eu/publications/marine-protected-areas/marine-protected-areas

European Environment Agency (EEA). (2024, June 26). *Global and European temperatures*. European Environment Agency's Home Page. https://www.eea.europa.eu/en/analysis/indicators/global-and-european-temperatures#:~:text=Global%20mean%20temperature%20between%202013,depending%20on%20the%20dataset%20used.

European Environment Agency (EEA). (2025). *Natura 2000 - version end 2023* (1.0) [Dataset]. https://www.eea.europa.eu/en/datahub/datahubitem-view/6fc8ad2d-195d-40f4-bdec-576e7d1268e4

European Hydrogen Backbone (EHB). (n.d.). *The European Hydrogen Backbone (EHB) initiative*. ehb.eu. https://ehb.eu/

European Union Agency for the Cooperation of Energy Regulators (ACER). (2023). UNIT INVESTMENT COSTS INDICATORS FOR ENERGY INFRASTRUCTURE CATEGORIES. In *European Union Agency for the Cooperation of Energy Regulators* (pp. 1–2). https://www.acer.europa.eu/sites/default/files/documents/Publications/ACER_UIC_indicators_table.pdf

Eurostat. (2025). *Shedding light on energy in Europe – 2025 edition*. https://ec.europa.eu/eurostat/web/interactive-publications/energy-2025#energy-consumption

Evans, H. (2014). Guidance on the Offshore Transmission Owner (OFTO) of Last resort mechanism. In *Guidance* [Guidance]. https://www.ofgem.gov.uk/sites/default/files/docs/2014/02/v0_4_ofto_of_last_resort_q1_2014_0.pdf

Equinor. (n.d.). *Hydrogen in Equinor*. https://www.equinor.com/energy/hydrogen

Farahmand, H., Günther, S. H., & Kristiansen, M. (2024). Evaluating the offshore wind business case and green hydrogen production: A case study of a future North Sea Offshore Grid. *Electric Power Systems Research*, *234*, 110814. https://doi.org/10.1016/j.epsr.2024.110814

Federal Maritime and Hydrographic Agency (FMHA). (n.d.). *BSH - State of the North Sea*. https://www.bsh.de/EN/TOPICS/Monitoring_systems/State_of_the_North_Sea/state_of_the_north_sea_node.html

Flanders Marine Institute. (2021). North Sea [Dataset]. In *Global Oceans and Seas* (Version 1). https://doi.org/10.14284/542

Fraley, C., & Raftery, A. E. (1998). How many clusters? which clustering method? Answers via Model-Based Cluster analysis. *The Computer Journal*, *41*(8), 578–588. https://doi.org/10.1093/comjnl/41.8.578

Fornito, A., Zalesky, A., & Bullmore, E. T. (2016). Chapter 2 - Nodes and Edges. In *Fundamentals of Brain Network Analysis*(pp. 37–88). Elsevier Inc. https://doi.org/10.1016/B978-0-12-407908-3.00002-9

Gaonkar, M. N., & Sawant, K. (2013). AutoEpsDBSCAN : DBSCAN with Eps Automatic for Large Dataset. *International Journal on Advanced Computer Theory and Engineering (IJACTE)*, *2*(2). https://www.researchgate.net/profile/Kedar-Sawant-3/publication/373246940_AutoEpsDBSCAN_DBSCAN_with_Eps_Automatic_for_Large_Dataset/links/64e2df291351f5785b7b41fe/AutoEpsDBSCAN-DBSCAN-with-Eps-Automatic-for-Large-Dataset.pdf

Gasunie. (n.d.). *Electrolysis in the North Sea: our role and the role of green hydrogen*. https://www.gasunie.nl/en/expertise/hydrogen/offshore-hydrogen/electrolysis-in-the-north-sea-our-role-and-the-role-of-green-hydrogen

Gasunie. (2025, April 30). Seven questions about offshore hydrogen. *Gasunie*. https://www.gasunie.nl/en/news/seven-questions-about-offshore-hydrogen

Gea-Bermúdez, J., Bramstoft, R., Koivisto, M., Kitzing, L., & Ramos, A. (2023). Going offshore or not: Where to generate hydrogen in future integrated energy systems? *Energy Policy*, *174*, 113382. https://doi.org/10.1016/j.enpol.2022.113382

Gertler, P. J., Shelef, O., Wolfram, C. D., & Fuchs, A. (2016). The Demand for Energy-Using Assets among the World's Rising Middle Classes. *The American Economic Review*, *106*(6), 1366–1401. https://www.jstor.org/stable/43861125

Ghosh, A., & Das, S. K. (2008). Coverage and connectivity issues in wireless sensor networks: A survey. *Pervasive and Mobile Computing*, *4*(3), 303–334. https://doi.org/10.1016/j.pmcj.2008.02.001

GIS Resources. (2020, September 21). *Understanding Shapefile (.shp) File Format*. https://gisresources.com/understanding-shapefile-shp-file-format/

Glaum, P., Neumann, F., & Brown, T. (2024). Offshore power and hydrogen networks for Europe's North Sea. *Applied Energy*, *369*, 123530. https://doi.org/10.1016/j.apenergy.2024.123530

Gluzman, R. (2025, April 3). *Why Government Regulation is Essential for the Energy Transition*. REN21. https://www.ren21.net/why-government-regulation-is-essential-for-the-energy-transition/

Gower, J. C., & Ross, G. J. S. (1969). Minimum spanning trees and single linkage cluster analysis. *Journal of the Royal Statistical Society Series C (Applied Statistics)*, *18*(1), 54. https://doi.org/10.2307/2346439

Greenpeace UK. (2025, July 8). *About Greenpeace - Greenpeace UK*. https://www.greenpeace.org.uk/about-greenpeace/#intro

Gualthérie Van Weezel, T. (2025, May 30). Hoogspanning op de Noordzee. *Volkskrant*. https://www.volkskrant.nl/kijkverder/v/2025/noordzee-energie-windenergie-windmolens-reportage~v1441385/

Gulski, E., Anders, G., Jongen, R., Parciak, J., Siemiński, J., Piesowicz, E., Paszkiewicz, S., & Irska, I. (2021). Discussion of electrical and thermal aspects of offshore wind farms' power cables reliability. *Renewable and Sustainable Energy Reviews*, *151*, 111580. https://doi.org/10.1016/j.rser.2021.111580

Gupta, N. A., Sharma, N. H., & Akhtar, N. A. (2021). A COMPARATIVE ANALYSIS OF K-MEANS AND HIERARCHICAL CLUSTERING. *EPRA International Journal of Multidisciplinary Research (IJMR)*, 412–418. https://doi.org/10.36713/epra8308

Gusatu, L. F., Yamu, C., Zuidema, C., & Faaij, A. (2020). A Spatial analysis of the potentials for offshore wind farm locations in the North Sea Region: Challenges and opportunities. *ISPRS International Journal of Geo-Information*, *9*(2), 96. https://doi.org/10.3390/ijgi9020096

Guşatu, L. F., Zuidema, C., Faaij, A., Martínez-Gordón, R., & Santhakumar, S. (2024). A framework to identify offshore spatial trade-offs in different space allocation options for Offshore Wind Farms, as part of the North Sea Offshore Grid. *Energy Reports*, *11*, 5874–5893. https://doi.org/10.1016/j.egyr.2024.05.052

Hafeezallah, A., Al-Dhamari, A., & Abu-Bakar, S. a. R. (2024). Motion segmentation using Ward's hierarchical agglomerative clustering for crowd disaster risk mitigation. *International Journal of Disaster Risk Reduction*, *102*, 104262. https://doi.org/10.1016/j.ijdrr.2024.104262

Halkidi, M. (2009). Hierarchial clustering. In *Encyclopedia of Database Systems* (pp. 1291–1294). https://doi.org/10.1007/978-0-387-39940-9_604

Hammes, N. (2023, November 8). *Reuse of offshore pipelines for hydrogen transport possible before 2030 - Noordgastransport*. Noordgastransport. https://noordgastransport.nl/reuse-of-offshore-pipelines-for-hydrogen-transport-possible-before-2030/

Hammond, J., Rosenberg, M., & Brown, S. (2025). Understanding costs in hydrogen infrastructure networks: A multi-stage approach for spatially-aware pipeline design. *International Journal of Hydrogen Energy*, *102*, 430–443. https://doi.org/10.1016/j.ijhydene.2024.12.273

Han, J., Kamber, M., & Pei, J. (2012). Data preprocessing. In *Elsevier eBooks* (pp. 83–124). https://doi.org/10.1016/b978-0-12-381479-1.00003-4

Heckman, K. (2024). *Haversine - Distance*. vCalc. https://www.vcalc.com/wiki/vcalc/haversine-distance

Heijnen, P. W. (n.d.-a). H2.1 Eigenschappen van grafen. In *brightspace.tudelft.nl*. https://brightspace.tudelft.nl/d2l/le/content/401755/viewContent/2245580/View

Heijnen, P. W. (2025). Minimum-cost network-layout tool with multi-sinks and multi-sources. In *gitlab.tudelft.nl* (Version 4). https://gitlab.tudelft.nl/pheijnen/optimal-network-layout/-/blob/master/ONLT/Tutorial_Optimal_Network_Layout_Version_3.pdf?ref_type=heads

Heijnen, P. W., Chappin, E. J., & Herder, P. M. (2019). A method for designing minimum-cost multisource multisink network layouts. *Systems Engineering*, *23*(1), 14–35. https://doi.org/10.1002/sys.21492

Herbert Smith Freehills (HSF). (2021). *COORDINATED OFFSHORE TRANSMISSION*. https://tinv.com/wp-content/uploads/2021/11/Coordinated-Offshore-Transmission.pdf

Hydrogen Europe. (2024). Hydrogen Infrastructure report. In *Hydrogen Europe* (pp. 2–6). https://hydrogeneurope.eu/wp-content/uploads/2024/10/2024.10_HE_Hydrogen-Infrastructure-Report.pdf

Ibrahim, O. S., Singlitico, A., Proskovics, R., McDonagh, S., Desmond, C., & Murphy, J. D. (2022). Dedicated large-scale floating offshore wind to hydrogen: Assessing design variables in proposed typologies. *Renewable and Sustainable Energy Reviews*, *160*, 112310. https://doi.org/10.1016/j.rser.2022.112310

International Energy Agency (IEA). (2024a). World Energy Outlook 2024. In *Iea*. https://iea.blob.core.windows.net/assets/140a0470-5b90-4922-a0e9-838b3ac6918c/WorldEnergyOutlook2024.pdf

International Marine Organization (IMO). (n.d.). *Ships' routeing*. https://www.imo.org/en/ourwork/safety/pages/shipsrouteing.aspx

Ismail, F. H., Ali, A. F., Esmat, S., & Hassanien, A. E. (2015). Newcastle Disease virus clustering based on swarm rapid Centroid estimation. In *Advances in intelligent systems and computing* (pp. 359–367). https://doi.org/10.1007/978-3-319-27400-3_32

Jacobsen, S. (2024, August 21). *Denmark's North Sea energy island delayed again by high costs*. reuters.com. https://www.reuters.com/business/energy/denmarks-north-sea-energy-island-delayed-again-by-high-costs-2024-08-21/

Jacquemin, J., Thiran, P., & Quoilin, S. (2024). Prioritizing the role of renewable fuels and hydrogen networks in the transition towards net zero emissions in Western Europe. *Energy*, 134069. https://doi.org/10.1016/j.energy.2024.134069

Jain, A. K. (2010). Data clustering: 50 years beyond K-means. *Pattern Recognition Letters*, 651–666. https://doi.org/10.1016/j.patrec.2009.09.011

James, G. M. (2003). Variance and Bias for General Loss Functions. *Machine Learning*, *51*(2), 115–135. https://doi.org/10.1023/a:1022899518027Jansen, M., Duffy, C., Green, T. C., & Staffell, I. (2022). Island in the Sea: The prospects and impacts of an offshore wind power hub in the North Sea. *Advances in Applied Energy*, *6*, 100090. https://doi.org/10.1016/j.adapen.2022.100090

Jansen, M., Duffy, C., Green, T. C., & Staffell, I. (2022). Island in the Sea: The prospects and impacts of an offshore wind power hub in the North Sea. *Advances in Applied Energy*, *6*, 100090. https://doi.org/10.1016/j.adapen.2022.100090

Janssen, M., Torres, M. P., Braendle, G., Schumacher, J., De Hita, D., & Frontier Economics. (2025). *HARNESSING THE NORTHERN SEAS ENERGY POTENTIAL TO MEET CLIMATE TARGETS*. https://www.frontier-economics.com/media/im3nrl4s/rep-frontier-metastudy-for-hynos-20250130.pdf

Jarman, A. M. (2020). Hierarchical Cluster Analysis: Comparison of Single linkage,Complete linkage, Average linkage and Centroid Linkage Method. *Georgia Southern University, 29*. https://doi.org/10.13140/RG.2.2.11388.90240

Jenkinson, O. (2024, August 22). Denmark's North Sea energy island facing more delays amid high costs. *Windpower Monthly*. https://www.windpowermonthly.com/article/1885854/denmarks-north-sea-energy-island-facing-delays-amid-high-costs

Jordaan, J., & Lategan, L. (2010). *Modelling as research methodology*. https://doi.org/10.18820/9781920383176

Joshi, P. M., & Verma, H. (2021). Synchrophasor measurement applications and optimal PMU placement: A review. *Electric Power Systems Research*, *199*, 107428. https://doi.org/10.1016/j.epsr.2021.107428

Karyotis, V., & Khouzani, M. (2016). Fundamentals of complex communications networks. In *Elsevier eBooks* (pp. 3–26). https://doi.org/10.1016/b978-0-12-802714-1.00011-6

Keck, F., Peller, T., Alther, R., Barouillet, C., Blackman, R., Capo, E., Chonova, T., Couton, M., Fehlinger, L., Kirschner, D., Knüsel, M., Muneret, L., Oester, R., Tapolczai, K., Zhang, H., & Altermatt, F. (2025). The global human impact on biodiversity. *Nature*. https://doi.org/10.1038/s41586-025-08752-2

Khan, M. A., Young, C., Layzell, D. B., THE TRANSITION ACCELERATOR, & CESAR, UNIVERSITY OF CALGARY. (2021). The Techno-Economics of Hydrogen Pipelines. *TRANSITION ACCELERATOR TECHNICAL BRIEFS*, *1*(2), 1–40. https://transitionaccelerator.ca/wp-content/uploads/2023/06/The-Techno-Economics-of-Hydrogen-Pipelines-v2.pdf

Konstantelos, I., Pudjianto, D., Strbac, G., De Decker, J., Joseph, P., Flament, A., Kreutzkamp, P., Genoese, F., Rehfeldt, L., Wallasch, A., Gerdes, G., Jafar, M., Yang, Y., Tidemand, N., Jansen, J., Nieuwenhout, F., Van Der Welle, A., & Veum, K. (2016). Integrated North Sea grids: The costs, the benefits and their distribution between countries. *Energy Policy*, *101*, 28–41. https://doi.org/10.1016/j.enpol.2016.11.024

Koo, B., Ha, Y., & Kwon, H. (2023). Preliminary evaluation of hydrogen blending into high-pressure natural gas pipelines through hydraulic analysis. *Energy*, *268*, 126639. https://doi.org/10.1016/j.energy.2023.126639

Kristiansen, M., Korpås, M., & Farahmand, H. (2018). Towards a fully integrated North Sea offshore grid: An engineering-economic assessment of a power link island. *Wiley Interdisciplinary Reviews Energy and Environment*, *7*(4). https://doi.org/10.1002/wene.296

Levalle, R. R., & Nof, S. Y. (2017). Resilience in supply networks: Definition, dimensions, and levels. *Annual Reviews in Control*, *43*, 224–236. https://doi.org/10.1016/j.arcontrol.2017.02.003

Lévy, J., & Belaïd, F. (2017). The determinants of domestic energy consumption in France: Energy modes, habitat, households and life cycles. *Renewable and Sustainable Energy Reviews*, *81*, 2104–2114. https://doi.org/10.1016/j.rser.2017.06.022

Lipu, H., Ansari, S., Miah, M. S., Hasan, K., Meraj, S. T., Faisal, M., Jamal, T., Ali, S. H., Hussain, A., Muttaqi, K. M., & Hannan, M. (2022). A review of controllers and optimizations based scheduling operation for battery energy storage system towards decarbonization in microgrid: Challenges and future directions. *Journal of Cleaner Production*, *360*, 132188. https://doi.org/10.1016/j.jclepro.2022.132188

Lloyd, S. (1982). Least squares quantization in PCM. *IEEE Transactions on Information Theory*, *28*(2), 129–137. https://doi.org/10.1109/tit.1982.1056489

Lüth, A., & Keles, D. (2024). Risks, strategies, and benefits of offshore energy hubs: A literature-based survey. *Renewable and Sustainable Energy Reviews*, *203*, 114761. https://doi.org/10.1016/j.rser.2024.114761

Lüth, A., Seifert, P. E., Egging-Bratseth, R., & Weibezahn, J. (2023a). How to connect energy islands: Trade-offs between hydrogen and electricity infrastructure. *Applied Energy*, *341*, 121045. https://doi.org/10.1016/j.apenergy.2023.121045

Lüth, A., Werner, Y., Egging-Bratseth, R., & Kazempour, J. (2023b). Electrolysis as a flexibility resource on energy islands: The case of the North Sea. *Energy Policy*, *185*, 113921. https://doi.org/10.1016/j.enpol.2023.113921

Machado, J., Neves, M. V., & Santos, P. J. (2015). Economic limitations of the HVAC transmission system when applied to offshore wind farms. *IEEE*, 69–75. https://doi.org/10.1109/cpe.2015.7231051

MacQueen, J. B. (1967). Some methods for classification and analysis of multivariate observations. *Fifth Berkeley Symposium on Mathematics, Statistics and Probability, University of California Press*, *1*, 281–297. http://digitalassets.lib.berkeley.edu/math/ucb/text/math_s5_v1_article-17.pdf

Marsh, A. (2023, July 7). *Established North Sea maritime borders*. Sovereign Limits. https://sovereignlimits.com/blog/the-north-sea-continental-shelf-cases

Martínez-Gordón, R., Gusatu, L., Morales-España, G., Sijm, J., & Faaij, A. (2022). Benefits of an integrated power and hydrogen offshore grid in a net-zero North Sea energy system. *Advances in Applied Energy*, *7*, 100097. https://doi.org/10.1016/j.adapen.2022.100097

Maptools. (n.d.). *Why use UTM coordinates*. https://www.maptools.com/tutorials/utm/why_use_utm#:~:text=UTM%20Provides%20a%20constant%20distance,of%20latitude%20at%20the%20equator

McKenna, R., D'Andrea, M., & González, M. G. (2021). Analysing long-term opportunities for offshore energy system integration in the Danish North Sea. *Advances in Applied Energy*, *4*, 100067. https://doi.org/10.1016/j.adapen.2021.100067

Melnykov, V., & Michael, S. (2019). Clustering large datasets by merging K-Means solutions. *Journal of Classification*, *37*(1), 97–123. https://doi.org/10.1007/s00357-019-09314-8

Memija, A. (2025, April 30). *First building blocks set for world's first artificial island in Belgian North Sea (VIDEO) | Offshore wind*. Offshore Wind. https://www.offshorewind.biz/2025/04/30/first-building-blocks-set-for-worlds-first-artificial-island-in-belgian-north-sea-video/

Ministry of Foreign Affairs Denmark. (n.d.). *Global Climate Action Strategy*. UM-ENEN. https://um.dk/en/foreign-policy/new-climate-action-strategy

Młodak, A. (2020). k-Means, Ward and Probabilistic Distance-Based Clustering Methods with Contiguity Constraint. *Journal of Classification*, *38*(2), 313–352. https://doi.org/10.1007/s00357-020-09370-5

Møller, K. T., Jensen, T. R., Akiba, E., & Li, H. (2017). Hydrogen - A sustainable energy carrier. *Progress in Natural Science Materials International*, *27*(1), 34–40. https://doi.org/10.1016/j.pnsc.2016.12.014

Murtagh, F., & Contreras, P. (2017). Algorithms for hierarchical clustering: an overview, II. *Wiley Interdisciplinary Reviews Data Mining and Knowledge Discovery*, *7*(6). https://doi.org/10.1002/widm.1219

National Geographic. (2024, April 10). *The importance of Marine Protected Areas (MPAs)*. https://education.nationalgeographic.org/resource/importance-marine-protected-areas/

National Grid. (n.d.). *Corporate information | National Grid*. https://www.nationalgrid.com/about-us/corporate-information

NetworkX. (n.d.). *single_source_dijkstra — NetworkX 3.5 documentation*. https://networkx.org/documentation/stable/reference/algorithms/generated/networkx.algorithms.shortest_paths.weighted.single_source_dijkstra.html

New Energy Coalition. (2024). On the potential of the North Sea region for the future energy supply. In *Energy Trends 2024 Congress* (p. 2). https://www.newenergycoalition.org/custom/uploads/2024/11/On-the-potential-of-the-North-Sea-region-for-the-future-energy-supply.pdf

Nieuwenhout, C., & Andreasson, L. M. (2023). The Legal Framework for Artificial Energy Islands in the Northern Seas. *International Journal of Marine and Coastal Law*, *39*(1), 39–72. https://doi.org/10.1163/15718085-bja10151

Noordgastransport. (2022, August 30). *Transport of gas - Noordgastransport*. https://noordgastransport.nl/transport-of-gas/

Noordzeeloket. (n.d.). *Functions and use*. https://www.noordzeeloket.nl/en/functions-use/

North Sea Energy. (n.d.). *System Integration Concepts — North Sea Energy*. https://northseaenergyroadmap.nl/system-integration-concepts

North Sea Energy. (2020). Unlocking potential of the North Sea. In *TNO*. https://publications.tno.nl/publication/34636747/ENOdsN/NSE-2020-unlocking.pdf

North Sea Energy. (2024). *Commodity specific actions — North Sea Energy*. https://northseaenergyroadmap.nl/commodity-specific-actions/#plan-and-develop-green

North Sea Energy. (2025). *Project Atlas*. https://northseaenergy.projectatlas.app/atlas/make-your-own-map/visibility?map=53.26642,6.91637,5.02,0,0

North Sea Wind Power Hub (NSWPH). (2022a). Unlocking the North Sea as a Green Powerplant - Key Insights 2022. In *northseawindpowerhub.eu*. https://northseawindpowerhub.eu/files/media/document/NSWPH_Insights_15.09.2022_CMYK_without%20cropmarks.pdf

North Sea Wind Power Hub (NSWPH). (2022b). NSWPH Technical Feasibility Report (Concept Stage). In *North Sea Wind Power Hub*. https://northseawindpowerhub.eu/files/media/document/424532-N-RP-0006%20-%20Technical%20Feasibility%20Report%20Rev%20C.pdf

North Sea Wind Power Hub (NSWPH). (2024a). Hubs-and-spokes: A feasible option for offshore infrastructure development in the North Sea. In *North Sea Wind Power Hub Programme Vision Paper* [Vision Paper]. North Sea Wind Power Hub. https://northseawindpowerhub.eu/files/media/document/North%20Sea%20Wind%20Power%20Hub_Vision%20Paper%202024.pdf

North Sea Wind Power Hub (NSWPH). (2024b). Offshore Energy Hubs: Blueprints with Offshore Electrolysis Technical feasibility. In *Discussion Paper*. https://northseawindpowerhub.eu/files/media/document/2024.09.16_NSWPH_Offshore%20Energy%20Hubs%20Blueprints%20with%20Offshore%20Electrolysis_Technical%20feasibility_Discussion%20paper%20%232.pdf

North SEE. (n.d.-a). *Nationally designated priority areas for shipping*. Interreg North Sea Region. https://northsearegion.eu/northsee/s-hipping/nationally-designated-priority-areas-for-shipping/

North SEE. (n.d.). *Transnational energy cooperation between North Sea countries, Interreg VB North Sea Region Programme*. Interreg North Sea Region. https://northsearegion.eu/northsee/e-energy/transnational-energy-cooperation-between-north-sea-countries/

Norton Rose Fulbright. (2025, July). *Understanding hydrogen in the EU*. Netherlands | Global Law Firm | Norton Rose Fulbright. https://www.nortonrosefulbright.com/en-nl/knowledge/publications/7b3fdaed/understanding-hydrogen-in-the-eu

Office of Gas and Electricity Markets (Ofgem). (n.d.). *Offshore Electricity Transmission (OFTO)*. Ofgem. https://www.ofgem.gov.uk/energy-policy-and-regulation/policy-and-regulatory-programmes/offshore-electricity-transmission-ofto

Offshore Transmission System Operators Collaboration (OTC). (2025). Joint planning in Europe's northern seas. In *Offshore TSO Collaboration Expert Paper III*. https://tennet-drupal.s3.eu-central-1.amazonaws.com/default/2025-04/Expert%20Paper%20III%20Offshore%20TSO%20Collaboration%20April%202025_1.pdfOne North Sea. (2021). Cross-border collaboration in the North Sea energy transition. In *One North Sea*. https://onenorthsea.com/storage/files/2eda2e0a-cec8-4cc8-bf45-2aa1a389b63f/One-North-Sea-report-r9.pdf

Ørsted. (n.d.). *Garracummer-Wind-Farm-2*. https://orsted.com/en/who-we-are/our-purpose/our-vision-and-values

OSPAR Commission. (2021). OSPAR Marine Protected Areas Network [Dataset]. In *odims.ospar.org* (Version v002). https://odims.ospar.org/en/submissions/ospar_mpa_2021_07/

Ostend Declaration of Energy Ministers on the North Seas as Europe's Green Power Plant. (2023). In *Government of the Netherlands*. https://www.government.nl/documents/diplomatic-statements/2023/04/24/ostend-declaration-on-the-north-sea-as-europes-green-power-plant

Öttl, A., Termansen, M., & University of Copenhagen, Department of Food and Resource Economics. (2025). Agent-Based Modelling of food systems: A scoping review on incorporation of behavioural insights. In *Environmental Modelling and Software* [Journal-article]. https://doi.org/10.1016/j.envsoft.2025.106617

Peters, R., Vaessen, J., & Van Der Meer, R. (2020). Offshore Hydrogen Production in the North Sea Enables Far Offshore Wind Development. *One Petro*. https://doi.org/10.4043/30698-ms

Pillay, C. J., Kabeya, M., & Davidson, I. E. (2020). Transmission Systems: HVAC vs HVDC. In *Proceedings of the 5th NA International Conference on Industrial Engineering and Operations Management* [Conference-proceeding]. https://www.ieomsociety.org/detroit2020/papers/450.pdf

PosHYdon. (n.d.). *Poshydon | Over PoSHYDon*. https://poshydon.com/nl/home/overposhydon/

Quirk, D. G., Underhill, J. R., Gluyas, J. G., Wilson, H. A., Howe, M. J., & Anderson, S. (2021). The North Sea through the energy transition. *First Break*, *39*(4), 31–43. https://doi.org/10.3997/1365-2397.fb2021026

Rahman, S. (2017). Basic graph Theory. In *Undergraduate Topics in Computer* Ramboll. (2025). *The rise of offshore hydrogen production at scale*. https://www.ramboll.com/net-zero-explorers/offshore-hydrogen-at-scale

Rettig, E., Fischhendler, I., & Schlecht, F. (2023). The meaning of energy islands: Towards a theoretical framework. *Renewable and Sustainable Energy Reviews*, *187*, 113732. https://doi.org/10.1016/j.rser.2023.113732

Reuters. (2025, May 16). *Dutch postpone offshore wind farm tenders due to low interest* [Press release]. https://www.reuters.com/business/energy/dutch-postpone-offshore-wind-farm-tenders-due-low-interest-2025-05-16/Rezaei, G., Afshar, M. H., & Rohani, M. (2014). Layout optimization of looped networks by constrained ant colony optimisation algorithm. *Advances in Engineering Software*, *70*, 123–133. https://doi.org/10.1016/j.advengsoft.2014.01.009

Rijksdienst voor Ondernemend Nederland (RVO). (2025, May 7). *Offshore hydrogen production*. RVO.nl. https://english.rvo.nl/topics/hydrogen/offshore-hydrogen-production

Rokach, L., & Maimon, O. (2006). Clustering methods. In *Springer eBooks* (pp. 321–352). https://doi.org/10.1007/0-387-25465-x_15

Roland Berger. (2024). *Standard beats size in Europe's offshore wind*. https://topsectorenergie.nl/nl/kennisbank/standaardisatie-verslaat-grootte-de-toekomst-van-offshore-windturbines/#:~:text=Volgens%20de%20studie%20%22Standard%20Beats,broodnodige%20groei%20van%20de%20sector

Romeo, G. (2020). Linear programming. In *Elsevier eBooks* (pp. 383–415). https://doi.org/10.1016/b978-0-12-817648-1.00007-4

RWE. (n.d.). *H2OPZEE – Demonstration project for green hydrogen in the Netherlands*. https://www.rwe.com/en/research-and-development/hydrogen-projects/h2opzee/

S&P Global. (n.d.). *Global Energy Security*. spglobal.com. https://www.spglobal.com/en/research-insights/market-insights/geopolitical-risk/global-energy-security

Salgado, C. M., Azevedo, C., Proença, H., & Vieira, S. M. (2016). Noise versus outliers. In *Springer eBooks* (pp. 163–183). https://doi.org/10.1007/978-3-319-43742-2_14

Salih, N. M., & Jacksi, K. (2020). Semantic Document Clustering using K-means algorithm and Ward's Method. *2020 International Conference on Advanced Science and Engineering (ICOASE)*, 978-1-6654-1579-8/20. https://doi.org/10.1109/icoase51841.2020.9436588

Sall, P. (2023, March 17). *DNV study shows high offshore hydrogen infrastructure potential for Europe*. DNV. https://www.dnv.com/news/dnv-study-shows-high-offshore-hydrogen-infrastructure-potential-for-europe-241164/

Santaella, M. I. (2025, February 7). *EU boosts energy infrastructure with €1.25bn in grants*. WindEurope. https://windeurope.org/newsroom/news/eu-boosts-energy-infrastructure-with-1-25bn-in-grants/#:~:text=The%20European%20Commission%20has%20allocated,and%20its%20wider%20energy%20transition.

Sayani, J. K. S., Wang, M., Ma, Z., Sharan, P., Mehana, M., & Chen, B. (2025). Techno-economic analysis of hydrogen transport via repurposed natural gas pipelines: Flow dynamics and infrastructure tradeoffs. *International Journal of Hydrogen Energy*, *147*, 150033. https://doi.org/10.1016/j.ijhydene.2025.150033

Sharma, N., & Kumar, K. (2021). Resource allocation trends for ultra dense networks in 5G and beyond networks: A classification and comprehensive survey. *Physical Communication*, *48*, 101415. https://doi.org/10.1016/j.phycom.2021.101415

Signorelli, G., & Leonardi, M. (2025, April 11). *GAS AND THE GREEN DEAL: THE GEOPOLITICS OF TARIFFS BETWEEN TRUMP, THE EU AND CHINA*. eccoclimate.org. https://eccoclimate.org/gas-and-the-green-deal-the-geopolitics-of-tariffs-between-trump-the-eu-and-china/Soares-Ramos, E. P., De Oliveira-Assis, L., Sarrias-Mena, R., & Fernández-Ramírez, L. M. (2020). Current status and future trends of offshore wind power in Europe. *Energy*, *202*, 117787. https://doi.org/10.1016/j.energy.2020.117787

Slowinski, R., Sagdur, Y., Van Rossum, R., Kozub, A., Overgaag, M., Blanco, A. A., Michelet, A., Ho, G., Kandathiparambil, S., & London, P. (2023). IMPLEMENTATION ROADMAP — CROSS BORDER PROJECTS AND COSTS UPDATE. In *European Hydrogen Backbone*. Guidehouse. https://ehb.eu/files/downloads/EHB-2023-Implementation-Roadmap-Part-1.pdf

Sovacool, B. K., & Mukherjee, I. (2011). Conceptualizing and measuring energy security: A synthesized approach. *Energy*, *36*(8), 5343–5355. https://doi.org/10.1016/j.energy.2011.06.043

SSE Renewables. (n.d.). *Dogger Bank Offshore Wind Farm | SSE Renewables*. https://www.sserenewables.com/offshore-wind/projects/dogger-bank

Staeb, J. (2025, January 8). *Spatial planning North Sea - DigiShape*. DigiShape. https://www.digishape.nl/en/program/spatial-planning-north-sea/

Starczewski, A., Goetzen, P., & Er, M. J. (2020). A new method for automatic determining of the DBSCAN parameters. *Journal of Artificial Intelligence and Soft Computing Research*, *10*(3), 209–221. https://doi.org/10.2478/jaiscr-2020-0014

Steinberg, F., & Anderson, J. (2025, April 14). The Possible European Response to Trump's "Reciprocal" Tariffs. *Center for Strategic & International Studies*. https://www.csis.org/analysis/possible-european-response-trumps-reciprocal-tariffs

Stichting De Noordzee. (2022, May 19). *Onze doelen - Stichting De Noordzee*. https://www.noordzee.nl/onze-doelen/

Svendsen, H. G. (2013). Planning tool for clustering and optimised grid connection of offshore wind farms. *Energy Procedia*, *35*, 297–306. https://doi.org/10.1016/j.egypro.2013.07.182

Swallow, T. (2024, February 11). EY: Will Consumers Pay More for Sustainably Sourced Energy? *SustainabilityMag*. https://sustainabilitymag.com/renewable-energy/ey-will-consumers-pay-more-for-sustainably-sourced-energy

Tang, A. (2022, November 17). *Energy islands coming to Europe's seas*. WindEurope. https://windeurope.org/newsroom/news/energy-islands-coming-to-europes-seas/

TenneT. (n.d.). *Offshore TSO Collaboration*. tennet.eu. https://www.tennet.eu/offshore-tso-collaboration

TenneT. (2025, April 19). *12 Offshore TSOs are striving for integrated offshore grid to strengthen European energy independence*. tennet.eu. https://www.tennet.eu/news/12-offshore-tsos-are-striving-integrated-offshore-grid-strengthen-european-energy-independenceTerenzi, A., Iacozza, C., Rossi, C., Scarsciafratte, D., Arcangeletti, G., & Aloigi, E. (2024). *Leading the Energy Transition: A Novel Approach to Existing Gas Pipelines Retrofitting for Hydrogen Transport*. Society of Petroleum Engineers (SPE). https://doi.org/10.2118/220011-ms

Thommessen, C., Otto, M., Nigbur, F., Roes, J., & Heinzel, A. (2021). Techno-economic system analysis of an offshore energy hub with an outlook on electrofuel applications. *Smart Energy*, *3*, 100027. https://doi.org/10.1016/j.segy.2021.100027

TNO. (n.d.). *15 things you need to know about hydrogen | TNO*. tno.nl/en. https://www.tno.nl/en/sustainable/industry/carbon-neutral-industry/clean-hydrogen-production/15-things-hydrogen/

Tobback, B. (2025, April 3). *Ensuring Europe's energy independence in the face of geopolitical crises: bringing clean and affordable energy to people and businesses*. The European Files. https://www.europeanfiles.eu/energy/ensuring-europes-energy-independence-in-the-face-of-geopolitical-crises-bringing-clean-and-affordable-energy-to-people-and-businesses

Tooki, O. O., & Popoola, O. M. (2024). A comprehensive review on recent advances in transactive energy system: Concepts, models, metrics, technologies, challenges, policies and future. *Renewable Energy Focus*, *50*, 100596. https://doi.org/10.1016/j.ref.2024.100596

Tosatto, A., Beseler, X. M., Østergaard, J., Pinson, P., & Chatzivasileiadis, S. (2022). North Sea Energy Islands: Impact on national markets and grids. *Energy Policy*, *167*, 112907. https://doi.org/10.1016/j.enpol.2022.112907

Traber, T., Koduvere, H., & Koivisto, M. (2017). Impacts of offshore grid developments in the North Sea region on market values by 2050: How will offshore wind farms and transmission lines pay? *2022 18th International Conference on the European Energy Market (EEM)*, 1–6. https://doi.org/10.1109/eem.2017.7981945

Tractebel. (2024, September 30). *World's first energy island takes shape in Belgium's North Sea*. https://tractebel-engie.com/en/news/2024/world-s-first-energy-island-takes-shape-in-belgium-s-north-sea

Transport & Environment (T&E). (2024, May 31). *Europe's hydrogen plans reliant on uncertain imports – report*. T&E. https://www.transportenvironment.org/articles/europes-hydrogen-plans-reliant-on-uncertain-imports-report

Travaglini, R., Frowijn, L., Bianchini, A., Lukszo, Z., & Bruninx, K. (2025). Offshore or onshore hydrogen production? A critical analysis on costs and operational considerations for the Dutch North Sea. *Applied Energy*, *397*, 126290. https://doi.org/10.1016/j.apenergy.2025.126290

United Kingdom (UK) Hydrographic Office. (2025). UK EEZ Ships' Routeing Measurs [Dataset]. In *Marine Data Portal*. https://datahub.admiralty.co.uk/portal/apps/sites/#/marine-data-portal/maps/ba5b015a34b24c298fb5e1038226502a/about

United Nations (UN). (2024). *The Paris Agreement*. unfccc.int. https://unfccc.int/process-and-meetings/the-paris-agreement

United Nations Convention on the Law of the Sea (UNCLOS). (1982). https://www.un.org/depts/los/convention_agreements/texts/unclos/unclos_e.pdf

United States Department of Energy (US DOE). (n.d.). *Hydrogen production: electrolysis*. Energy.gov. https://www.energy.gov/eere/fuelcells/hydrogen-production-electrolysis

Valencia-Rivera, G. H., Benavides-Robles, M. T., Morales, A. V., Amaya, I., Cruz-Duarte, J. M., Ortiz-Bayliss, J. C., & Avina-Cervantes, J. G. (2023). A systematic review of metaheuristic algorithms in electric power systems optimization. *Applied Soft Computing*, *150*, 111047. https://doi.org/10.1016/j.asoc.2023.111047

Van De Weijer, B. (2024, April 6). De Noordzee van fossiel naar Groen. *Volkskrant*. https://www.volkskrant.nl/kijkverder/v/2024/staat-hier-de-toekomst-van-groene-waterstof~v1051103/

Van De Weijer, B. (2025, April 10). Netbeheerders willen gezamenlijk stroomnet op de Noordzee bouwen. *Volkskrant*. https://www.volkskrant.nl/economie/netbeheerders-willen-gezamenlijk-stroomnet-op-de-noordzee-bouwen-waarmee-duizend-miljard-euro-kan-worden-bespaard~b2024c5a/

Van Den Assum, J. C. (2022). *Traversing obstacles: Designing energy infrastructure networks in a geographical cost-differentiated context* [Master thesis, Delft University of Technology]. https://repository.tudelft.nl/record/uuid:512431bf-13f5-4c6d-808a-8c961b780d48

Van Der Veer, E., Sweers, B., Kawale, D., Van Unen, M., Van Schot, M., Kee, J., Howell, F., Renz, M., De Vries, E., Tak, S., Knoors, B., Meijer, S., Audenaert, S., Van Der Keere, L., De Schutter, R., Xiao, M., Ter Veld, H., Rajavelu, K., & Pernot, E. (2020).

Offshore energy islands Deliverable D3.8. In *North Sea Energy*. https://north-sea-energy.eu/static/0856dd12a36d1f321aaf757706bd5913/8a.-FINAL-NSE3_D3.8-Final-report-on-the-techno-economic-environmental-and-legal-assessment-of-offshore-energy-islands.pdf

Van Dyke, J. M. (1991). Military exclusion and warning zones on the high seas. *Marine Policy*, *15*(3), 147–169. https://www.sciencedirect.com/science/article/pii/0308597X9190059K

Van Rossum, R., Jens, J., La Guardia, G., Wang, A., Kühnen, L., & Overgaag, M. (2022). *A EUROPEAN HYDROGEN INFRASTRUCTURE VISION COVERING 28 COUNTRIES* [Report]. Guidehouse. https://www.europeangashub.com/wp-content/uploads/2022/04/EHB-A-European-hydrogen-infrastructure-vision-covering-28-countries.pdf

Van Tongeren, D. H. J. (2022). Constructing and analysing offshore hydrogen system design powered by wind farms in the North Sea: A multi-sink multi-source network optmisation approach [Master thesis, Delft University of Technology]. https://repository.tudelft.nl/record/uuid:9976f270-509a-4236-be65-0a71ac95b5e7

Van Wingerden, T., Geerdink, D., Taylor, C., & Hülsen, C. F. (2023). Specification of a European offshore hydrogen backbone. In *DNV*. DNV. https://aquaventus.org/wp-content/uploads/2023/03/DNV-Study_Specification_of_a_European_Offshore_Hydrogen_Backbone.pdf

Vattenfall. (n.d.-a). *About us - Our company*. https://group.vattenfall.com/about-us

Vattenfall. (n.d.-b). *Our strategy and vision*. https://group.vattenfall.com/about-us/strategy

Vattenfall. (2024, February 26). *Wind op zee blijft grote rol spelen in energietransitie*. https://group.vattenfall.com/nl/newsroom/achtergrondartikel/2024/wind-op-zee-blijft-grote-rol-spelen-in-energietransitie

Veness, C. (n.d.). *Calculate distance and bearing between two Latitude/Longitude points using haversine formula in JavaScript*. https://www.movable-type.co.uk/scripts/latlong.html

Venugopalan, S., Garcia Navarro, J., & Buijs, L. (2024). State of art in Offshore Hydrogen production. In *topsectorenergie.nl*. https://topsectorenergie.nl/documents/1302/State_of_art_in_Offshore_Hydrogen_production.pdf

Vijaya, N., Sharma, S., & Batra, N. (2019). Comparative study of single linkage, complete linkage, and Ward method of agglomerative clustering. *2022 International Conference on Machine Learning, Big Data, Cloud and Parallel Computing (COM-IT-CON)*. https://doi.org/10.1109/comitcon.2019.8862232

Von Meier, A. (2006). *Electric Power Systems: A Conceptual Introduction*. https://gacbe.ac.in/images/E%20books/Electric%20Power%20Systems%20-%20A%20Conceptual%20Introduction%20-%20A.%20von%20Meier%20(Wiley,%202006).pdf

Wang, A., Van Der Leun, K., Peters, D., & Buseman, M. (2020). European Hydrogen Backbone: How a dedicated hydrogen infrastructure can be created. In *European Hydrogen Backbone (EHB)*. Guidehouse. https://ehb.eu/files/downloads/2020_European-Hydrogen-Backbone_Report.pdf

Wang, X., Ning, F., Lin, Z., & Zhang, Z. (2025). Efficient ship pipeline routing with dual-strategy enhanced ant colony optimization: Active behavior adjustment and passive environmental adaptability. *Journal of Manufacturing Systems*, *80*, 673–693. https://doi.org/10.1016/j.jmsy.2025.04.003

Wang, Y., Wu, Q., Liu, H., & Kang, Z. (2023). Research progress of hydrogen compatibility testing methods and hydrogen embrittlement prevention measures for pipeline steel. *You Qi Chu Yun/Oil and Gas Storage and Transportation*, *42*(11), 1251–1260. https://doi.org/10.6047/j.issn.1000-8241.2023.11.005

Ward, J. H. (1963). Hierarchical grouping to optimize an objective function. *Journal of the American Statistical Association*, *58*(301), 236–244. https://doi.org/10.1080/01621459.1963.10500845

Wen, Q., Huang, F., Xiao, H., Xu, Y., Hu, Q., & Liu, J. (2023). Improving hydrogen induced cracking resistance of high strength acid-resistant submarine pipeline steels via trace-Mg treatment. *International Journal of Hydrogen Energy*, *48*(39), 14808–14821. https://doi.org/10.1016/j.ijhydene.2022.12.322

Wiegner, J., Andreasson, L., Kusters, J., & Nienhuis, R. (2023). Interdisciplinary perspectives on offshore energy system integration in the North Sea: A systematic literature review. *Renewable and Sustainable Energy Reviews*, *189*, 113970. https://doi.org/10.1016/j.rser.2023.113970

Wikipedia contributors. (2010, October 6). *Map of the North Sea*. Wikipedia. https://en.wikipedia.org/wiki/North_Sea#/media/File:North_Sea_map-en.png

WindEurope. (2019). Industry position on how offshore grids should develop. In *windeurope.org*. https://windeurope.org/wp-content/uploads/files/policy/position-papers/WindEurope-Industry-position-on-how-offshore-grids-should-develop.pdf

WindEurope. (2024, December 6). *No offshore bids in Denmark – disappointing but sadly not surprising* [Press release]. https://windeurope.org/newsroom/press-releases/no-offshore-bids-in-denmark-disappointing-but-sadly-not-surprisingWorld Meteorological Organization (WMO). (2024, October 25). *Greenhouse gas concentrations surge again to new record in 2023*. World

Meteorological Organization. https://wmo.int/news/media-centre/greenhouse-gas-concentrations-surge-again-new-record-2023

Winzer, C. (2012). Conceptualizing energy security. *Energy Policy*, *46*, 36–48. https://doi.org/10.1016/j.enpol.2012.02.067

World Wide Fund for Nature (WWF). (n.d.). *Our values*. WWF. https://www.wwf.eu/about_us/our_values/

Wu, Q., Peng, L., Han, G., Shu, J., Yuan, M., & Wang, B. (2025). Deep-Learning-Based scheduling optimization of Wind-Hydrogen-Energy storage system on energy islands. *Energy*, 135107. https://doi.org/10.1016/j.energy.2025.135107

Xiang, X., Merlin, M., & Green, T. (2016). Cost analysis and comparison of HVAC, LFAC and HVDC for offshore wind power connection. *The 16th IET International Conference on AC and DC Power Transmission (ACDC 2020)*, 6 (6 .). https://doi.org/10.1049/cp.2016.0386

Xu, L. (2024). Optimizing energy hub systems: A comprehensive analysis of integration, efficiency, and sustainability. *Computers & Electrical Engineering*, *120*, 109779. https://doi.org/10.1016/j.compeleceng.2024.109779

York, T. (2025, June 9). *Why wind farm developers are pulling out at the last minute*. The Conversation. https://theconversation.com/why-wind-farm-developers-are-pulling-out-at-the-last-minute-256842

Younas, M., Shafique, S., Hafeez, A., Javed, F., & Rehman, F. (2022). An overview of hydrogen production: current status, potential, and challenges. *Fuel*, *316*, 123317. https://doi.org/10.1016/j.fuel.2022.123317

Zhang, C., Song, P., Hou, J., Xiao, L., Wang, X., Yang, F., & Wang, X. (2024a). Technical and economic analysis of hydrogen production, storage and transportation by offshore wind power in different scenarios: A Guangdong case study. *International Journal of Hydrogen Energy*, *94*, 829–837. https://doi.org/10.1016/j.ijhydene.2024.10.346

Zhang, Z., Li, J., Lei, Z., Zhu, Q., Cheng, J., & Gao, S. (2024b). Reinforcement learning-based particle swarm optimization for wind farm layout problems. *Energy*, 134050. https://doi.org/10.1016/j.energy.2024.134050

Zhou, J., Peng, J., Liang, G., & Deng, T. (2018). Layout optimization of tree-tree gas pipeline network. *Journal of Petroleum Science and Engineering*, *173*, 666–680. https://doi.org/10.1016/j.petrol.2018.10.067

Appendix A: Background Research Methodology

In this Appendix, required background theory is provided for Ward's clustering, the haversine formula and the hydrogen backbone rerouting procedure.

A1. Mathematical Explanation of Ward's Clustering

In Ward's method (Ward, 1963), each data point initially forms its own cluster. Given n OWFs, there are n initial clusters. Then, two clusters are merged incrementally if it results in the smallest increase in within-cluster variance.

The increase in variance is formally expressed using the error sum of squares (ESS). ESS is defined for a cluster c as the sum of squared Euclidean distances between the position each OWF i, denoted as x_i, and a cluster centroid x_c. The centroid x_c is the average position of all OWFs in cluster c. ESS of cluster c is calculated as:

$$ESS_c = \sum_{i=1}^{n_c} \|x_i - x_c\|^2$$

Where n_c represents the number of OWFs in cluster c. The Euclidean distance (Engati, n.d.) is indicated as $\|\cdot\|$, and is calculated as:

$$d_{AB} = \sqrt{(lat_B - lat_A)^2 + (lon_B - lon_A)^2}$$

Here, d_{AB} is the distance between point A and B in degrees, with (lat_A, lon_A) and (lat_B, lon_B) representing the geographic coordinates for, respectively, point A and B.

The ESS is presented for an individual cluster c. The total ESS, which is the sum over all clusters, reflects the compactness of the clustering. At each step, the cluster pair that results in the smallest increase in total ESS are merged. In the context of this thesis, compact clusters directly translate to shorter average cable lengths between OWFs and the island they are connected to. Minimizing ESS therefore contributes to minimizing electricity cabling, and thus on costs.

Based on Hafeezallah et al. (2024), the increase is given by:

$$\Delta ESS(c_1, c_2) = \frac{n_{c_1} \cdot n_{c_2}}{n_{c_1} + n_{c_2}} \left\| x_{c_1} - x_{c_2} \right\|^2$$

Here, clusters c_1 and c_2, with sizes n_{c_1} and n_{c_2}respectively, and centroids x_{c_1} and x_{c_2} respectively, are merged. $\left\| x_{c_1} - x_{c_2} \right\|$ is the Euclidean distance between the centroids of each cluster c_1 and c_2. $\frac{n_{c_1} \cdot n_{c_2}}{n_{c_1} + n_{c_2}}$ is a factor that increases with the size of the clusters, meaning that when larger clusters are merged, the contribution to the total variance is larger.

A2. Haversine Formula

The haversine formula (Heckman, 2024) is:

$$d_i = 2 \cdot R_{Earth} \cdot \sin^{-1}\left(\sqrt{\sin\left(\frac{(lat_2 - lat_1)}{2}\right)^2 + \sin\left(\frac{(lon_2 - lon_1)}{2}\right)^2 \cdot \cos(lat_1) \cdot \cos(lat_2)}\right)$$

Here, R_{Earth} is the Earth's radius, equal to 6371 km, lat_1 and lat_2 are the latitude coordinates of the two nodes in radians and lon_1 and lon_2 are the longitude coordinates in radians. This formulation accounts for the North-South distance via $\sin\left(\frac{(lat_2 - lat_1)}{2}\right)^2$, via the East-West distance via $\sin\left(\frac{(lon_2 - lon_1)}{2}\right)^2$, which is weighted by the proximity to the Equator via $\cos(lat_1) \cdot \cos(lat_2)$.

A3. Hydrogen Backbone Rerouting Procedure

The rerouting procedure for infeasible segments of the hydrogen backbone costs of five steps, which are discussed below.

Step 1: Supply and demand nodes

The two end nodes of each edge that is to be rerouted, are assigned as supply and demand nodes. If one is a terminal, meaning energy islands are supply nodes, entry points are demand nodes, its roles are fixed. If both end nodes are terminals with different functions, its roles are also fixed. However, if both are terminals of the same type, it is assigned arbitrarily what its role will be. This also happens if none of the end nodes are terminals. If an end node lies inside a forbidden area, it is moved to the nearest reachable node outside this area, using Dijkstra's shortest path algorithm on the initial backbone (NetworkX, n.d.). This nearest reachable node is in opposite direction of the neighbour node which is connected via the infeasible segment. The infeasible segment is thereby extended, and multiple edges are included for rerouting.

Additionally, there is a special case. If both end nodes are entry points, and one has node degree equal to 1, that entry point is removed and its demand is merged into the other. This assumes that its connection would be provided via the onshore network instead.

Step 2: Rerouting area

The rerouting area is defined as the area between the supply and demand nodes, covering the total segment that is to be rerouted, and this is expanded by a buffer zone.

Step 3: Supply and demand capacity

The supply and demand for the end nodes of the rerouted segment are based on the capacity of the original edge. For multi-edge segments, the maximum capacity is taken to avoid underestimating the required flow.

Step 4: Obstacles

All forbidden areas within the rerouting area are identified and extracted as closed polygons.

Step 5: Existing connections

The identification of existing connections in the rerouted area is based on the edge classification. If an edge is classified as *not used*, it is included in the rerouting process. *Repurposed* pipelines are included with their remaining unused diameter, which is determined as:

$$D_{initial} - D_{final} > 0$$

These pipelines are cut into usable segments, and the remaining unused part is added as available infrastructure for the rerouting process.

Appendix B: Final Offshore Wind Farm Dataset

In this Appendix, an overview of all OWFs that are included in modelling are presented. For each OWF, it includes detailed information including its name, coordinates, electrical capacity, distance from shore, average distance to all other OWFs and appropriate parameter values for the distance-based categories. This information is presented in Table B.1 and Table B.2.

Wind Farm	Latitude	Longitude	Electrical Capacity (MW)	Distance to Shore (km)	Share of Electricity to Island	Share of Hydrogen Production	Average Distance to Other OWFs (km)
Albatros	54.48599838	6.248965584	10000	125.0	100%	100%	286.0
Alpha Ventus	54.0107831	6.606859144	6000	136.3	100%	100%	286.6
Amrumbank West	54.52295552	7.705657429	1000	197.5	100%	100%	287.0
Aspen	57.73950507	-0.224128781	2000	221.5	100%	100%	292.3
Avalon	58.23	-0.43	1200	195.8	100%	100%	293.7
Bard Offshore 1	54.35528757	5.980842648	12000	145.7	100%	100%	294.2
Beech	57.8957789	1.681856621	1500	99.7	100%	50%	295.4
Beech North	57.97	0.49	2000	112.8	100%	100%	295.9
Beech South	56.67	1.4	2000	98.8	100%	50%	297.5
Bellrock	56.84559681	0.035515129	2000	105.0	100%	100%	297.8
Belwind Alstom Haliade Demonstration	51.69	2.84	4000	82.9	100%	50%	297.9
Belwind phase 1	51.6687628	2.804547819	2000	108.0	100%	100%	299.0
Belwind phase 2 (Nobelwind) (Zone 1)	51.67886682	2.787309893	500	119.3	100%	100%	299.7
Belwind phase 2 (Nobelwind) (Zone 2)	51.65659836	2.829339971	270	94.1	100%	50%	300.2
Berwick Bank Wind Farm	56.29191816	-1.467124249	252	89.3	100%	50%	300.5
Borkum Riffgrund 1	53.96736369	6.554129207	402	87.6	100%	50%	301.7
Borkum Riffgrund 2	53.95174172	6.487406878	400	89.5	100%	50%	303.1
Borkum Riffgrund 3	54.04678221	6.19424311	9000	116.7	100%	100%	303.5
Borssele Kavel I	51.74725302	3.060109669	1400	164.9	100%	100%	303.6
Borssele Kavel II	51.63497752	3.069337933	2000	109.5	100%	100%	303.8
Borssele Kavel III	51.66887935	2.969346058	630	83.7	100%	50%	304.6
Borssele Kavel IV	51.7362141	2.882120202	2500	112.0	100%	100%	307.2
Borssele Kavel V	51.70915687	3.003305575	117.6	97.9	100%	50%	307.7
Bowdun Offshore Wind Farm	56.9749046	-1.345889487	960	83.0	100%	50%	308.0
Broadshore	58.17323757	-1.802029175	2500	113.0	100%	100%	308.3
Buchan Deep Demo	57.48427079	-1.362140464	4000	40.0	50%	50%	308.4
Buchan Offshore Wind Farm	58.40883352	-1.235008822	2500	110.0	100%	100%	308.7
Butendiek	55.01757524	7.774023087	700	56.0	50%	50%	309.2
C-Power (Zone A)	51.53911194	2.921967755	3500	106.4	100%	100%	309.4
C-Power (Zone B)	51.56316742	2.984985241	2500	112.0	100%	100%	309.5
Caledonia Offshore Wind Farm	58.19710311	-2.486717694	300	57.8	50%	50%	310.6
CampionWind	57.30623508	0.113762015	497	86.9	100%	50%	310.6
Cedar	56.97128098	0.718430479	980	75.9	100%	50%	310.7
Cenos	57.12193846	1.429374466	1200	131.0	100%	100%	310.8
Central North Sea Electrification	57.11	1.96	400	93.8	100%	50%	310.8
Culzean	57.19147016	1.876484997	2400	121.1	100%	100%	311.1
Dan Tysk	55.13718305	7.200771829	5500	107.8	100%	100%	311.2
Deutsche Bucht	54.30499854	5.792052217	2500	110.0	100%	100%	311.7
Dogger Bank A	54.76947456	1.908959638	2500	112.0	100%	100%	312.4
Dogger Bank B	54.97737666	1.679728774	1000	260.0	100%	100%	312.5
Dogger Bank C	55.03972759	2.8226577	1500	122.2	100%	100%	313.0
Dogger Bank D	55.06	2.94	300	56.0	50%	50%	313.9
Dudgeon	53.26535507	1.380715375	2500	109.0	100%	100%	314.1
Dudgeon Extension	53.27895727	1.373070395	2500	112.0	100%	100%	314.8
East Anglia North Tranche 2 (Norfolk Boreas)	53.0384249	2.941607792	1000	146.0	100%	100%	314.9
East Anglia North Tranche One East (Norfolk Vanguard East)	52.82861535	2.925100007	1020	101.0	100%	100%	315.9
East Anglia North Tranche One West (Norfolk Vanguard West)	52.91205059	2.47338818	1200	131.0	100%	100%	316.0
East Anglia One	52.2373483	2.503504787	4000	91.9	100%	50%	316.6
East Anglia One North	52.38105833	2.431137626	913	53.1	50%	50%	317.3
East Anglia Three	52.66515209	2.855666975	4000	32.5	50%	50%	320.9
East Anglia Two	52.15338928	2.201472319	2100	200.0	100%	100%	321.3
EN11	54.78934202	6.372875137	1000	117.0	100%	100%	321.6
EN12	54.85016443	6.147061706	1500	99.5	100%	50%	323.0
EN13	55.0807226	6.395384863	1218	105.7	100%	100%	324.5
EN13-Nord	55.29488867	6.479948157	200	45.0	50%	50%	324.7
EN14	54.78147118	5.077249514	203.2	46.7	50%	50%	324.8
EN16	55.25050315	5.489048158	1000	139.0	100%	100%	326.3
EN17	55.26128471	4.698772634	288	83.3	100%	50%	326.5
EN19	55.78422029	3.637845755	378	42.6	50%	50%	327.9
EN20	55.2521955	4.764952301	1386	89.5	100%	50%	328.9
EnBW He Dreiht	54.36522994	6.186484129	465.4	34.6	50%	50%	329.5
EnBW Hohe See	54.44337185	6.329969754	62	40.5	50%	50%	330.9
Five Estuaries	51.90196402	2.161681604	312	34.9	50%	50%	330.9
Flora	57.4949796	-1.177342776	2000	92.6	100%	50%	332.1
Freya	57.27	7.54	2100	170.0	100%	100%	333.9
Future Tender A	53.638125	3.197021	2000	49.5	50%	50%	334.1
Future Tender B	53.602285	3.191528	1000	155.0	100%	100%	334.9
Future Tender C	53.520717	3.197021	1800	73.2	100%	50%	335.3
Future Tender D	53.646266	3.289032	480	37.1	50%	50%	335.3
Future Tender E	53.602285	3.284912	1000	95.0	100%	50%	335.5
Future Tender F	53.525615	3.260193	1000	176.7	100%	100%	336.6
Future Tender G	53.461202	3.197021	15	259.6	100%	100%	336.9
Future Tender H	53.461202	3.284912	2100	73.2	100%	50%	337.7
Galloper	51.88	2.04	298.62	66.4	100%	50%	338.8
Gebied 1 Noord (Nederwiek Noord)	53.40896991	3.255527111	1000	65.4	100%	50%	338.8
Gebied 1 Zuid (Nederwiek Zuid)	53.09957948	3.178078923	420	33.8	50%	50%	338.9
Gebied 2 Noord (Lagelander)	53.2961757	3.988358576	1500	200.0	100%	100%	339.0
Gebied 5 Oost (Doordewind)	54.27224701	5.577185063	433	37.0	50%	50%	339.1
Global Tech I	54.50895719	6.364885326	332.1	33.0	50%	50%	339.5
Gode Wind 01	54.01611259	6.98495433	867	49.5	50%	50%	342.4
Gode Wind 02	54.07579074	7.00767447	263.1	37.6	50%	50%	343.4
Gode Wind 3	54.03819066	7.105996809	4000	62.0	100%	50%	343.9
Greater Gabbard	51.88398384	1.935838464	344.52	31.7	50%	50%	344.6
Green Volt	57.88264697	-0.639907721	1000	122.0	100%	100%	345.0
HKW Kavel VI (Ecowende)	52.72319732	3.815989564	1000	205.0	100%	100%	345.4
HKW Kavel VII (Oranjewind)	52.63765598	3.70942861	225	33.9	50%	50%	346.7
HKZ Kavel I	52.37317288	4.040900261	242	32.0	50%	50%	348.8
HKZ Kavel II	52.29120292	3.983367586	1800	69.9	100%	50%	350.0
Horns Rev II	55.60016512	7.582754628	2100	67.4	100%	50%	351.1
Horns Rev III	55.69483326	7.659057832	867	82.0	100%	50%	351.4
Hornsea Project 1 (Centre)	53.88131208	1.91250509	1500	211.7	100%	100%	351.7
Hornsea Project 2 (HOW02) Wind Farm	53.94023543	1.68766321	1800	47.5	50%	50%	352.3
Hornsea Project Four (HOW04)	54.03860767	1.271072174	1500	53.3	50%	50%	352.6
Hornsea Project Three (HOW03)	53.87299926	2.537160732	756	51.6	50%	50%	352.9
Hywind Scotland Pilot Park	57.5	-1.3	1000	122.0	100%	100%	356.4
IJmuiden Ver	52.85956056	3.528930505	1000	70.0	100%	50%	356.9
IJmuiden Ver Development zone	52.7468837	3.395985	6978	47.0	50%	50%	358.0
IJmuiden Ver Noord (IJ-Ver-n)	53.0282744	3.729450341	760	53.6	50%	50%	358.4
Judy	56.65529317	2.271971889	209.3	28.7	50%	50%	359.4

Table B.1. Final dataset for the OWFs in the North Sea (1/2).

Wind Farm	Latitude	Longitude	Electrical Capacity (MW)	Distance to Shore (km)	Share of Electricity to Island	Share of Hydrogen Production	Average Distance to Other OWFs (km)
Jyske Banke Nord	57.29	7.7	250	228.5	100%	100%	360.5
London Array	51.62556023	1.496323993	1500	200.0	100%	100%	360.8
MacColl	58.14029716	-2.704897865	2250	130.4	100%	100%	360.9
Marr Bank Wind Farm	56.34486648	-1.794374783	1400	67.8	100%	50%	361.2
MarramWind	58.15283755	-0.654642017	1000	160.0	100%	100%	361.3
Meerwind Sued/Ost	54.39220139	7.704169097	402	26.9	50%	50%	361.7
Merkur Offshore (MEG Offshore I)	54.0430854	6.553891046	402	32.1	50%	50%	362.1
Mermaid	51.71863092	2.740509017	1000	100.0	100%	100%	362.4
Moray Offshore Windfarm (East)	58.1603489	-2.630133032	288	32.5	50%	50%	362.8
Moray West	58.09715554	-3.006924151	302.4	36.1	50%	50%	363.2
Morven	56.65795877	-0.875405066	342	33.5	50%	50%	363.2
Muir Mhor	57.4186613	-0.569817036	295.2	28.1	50%	50%	363.4
N-10.1	54.60203838	6.143058794	700	54.1	50%	50%	364.0
N-10.2	54.67527766	5.984668414	407	22.5	50%	50%	364.3
N-3.5	54.02592987	6.848543511	120	23.1	50%	50%	365.1
N-3.6	54.04579946	6.772103329	288	23.1	50%	50%	365.6
N-3.7	54.04490226	7.062126089	3	221.0	100%	100%	365.6
N-3.8	54.06807013	6.893242266	1400	187.8	100%	100%	369.2
N-6.6	54.26586654	5.953197108	1000	27.0	50%	50%	369.5
N-6.7	54.3609664	5.846058225	285	32.3	50%	50%	371.2
N-7.2	54.28838527	6.223845345	4000	115.1	100%	100%	371.3
N-9.1	54.43716421	5.765083393	100	28.0	50%	50%	371.3
N-9.2	54.5209024	5.900578151	100	32.0	50%	50%	373.8
N-9.3	54.43636135	5.630797817	1008	146.0	100%	100%	377.3
N-9.4	54.55986831	5.754170204	129	22.3	50%	50%	377.9
NE6	58.05833093	-1.65672396	380	22.4	50%	50%	379.3
Neos	58.15	1.53	283.5	26.6	50%	50%	379.7
Nordsee One	53.98095847	6.816739626	573	32.7	50%	50%	379.7
Nordsee Ost	54.44456228	7.682155213	1000	46.0	50%	50%	380.9
Nordsøen 1 - A1	55.8573944	7.6987885	380	23.5	50%	50%	385.3
Nordsøen 1 - A2	56.0142511	7.6438751	900	36.1	50%	50%	387.0
Nordsøen 1 - A3	56.1674636	7.5861817	1000	174.0	100%	100%	389.4
Nordsøen 1 - Subarea 2	55.9543728	7.3471921	1200	115.5	100%	100%	390.6
Nordsøen Tender 1	56.5841986	6.1000615	714	50.6	50%	50%	396.1
Nordsøen Tender 10	55.8396205	6.2887621	2610	79.5	100%	50%	399.2
Nordsøen Tender 2	56.7215099	6.5375905	2000	93.2	100%	50%	405.9
Nordsøen Tender 3	56.2606641	6.2739431	960	29.7	50%	50%	408.0
Nordsøen Tender 4	56.7773487	6.1768433	1008	201.5	100%	100%	409.1
Nordsøen Tender 5	56.2564984	5.8802963	15	183.1	100%	100%	413.8
Nordsøen Tender 6	56.5804268	7.3410183	2907	61.2	100%	50%	415.1
Nordsøen Tender 7	56.3196054	6.9674804	1500	60.4	100%	50%	423.8
Nordsøen Tender 8	56.0457987	6.5854313	25	208.0	100%	100%	428.4
Nordsøen Tender 9	55.9651759	5.8032926	1100	37.5	50%	50%	428.5
Nordsren II	56.29296643	6.820367486	376	27.3	50%	50%	429.0
Nordsren III	56.58679097	6.553402928	1000	70.0	100%	50%	429.2
Nordsren III vest	56.19203215	5.951498855	798	62.9	100%	50%	430.1
Norfolk Boreas	53.08751586	2.929058901	1050	54.1	50%	50%	430.5
Norfolk Vanguard	52.87	2.67	380	40.2	50%	50%	431.0
North Falls	51.73606573	2.039214541	2300	43.4	50%	50%	431.6
Northwester 2	51.68653676	2.752631217	19	34.8	50%	50%	432.6
Northwind	51.61595907	2.905150268	353	39.1	50%	50%	432.9
Odin (DK)	56.96	5.91	1500	143.4	100%	100%	433.1
Orcadian Microgrid	58.12	-0.56	235.2	48.3	50%	50%	434.0
Ossian Offshore Wind Farm	56.68759059	-0.393592014	504	24.8	50%	50%	435.1
OWF Luchterduinen	52.40508973	4.163094644	6	43.9	50%	50%	435.4
OWF Prinses Amalia	52.58786535	4.223826289	1760	45.5	50%	50%	435.7
R4 Project 1 (Dogger Bank South West)	54.62494245	1.478649484	1008	84.1	100%	50%	435.9
R4 Project 2 (Dogger Bank South East)	54.50070479	1.903768465	351.5	29.5	50%	50%	436.4
R4 Project 3 (Outer Dowsing)	53.56836744	1.284806083	218.5	44.5	50%	50%	436.7
Race Bank	53.27657931	0.841376795	165	42.6	50%	50%	436.9
Race Bank Extension	53.276	0.841	165	40.6	50%	50%	437.7
Rentel	51.59140071	2.944544671	165	39.2	50%	50%	438.5
Salamander	57.58	-1.06	376	24.2	50%	50%	439.1
Sandbank	55.19975908	6.85247825	252	36.1	50%	50%	440.3
Scaraben	58.23	-1.58	1008	38.4	50%	50%	441.2
Seagreen 1A Offshore Wind Farm	56.55843286	-1.87025557	216	33.7	50%	50%	441.7
Seagreen Wind Farm	56.57257043	-1.657122947	309	28.4	50%	50%	443.8
SeaStar	51.63418029	2.86165196	1140	38.2	50%	50%	444.0
Sinclair	58.29	-1.71	504	22.4	50%	50%	445.2
Sofia	54.98994051	2.228543592	1800	30.9	50%	50%	446.3
Sønnavind A	57.4135505	7.4395825	184.5	25.0	50%	50%	446.3
Sørlige Nordsjø 2 - Phase 1 (Sørvest F)	56.7850253	5.118057	141.15	24.8	50%	50%	449.1
Sørlige Nordsjø 2 - Phase 2 (Sørvest F)	56.7804175	4.568783	500	32.4	50%	50%	452.9
Sørlige Nordsjø 2 - Phase 3 (Sørvest F)	56.4794326	4.7850087	200	43.1	50%	50%	452.9
Sorlige Nordsjo II	56.78	4.92	50	32.3	50%	50%	453.2
Sørvest A	57.7545173	3.141372	560	68.1	100%	50%	455.2
Sørvest B (Sørlige Nordsjø 1)	57.3063843	3.2291128	30	28.0	50%	50%	457.8
Sørvest C	57.0447216	3.6686463	30	22.4	50%	50%	459.5
Sørvest D	56.3233705	3.8106814	105	94.1	100%	50%	467.0
Sørvest E	57.2637125	4.5640245	630	20.5	50%	50%	468.6
Spiorad na Mara	58.41	-0.679	1500	107.7	100%	100%	470.8
Stevenson	58.19724348	-2.778661853	3000	75.7	100%	50%	471.7
Stromar	58.51446242	-2.145706678	1000	115.0	100%	100%	486.1
Telford	58.24592768	-2.688518534	840	110.3	100%	100%	489.8
Ten Noorden van de Wadden	54.02841013	5.800357928	1500	33.3	50%	50%	498.1
Thybo	57.07	6.1	500	24.4	50%	50%	502.8
Thybo II	57.28	7.86	100	64.5	100%	50%	505.4
Trianel Windpark Borkum Phase 1	54.04621997	6.457645411	960	74.9	100%	50%	505.8
Trianel Windpark Borkum Phase 2	54.05034224	6.463669108	500	47.5	50%	50%	509.9
Triton Knoll	53.47846028	0.838582968	100	68.3	100%	50%	513.6
Utsira Nord 1	59.41	4.43	500	20.3	50%	50%	514.6
Utsira Nord 2	59.27	4.49	500	26.7	50%	50%	526.7
Utsira Nord 3	59.13	4.54	2000	23.3	50%	50%	537.8
Veja Mate	54.3181454	5.872901416	953	22.3	50%	50%	541.8
Vestavind E	58.9985565	3.5574129	313.5	28.5	50%	50%	543.9
Wind Energy Search Area 3	53.884916	3.867188	1000	36.9	50%	50%	544.0
Wind Energy Search Area 4	53.923751	5.515	1000	36.9	50%	50%	544.0
Wind Energy Search Area 6&7	54.508327	3.823242	313.5	22.3	50%	50%	549.0
ZeeEnergie / Gemini II	54.03450001	5.884241837	323	22.3	50%	50%	550.2
#no name	58.51446241	-2.145706693	882	22.2	50%	50%	555.2

Table B.2. Final dataset for the OWFs in the North Sea (2/2).

Appendix C: Existing Natural Gas Pipeline Dataset

In this Appendix, the data preparation for natural gas pipelines, as outlined in *5.4 Existing Natural Gas Pipelines*, is complemented. In *C1. Pipeline Data Simplification Steps*, the three simplification steps are discussed. The calculations regarding pipeline capacity are detailed in *C2. Hydrogen Pipeline Capacity*. The final pipeline dataset is ultimately presented in *C3. Final Dataset Existing Natural Gas Pipelines*.

C1. Pipeline Data Simplification Steps

To lower computational time while preserving network accuracy, the pipeline network is simplified in three steps. Let the gas pipelines be an undirected graph $G = (V, E)$, where each node $v \in V$ is a coordinate, and each edge $e \in E$ is a pipeline segment with diameter $D(u, v)$ in inches, and a length $l(u, v)$ in m. Distances are computed after the conversion of coordinates to UTM.

Data Simplification Step 1: *contracting nearby nodes*.
In the raw dataset, multiple coordinates can lie within a few tens of meters of one another due to how geometry is approached. To account for this, points within a radius of 50 m ($r = 50\ m$) are considered to represent the same physical location in the network. These points are therefore merged into a single node, which is shown in Figure C1.1. It shows that the node above is merged with the node below. To preserve data integrity, the nodes are only contracted if their connected pipeline segments have the same diameter, ensuring that edges with different capacities are merged.

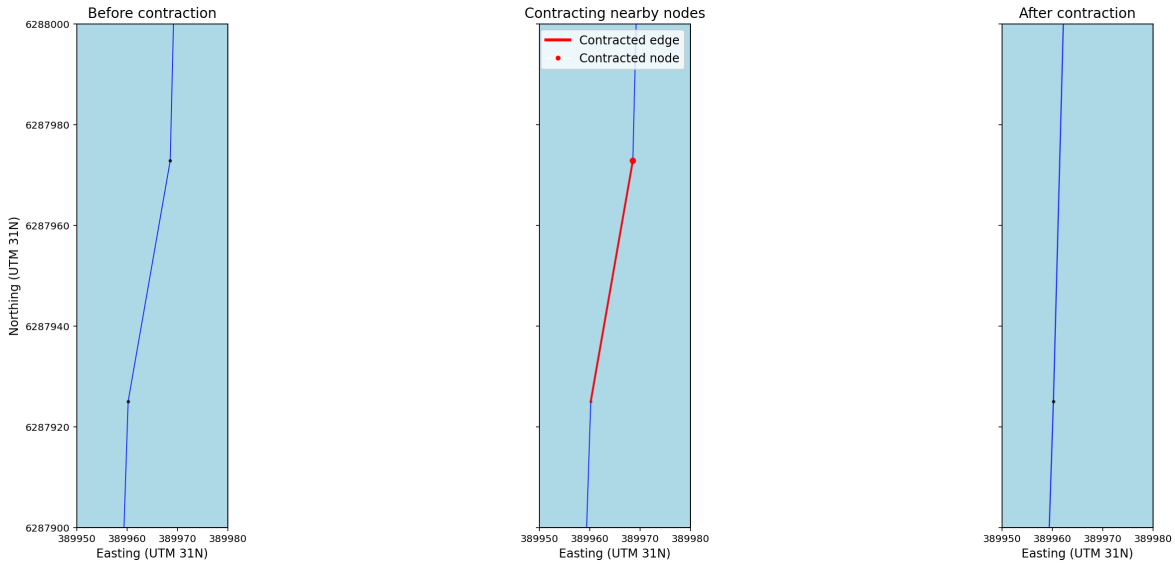

Figure C1.1. The steps of contracting nearby nodes in the existing gas pipeline dataset (data simplification step 1).

Formally, for any $u, v \in V$, nodes u and v are contracted into one single representative node when $l(u, v) \leq r \; and \; D(u,\cdot) = D(v,\cdot)$ for all incident edges.

After the contraction is completed, the number of data points is reduced from 307,751 to 57,036 coordinates. The result for the complete network is shown in Figure 29 (left) Visually, the plot closely resembles the pre-simplification network (Figure 28), which is expected given the small radius r relative to the entire North Sea.

Data Simplification Step 2: *removing small deviations*.
Some pipelines contain minor bends, which result in small deviations from an otherwise straight path. These deviations create nodes with $\deg(u) = 2$, meaning that exactly two other nodes are connected in sequence. If such node u has neighbours a and b, node u is removed if the total path length between a and b is not larger than 1,000 m. When node u is removed, a direct edge between a and b is added, which the diameter is the average of the two original edges. This can be seen in Figure C1.2, as the red nodes are removed and replaced by direct connections, thereby straightening segments with minor bends.

Formally, node u is removed if $[l(a,u) + l(u,b)] - l(a,b) \leq 1{,}000\ m$. Then, a direct edge (a,b) is added with: $D(a,b) = \frac{D(a,u)+D(u,b)}{2}$.

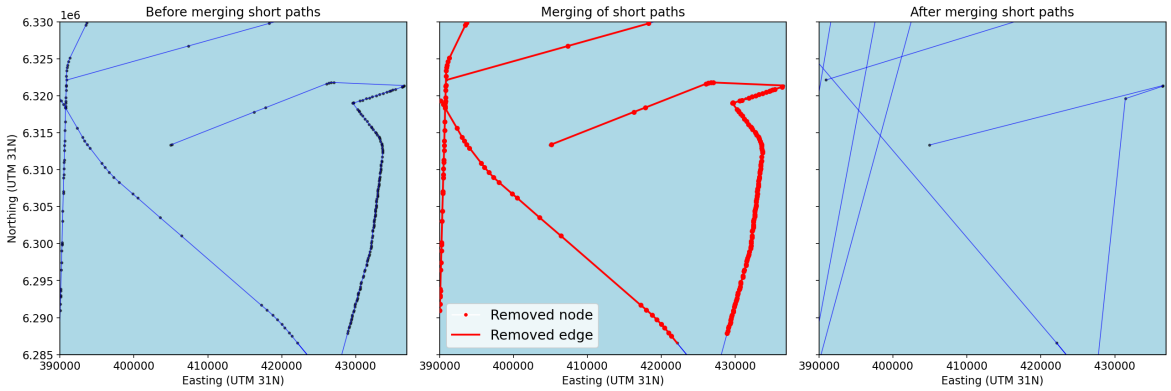

Figure C1.2. The steps of removing small deviations in the gas pipeline dataset (data simplification step 2).

This way, unnecessary curvature is removed while a realistic route geometry at a large scale is maintained. In Figure C1.2 (right) the geometric shape resulting from this step seems odd, which is an effect of the merging criteria. Ultimately, the number of points is reduced to 600 coordinates. The result is shown in Figure 29 (middle).

Data Simplification Step 3: *merging short paths*.
Long and continuous pipelines are often stored as a series of short, connected segments. This can include a node u with $\deg(u) = 2$. Therefore, if the combined length between neighbor nodes a and b is equal or smaller than 100,000 m, node u is removed, and a direct connection between is added a and b. The outcomes are shown in Figure C1.3, where two edges are merged into one new, direct connection.

Formally, if $l(a,u) + l(u,b) \leq 100{,}000\ m$ for a node u with $\deg(u) = 2$, and neighbor nodes a and b, then u is removed and $e(a,b)$ is added with $D(a,b) = \frac{D(a,u)+D(u,b)}{2}$.

This connection then has the length equal to the full distance between the neighboring nodes of u. This step ensures that long, straight pipeline segments are represented in an efficient way without fragmenting the network into unnecessarily small parts. The number of points in the data set is, as result from this step, reduced to 537 coordinates. The outcomes are shown in Figure 29 (right).

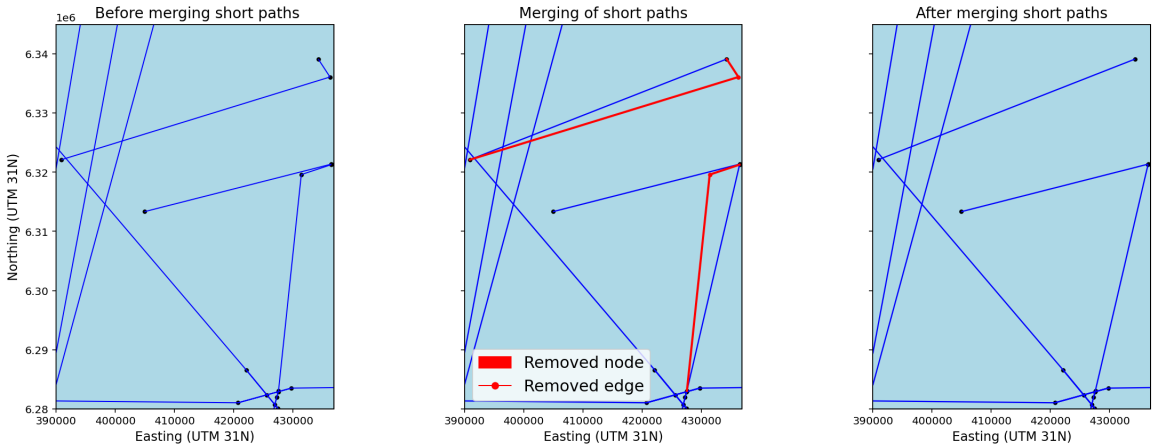

Figure C1.3. The steps of merging short paths in the gas pipeline dataset (data simplification step 3).

C2. Hydrogen Pipeline Capacity

The mass flow rate $\dot{m}$ through a pipeline, expressed in kg/s, and the energy density of hydrogen LHV_{H_2}, expressed in MJ/kg, are appropriate parameters to determine the capacity flow $\dot{C}$, expressed in MW as it is equal to MJ/s (Khan et al., 2021; Møller et al., 2017). Since the units are equal, the hydrogen capacity flow is calculated as:

$$\dot{C} = \dot{m} \cdot LHV_{H_2} \quad with \ \dot{m} = M_{H_2} \cdot \dot{n} \ gives \ \dot{C} = M_{H_2} \cdot \dot{n} \cdot LHV_{H_2}$$

where M_{H_2} is the molar mass of hydrogen in kg/mol and $\dot{n}$ is the molar flow rate in mol/s.

For hydrogen, $M_{H_2} = 0.002016\, kg/mol$ and $LHV_{H_2} = 120\, MJ/kg$ (Khan et al., 2021; Møller et al., 2017). The molar flow rate $\dot{n}$ can be calculated using the ideal gas law:

$$\dot{n} = \frac{\dot{p} \cdot \dot{V}}{R \cdot T}$$

where $\dot{p}$ is the operating pressure in the pipeline in Pa, $\dot{V}$ is the volumetric flow rate in m^3/s, R is the universal gas constant equal to $8.314\, J/mol \cdot K$, and T is the operating temperature in K. The volumetric flow rate $\dot{V}$ is calculated as:

$$\dot{V} = A \cdot \dot{v} \quad with\ A = \frac{\pi}{4} D^2$$

where $\dot{v}$ is the average velocity flow of the gas through the pipeline in m/s, and A is the cross-sectional area of the pipeline in m^2. In this context, D is the inner diameter of a pipeline expressed in m, Since the diameters in the pipeline dataset are expressed in inches, so this must be converted into m via: $D_m = D_{inch} \cdot 0.0254$

For the North Sea, the following parameters are assumed: $T = 283.15\, K$ (FMHA, n.d.); $\dot{v} = 15\, m/s$ (Hammond et al., 2025); $\dot{p} = 8 \cdot 10^6\, Pa$ (Noordgastransport, 2022).

By applying these equations to each pipeline segment, the potential hydrogen transport capacity in MW can be calculated from the diameter values in the dataset.

C3. Final Existing Natural Gas Pipeline Dataset

Tables C3.1 and C3.1 present the natural gas pipeline dataset that is for the hydrogen backbone.

Coordinate node *u*	Coordinate node *v*	Diameter (inch)	Capacity (MW)	Coordinate node *u*	Coordinate node *v*	Diameter (inch)	Capacity (MW)
(496325.5911795729, 5963770.152148962)	(509803.49749648187, 5959005.184786638)	24	3599	(427571.6371030377, 6283027.186169165)	(436462.7118864687, 6321279.261368385)	34	7223
(509803.49749648187, 5959005.184786638)	(509882.47787054896, 5958977.79032274)	24	3599	(397785.4959342622, 5969374.27611221)	(397686.5899086616, 5967817.540572374)	34	7223
(509803.49749648187, 5959005.184786638)	(514536.46250227944, 5896489.626561847)	24	3599	(397785.4959342622, 5969374.27611221)	(397734.8451872991, 5968577.056555183)	34	7223
(509882.47787054896, 5958977.79032274)	(518315.10427135916, 6054217.247279612)	42	11021.9	(397686.5899086616, 5967817.540572374)	(397734.8451872991, 5968577.056555183)	34	7223
(509882.47787054896, 5958977.79032274)	(509055.55828324164, 5949638.425728741)	42	11021.9	(397686.5899086616, 5967817.540572374)	(396073.7105586097, 5858415.580034024)	34	7223
(518315.10427135916, 6054217.247279612)	(513740.772409056, 6002553.997682261)	42	11021.9	(397734.8451872991, 5968577.056555183)	(393282.81642501097, 5966696.837017953)	26	4223.8
(518315.10427135916, 6054217.247279612)	(519299.8107472225, 6070911.089621851)	42	11021.9	(397734.8451872991, 5968577.056555183)	(402706.7479582354, 5970676.833808714)	26	4223.8
(518315.10427135916, 6054217.247279612)	(509055.55828324164, 5949638.425728741)	42	11021.9	(393282.81642501097, 5966696.837017953)	(402706.7479582354, 5970676.833808714)	26	4223.8
(509055.55828324164, 5949638.425728741)	(513740.772409056, 6002553.997682261)	42	11021.9	(393282.81642501097, 5966696.837017953)	(316626.73297181487, 5916384.0412508)	26	4223.8
(509055.55828324164, 5949638.425728741)	(508650.47540595144, 5883311.908526756)	42	11021.9	(402706.7479582354, 5970676.833808714)	(411734.7204030825, 5984348.741160766)	26	4223.8
(513740.772409056, 6002553.997682261)	(513609.4701896167, 6002673.882105763)	36	8097.8	(411734.7204030825, 5984348.741160766)	(415233.71233143867, 5987964.709589604)	26	4223.8
(513740.772409056, 6002553.997682261)	(513770.4719206936, 6002526.8806863865)	36	8097.8	(411734.7204030825, 5984348.741160766)	(413025.4983400906, 5985682.671722605)	26	4223.8
(524432.8982720445, 5927839.130692187)	(541667.4167817289, 5902431.989014162)	24	3599	(441668.9842966264, 5882696.621091141)	(437461.8481340508, 5884684.041519839)	20	2499.3
(445070.9069545813, 5881578.331988309)	(442200.5089349678, 5882466.455997907)	30	5623.4	(441668.9842966264, 5882696.621091141)	(441711.3772883055, 5882574.722203689)	20	2499.3
(445070.9069545813, 5881578.331988309)	(401274.6652322256, 5866304.194026764)	30	5623.4	(441668.9842966264, 5882696.621091141)	(447997.8239024533, 5885563.402689154)	20	2499.3
(445070.9069545813, 5881578.331988309)	(396735.76104394096, 5857675.961683429)	30	5623.4	(441711.3772883055, 5882574.722203689)	(441693.4344097613, 5882575.384879942)	20	2499.3
(442200.5089349678, 5882466.455997907)	(441664.7872980522, 5882566.052859158)	30	5623.4	(447997.8239024533, 5885563.402689154)	(450644.44399616396, 5886771.092486433)	20	2499.3
(442200.5089349678, 5882466.455997907)	(441712.8423570225, 5882582.234627323)	30	5623.4	(447997.8239024533, 5885563.402689154)	(449047.95791780617, 5886042.593540584)	20	2499.3
(401274.6652322256, 5866304.194026764)	(445030.57316780125, 5877647.828308034)	30	5623.4	(488407.38546546036, 5897350.1975325085)	(490671.32087980607, 5893287.00701737)	20	2499.3
(401274.6652322256, 5866304.194026764)	(396461.62469697744, 5857940.436575574)	30	5623.4	(458427.2244577096, 5876580.237625821)	(452380.1652624203, 5878168.414267608)	24	3599
(401274.6652322256, 5866304.194026764)	(441664.7872980522, 5882566.052859158)	30	5623.4	(471530.35774421075, 5908168.328104466)	(460922.60761710524, 5891647.164325486)	30	5623.4
(441664.7872980522, 5882566.052859158)	(441712.8423570225, 5882582.234627323)	30	5623.4	(460922.60761710524, 5891647.164325486)	(460645.1800313962, 5891189.61856394)	30	5623.4
(441712.8423570225, 5882582.234627323)	(441668.9842966264, 5882696.621091141)	20	2499.3	(460922.60761710524, 5891647.164325486)	(460848.4123196157, 5891524.79818152)	30	5623.4
(441712.8423570225, 5882582.234627323)	(441711.3772883055, 5882574.722203689)	20	2499.3	(460645.1800313962, 5891189.61856394)	(460848.4123196157, 5891524.79818152)	30	5623.4
(445239.1746528493, 5873559.755415794)	(445177.6417073175, 5877509.304534158)	24	3599	(460645.1800313962, 5891189.61856394)	(456328.49521544366, 5884502.168965643)	30	5623.4
(445177.6417073175, 5877509.304534158)	(445154.0683091626, 5877735.425787922)	24	3599	(460848.4123196157, 5891524.79818152)	(463045.61169940344, 5892541.837988338)	20	2499.3
(445177.6417073175, 5877509.304534158)	(445160.4454394664, 5877674.254942284)	24	3599	(460848.4123196157, 5891524.79818152)	(455931.8954685993, 5889249.040508195)	20	2499.3
(445154.0683091626, 5877735.425787922)	(445160.4454394664, 5877674.254942284)	24	3599	(456328.49521544366, 5884502.168965643)	(456208.15089017776, 5884336.382298215)	30	5623.4
(445154.0683091626, 5877735.425787922)	(445047.8757785893, 5881562.017643185)	24	3599	(456328.49521544366, 5884502.168965643)	(456281.05477838, 5884436.81489145)	30	5623.4
(445160.4454394664, 5877674.254942284)	(445346.42934050254, 5877712.099267836)	30	5623.4	(463045.61169940344, 5892541.837988338)	(455931.8954685993, 5889249.040508195)	20	2499.3
(445160.4454394664, 5877674.254942284)	(445030.57316780125, 5877647.828308034)	30	5623.4	(463045.61169940344, 5892541.837988338)	(479856.1619723098, 5921477.116712464)	20	2499.3
(445346.42934050254, 5877712.099267836)	(448566.6880573332, 5878528.842516795)	30	5623.4	(455931.8954685993, 5889249.040508195)	(450644.44399616396, 5886771.092486433)	20	2499.3
(445346.42934050254, 5877712.099267836)	(445030.57316780125, 5877647.828308034)	30	5623.4	(456208.15089017776, 5884336.382298215)	(456281.05477838, 5884436.81489145)	30	5623.4
(211468.088086312, 6392142.606432608)	(223481.48588759732, 6394729.046561126)	36	8097.8	(456208.15089017776, 5884336.382298215)	(452154.690703323, 5878300.817880876)	30	5623.4
(223481.48588759732, 6394729.046561126)	(296952.4318162743, 6574741.934692313)	36	8097.8	(456281.05477838, 5884436.81489145)	(455255.36440149584, 5884652.000366799)	24	3599
(296952.4318162743, 6574741.934692313)	(297325.7931715187, 6575212.46313234)	36	8097.8	(456281.05477838, 5884436.81489145)	(456755.2809200805, 5884337.324265406)	24	3599
(296952.4318162743, 6574741.934692313)	(297266.3750192009, 6575137.581438971)	36	8097.8	(450644.44399616396, 5886771.092486433)	(449047.95791780617, 5886042.593540584)	20	2499.3
(297325.7931715187, 6575212.46313234)	(297266.3750192009, 6575137.581438971)	36	8097.8	(455255.36440149584, 5884652.000366799)	(453329.2866726973, 5885085.084155323)	24	3599
(297325.7931715187, 6575212.46313234)	(424145.7874263197, 6746663.510533108)	36	8097.8	(455255.36440149584, 5884652.000366799)	(456755.2809200805, 5884337.324265406)	24	3599
(297266.3750192009, 6575137.581438971)	(297400.6867935585, 6577965.802228212)	30	5623.4	(456755.2809200805, 5884337.324265406)	(469541.23998135864, 5881641.279608205)	24	3599
(297266.3750192009, 6575137.581438971)	(296623.0904381143, 6561591.852970045)	30	5623.4	(453329.2866726973, 5885085.084155323)	(449047.95791780617, 5886042.593540584)	24	3599
(424145.7874263197, 6746663.510533108)	(429746.7823500872, 6766761.568699479)	36	8097.8	(453329.2866726973, 5885085.084155323)	(448401.3275321805, 5886187.210947581)	24	3599
(297400.6867935585, 6577965.802228212)	(296827.6016144862, 6682280.471504648)	30	5623.4	(419084.58238388435, 5874792.51263237)	(396279.7265778803, 5858299.656176352)	30	5623.4
(297400.6867935585, 6577965.802228212)	(296623.0904381143, 6561591.852970045)	30	5623.4	(422561.5777433403, 5872771.474665573)	(419106.4887352072, 5874798.375842747)	24	3599
(296623.0904381143, 6561591.852970045)	(310813.9595239366, 6525394.629348803)	30	5623.4	(411851.741918748, 5879064.46793002)	(419083.51546872035, 5874808.887344948)	24	3599
(296827.6016144862, 6682280.471504648)	(268851.8087805821, 6708269.331331016)	30	5623.4	(417279.6032908464, 5883760.224652669)	(419083.7952225405, 5874813.555954336)	24	3599
(433752.4189852774, 5916078.953754209)	(410388.1783687296, 5915798.439766941)	36	8097.8	(450578.33897818957, 5931861.921059969)	(455575.31412610656, 5922237.025667818)	24	3599
(410388.1783687296, 5915798.439766941)	(404289.2961345687, 5915911.25363371)	36	8097.8	(445417.0172366735, 5881060.934485169)	(445070.23549919203, 5881572.331696676)	24	3599
(410388.1783687296, 5915798.439766941)	(406835.9793459728, 5915864.146447592)	36	8097.8	(391902.79160433734, 5919030.158107001)	(396110.0782578801, 5858343.46685694)	20	2499.3
(404289.2961345687, 5915911.25363371)	(406835.9793459728, 5915864.146447592)	36	8097.8	(435980.6270071968, 6470362.328010995)	(432756.12699657865, 6467358.807705848)	44	12096.6
(404289.2961345687, 5915911.25363371)	(316709.4061996511, 5916140.490084777)	36	8097.8	(432756.12699657865, 6467358.807705848)	(435723.7637499772, 6469871.955752278)	44	12096.6
(406835.9793459728, 5915864.146447592)	(406812.5389387147, 5916010.108841138)	24	3599	(432756.12699657865, 6467358.807705848)	(399339.43734338216, 6376075.242201257)	44	12096.6
(406835.9793459728, 5915864.146447592)	(406891.58374413, 5915517.900285684)	24	3599	(432756.12699657865, 6467358.807705848)	(418058.9700635129, 6439856.151090887)	44	12096.6
(406812.5389387147, 5916010.108841138)	(410935.5608747949, 5968722.8434132105)	24	3599	(399339.43734338216, 6376075.242201257)	(340039.919966061, 6023008.709724082)	44	12096.6
(406812.5389387147, 5916010.108841138)	(406891.58374413, 5915517.900285684)	24	3599	(418058.9700635129, 6439856.151090887)	(341024.0990019954, 6026552.433711446)	44	12096.6
(406891.58374413, 5915517.900285684)	(396194.1775267548, 5858235.944046174)	24	3599	(340039.919966061, 6023008.709724082)	(309953.29871949705, 5950318.262707201)	44	12096.6
(410935.5608747949, 5968722.8434132105)	(413025.4983400906, 5985682.671722605)	24	3599	(341024.0990019954, 6026552.433711446)	(309953.29871949705, 5950318.262707201)	44	12096.6
(410935.5608747949, 5968722.8434132105)	(414971.52361402166, 6001474.653578361)	24	3599	(309953.29871949705, 5950318.262707201)	(309550.4797351507, 5949708.183172109)	44	12096.6
(396194.1775267548, 5858235.944046174)	(415747.4496093886, 5924049.107762601)	24	3599	(309953.29871949705, 5950318.262707201)	(309440.54417601076, 5949473.126186414)	44	12096.6
(450595.45211790374, 5931862.966293803)	(435456.37424956966, 5924652.071606926)	28	4898.6	(490648.5132495848, 5893240.993983228)	(426958.83428842307, 5853977.820893986)	30	5623.4
(435456.37424956966, 5924652.071606926)	(434472.57858457055, 5924459.052443639)	28	4898.6	(426958.83428842307, 5853977.820893986)	(396792.9418969744, 5857631.564962173)	30	5623.4
(435456.37424956966, 5924652.071606926)	(434591.4281454549, 5924482.370540694)	28	4898.6	(445659.39862218197, 6708085.633873985)	(444924.7572939796, 6640049.861418651)	24	3599
(434472.57858457055, 5924459.052443639)	(434591.4281454549, 5924482.370540694)	28	4898.6	(211477.62623263022, 6392008.637738333)	(213655.34933597653, 6392353.654575056)	32	6398.2
(434472.57858457055, 5924459.052443639)	(316883.8469508887, 5915790.041405502)	28	4898.6	(213655.34933597653, 6392353.654575056)	(215553.12692456518, 6392426.54303275)	32	6398.2
(434591.4281454549, 5924482.370540694)	(434594.50522024144, 5924648.086150544)	20	2499.3	(213655.34933597653, 6392353.654575056)	(231196.62828751962, 6399336.931342541)	32	6398.2
(434591.4281454549, 5924482.370540694)	(434508.39941327414, 5920010.8649899475)	20	2499.3	(215553.12692456518, 6392426.54303275)	(211582.36966544494, 6392069.208393465)	32	6398.2
(434594.50522024144, 5924648.086150544)	(434722.4202593818, 5932727.39560303)	20	2499.3	(215553.12692456518, 6392426.54303275)	(222335.59605367592, 6390766.122700939)	32	6398.2
(434594.50522024144, 5924648.086150544)	(434508.39941327414, 5920010.8649899475)	20	2499.3	(231196.62828751962, 6399336.931342541)	(222335.59605367592, 6390766.122700939)	32	6398.2
(434508.39941327414, 5920010.8649899475)	(433774.63950210623, 5916337.011913868)	20	2499.3	(231196.62828751962, 6399336.931342541)	(242899.76367668508, 6415600.6312976675)	32	6398.2
(309409.3264835842, 5949878.889335523)	(351021.69188387797, 5989508.2246154435)	36	8097.8	(231196.62828751962, 6399336.931342541)	(248432.01123689703, 6423661.973197386)	32	6398.2
(431058.9609875996, 6742226.511676711)	(447494.9617654755, 6638321.790868728)	24	3599	(222335.59605367592, 6390766.122700939)	(242899.76367668508, 6415600.6312976675)	32	6398.2
(425399.96347015776, 6623487.934469281)	(426933.7281269183, 6618402.676017112)	32	6398.2	(242899.76367668508, 6415600.6312976675)	(248432.01123689703, 6423661.973197386)	32	6398.2
(426933.7281269183, 6618402.676017112)	(447503.84022583556, 6638355.749063378)	32	6398.2	(248432.01123689703, 6423661.973197386)	(283813.5652461441, 6474945.513174574)	32	6398.2
(426933.7281269183, 6618402.676017112)	(383883.29316635546, 6592784.58325065)	32	6398.2	(283813.5652461441, 6474945.513174574)	(311113.206032237, 6525865.380980029)	32	6398.2
(383883.29316635546, 6592784.58325065)	(320557.0001499574, 6531150.339209928)	32	6398.2	(449047.95791780617, 5886042.593540584)	(448401.3275321805, 5886187.210947581)	24	3599
(383883.29316635546, 6592784.58325065)	(382139.0530782275, 6591138.947436609)	32	6398.2	(310277.4845231343, 6526482.976147089)	(309271.69206341635, 6524985.388093214)	40	9997.2
(383883.29316635546, 6592784.58325065)	(389958.5756860956, 6598869.919460719)	32	6398.2	(309747.82494035317, 5948805.43558867)	(375786.23360901535, 5953825.487283315)	24	3599
(310275.1134558208, 6526519.453143631)	(309259.1182601709, 6524972.066685413)	32	6398.2	(417149.456697279, 6601540.56651948)	(418958.7459397973, 6589789.325671904)	40.5	10248.7
(310275.1134558208, 6526519.453143631)	(311438.1950596592, 6528444.43634436)	32	6398.2	(415233.71233143867, 5987964.709589604)	(413025.4983400906, 5985682.671722605)	26	4223.8
(310275.1134558208, 6526519.453143631)	(320557.0001499574, 6531150.339209928)	32	6398.2	(415233.71233143867, 5987964.709589604)	(455886.4433797279, 6013481.569375843)	26	4223.8
(311438.1950596592, 6528444.43634436)	(312328.1205943241, 6528905.961999789)	32	6398.2	(413025.4983400906, 5985682.671722605)	(414971.52361402166, 6001474.653578361)	24	3599
(311438.1950596592, 6528444.43634436)	(311517.4369010336, 6518847.987852949)	32	6398.2	(414971.52361402166, 6001474.653578361)	(398213.77682200866, 6050024.246845489)	24	3599
(320557.0001499574, 6531150.339209928)	(312328.1205943241, 6528905.961999789)	32	6398.2	(460187.9112598726, 6770747.408511071)	(429580.501354053, 6765833.080657949)	28	4898.6
(320557.0001499574, 6531150.339209928)	(326198.8550795516, 6536800.90945419)	32	6398.2	(211442.06917543238, 6393195.246037182)	(230666.78253355605, 6394441.59103683)	30	5623.4
(312328.1205943241, 6528905.961999789)	(326198.8550795516, 6536800.90945419)	32	6398.2	(230666.78253355605, 6394441.59103683)	(356823.5217228604, 6460485.303297232)	30	5623.4
(311517.4369010336, 6518847.987852949)	(260178.16349735472, 6440143.192187782)	32	6398.2	(356823.5217228604, 6460485.303297232)	(394859.5672316896, 6526701.969993151)	30	5623.4
(326198.8550795516, 6536800.90945419)	(382139.0530782275, 6591138.947436609)	32	6398.2	(394859.5672316896, 6526701.969993151)	(417075.1630999993, 6601547.105260702)	30	5623.4
(260178.16349735472, 6440143.192187782)	(242899.76367668508, 6415600.6312976675)	32	6398.2	(434286.9868546203, 6339147.332603614)	(390935.48354326555, 6322123.988333836)	22	3024.2
(260178.16349735472, 6440143.192187782)	(248432.01123689703, 6423661.973197386)	32	6398.2	(416048.21573718096, 6456131.656943004)	(405794.35765372193, 6435028.685078592)	34.5	7437
(260178.16349735472, 6440143.192187782)	(283813.5652461441, 6474945.513174574)	32	6398.2	(443906.0550307203, 5883320.2989675915)	(445044.29586453264, 5881571.181734088)	24	3599
(382139.0530782275, 6591138.947436609)	(389958.5756860956, 6598869.919460719)	32	6398.2	(445491.48793825, 5878378.33308849)	(445431.69387084385, 5881037.626278247)	20	2499.3
(389958.5756860956, 6598869.919460719)	(404757.689548723, 6612745.814336248)	32	6398.2	(471543.4267311314, 5908226.325019224)	(471295.44879019127, 5912710.828103167)	22	3024.2
(389958.5756860956, 6598869.919460719)	(405105.86317313835, 6612817.488942608)	32	6398.2	(448401.3275321805, 5886187.210947581)	(396213.8588485973, 5858189.562172096)	24	3599
(405105.86317313835, 6612817.488942608)	(456276.86000093876, 6604306.61792139)	32	6398.2	(495807.8140810185, 6019667.764651982)	(513609.4701896167, 6002673.882105763)	36	8097.8
(405105.86317313835, 6612817.488942608)	(447650.875753692, 6638415.826404523)	32	6398.2	(513609.4701896167, 6002673.882105763)	(513770.4719206936, 6002526.8806863865)	36	8097.8
(309464.63186397904, 5949545.9026090475)	(331650.8667101733, 5968183.253946175)	36	8097.8	(513770.4719206936, 6002526.8806863865)	(534008.3304058086, 5983632.012581529)	36	8097.8
(211436.96129758755, 6393162.3157725)	(390107.1505200692, 6435582.23431319)	28	4898.6	(534008.3304058086, 5983632.012581529)	(579872.9998889283, 5917577.471097438)	36	8097.8
(466146.85319994995, 6033573.000476985)	(412695.30499415065, 6017678.357543591)	20	2499.3	(614925.4821655519, 5860278.54303011)	(566844.5476186358, 5873380.928544635)	36	8097.8
(452331.31197348685, 5878102.478606805)	(453990.2320719792, 5876998.274784747)	20	2499.3	(566844.5476186358, 5873380.928544635)	(533983.2629795704, 5871607.368610832)	36	8097.8
(452388.4424670055, 5877893.644249394)	(455684.4256815265, 5874345.020452828)	30	5623.4	(566844.5476186358, 5873380.928544635)	(558893.2210562906, 5872951.786642045)	36	8097.8
(448593.5906294645, 5878518.319589589)	(451723.67781740095, 5878237.143820745)	20	2499.3	(533983.2629795704, 5871607.368610832)	(558893.2210562906, 5872951.786642045)	36	8097.8
(448593.5906294645, 5878518.319589589)	(447086.01867825835, 5879272.2904707575)	20	2499.3	(533983.2629795704, 5871607.368610832)	(532877.418795741, 5871421.7709486205)	36	8097.8
(448593.5906294645, 5878518.319589589)	(450092.02646636707, 5875465.60967714)	20	2499.3	(558893.2210562906, 5872951.786642045)	(558846.7447822513, 5872782.09357595)	20	2499.3
(448593.5906294645, 5878518.319589589)	(447206.1295653985, 5873006.344096696)	20	2499.3	(558893.2210562906, 5872951.786642045)	(558900.6441999713, 5872978.889847655)	20	2499.3
(432168.6813275439, 6767337.632048879)	(429628.4425008194, 6765821.432189478)	32	6398.2	(532877.418795741, 5871421.7709486205)	(473185.261875502, 5854343.890212997)	36	8097.8
(309866.52951908467, 5948706.8340890845)	(353784.5249186058, 5943727.247365459)	30	5623.4	(532877.418795741, 5871421.7709486205)	(511478.2072492009, 5865299.472786125)	36	8097.8
(234961.5966639385, 6060681.570293155)	(387654.5784648076, 6275308.858576357)	36	8097.8	(558846.7447822513, 5872782.09357595)	(551040.2977820637, 5845384.49217687)	20	2499.3
(387654.5784648076, 6275308.858576357)	(419249.9194883989, 6391992.3794693025)	36	8097.8	(558846.7447822513, 5872782.09357595)	(558900.6441999713, 5872978.889847655)	20	2499.3
(419249.9194883989, 6391992.3794693025)	(428696.74675705255, 6402336.3178242445)	36	8097.8	(558900.6441999713, 5872978.889847655)	(566497.8906079897, 5891536.856196745)	20	2499.3
(468335.15771420504, 5915943.3271421315)	(471101.6180427462, 5906547.8130771285)	20	2499.3	(473185.261875502, 5854343.890212997)	(511478.2072492009, 5865299.472786125)	36	8097.8
(378998.47432518646, 6339699.896413925)	(377118.82222721865, 6339475.460538382)	20	2499.3	(473185.261875502, 5854343.890212997)	(396848.5889924612, 5857624.225035833)	36	8097.8
(377118.82222721865, 6339475.460538382)	(422125.6572177331, 6286562.972704994)	20	2499.3	(511478.2072492009, 5865299.472786125)	(513828.3138757374, 5850328.596456128)	42	11021.9
(377118.82222721865, 6339475.460538382)	(348986.43283211114, 6370678.407589518)	20	2499.3	(566497.8906079897, 5891536.856196745)	(566543.8862761182, 5891625.762702832)	20	2499.3
(422125.6572177331, 6286562.972704994)	(427464.3248525256, 6280078.9360657325)	20	2499.3	(566497.8906079897, 5891536.856196745)	(566554.0920052852, 5891641.257588403)	20	2499.3
(422125.6572177331, 6286562.972704994)	(426964.876009079, 6280685.537716534)	20	2499.3	(513828.3138757374, 5850328.596456128)	(506228.6875659872, 5743058.70224418)	42	11021.9
(422125.6572177331, 6286562.972704994)	(425597.98299873, 6282345.686833758)	20	2499.3	(506228.6875659872, 5743058.70224418)	(505591.57909282704, 5742189.853602463)	42	11021.9
(348986.43283211114, 6370678.407589518)	(211496.7787027526, 6391328.874316044)	20	2499.3	(506228.6875659872, 5743058.70224418)	(506054.5537028796, 5742791.185589799)	42	11021.9
(427464.3248525256, 6280078.9360657325)	(426964.876009079, 6280685.537716534)	20	2499.3	(468958.70008902653, 6449710.564787086)	(476176.7036923132, 6369617.491576042)	36	8097.8
(427464.3248525256, 6280078.9360657325)	(425597.98299873, 6282345.686833758)	20	2499.3	(476176.7036923132, 6369617.491576042)	(513008.24711305933, 6267591.296656276)	36	8097.8
(427464.3248525256, 6280078.9360657325)	(447775.7433325332, 6261305.552331929)	20	2499.3	(466956.5617059467, 6448402.840804987)	(466004.6060877425, 6400495.019638664)	40	9997.2
(426964.876009079, 6280685.537716534)	(427264.27895953535, 6281935.372892571)	34	7223	(466956.5617059467, 6448402.840804987)	(472151.6466141608, 6376332.838276971)	40	9997.2
(426964.876009079, 6280685.537716534)	(426778.452915229, 6279907.328483912)	34	7223	(466956.5617059467, 6448402.840804987)	(468796.707503678, 6449936.750162235)	40	9997.2
(425597.98299873, 6282345.686833758)	(429735.44206357945, 6283486.026921186)	20	2499.3	(466004.6060877425, 6400495.019638664)	(576475.84133988, 6174496.775475628)	40	9997.2
(425597.98299873, 6282345.686833758)	(420744.5412309372, 6281008.0121587785)	20	2499.3	(472151.6466141608, 6376332.838276971)	(595086.7729137045, 6155602.55027287)	40	9997.2
(427264.27895953535, 6281935.372892571)	(427529.6631649181, 6282878.0842049625)	34	7223	(595086.7729137045, 6155602.55027287)	(794964.0789205681, 5959543.495570813)	40	9997.2
(427264.27895953535, 6281935.372892571)	(427571.6371030377, 6283027.186169165)	34	7223	(541764.2701797213, 5902342.583106947)	(541767.2687144477, 5902203.5837321095)	24	3599
(427264.27895953535, 6281935.372892571)	(426778.452915229, 6279907.328483912)	34	7223	(447390.86990423495, 5654612.313002765)	(457079.6919239637, 5683864.889907337)	42	11021.9
(426778.452915229, 6279907.328483912)	(397785.4959342622, 5969374.27611221)	34	7223	(457079.6919239637, 5683864.889907337)	(447615.5257344601, 5655251.097589423)	42	11021.9
(429735.44206357945, 6283486.026921186)	(459382.93190344214, 6283850.304170418)	20	2499.3	(457079.6919239637, 5683864.889907337)	(505591.57909282704, 5742189.853602463)	42	11021.9
(429735.44206357945, 6283486.026921186)	(420744.5412309372, 6281008.0121587785)	20	2499.3	(505591.57909282704, 5742189.853602463)	(506054.5537028796, 5742791.185589799)	42	11021.9
(429735.44206357945, 6283486.026921186)	(427529.6631649181, 6282878.0842049625)	20	2499.3	(506054.5537028796, 5742791.185589799)	(507764.63808208413, 5766648.902708014)	42	11021.9
(420744.5412309372, 6281008.0121587785)	(427529.6631649181, 6282878.0842049625)	20	2499.3	(507764.63808208413, 5766648.902708014)	(507769.48857158265, 5766723.21263516)	42	11021.9
(420744.5412309372, 6281008.0121587785)	(389810.7288901388, 6281318.893531999)	20	2499.3	(507764.63808208413, 5766648.902708014)	(509119.5128037765, 5774088.803248421)	42	11021.9
(427529.6631649181, 6282878.0842049625)	(427571.6371030377, 6283027.186169165)	34	7223	(507769.48857158265, 5766723.21263516)	(507964.6680067731, 5769006.074073006)	40	9997.2

Table C3.1. Final dataset for the existing natural gas pipelines in the North Sea (1/2).

Coordinate node *u*	Coordinate node *v*	Diameter (inch)	Capacity (MW)
(507769.48857158265, 5766723.21263516)	(505678.2671592704, 5742263.828809675)	40	9997.2
(509119.5128037765, 5774088.803248421)	(509128.8987418024, 5774115.501670484)	42	11021.9
(509119.5128037765, 5774088.803248421)	(510717.5589903855, 5780081.955717049)	42	11021.9
(507964.6680067731, 5769006.074073006)	(508700.97415796964, 5772863.692963317)	40	9997.2
(507964.6680067731, 5769006.074073006)	(505678.2671592704, 5742263.828809675)	40	9997.2
(505678.2671592704, 5742263.828809675)	(516002.9598789426, 5688828.9394348655)	40	9997.2
(509128.8987418024, 5774115.501670484)	(510133.9593438252, 5777055.607615262)	40	9997.2
(509128.8987418024, 5774115.501670484)	(508700.97415796964, 5772863.692963317)	40	9997.2
(510717.5589903855, 5780081.955717049)	(510718.9769753066, 5780090.125898196)	42	11021.9
(510717.5589903855, 5780081.955717049)	(511919.55283127207, 5796463.666088172)	42	11021.9
(508700.97415796964, 5772863.692963317)	(510133.9593438252, 5777055.607615262)	40	9997.2
(510133.9593438252, 5777055.607615262)	(510705.29953819193, 5779903.530737079)	40	9997.2
(510718.9769753066, 5780090.125898196)	(512575.98653197655, 5805424.477247665)	40	9997.2
(510718.9769753066, 5780090.125898196)	(510705.29953819193, 5779903.530737079)	40	9997.2
(511919.55283127207, 5796463.666088172)	(511925.5799167384, 5796551.2705098335)	42	11021.9
(511919.55283127207, 5796463.666088172)	(512586.6253187486, 5806415.707136869)	42	11021.9
(510705.29953819193, 5779903.530737079)	(512575.98653197655, 5805424.477247665)	40	9997.2
(510705.29953819193, 5779903.530737079)	(511925.5799167384, 5796551.2705098335)	40	9997.2
(512575.98653197655, 5805424.477247665)	(511925.5799167384, 5796551.2705098335)	40	9997.2
(512575.98653197655, 5805424.477247665)	(512585.6268380995, 5806501.062127923)	40	9997.2
(512575.98653197655, 5805424.477247665)	(512592.2828221936, 5807244.371702075)	40	9997.2
(512586.6253187486, 5806415.707136869)	(512585.6268380995, 5806501.062127923)	42	11021.9
(512586.6253187486, 5806415.707136869)	(513991.4201983525, 5847705.281247163)	42	11021.9
(512585.6268380995, 5806501.062127923)	(512592.2828221936, 5807244.371702075)	40	9997.2
(512592.2828221936, 5807244.371702075)	(513948.2928125484, 5845220.097395049)	40	9997.2
(513991.4201983525, 5847705.281247163)	(513990.03341960383, 5847759.79299686)	42	11021.9
(513991.4201983525, 5847705.281247163)	(524529.4160683086, 6161793.367278717)	42	11021.9
(513990.03341960383, 5847759.79299686)	(513995.77419024403, 5848109.088586324)	40	9997.2
(513990.03341960383, 5847759.79299686)	(513948.2928125484, 5845220.097395049)	40	9997.2
(524529.4160683086, 6161793.367278717)	(463168.7946721789, 6357472.951859608)	42	11021.9
(513948.2928125484, 5845220.097395049)	(513995.77419024403, 5848109.088586324)	40	9997.2
(513995.77419024403, 5848109.088586324)	(508735.18205012626, 5882321.335293145)	40	9997.2
(463168.7946721789, 6357472.951859608)	(464987.47792804556, 6447263.997837251)	42	11021.9
(464987.47792804556, 6447263.997837251)	(463480.77213576256, 6326469.96377266851)	42	11021.9
(464987.47792804556, 6447263.997837251)	(468849.3549968335, 6449911.983886492)	42	11021.9
(463480.77213576256, 6326469.96377266851)	(525958.7327554708, 6184983.55245338)	42	11021.9
(525958.7327554708, 6184983.55245338)	(519358.01391143433, 6071899.211723003)	42	11021.9
(519186.6067866278, 6071317.61784034)	(501158.69302057451, 5716799.536386963)	40	9997.2
(501158.69302057451, 5716799.536386963)	(515923.4009004284, 5688784.559180301)	40	9997.2
(512912.49916899943, 6267301.588270561)	(516652.4258971926, 6266665.81521927)	36	8097.8
(516652.4258971926, 6266665.81521927)	(756250.7740279936, 5954327.921702382)	36	8097.8
(397010.0209094289, 5857666.841837019)	(431865.2313192251, 5849579.97195162)	40	9997.2
(431865.2313192251, 5849579.97195162)	(465583.55059510225, 5761436.556125671)	40	9997.2
(465583.55059510225, 5761436.556125671)	(512217.3423863864, 5686007.991640626)	40	9997.2
(555649.1573889885, 5793503.369555352)	(571877.4932120459, 5759445.380421263)	26	4223.8
(447698.8395861225, 6638312.3310577525)	(453504.88301225414, 6660159.796814813)	20	2499.3
(598590.9005969545, 6711455.264783611)	(600852.7839705185, 6713558.853327209)	40	9997.2
(598590.9005969545, 6711455.264783611)	(592841.98812108, 6707069.540223511)	40	9997.2
(598590.9005969545, 6711455.264783611)	(595074.9142741413, 6708768.98885496)	40	9997.2
(592841.98812108, 6707069.540223511)	(592262.9454241535, 6706525.425372319)	40	9997.2
(592841.98812108, 6707069.540223511)	(595074.9142741413, 6708768.98885496)	40	9997.2
(595074.9142741413, 6708768.98885496)	(593011.366382251, 6707093.397413537)	40	9997.2
(592262.9454241535, 6706525.425372319)	(581093.9680237537, 6684392.282222671)	40	9997.2
(593011.366382251, 6707093.397413537)	(592107.7149779751, 6706128.680634178)	40	9997.2
(593011.366382251, 6707093.397413537)	(600853.9256178074, 6713557.695677103)	40	9997.2
(588721.0869262554, 6698127.423294615)	(581093.9680237537, 6684392.282222671)	40	9997.2
(588721.0869262554, 6698127.423294615)	(592107.7149779751, 6706128.680634178)	40	9997.2
(581093.9680237537, 6684392.282222671)	(579061.2994041044, 6680201.983649858)	40	9997.2
(581093.9680237537, 6684392.282222671)	(576500.1609000246, 6676018.585508968)	40	9997.2
(592107.7149779751, 6706128.680634178)	(579150.2211248266, 6680261.60145357)	40	9997.2
(579061.2994041044, 6680201.983649858)	(576500.1609000246, 6676018.585508968)	40	9997.2
(579061.2994041044, 6680201.983649858)	(527030.9378049979, 6572691.292147379)	40	9997.2
(576500.1609000246, 6676018.585508968)	(480449.6329021302, 6534142.4535682555)	40	9997.2
(527030.9378049979, 6572691.292147379)	(512377.0986185207, 6542975.000315439)	40	9997.2
(527030.9378049979, 6572691.292147379)	(558855.4371591279, 6636446.008471912)	40	9997.2
(480449.6329021302, 6534142.4535682555)	(449803.480810513, 6485989.189023579)	40	9997.2
(480449.6329021302, 6534142.4535682555)	(463159.2031449836, 6506937.776017228)	40	9997.2
(480449.6329021302, 6534142.4535682555)	(444491.80919345224, 6478608.282985803)	40	9997.2
(579150.2211248266, 6680261.60145357)	(578501.1872087056, 6679149.11729412)	40	9997.2
(579150.2211248266, 6680261.60145357)	(576627.4061935832, 6675937.341074381)	40	9997.2
(512377.0986185207, 6542975.000315439)	(468755.0578203525, 6450326.035762492)	40	9997.2
(512377.0986185207, 6542975.000315439)	(468412.86878520244, 6450715.412074596)	40	9997.2
(558855.4371591279, 6636446.008471912)	(561056.3317558677, 6640149.327758006)	40	9997.2
(558855.4371591279, 6636446.008471912)	(561856.9137225933, 6641496.4211816825)	40	9997.2
(449803.480810513, 6485989.189023579)	(444491.80919345224, 6478608.282985803)	40	9997.2
(449803.480810513, 6485989.189023579)	(463159.2031449836, 6506937.776017228)	40	9997.2
(463159.2031449836, 6506937.776017228)	(457704.2970111947, 6558582.480936416)	36	8097.8
(463159.2031449836, 6506937.776017228)	(468890.7624966315, 6452673.837430064)	36	8097.8
(444491.80919345224, 6478608.282985803)	(439329.76950959937, 6473148.724804737)	40	9997.2
(457704.2970111947, 6558582.480936416)	(456569.54579270305, 6592946.576390092)	36	8097.8
(457704.2970111947, 6558582.480936416)	(468890.7624966315, 6452673.837430064)	36	8097.8
(457704.2970111947, 6558582.480936416)	(461750.2893859317, 6520276.765462364)	36	8097.8
(468890.7624966315, 6452673.837430064)	(461750.2893859317, 6520276.765462364)	36	8097.8
(468890.7624966315, 6452673.837430064)	(469013.20548602834, 6450345.493910545 5)	36	8097.8
(439329.76950959937, 6473148.724804737)	(436728.29091241234, 6470691.040594641)	40	9997.2
(439329.76950959937, 6473148.724804737)	(436043.43258448805, 6470170.511448721)	40	9997.2
(461750.2893859317, 6520276.765462364)	(480941.9666224093, 6566885.304208473)	42	11021.9
(461750.2893859317, 6520276.765462364)	(458979.02490126775, 6513546.525759099)	42	11021.9
(524507.4064217092, 6236936.310304307)	(512852.5378762526, 6267086.573465784)	20	2499.3
(608911.7310092347, 6079737.843029308)	(617500.5598142991, 6018508.858514806)	24	3599
(617500.5598142991, 6018508.858514806)	(588685.9471917347, 5964965.135446918)	24	3599
(588685.9471917347, 5964965.135446918)	(613458.0187322123, 5933567.8498038715)	24	3599
(613458.0187322123, 5933567.8498038715)	(629731.057669261, 5942348.829731853)	24	3599
(613458.0187322123, 5933567.8498038715)	(618872.9126761183, 5918830.953984269)	24	3599
(618872.9126761183, 5918830.953984269)	(618912.1008888567, 5918738.9529059725)	24	3599
(618872.9126761183, 5918830.953984269)	(618879.10265171, 5918816.421950546)	24	3599
(618912.1008888567, 5918738.9529059725)	(618879.10265171, 5918816.421950546)	24	3599
(618912.1008888567, 5918738.9529059725)	(614843.240564859, 5860496.370864442)	24	3599
(618879.10265171, 5918816.421950546)	(618734.7271158351, 5918790.451977293)	36	8097.8
(618879.10265171, 5918816.421950546)	(618879.826002495, 5918816.552065391)	36	8097.8
(618734.7271158351, 5918790.451977293)	(618879.826002495, 5918816.552065391)	36	8097.8
(618734.7271158351, 5918790.451977293)	(619920.5013178656, 5917665.069761312)	36	8097.8
(618734.7271158351, 5918790.451977293)	(618879.826002495, 5918816.552065391)	36	8097.8
(618879.826002495, 5918816.552065391)	(739285.8863002735, 5938266.27058667)	36	8097.8
(739285.8863002735, 5938266.27058667)	(744835.8432697698, 5930540.322295495)	36	8097.8
(490548.32070507837, 6705893.305980375)	(490179.64392124745, 6705549.668073598)	36	8097.8
(490179.64392124745, 6705549.668073598)	(456254.80642135075, 6604842.311291549)	36	8097.8
(490179.64392124745, 6705549.668073598)	(456296.5322142084, 6604351.4241977555)	36	8097.8
(695346.1927666434, 5938074.291364197)	(693968.3084829613, 5927922.8471997855)	20	2499.3
(613095.9032291935, 6176464.721088673)	(704454.2899676798, 6182207.782564193)	30	5623.4
(704454.2899676798, 6182207.782564193)	(728217.0186004539, 6184407.428588503)	30	5623.4
(704454.2899676798, 6182207.782564193)	(721831.1132356221, 6183816.3040773233)	30	5623.4
(728217.0186004539, 6184407.428588503)	(721831.1132356221, 6183816.3040773233)	30	5623.4
(728217.0186004539, 6184407.428588503)	(823731.3892758468, 6183855.51476786)	30	5623.4
(721831.1132356221, 6183816.3040773233)	(721808.4541703671, 6183897.9335544429)	42	11021.9
(721808.4541703671, 6183897.933554429)	(631929.9735011158, 6514390.953443488)	42	11021.9
(721808.4541703671, 6183897.933554429)	(779696.6917922054, 5975433.91147569)	42	11021.9
(631929.9735011158, 6514390.953443488)	(634076.7849729586, 6564189.2549567 5)	42	11021.9
(779696.6917922054, 5975433.91147569)	(789080.7565834202, 5970305.566215284)	42	11021.9
(565808.097674278, 5900222.596133777)	(565787.0994171078, 5900173.595991878)	24	3599
(514228.4494237759, 5906699.686984414)	(515519.02947017713, 5906711.405489288)	20	2499.3
(643034.6837887766, 6572795.069873585)	(641628.6253193096, 6569518.897271926)	42	11021.9
(641556.6606088676, 6569445.65844189)	(640105.0075232913, 6568007.3804974 71)	42	11021.9
(640105.0075232913, 6568007.3804974 71)	(634850.0752097282, 6564975.460136864)	42	11021.9
(640105.0075232913, 6568007.3804974 71)	(643210.9806089415, 6573054.444530298)	42	11021.9
(640105.0075232913, 6568007.3804974 71)	(635701.5885887065, 6565436.063565598)	42	11021.9
(634850.0752097282, 6564975.460136864)	(634076.7849729586, 6564189.2549567 5)	42	11021.9
(634850.0752097282, 6564975.460136864)	(635559.1172252515, 6565366.339393144)	42	11021.9
(634076.7849729586, 6564189.2549567 5)	(630134.7338343337, 6525569.652539354)	42	11021.9
(630134.7338343337, 6525569.652539354)	(776775.1854117303, 5977054.429426003)	42	11021.9
(776775.1854117303, 5977054.429426003)	(794347.1132956182, 5958525.556589705)	42	11021.9
(496228.5532835825, 6277561.707900784)	(516312.5515770916, 6247826.27386562)	27	4555

Coordinate node *u*	Coordinate node *v*	Diameter (inch)	Capacity (MW)
(514304.4547658421, 6267276.253107279)	(510466.0333059424, 6271344.285195684)	36	8097.8
(510466.0333059424, 6271344.285195684)	(468989.968860959, 6400465.059057727)	36	8097.8
(540225.806258186, 6723588.527228442)	(594616.250174526, 6708568.932608865)	36	8097.8
(594616.250174526, 6708568.932608865)	(595203.2435902387, 6708943.921100869)	36	8097.8
(594616.250174526, 6708568.932608865)	(594193.2837895091, 6708350.856016202)	36	8097.8
(594616.250174526, 6708568.932608865)	(594830.9428235356, 6708613.256848234)	36	8097.8
(595203.2435902387, 6708943.921100869)	(594988.9496761939, 6708729.954349294)	36	8097.8
(595203.2435902387, 6708943.921100869)	(600851.0013707281, 6713560.66099944)	36	8097.8
(595203.2435902387, 6708943.921100869)	(598593.9868259749, 6711480.979503778)	36	8097.8
(595203.2435902387, 6708943.921100869)	(598604.9723748714, 6711476.822114426)	36	8097.8
(594193.2837895091, 6708350.856016202)	(594988.9496761939, 6708729.954349294)	36	8097.8
(594193.2837895091, 6708350.856016202)	(593285.3262572779, 6708074.042353485)	36	8097.8
(594830.9428235356, 6708613.256848234)	(594002.0188107104, 6708096.83314098)	36	8097.8
(594830.9428235356, 6708613.256848234)	(594988.9496761939, 6708729.954349294)	36	8097.8
(594988.9496761939, 6708729.954349294)	(598604.9723748714, 6711476.822114426)	36	8097.8
(598604.9723748714, 6711476.822114426)	(594002.0188107104, 6708096.83314098)	36	8097.8
(598604.9723748714, 6711476.822114426)	(600684.4855593563, 6714090.272122908)	36	8097.8
(593285.3262572779, 6708074.042353485)	(540226.3134152555, 6723506.800989305)	36	8097.8
(593285.3262572779, 6708074.042353485)	(594002.0188107104, 6708096.83314098)	36	8097.8
(562257.4409090907, 6183224.651138106)	(569040.52938828, 6129230.86570553)	20	2499.3
(569040.52938828, 6129230.86570553)	(608812.8392899456, 6079763.416162286)	20	2499.3
(566051.0990061018, 5996815.2773645)	(540855.7119882702, 5977364.7739370465)	24	3599
(447988.87988246826, 6639032.8152595395)	(447650.9001070283, 6638367.139408074)	26	4223.8
(447371.9379140336, 6638231.868188095)	(447533.4033881319 4, 6638293.94603151)	26	4223.8
(558148.1535864604, 5903223.575478802)	(566488.09299910 16, 5891680.656773084)	24	3599
(566488.09299916, 5891680.656773084)	(566550.09210803 92, 5891619.656888804)	24	3599
(566488.09299916, 5891680.656773084)	(566543.88627611 82, 5891625.762702832)	24	3599
(566550.09210803 92, 5891619.656888804)	(566543.88627611 82, 5891625.762702832)	24	3599
(566550.09210803 92, 5891619.656888804)	(614995.738930376, 5860352.833067314)	24	3599
(566543.88627611 82, 5891625.762702832)	(566554.09200528 52, 5891641.257588403)	20	2499.3
(566554.09200528 52, 5891641.257588403)	(579886.9997967046, 5917589.9700821405)	20	2499.3
(610282.9424204874, 6174769.100159586)	(609381.8434280441, 6141403.069665399)	26	4223.8
(609381.8434280441, 6141403.069665399)	(609359.5530733246, 6140903.564470005)	26	4223.8
(609381.8434280441, 6141403.069665399)	(609380.8005378912, 6141379.699510185)	26	4223.8
(609359.5530733246, 6140903.564470005)	(609380.8005378912, 6141379.699510185)	26	4223.8
(609359.5530733246, 6140903.564470005)	(609363.4419900374, 6135908.496417594)	26	4223.8
(609380.8005378912, 6141379.699510185)	(577176.6108449113, 6173791.611592496)	40	9997.2
(609380.8005378912, 6141379.699510185)	(676985.3257706618, 6073339.113825504)	40	9997.2
(609363.4419900374, 6135908.496417594)	(609386.0905746187, 6135409.020372901)	26	4223.8
(609363.4419900374, 6135908.496417594)	(609379.9515982176, 6135544.405065057)	26	4223.8
(577176.6108449113, 6173791.611592496)	(676985.3257706618, 6073339.113825504)	40	9997.2
(676985.3257706618, 6073339.113825504)	(794347.1132956182, 5958525.556589705)	40	9997.2
(609386.0905746187, 6135409.020372901)	(609379.9515982176, 6135544.405065057)	26	4223.8
(609386.0905746187, 6135409.020372901)	(609044.5623189479, 6079504.074392224)	26	4223.8
(609379.9515982176, 6135544.405065057)	(604604.9087471823, 6140475.552033862)	36	8097.8
(609379.9515982176, 6135544.405065057)	(614861.2899986281, 6129883.87256694)	36	8097.8
(794347.1132956182, 5958525.556589705)	(785686.341406351, 5956583.523985193)	42	11021.9
(604604.9087471823, 6140475.552033862)	(598449.7483623315, 6146972.709773813)	36	8097.8
(604604.9087471823, 6140475.552033862)	(614861.2899986281, 6129883.87256694)	36	8097.8
(614861.2899986281, 6129883.87256694)	(696138.8247262202, 6044738.839676155)	36	8097.8
(578501.1872087056, 6679149.11729412)	(578273.0201351175, 6680130.509550559)	42	11021.9
(578501.1872087056, 6679149.11729412)	(584000.2472227109, 6655496.559409356)	42	11021.9
(578501.1872087056, 6679149.11729412)	(576627.4061935832, 6675937.341074381)	40	9997.2
(576627.4061935832, 6675937.341074381)	(561856.9137225933, 6641496.4211816825)	40	9997.2
(468412.86878520244, 6450715.412074596)	(436180.9507158491, 6470178.85682039 15)	40	9997.2
(561056.3317558677, 6640149.327758006)	(550825.1455740231, 6653220.317460986)	30	5623.4
(561056.3317558677, 6640149.327758006)	(561678.7423073115, 6639354.158775216)	30	5623.4
(561056.3317558677, 6640149.327758006)	(561856.9137225933, 6641496.4211816825)	40	9997.2
(624194.7286227051, 6579231.412158546)	(622093.3617241377, 6579500.703570451)	28	4898.6
(622093.3617241377, 6579500.703570451)	(624382.8494263487, 6579227.863784319)	28	4898.6
(622093.3617241377, 6579500.703570451)	(549710.0988079049, 6513770.729156511)	28	4898.6
(549710.0988079049, 6513770.729156511)	(468918.88671169226, 6449717.667198925)	28	4898.6
(456457.03561948927, 6604145.747864203 5)	(468944.6791272268, 6449827.585687216)	36	8097.8
(644698.8705859517, 5895203.691567047 5)	(661840.5275839407, 5895815.586845919)	20	2499.3
(468810.8569156975, 6449784.207370684 5)	(436156.47367511364, 6470137.49717957)	30	5623.4
(519249.6736165643, 6070911.717822441)	(508581.7190407142 6, 5883299.253302768)	40	9997.2
(535920.7385778576, 6715480.65162958)	(490488.02960922685, 6706312.589468942)	20	2499.3
(453403.11811154906, 6766228.79545813)	(613815.7859869427, 6578501.711758941)	30	5623.4
(613815.7859869427, 6578501.711758941)	(620471.2616768345, 6579406.372534621)	30	5623.4
(620471.2616768345, 6579406.372534621)	(623725.0584878552, 6579164.768430137)	30	5623.4
(620471.2616768345, 6579406.372534621)	(561678.7423073115, 6639354.158775216)	30	5623.4
(623725.0584878552, 6579164.768430137)	(624382.9056855564, 6579234.831812205)	30	5623.4
(623725.0584878552, 6579164.768430137)	(624087.0914709191, 6579207.820720336)	30	5623.4
(561678.7423073115, 6639354.158775216)	(550825.1455740231, 6653220.317460986)	30	5623.4
(514581.4632887878, 5896531.62717084)	(575949.025475991, 5897363.614609873)	36	8097.8
(575949.025475991, 5897363.614609873)	(614910.7392920713, 5860444.871606298)	36	8097.8
(460750.6766183828, 6702694.507290499)	(477264.0957517021, 6738513.658445945)	22	3024.2
(460750.6766183828, 6702694.507290499)	(459833.8464966053, 6613539.205264947)	22	3024.2
(477264.0957517021, 6738513.658445945)	(447270.8857893112, 6773528.156714196)	30	5623.4
(477264.0957517021, 6738513.658445945)	(488019.7652230964, 6725957.337513566)	30	5623.4
(447270.8857893112, 6773528.156714196)	(488019.7652230964, 6725957.337513566)	30	5623.4
(488019.7652230964, 6725957.337513566)	(494141.3140381553, 6714335.138795109)	30	5623.4
(459393.59941006626, 6612846.142629294)	(456168.25619435357, 6604805.544919367)	22	3024.2
(456751.6694823465, 6603856.945329733)	(456530.2381833084 5, 6593940.2940353)	36	8097.8
(480941.9666224093, 6566885.304208473)	(506891.6515554196, 6695628.597819027)	42	11021.9
(480941.9666224093, 6566885.304208473)	(458979.02490126775, 6513546.525759099)	42	11021.9
(458979.02490126775, 6513546.525759099)	(443982.90676414984, 6478605.527032213)	42	11021.9
(506891.6515554196, 6695628.597819027)	(509479.5201875334, 6699157.340276232)	42	11021.9
(506891.6515554196, 6695628.597819027)	(507769.00357350585, 6696824.929532977)	42	11021.9
(520526.0054784045, 6260242.350235772)	(597764.724539309, 6147693.504057382)	36	8097.8
(480127.14235663763, 6766539.7971019065)	(518659.9864000518, 6735472.2120956)	30	5623.4
(518659.9864000518, 6735472.2120956)	(522563.1135586641, 6731956.161778787)	30	5623.4
(518659.9864000518, 6735472.2120956)	(520823.2126610343, 6733523.515045472)	30	5623.4
(522563.1135586641, 6731956.161778787)	(520823.2126610343, 6733523.515045472)	30	5623.4
(522563.1135586641, 6731956.161778787)	(560682.4214687624, 6719523.23568152)	30	5623.4
(520823.2126610343, 6733523.515045472)	(520932.96051015914, 6734570.77703081)	42	11021.9
(520823.2126610343, 6733523.515045472)	(520742.9939478428, 6732758.032992673)	42	11021.9
(560682.4214687624, 6719523.23568152)	(581869.1231717295, 6712911.644172993)	30	5623.4
(560682.4214687624, 6719523.23568152)	(569804.8810037818, 6716676.451087853)	30	5623.4
(520932.96051015914, 6734570.77703081)	(520950.9574453629, 6768696.469904407)	42	11021.9
(520932.96051015914, 6734570.77703081)	(520742.9939478428, 6732758.032992673)	42	11021.9
(520742.9939478428, 6732758.032992673)	(509479.5201875334, 6699157.340276232)	42	11021.9
(581869.1231717295, 6712911.644172993)	(569804.8810037818, 6716676.451087853)	30	5623.4
(581869.1231717295, 6712911.644172993)	(600168.0037397683, 6713413.5325082)	30	5623.4
(569804.8810037818, 6716676.451087853)	(578273.0201351175, 6680130.509550559)	42	11021.9
(509479.5201875334, 6699157.340276232)	(507769.00357350585, 6696824.929532977)	42	11021.9
(578273.0201351175, 6680130.509550559)	(584000.2472227109, 6655496.559409356)	42	11021.9
(507769.00357350585, 6696824.929532977)	(495946.5624632121, 6710839.797995434)	30	5623.4
(507769.00357350585, 6696824.929532977)	(508331.9049811784, 6696157.640170969)	30	5623.4
(495946.5624632121, 6710839.797995434)	(494626.683722565, 6713395.385706601)	30	5623.4
(495946.5624632121, 6710839.797995434)	(508331.9049811784, 6696157.640170969)	30	5623.4
(508331.9049811784, 6696157.640170969)	(550825.1455740231, 6653220.317460986)	30	5623.4
(443730.3112645393, 6478017.213549422)	(436712.3860958606, 6470707.229872571)	42	11021.9
(471793.4963156098, 6774146.340864677)	(430243.2183826237, 6765733.007473995)	28	4898.6
(436566.11604688456, 6469848.210163634)	(466211.0269454223 5, 6318328.431179547)	40	9997.2
(466211.0269454223 5, 6318328.431179547)	(525915.6120538256, 6185434.937102802)	40	9997.2
(525915.6120538256, 6185434.937102802)	(519308.3572884777, 6071904.573975763)	40	9997.2
(405729.69755618204, 6612947.646914011)	(456051.3352329262 4, 6604714.998606688)	32	6398.2
(469053.07292848185, 6449354.604760197)	(468989.968860959, 6400465.059057727)	36	8097.8
(558260.588663378, 6788946.313120315)	(569025.0952207722, 6719933.665234513)	42	11021.9
(584000.2472227109, 6655496.559409356)	(624382.7793625315, 6579219.190421076)	42	11021.9
(468298.3681443451, 6450201.72488491)	(436591.5924246112, 6469883.365931111)	30	5623.4
(432573.3689588419, 6767587.633940245)	(430106.0080413448, 6766144.824977016)	32	6398.2
(696880.3661122861, 6044061.571639439)	(763901.1847008099, 5949250.610525062)	36	8097.8
(763901.1847008099, 5949250.610525062)	(767806.791515118, 5919202.962408417)	36	8097.8
(464622.04349942, 6767120.529371061)	(480768.966655080 73, 6746175.277428134)	22	3024.2
(450393.24745205976, 6349611.3058971284)	(428726.47548090457, 6402320.982145284)	20	2499.3
(414590.67697332415, 6526967.637629045)	(393831.3417949726, 6525009.59800982)	30	5623.4
(436514.6890215057, 6321379.116033549)	(404956.1876326564, 6313335.091253902)	20	2499.3
(453982.87479135016, 6047128.8251697)	(413861.6193195897, 6017832.979861609)	24	3599
(265611.711503746, 6712068.932880976)	(269943.3706383372, 6730776.29241769)	20	2499.3
(375564.99552317645, 5988522.561782737)	(351080.5859562901 3, 5989447.8728110725)	24	3599
(428728.7860789502, 6402347.332986572)	(431620.4796423411, 6424511.268114423)	20	2499.3
(269865.56858341047, 6730872.192659691)	(265929.766387051, 6712862.969818345)	20	2499.3
(265435.073241435, 6710614.470901158)	(260448.60484375976, 6711069.291565503)	20	2499.3

Table C3.2. Final dataset for the existing natural gas pipelines in the North Sea (2/2).

Appendix D: Dataset Onshore Entry Points

In Table D.1, the relevant data regarding onshore entry points is provided, including ID, country, coordinates, the total pipeline diameters and share of pipeline diameter. Using the equation described in *5.5 Onshore Entry Points*, and the total pipeline diameter, the share of hydrogen demand per entry point is calculated.

ID	Location	Country	Coordinates	Total pipeline diameter (inch)	Share (%)
BE01	Zeebrugge	Belgium	(514356.249, 5688685.812)	120	7.2%
DK01	Jutland	Denmark	(823627.379, 6183927.967)	30	1.8%
FR01	Dunkerque	France	(447686.958, 5654786.189)	84	5.0%
DE01	Emden	Germany	(778386.84, 5917696.808)	36	2.2%
DE02	Dornum	Germany	(795076.595, 5957585.486)	122	7.3%
NL01	Maasvlakte	Netherlands	(571920.399, 5759680.069)	26	1.6%
NL02	IJmuiden	Netherlands	(606990.825, 5816054.688)	20	1.2%
NL03	Den Helder	Netherlands	(614906.779, 5860447.736)	120	7.2%
NL04	Eemshaven	Netherlands	(745542.557, 5930167.33)	36	2.2%
NO01	Karsto	Norway	(644273.739, 6573213.843)	42	2.5%
NO02	Sleipner	Norway	(624417.51, 6579863.949)	100	6.0%
NO03	Kollsnes	Norway	(600053.306, 6713079.594)	106	6.3%
UK01	Bacton	UK	(396489.989, 5858276.384)	292	17.5%
UK02	Shetland	UK	(273423.414, 6708581.79)	30	1.8%
UK03	St. Fergus	UK	(211639.759, 6391901.537)	210	12.6%
UK04	Teeside	UK	(234794.842, 6061404.731)	36	2.2%
UK05	Easington	UK	(310253.076, 5948737.723)	170	10.2%
UK06	Theddlethorpe	UK	(316902.085, 5917711.042)	90	5.4%

Table D.1. Dataset for onshore entry points for the hydrogen backbone.

Appendix E: Specification of Clustering Results

In this Appendix, the resulting clustering output is visualized. The results for the first clustering round are presented in *E1. Result Specification of First Clustering Round*. In *E2. Specification of Filtering Results,* the results of the filtering after the first round are shown. The techno-economic details for $k = [3,20]$ are specified in *E3. Techno-Economic Details Post-Filtering*. Finally, some relevant cluster-specific results for $k = \{6,7,8\}$ after the second clustering round are provided in *E4. Cluster-Specific Results for* $k = \{6,7,8\}$.

E1. Result Specification of First Clustering Round

The resulting distribution of OWFs per cluster for each configuration in $k = [3,20]$ is presented in Figures E1.1 and E1.2. The OWFs belonging to the same cluster are indicated with a same color and black crosses indicate initial centroid locations

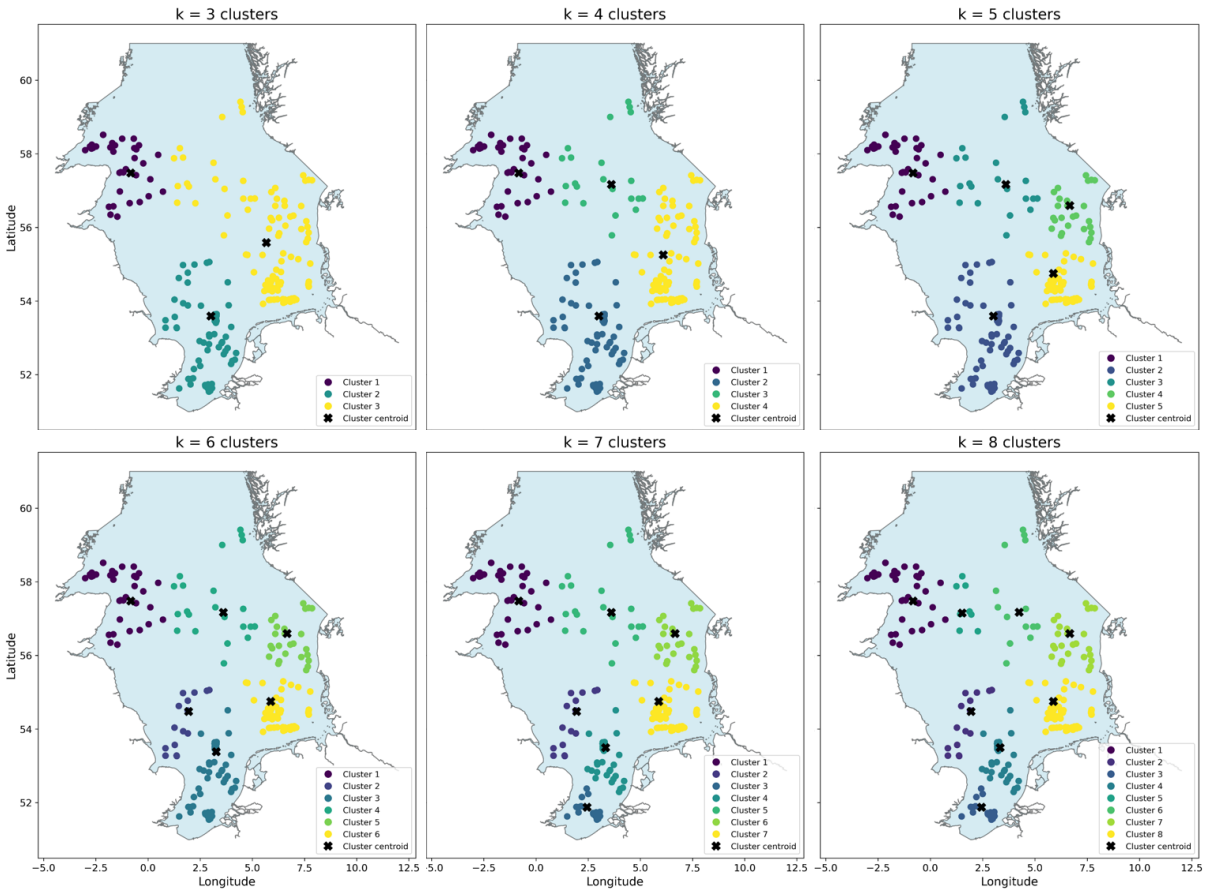

Figure E1.1. Results for Ward's clustering in the first round for $k = [3,8]$.

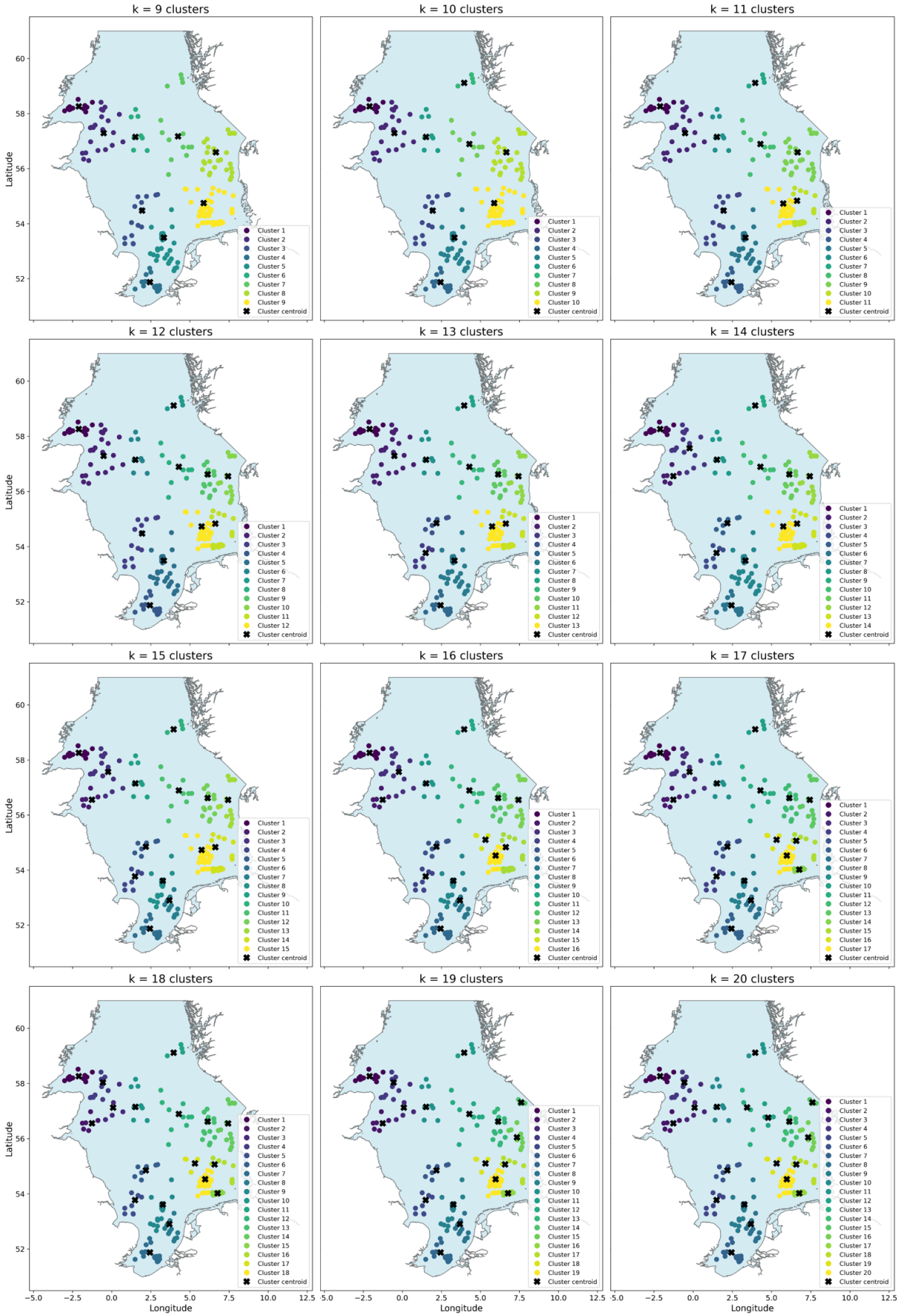

Figure E1.2. Results for Ward's clustering in the first round for $k = [12,20]$.

E2. Specification of Filtering Results

Based on the distance criterion defined in *4.3.1.3 Post-Clustering*, OWFs are filtered from the clusters that are generated in the first clustering round. Their island connection is then rearranged to one single connection to shore. The results of this filtering are presented in Figures E2.1 and E2.2 for each configuration in $k = [3,20]$. The OWFs belonging to the same cluster are indicated with a same color, the filtered OWFs are indicated by red crosses, and the black crosses indicate initial centroid locations.

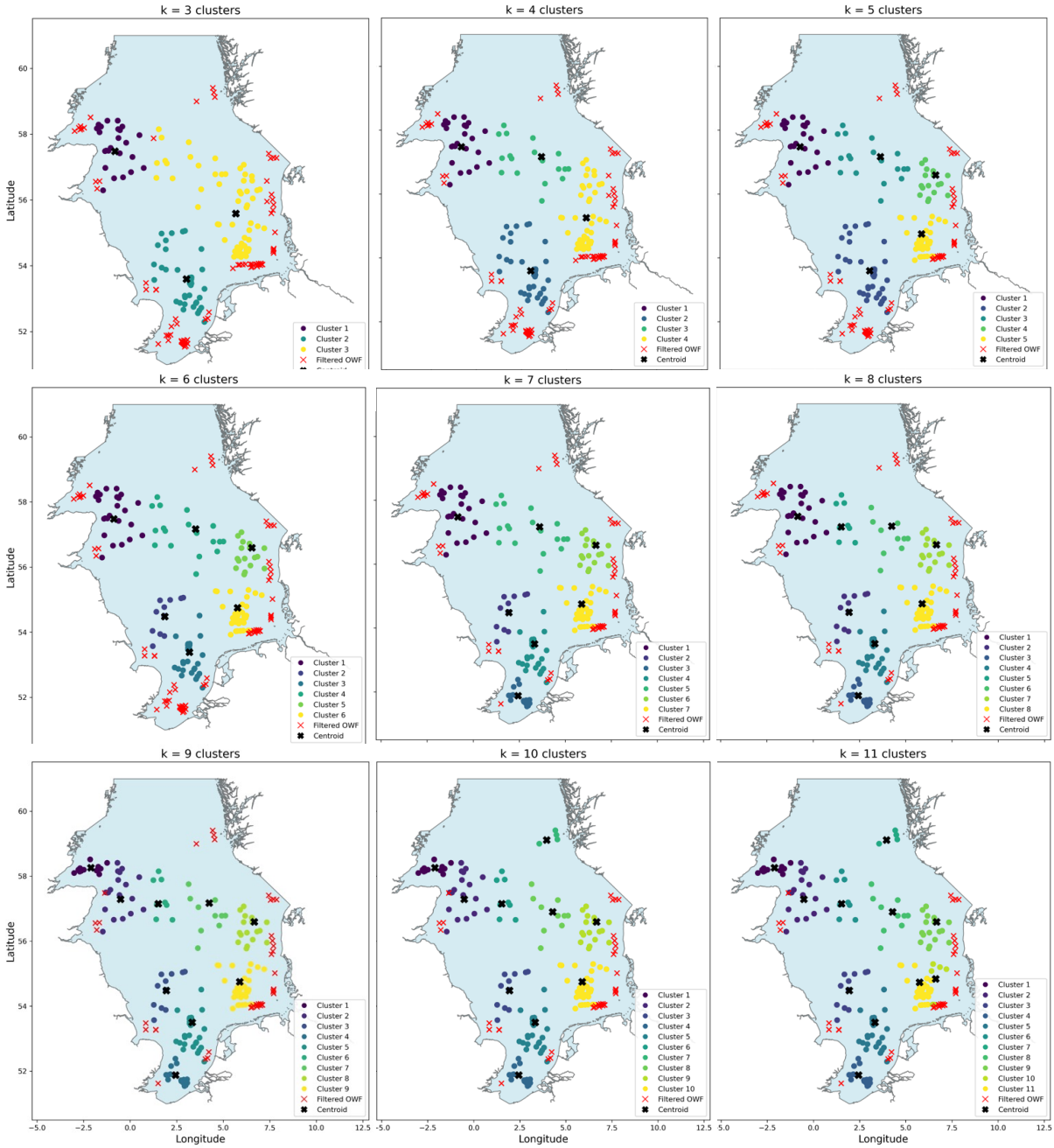

Figure E2.1. Results for filtering the output of the first clustering round based on the distance criterion for $k = [3,11]$.

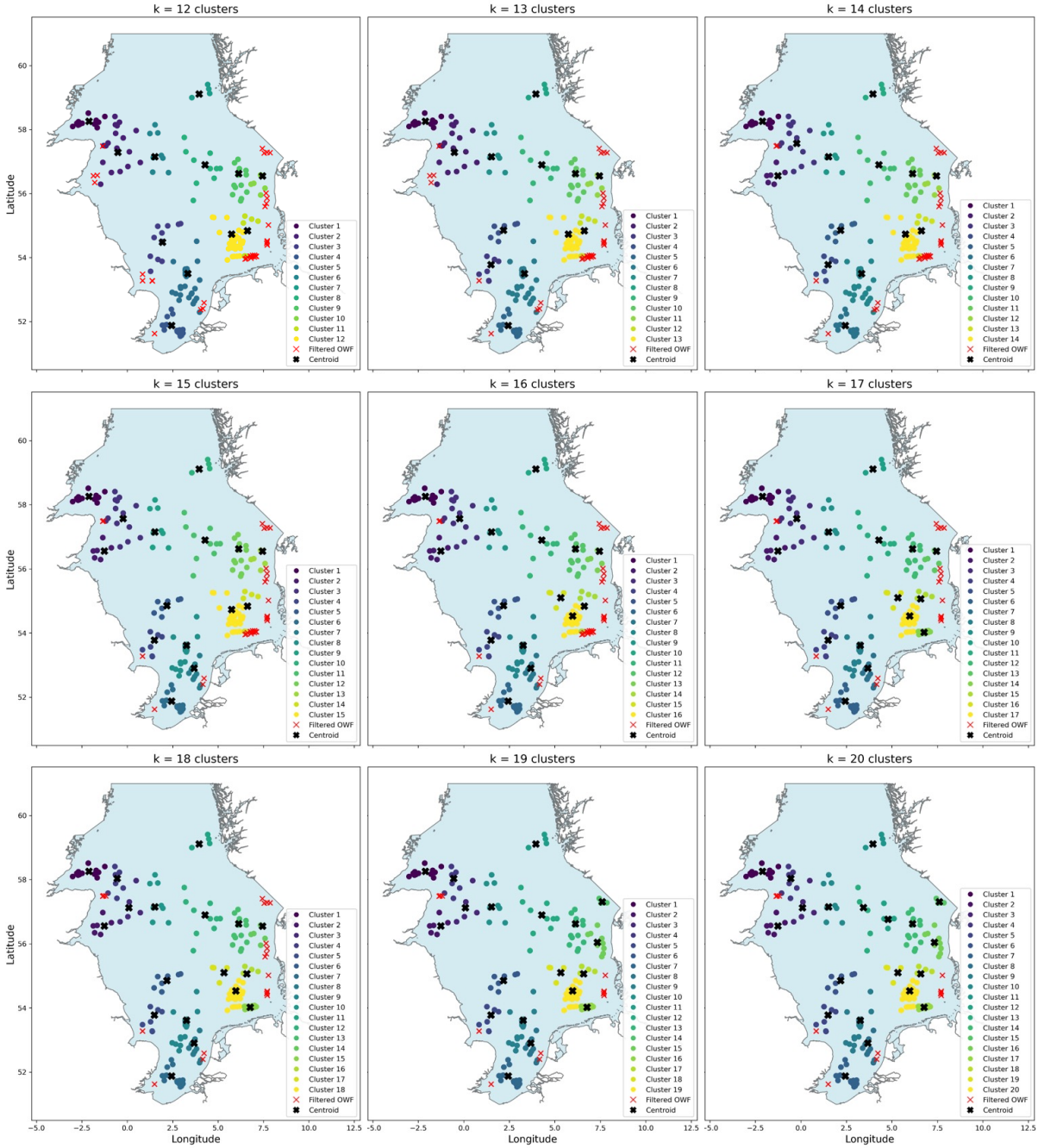

Figure E2.2. Results for filtering the output of the first clustering round based on the distance criterion for $k = [12,20]$.

E3. Techno-Economic Details Post-Filtering

The techno-economic details for $k = [3,20]$ after filtering are specified in this section. The specifications for the economic assessment are presented in Table E3.1. It shows that the subtotal costs consist of island construction, OWF-to-island cabling and OWF-to-shore cabling costs. It shows a trade-off between the energy island construction costs and total cabling costs, consisting of both OWF-to-island and OWF-to-shore connections.

k	Island construction costs (billion euros)	OWF-to-island cable costs (billion euros)	OWF-to-shore cable costs (billion euros)	Subtotal (billion euros)
3	€19.1	€21.2	€3.2	€43.6
4	€19.1	€18.1	€3.2	€40.4
5	€20.0	€16.2	€2.3	€38.5
6	€20.0	€14.7	€2.3	€37.0
7	€21.0	€14.7	€1.8	€37.5
8	€21.6	€14.2	€1.8	€37.5
9	€22.7	€14.2	€1.3	€38.3
10	€23.4	€14.2	€1.2	€38.7
11	€24.4	€14.2	€1.2	€39.8
12	€25.1	€14.0	€1.2	€40.3
13	€26.0	€13.7	€1.1	€40.8
14	€27.3	€13.4	€0.9	€41.6
15	€27.3	€12.9	€0.9	€41.1
16	€27.3	€12.7	€0.9	€40.8
17	€28.1	€12.5	€0.6	€41.1
18	€30.1	€12.0	€0.6	€42.3
19	€31.4	€12.0	€0.2	€43.6
20	€33.1	€11.8	€0.2	€45.1

Table E3.1. Specifications of subtotal costs for $k = [3,20]$, in billion euros: island construction, OWF-to-island cabling and OWF-to-shore cabling costs.

The technical details for $k = [3,20]$ after filtering are specified in Table E3.2. The values for all parameters increase when k increases.

k	Island surface area (km²)	Total electrical capacity to energy island (GW)	Total electrical capacity for hydrogen production (GW)	Total hydrogen production capacity (GW)
3	5.43	191	174	87
4	7.24	191	174	87
5	9.05	200	181	91
6	10.9	200	181	91
7	11.4	204	186	93
8	12.0	204	186	93
9	12.0	208	189	95
10	12.8	209	190	95
11	13.4	209	190	95
12	13.9	210	190	95
13	14.5	210	191	96
14	15.0	212	193	96
15	16.8	212	193	96
16	18.7	212	193	96
17	19.0	214	195	97
18	18.2	214	195	97
19	18.5	217	198	99
20	17.8	217	198	99

Table E3.2. Technical details for $k = [3,20]$ of the post-filtering results.

E4. Cluster-Specific Results for $k = \{6,7,8\}$

The island construction costs per island for $k = \{6,7,8\}$ after the second clustering round is provided in Table E4.1.

Island	Cluster 6	Cluster 7	Cluster 8
1	1.3	1.3	1.3
2	1.3	1.3	1.3
3	7.8	1.0	1.0
4	6.2	7.8	1.5
5	1.9	6.2	6.2
6	1.2	1.9	6.2
7	-	1.2	1.9
8	-	-	1.2

Table E4.1. Island construction costs per energy island, in billion euros, after the second clustering round for $k = \{6,7,8\}$.

The distribution of aggregated electricity capacity across the islands for $k = \{6,7,8\}$ after the second clustering round are shown in Table E4.2.

Island	Cluster 6	Cluster 7	Cluster 8
1	16.3	16.3	16.3
2	12.5	12.5	12.5
3	77.6	4.3	4.3
4	62.1	77.6	15.1
5	19.2	62.1	62.5
6	12.2	19.2	62.1
7	-	12.2	19.2
8	-	-	12.2

Table E4.2. Aggregated electrical capacity, in GW, to energy island after the second clustering round for $k = \{6,7,8\}$.

The resulting island sizes for each island across $= \{6,7,8\}$ after the second clustering round are shown in Table E4.3.

Island	Cluster 6	Cluster 7	Cluster 8
1	1.16	1.16	1.16
2	1.81	1.81	1.81
3	1.81	0.56	0.56
4	1.81	1.81	1.81
5	1.81	1.81	1.81
6	1.81	1.81	1.81
7	-	1.81	1.81
8	-	-	1.81

Table E4.3. Required surface area per energy island, in km^2, after the second clustering round for $k = \{6,7,8\}$.

Appendix F: Specification per Cluster for $k = 8$

The technical and economic details per cluster are specified in this Appendix for the results of the second round for $k = 8$. The location details for the resulting cluster centroids are presented per cluster in Table F.1

Cluster	Centroid coordinates
1	(57.50840131, -0.914016247)
2	(57.13414072, 0.565275638)
3	(51.8971087, 2.509088111)
4	(54.50993415, 1.961997947)
5	(53.47786412, 3.340664388)
6	(54.76157624, 5.833630136)
7	(56.48554708, 6.425285279)
8	(56.89746898, 4.284298481)

Table F.1. Cluster centroid coordinates per cluster.

In Table F.2, the technical details regarding energy potential are shown. Considering each island's hydrogen conversion rate (Table F.3), it is defined how much electrical capacity is used for hydrogen production. Including electrolyzer efficiency results in the potential hydrogen production capacity per cluster.

Cluster	Potential electrical capacity (GW)	Total electrical capacity for hydrogen production (GW)	Potential hydrogen production (GW)
1	16	11	5.7
2	13	13	6.3
3	4.3	4.3	2.2
4	15	14	7.2
5	62	56	28
6	62	57	29
7	19	18	9.1
8	12	12	6.1

Table F. 2. Technical details regarding energy potential of energy islands per cluster.

The other technical results are detailed in Table F.2, including island hydrogen conversion rate, required island surface area, island category and number of OWFs per cluster.

Cluster	Hydrogen conversion rate (%)	Required island surface area (km^2)	Appropriate category	Number of OWFs
1	70%	1.16	GL	19
2	100%	1.81	GH	13
3	100%	0.56	MH	23
4	95%	1.81	GH	11
5	89%	1.81	GH	28
6	92%	1.81	GH	35
7	95%	1.81	GH	17
8	100%	1.81	GH	10

Table F.3. Other technical details per cluster.

The results of the economic assessment are specified in Table F.3.

Cluster	Island construction cost (billion euros)	OWF-to-island cable cost (billion euros)	OWF-to-shore cable cost (billion euros)	Subtotal (billion euros)
1	€ 1.31	€ 1.56	€ 0.61	€ 3.48
2	€ 1.25	€ 0.96	€ 0.15	€ 2.36
3	€ 1.03	€ 0.30	€ 0.03	€ 1.37
4	€ 1.51	€ 1.10	€ 0.04	€ 2.65
5	€ 6.25	€ 4.04	€ 0.00	€ 10.3
6	€ 6.21	€ 3.87	€ 0.16	€ 10.2
7	€ 1.92	€ 1.36	€ 0.42	€ 3.71
8	€ 1.22	€ 0.78	€ 0.35	€ 2.35

Table F.4. Cost specification per cluster, in billion euros.

It shows that the most electrical energy is aggregated at the islands in Cluster 5 and 6. As a result, the island construction costs for these two clusters are significantly higher than for the other clusters.

Appendix G: Specifications for Island Location Results

In this Appendix, the results shown in *6.2 Energy Island Locations* are further specified.

G1. Visualization of Identification of Energy Island Locations

In this section, the last step of the spatial analysis is visualized. The optimal energy island locations are determined after three rounds. In Figures G1.1 to G1.7, candidate island locations are identified for each cluster in Round 1 and 3.

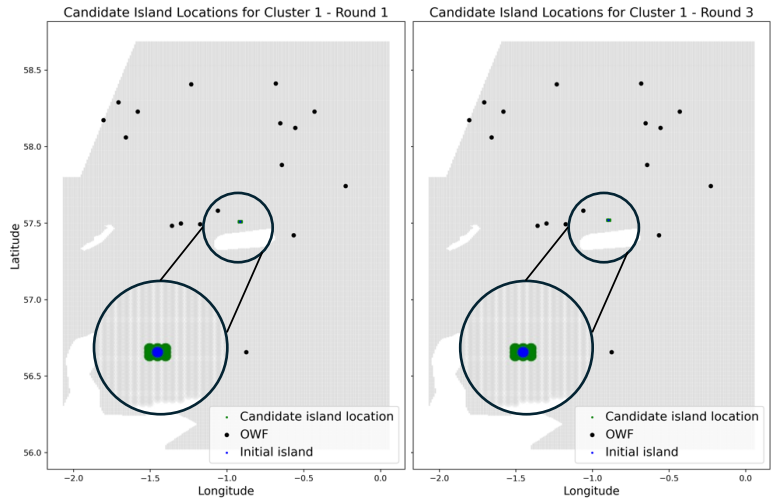

Figure G1.1. Identification of candidate island locations for Round 1 and 3, Cluster 1.

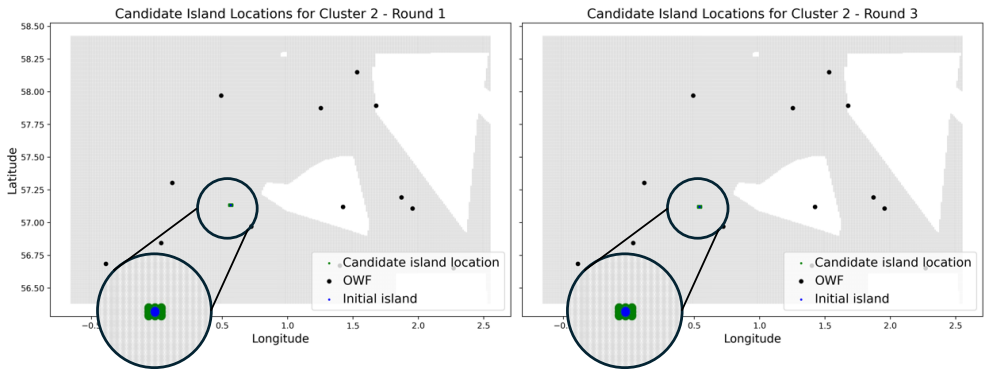

Figure G1.2. Identification of candidate island locations for Round 1 and 3, Cluster 2.

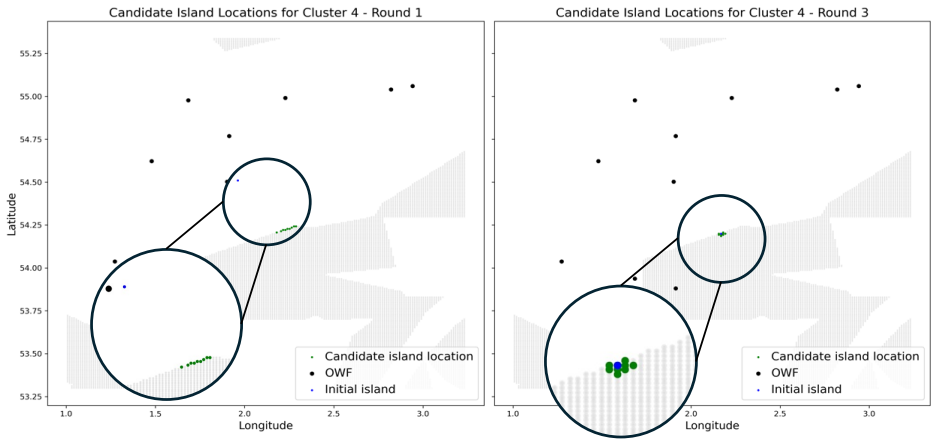

Figure G1.3. Identification of candidate island locations for Round 1 and 3, Cluster 4.

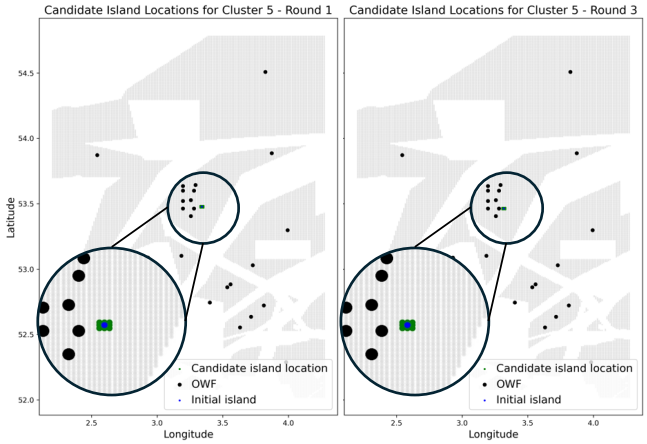

Figure G1.4. Identification of candidate island locations for Round 1 and 3, Cluster 5.

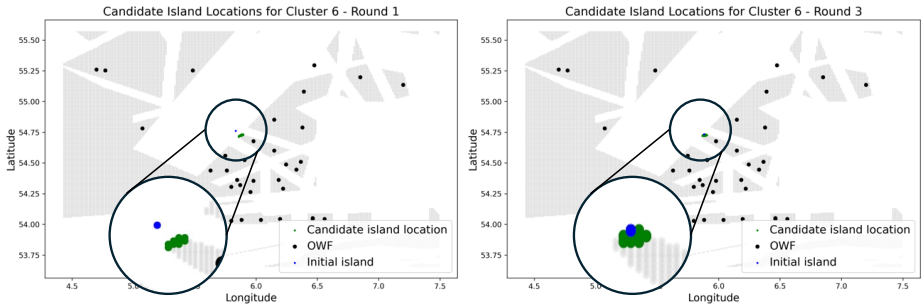

Figure G1.5. Identification of candidate island locations for Round 1 and 3, Cluster 6.

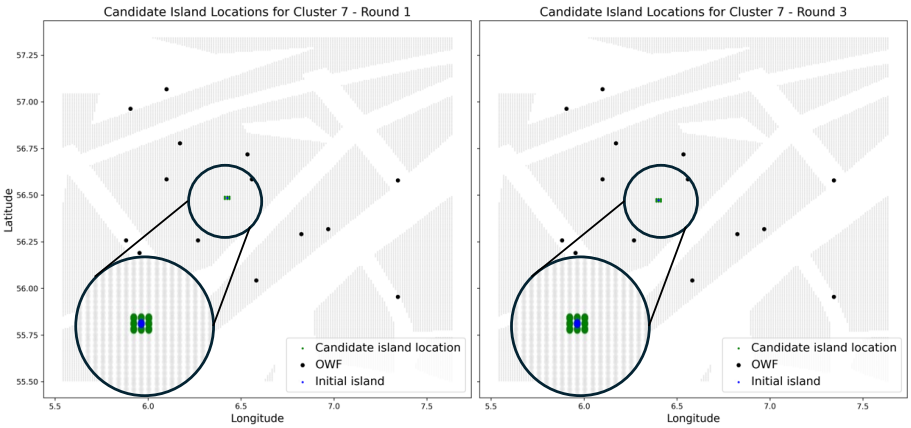

Figure G1.6. Identification of candidate island locations for Round 1 and 3, Cluster 7.

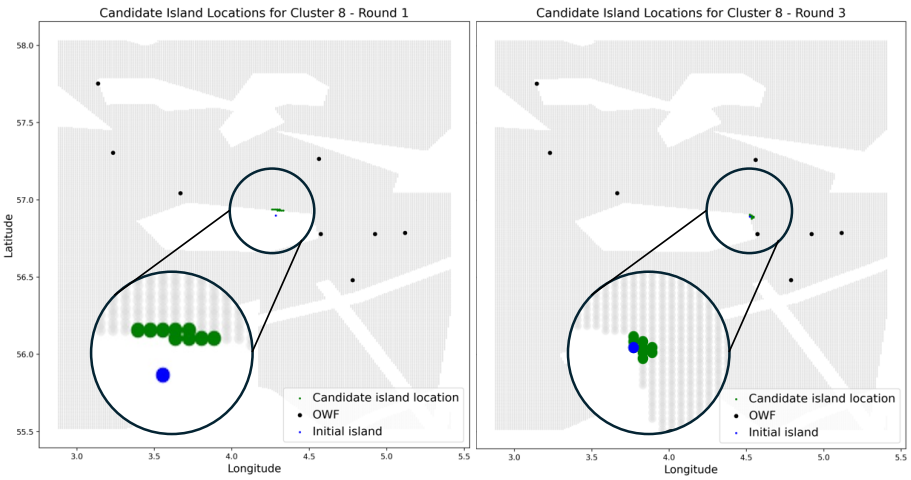

Figure G1.7. Identification of candidate island locations for Round 1 and 3, Cluster 8.

G2. Specifications of Optimal Island Locations per Round

In this section, the results for optimal island locations in each round is presented. Tables G2.1, G2.2 and G2.3 provide an overview per cluster. These tables present which candidate island location is found optimal, with corresponding network costs and cluster centroid coordinates.

Cluster	Round 1			
	Candidate number	*Network costs (monetary unit)*	*Network costs (million euros)*	*Cluster centroid coordinates*
1	9	309.8	€ 33.9	(57.51359820, -0.90434110)
2	7	239.3	€ 23.6	(57.12758160, 0.55319004)
3	6	70.2	€ 11.8	(51.78912565, 2.46875385)
4	5	234.4	€ 32.9	(54.20711203, 2.17953868)
5	7	527.7	€ 71.9	(53.47067097, 3.32857879)
6	1	455.9	€ 62.3	(54.73367403, 5.88197252)
7	7	250.3	€ 40.0	(56.47887347, 6.41319968)
8	1	187.8	€ 19.6	(56.90661000, 4.51045000)

Table G2.1. Results of the optimal island locations per cluster in Round 1.

Cluster	Round 2			
	Candidate number	*Network costs (monetary unit)*	*Network costs (million euros)*	*Cluster centroid coordinates*
1	8	309.3	€ 33.9	(57.51879435, -0.89466594)
2	7	239.0	€ 23.5	(57.12102132, 0.54110445)
3	1	70.2	€ 11.8	(51.78912565, 2.46875385)
4	4	233.2	€ 36.4	(54.20004308, 2.16745308)
5	7	524.6	€ 71.4	(53.46347660, 3.31649320)
6	1	455.9	€ 62.3	(54.73367403, 5.88197252)
7	7	248.8	€ 39.8	(56.47219868, 6.40111409)
8	9	180.1	€ 18.4	(56.89341007, 4.52253560)

Table G2.2. Results of the optimal island locations per cluster in Round 2.

Cluster	Round 3			
	Candidate number	*Network costs (monetary unit)*	*Network costs (million euros)*	*Cluster centroid coordinates*
1	9	308.7	€ 33.8	(57.52398976, -0.88499079)
2	7	238.7	€ 23.5	(57.11445988, 0.52901885)
3	1	70.2	€ 11.8	(51.78912565, 2.46875385)
4	3	232.0	€ 36.3	(54.20004308, 2.15536748)
5	4	521.8	€ 71.1	(53.46347660, 3.30440760)
6	1	455.9	€ 62.3	(54.73367403, 5.88197252)
7	7	247.3	€ 39.7	(56.46552271, 6.38902849)
8	1	180.1	€ 18.4	(56.89341007, 4.52253560)

Table G2.3. Results of the optimal island locations per cluster in Round 3.

The corresponding networks for each optimal island locations are shown in Figures G2.1 to G2.8. For each round, the network with lowest costs, which presents the optimal island locations, is shown per cluster.

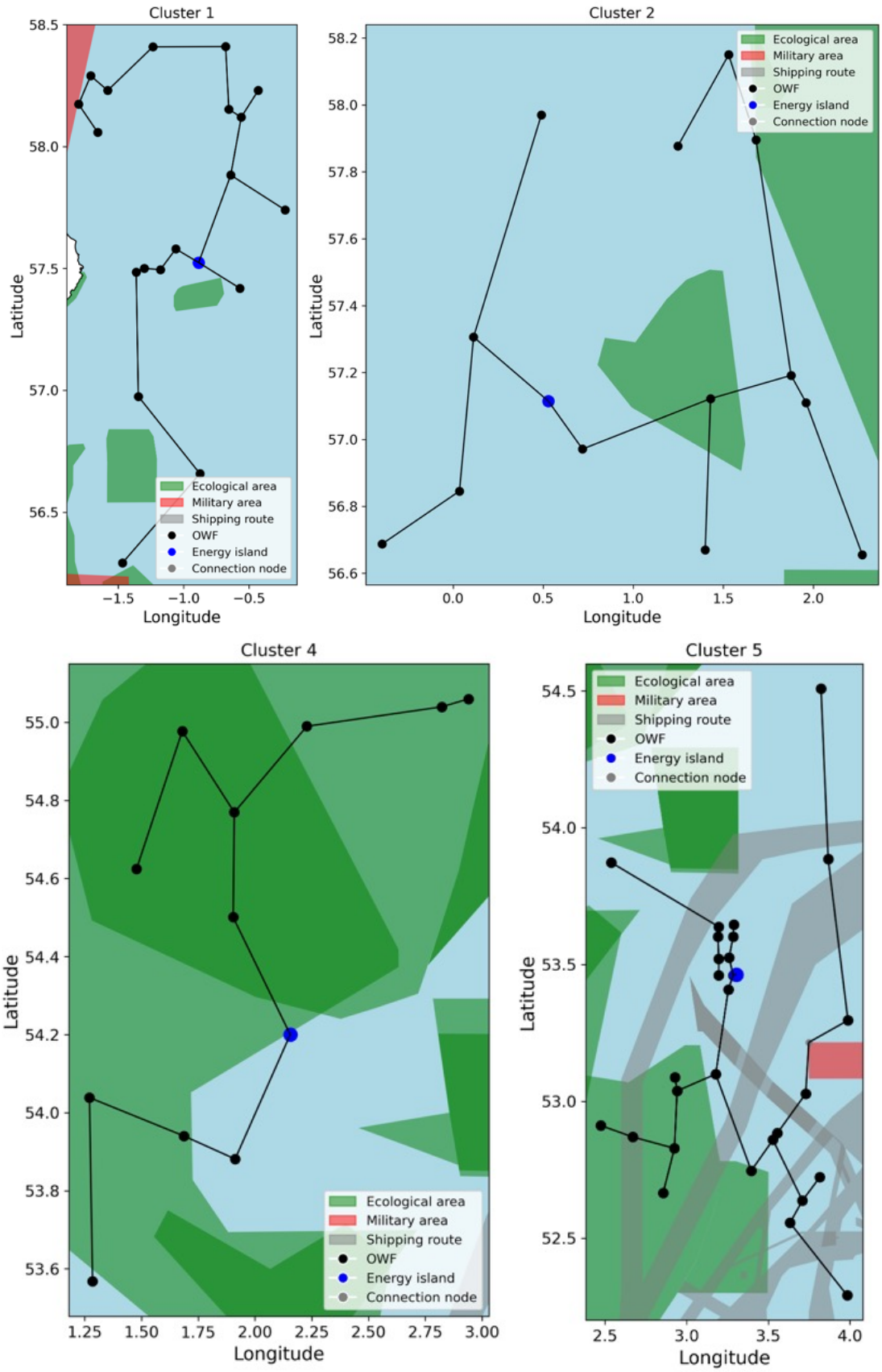

Figure G2.1. Final network layouts for optimal candidate island location in Round 3 for Clusters 1, 2, 4 and 5.

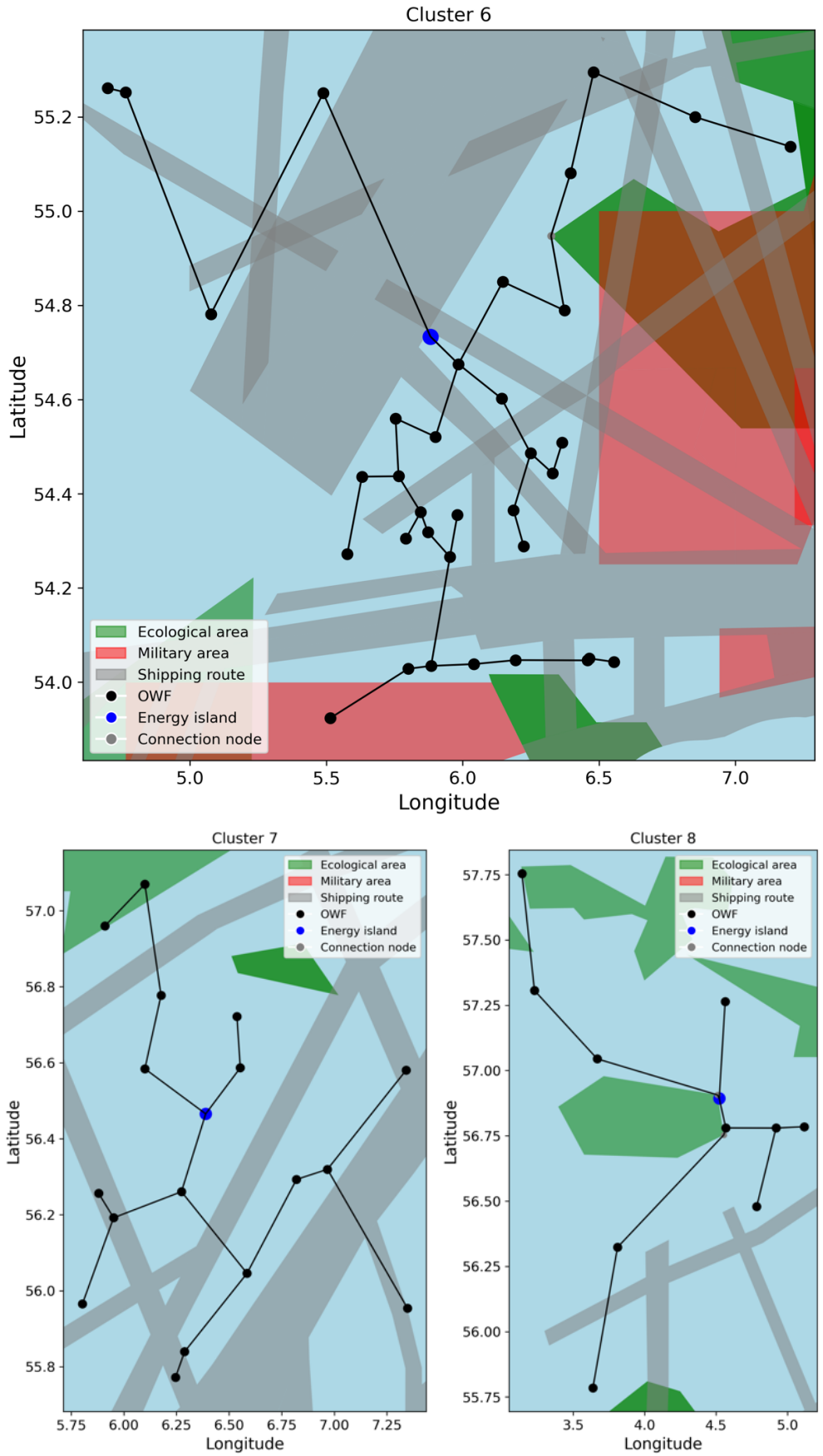

Figure G2.2. Final network layouts for optimal candidate island location in Round 3 for Clusters 6, 7 and 8.

G3. Final Network Details per Cluster

In this section, the electricity network details resulting from the ONLT, are shown for each cluster. Tables G3.1 to G3.8 show the node and edge details of the network. For each node, which can be recognized with its node ID, its coordinate and node type is provided. Most clusters only have terminal nodes, which represent OWFs or energy islands. Some clusters include corner nodes, which are added nodes to let the network go around forbidden areas. The nodes that are connected are shown. For each edge, its capacity in MW, relative (monetary units) and absolute (euros) costs, length in km and appropriate cable type are presented.

Nodes			Edges						
ID	Coordinate	Node type	Node1	Node2	Capacity (MW)	Cost (MU)	Length (km)	Cable type	Cost (€)
0	(-0.2241287813268451, 57.73950507148591)	terminal	0	8	1008	13.39	29.3	HVAC	€ 1,790,000.00
1	(-0.4300000002996285, 58.23000000010012)	terminal	8	14	7605	20.69	26.8	HVAC	€ 4,430,000.00
2	(-1.467124248947324, 56.29191815823793)	terminal	8	19	9173	39.37	42.5	HVDC	€ 2,450,000.00
3	(-1.345889486638461, 56.97490460347779)	terminal	1	14	1500	6.31	14.4	HVAC	€ 1,070,000.00
4	(-1.802029175413933, 58.17323757434305)	terminal	14	10	6000	7.36	6.6	HVAC	€ 980,000.00
5	(-1.36214046364462, 57.48427079190962)	terminal	2	11	2300	31.84	54.6	HVDC	€ 1,730,000.00
6	(-1.235008821765836, 58.40883352392847)	terminal	11	3	5207	38.87	45.4	HVDC	€ 2,050,000.00
7	(-1.177342776229102, 57.49497960246418)	terminal	3	5	6215	38.11	56.6	HVDC	€ 2,760,000.00
8	(-0.6399077209292461, 57.88264697347679)	terminal	5	9	6230	4.8	4.1	HVAC	€ 610,000.00
9	(-1.299999999999841, 57.50000000029996)	terminal	4	17	1000	4.51	14.1	HVAC	€ 850,000.00
10	(-0.6546420166631879, 58.15283754740661)	terminal	4	13	750	4.87	15.4	HVAC	€ 810,000.00
11	(-0.8754050662454984, 56.65795876836203)	terminal	17	16	1100	4.55	10.1	HVAC	€ 640,000.00
12	(-0.5698170359938713, 57.41866130351726)	terminal	9	7	6245	9.2	7.3	HVAC	€ 1,100,000.00
13	(-1.656723959507989, 58.05833092872347)	terminal	6	16	1200	12.9	28.3	HVAC	€ 1,880,000.00
14	(-0.5600000003995547, 58.11999999960045)	terminal	6	18	2160	24.67	32.4	HVAC	€ 2,870,000.00
15	(-1.060000000299624, 57.57999999960049)	terminal	18	10	3000	13.48	28.6	HVAC	€ 2,990,000.00
16	(-1.579999999800009, 58.23000000010012)	terminal	7	15	6270	10.88	11.8	HVAC	€ 1,770,000.00
17	(-1.709999999899935, 58.28999999980033)	terminal	15	19	6370	13.91	12.2	HVAC	€ 1,840,000.00
18	(-0.6790000004494914, 58.41000000010007)	terminal	19	12	798	9.02	22.2	HVAC	€ 1,200,000.00
19	(-0.8849907918822678, 57.52398975773351)	terminal							

Table G3.1. Final electricity network details Cluster 1.

Nodes			Edges						
ID	Coordinate	Node type	Node1	Node2	Capacity (MW)	Cost (MU)	Length (km)	Cable type	Cost (€)
0	(1.681856620570676, 57.89577890061297)	terminal	0	11	40	1.83	29.6	HVAC	€ 370,000.00
1	(0.4900000001999842, 57.96999999990027)	terminal	0	8	1048	22.68	79.2	HVDC	€ 1,780,000.00
2	(1.400000000000148, 56.66999999980032)	terminal	11	9	15	1.49	34.6	HVAC	€ 260,000.00
3	(0.03551512941122771, 56.84559680573891)	terminal	8	6	1316	15.72	28	HVAC	€ 1,950,000.00
4	(0.1137620149293769, 57.30623508310019)	terminal	8	7	265	1.84	10.4	HVAC	€ 330,000.00
5	(0.7184304794129261, 56.97128098070188)	terminal	1	4	1500	28.27	77.1	HVDC	€ 2,030,000.00
6	(1.429374466289097, 57.12193845648692)	terminal	4	3	3810	27.44	51.4	HVDC	€ 2,030,000.00
7	(1.959999999600484, 57.11000000000018)	terminal	4	13	7310	37.06	32.9	HVAC	€ 5,330,000.00
8	(1.876484996538487, 57.19147016000633)	terminal	2	6	1500	16.78	50.3	HVDC	€ 1,320,000.00
9	(1.248342575402418, 57.87720391193067)	terminal	6	5	4216	44.87	46.1	HVDC	€ 1,900,000.00
10	(2.27197188900498, 56.65529317005547)	terminal	3	12	2610	22.28	31.5	HVAC	€ 3,070,000.00
11	(1.530000000100074, 58.14999999990022)	terminal	13	5	5224	16.3	19.6	HVAC	€ 2,690,000.00
12	(-0.3935920140364463, 56.68759058515457)	terminal	7	10	15	2.1	54	HVAC	€ 410,000.00
13	(0.5290188499601172, 57.11445987562658)	terminal							

Table G3.2. Final electricity network details Cluster 2.

Nodes			Edges						
ID	Coordinate	Node type	Node1	Node2	Capacity (MW)	Cost (MU)	Length (km)	Cable type	Cost (€)
0	(2.840000000000146, 51.69000000039989)	terminal	0	3	193	0.47	3.8	HVAC	€ 100,000.00
1	(2.804547819256695, 51.66876280333216)	terminal	0	7	190	0.83	5.9	HVAC	€ 160,000.00
2	(2.787309893053644, 51.67886681503051)	terminal	3	1	1388	0.98	2.2	HVAC	€ 160,000.00
3	(2.829339971236801, 51.65659836377736)	terminal	3	22	1113	1.26	3.3	HVAC	€ 210,000.00
4	(3.060109668596215, 51.74725302002192)	terminal	1	2	1471	0.73	1.6	HVAC	€ 120,000.00
5	(3.069337932864629, 51.63497752030088)	terminal	2	19	1553	1.34	2.5	HVAC	€ 190,000.00
6	(2.969346057558508, 51.66887934829197)	terminal	19	17	1662	1.34	3.7	HVAC	€ 290,000.00
7	(2.88212020213598, 51.73621409780243)	terminal	22	20	987	1.42	3.6	HVAC	€ 220,000.00
8	(3.003305574677521, 51.70915686848802)	terminal	4	8	188	0.91	5.8	HVAC	€ 150,000.00
9	(2.921967754573779, 51.53911194296214)	terminal	8	5	188	1.32	9.4	HVAC	€ 250,000.00
10	(2.984985241401728, 51.56316741520779)	terminal	8	6	386	1	5.1	HVAC	€ 190,000.00
11	(2.503504787450113, 52.2373482954515)	terminal	6	21	561	1.85	8.8	HVAC	€ 400,000.00
12	(2.431137625824248, 52.38105832974655)	terminal	21	9	71	0.47	6	HVAC	€ 100,000.00
13	(2.201472318755577, 52.15338927889736)	terminal	21	10	92	0.46	4.2	HVAC	€ 80,000.00
14	(2.161681604342601, 51.90196402169332)	terminal	21	20	879	1.32	3.9	HVAC	€ 220,000.00
15	(2.03999999980033, 51.88000000020003)	terminal	11	12	450	3.29	16.7	HVAC	€ 680,000.00
16	(1.935838463788541, 51.88398383885107)	terminal	11	13	807	8.55	22.6	HVAC	€ 1,230,000.00
17	(2.74050901699696, 51.71863091617327)	terminal	13	14	1287	8.75	28.1	HVAC	€ 1,930,000.00
18	(2.039214540918465, 51.73606572895039)	terminal	14	15	681	3.1	8.7	HVAC	€ 440,000.00
19	(2.752631216749528, 51.6865367646383)	terminal	14	23	2518	15.66	24.5	HVAC	€ 2,350,000.00
20	(2.905150268420459, 51.61595907357072)	terminal	15	16	252	1.6	7.2	HVAC	€ 220,000.00
21	(2.944544670898149, 51.59140070739825)	terminal	15	18	252	2.21	16	HVAC	€ 490,000.00
22	(2.861651960048513, 51.63418029005438)	terminal	23	17	1780	11.32	20.3	HVAC	€ 1,640,000.00
23	(2.468753854325262, 51.78912564796965)	terminal							

Table G3.3. Final electricity network details Cluster 3.

Nodes			Edges						
ID	Coordinate	Node type	Node1	Node2	Capacity (MW)	Cost (MU)	Length (km)	Cable type	Cost (€)
0	(1.908959637871118, 54.76947455619769)	terminal	0	8	8500	23.46	29.9	HVAC	€ 5,220,000.00
1	(1.679728774201604, 54.97737666038179)	terminal	0	1	2700	15.33	27.4	HVAC	€ 2,710,000.00
2	(2.822657700333952, 55.03972759016633)	terminal	0	10	4600	25.02	31.9	HVAC	€ 4,120,000.00
3	(2.939999999800307, 55.05999999960045)	terminal	8	11	10000	37.08	37.2	HVAC	€ 7,040,000.00
4	(1.912505089624181, 53.88131207848838)	terminal	1	7	1500	15.04	41.3	HVDC	€ 1,080,000.00
5	(1.687663209947021, 53.94023543396888)	terminal	10	2	3200	32.12	38.3	HVAC	€ 4,130,000.00
6	(1.271072174403554, 54.03860767457125)	terminal	2	3	2000	5.09	7.8	HVAC	€ 670,000.00
7	(1.478649483841307, 54.62494245476375)	terminal	4	5	3886	13.78	16.1	HVAC	€ 1,910,000.00
8	(1.903768464871134, 54.50070478815031)	terminal	4	11	5104	27.19	38.8	HVAC	€ 5,270,000.00
9	(1.284806082828831, 53.56836744018435)	terminal	5	6	2500	20.41	29.3	HVAC	€ 2,800,000.00
10	(2.22854359206588, 54.98994050542708)	terminal	6	9	1500	17.43	52.3	HVDC	€ 1,370,000.00
11	(2.155367484848909, 54.20004307947497)	terminal							

Table G3.4. Final electricity network details Cluster 4.

Nodes			Edges						
ID	Coordinate	Node type	Node1	Node2	Capacity (MW)	Cost (MU)	Length (km)	Cable type	Cost (€)
0	(2.94160779221851, 53.03842490136384)	terminal	0	15	1800	2.05	5.5	HVAC	€ 450,000.00
1	(2.925100006964492, 52.82861535307375)	terminal	0	1	6200	15.72	23.4	HVAC	€ 3,490,000.00
2	(2.473388179710614, 52.9120505932918)	terminal	0	5	10100	23.22	17.2	HVAC	€ 3,270,000.00
3	(2.855666974625587, 52.66515209081561)	terminal	1	3	1400	6.36	18.8	HVAC	€ 1,340,000.00
4	(3.255527111340663, 53.40896990647311)	terminal	1	16	3000	13.49	17.7	HVAC	€ 1,850,000.00
5	(3.178078922855024, 53.09957947986568)	terminal	5	4	36052	56.84	34.8	HVAC	€ 12,400,000.00
6	(3.988358575685357, 53.29617569765576)	terminal	5	17	23952	60.37	41.9	HVDC	€ 3,660,000.00
7	(3.815989564223043, 52.72319732454788)	terminal	16	2	900	5.79	14	HVAC	€ 810,000.00
8	(3.709428610111534, 52.63765597800361)	terminal	4	27	40052	11.25	6.1	HVAC	€ 2,300,000.00
9	(3.633215530159725, 52.55628331676841)	terminal	27	25	19900	9.17	7.3	HVAC	€ 1,950,000.00
10	(3.983367585775589, 52.2912029238259)	terminal	27	28	62452	4.59	1.3	HVAC	€ 620,000.00
11	(2.537160731788825, 53.87299925755025)	terminal	17	12	23085	24.92	15.4	HVAC	€ 4,400,000.00
12	(3.528930504917196, 52.8595605607246)	terminal	6	18	12000	62.21	66	HVDC	€ 4,280,000.00
13	(3.729450341000432, 53.02827439691653)	terminal	6	29	14000	28.26	18.3	HVAC	€ 4,090,000.00
14	(3.555685831150927, 52.8840469708804)	terminal	18	19	10000	59.11	69.4	HVDC	€ 4,160,000.00
15	(2.929058900952548, 53.08751585721125)	terminal	29	13	14000	21.04	20.9	HVAC	€ 4,670,000.00
16	(2.669999999800325, 52.87000000020004)	terminal	7	8	378	2.56	11.9	HVAC	€ 450,000.00
17	(3.395985, 52.7468837)	terminal	8	9	1080	3.51	10.4	HVAC	€ 660,000.00
18	(3.867188, 53.884916)	terminal	8	12	2218	12.86	27.5	HVAC	€ 2,470,000.00
19	(3.823242, 54.508327)	terminal	9	10	380	8.26	37.8	HVAC	€ 1,420,000.00
20	(3.197021, 53.638125)	terminal	12	14	16867	4.44	3.3	HVAC	€ 800,000.00
21	(3.191528, 53.602285)	terminal	11	20	2400	32.74	50.6	HVDC	€ 1,630,000.00
22	(3.197021, 53.520717)	terminal	20	21	4900	2.41	4	HVAC	€ 530,000.00
23	(3.289032, 53.646266)	terminal	14	13	16000	26.94	19.8	HVAC	€ 4,730,000.00
24	(3.284912, 53.602285)	terminal	21	22	7400	6.66	9.1	HVAC	€ 1,480,000.00
25	(3.260193, 53.525615)	terminal	22	26	2500	2.84	6.6	HVAC	€ 630,000.00
26	(3.197021, 53.461202)	terminal	22	25	12400	6.66	4.2	HVAC	€ 890,000.00
27	(3.284912, 53.461202)	terminal	25	24	5000	5.41	8.7	HVAC	€ 1,170,000.00
28	(3.304407600123638, 53.46347660151039)	terminal	23	24	2500	2.11	4.9	HVAC	€ 470,000.00
29	(3.74844, 53.21567)	corner							

Table G3.5. Final electricity network details Cluster 5.

Nodes			Edges						
ID	Coordinate	Node type	Node1	Node2	Capacity (MW)	Cost (MU)	Length (km)	Cable type	Cost (€)
0	(6.248965584108899, 54.48599838152071)	terminal	0	15	897	2.63	7.1	HVAC	€ 410,000.00
1	(5.980842648320444, 54.35528756519825)	terminal	0	14	1940	5.72	14	HVAC	€ 1,180,000.00
2	(6.194243109518605, 54.0467822064183)	terminal	0	19	2955	8.14	14.6	HVAC	€ 1,510,000.00
3	(6.041711602743167, 54.03833426325583)	terminal	15	17	400	1.43	7.6	HVAC	€ 290,000.00
4	(7.200771829437993, 55.1371830477821)	terminal	14	23	980	2.57	8.9	HVAC	€ 530,000.00
5	(5.792052217263183, 54.30499853955641)	terminal	19	20	4955	11.67	13	HVAC	€ 1,750,000.00
6	(6.37287513717794, 54.78934202443696)	terminal	1	21	400	1.81	10.1	HVAC	€ 390,000.00
7	(6.147061705733297, 54.85016442804606)	terminal	21	32	5634	6.83	7.8	HVAC	€ 1,110,000.00
8	(6.395384863386274, 55.08072259682778)	terminal	21	33	4604	15.57	26.1	HVAC	€ 3,370,000.00
9	(6.479948157184076, 55.29488867130862)	terminal	2	3	1304	5.28	10	HVAC	€ 690,000.00
10	(5.077249513816356, 54.7814711844234)	terminal	2	30	391	5.02	17.2	HVAC	€ 660,000.00
11	(5.489048157902596, 55.25050315021537)	terminal	3	33	1604	6.03	10.3	HVAC	€ 790,000.00
12	(4.698772634410144, 55.26128471105852)	terminal	30	31	291	0.12	0.6	HVAC	€ 20,000.00
13	(4.764952301123672, 55.25219549984212)	terminal	33	29	2700	4.17	5.5	HVAC	€ 550,000.00
14	(6.186484129121948, 54.36522994493417)	terminal	4	28	299	5.91	23.2	HVAC	€ 770,000.00
15	(6.329969754232261, 54.44337185404613)	terminal	28	9	587	8.96	25.9	HVAC	€ 1,210,000.00
16	(5.577185063188773, 54.272247006362)	terminal	5	22	252	1.19	7.1	HVAC	€ 220,000.00
17	(6.364885326294059, 54.5089571887197)	terminal	22	32	6036	3.73	5.1	HVAC	€ 750,000.00
18	(6.553891045875946, 54.04308540360893)	terminal	22	24	6558	8.54	10	HVAC	€ 1,530,000.00
19	(6.143058793971182, 54.60203838236428)	terminal	6	7	10607	22.77	16	HVAC	€ 3,110,000.00
20	(5.984668413584175, 54.67527765859759)	terminal	6	36	7107	13.23	17.9	HVAC	€ 2,860,000.00
21	(5.953197107735637, 54.26586653618797)	terminal	7	20	19607	31.48	22.1	HVAC	€ 5,820,000.00
22	(5.846058225492551, 54.36096640333341)	terminal	36	8	7107	12.08	15.5	HVAC	€ 2,480,000.00
23	(6.223845345417109, 54.28838527351517)	terminal	20	35	43119	23	9.3	HVAC	€ 3,610,000.00
24	(5.765083393052065, 54.43716421305415)	terminal	20	25	18058	22.26	18	HVAC	€ 4,560,000.00
25	(5.900578150850725, 54.52090240326622)	terminal	8	9	1607	8.83	24.4	HVAC	€ 1,870,000.00
26	(5.630797816612235, 54.43636134736371)	terminal	10	13	1000	17.13	56	HVDC	€ 1,230,000.00
27	(5.754170203788265, 54.55986831107155)	terminal	10	11	7000	49.5	58.4	HVDC	€ 3,000,000.00
28	(6.8524782500495, 55.19975908158165)	terminal	11	35	19000	84.32	62.7	HVDC	€ 4,960,000.00
29	(5.800357928151044, 54.02841012804354)	terminal	16	26	4000	10.39	18.6	HVAC	€ 2,240,000.00
30	(6.457645410575332, 54.04621997351752)	terminal	26	24	5500	9.45	8.7	HVAC	€ 1,220,000.00
31	(6.463669108012017, 54.05034224033129)	terminal	18	31	189	1.21	5.9	HVAC	€ 160,000.00
32	(5.872901415579957, 54.31814540042453)	terminal	25	27	16058	18.11	10.4	HVAC	€ 2,480,000.00
33	(5.884241837463754, 54.03450000926983)	terminal	24	27	14058	13.79	13.7	HVAC	€ 3,060,000.00
34	(5.515, 53.923751)	terminal	29	34	2000	12.98	22	HVAC	€ 1,880,000.00
35	(5.881972520635403, 54.73367403397311)	terminal							
36	(6.32389, 54.9475)	corner							

Table G3.6. Final electricity network details Cluster 6.

Nodes			Edges						
ID	Coordinate	Node type	Node1	Node2	Capacity (MW)	Cost (MU)	Length (km)	Cable type	Cost (€)
0	(6.820367486056404, 56.29296643152518)	terminal	0	13	4989	10.03	9.5	HVAC	€ 1,280,000.00
1	(6.245791936592718, 55.77202864714343)	terminal	0	14	4989	22.88	31.1	HVAC	€ 4,170,000.00
2	(6.55340292770314, 56.58679097303798)	terminal	13	6	3489	29.62	46.9	HVDC	€ 1,780,000.00
3	(5.951498854851582, 56.19203214909348)	terminal	13	12	500	9.81	37	HVAC	€ 1,590,000.00
4	(5.909999999800334, 56.96000000029994)	terminal	14	9	6989	29.99	30.7	HVAC	€ 4,870,000.00
5	(6.09999999960047, 57.06999999990023)	terminal	14	16	1000	10.96	29.4	HVAC	€ 1,790,000.00
6	(7.3471921, 55.9543728)	terminal	2	8	1000	4.11	15	HVAC	€ 910,000.00
7	(6.1000615, 56.5841986)	terminal	2	17	1000	6.2	16.8	HVAC	€ 1,020,000.00
8	(6.5375905, 56.7215099)	terminal	17	7	8250	26.87	22.1	HVAC	€ 3,800,000.00
9	(6.2739431, 56.2606641)	terminal	17	9	9989	22.21	23.9	HVAC	€ 4,510,000.00
10	(6.1768433, 56.7773487)	terminal	3	11	1000	2.91	8.4	HVAC	€ 510,000.00
11	(5.8802963, 56.2564984)	terminal	3	15	1000	8.22	26.8	HVAC	€ 1,630,000.00
12	(7.3410183, 56.5804268)	terminal	3	9	2000	14.08	21.3	HVAC	€ 1,820,000.00
13	(6.9674804, 56.3196054)	terminal	4	5	2250	9.94	16.8	HVAC	€ 1,520,000.00
14	(6.5854313, 56.0457987)	terminal	5	10	6250	22.69	32.9	HVAC	€ 4,930,000.00
15	(5.8032926, 55.9651759)	terminal	10	7	7250	16.77	22	HVAC	€ 3,550,000.00
16	(6.2887621, 55.8396205)	terminal							
17	(6.389028490787987, 56.46552271154396)	terminal							

Table G3.7. Final electricity network details Cluster 7.

Nodes			Edges						
ID	Coordinate	Node type	Node1	Node2	Capacity (MW)	Cost (MU)	Length (km)	Cable type	Cost (€)
0	(3.637845755109761, 55.7842202898433)	terminal	8	11	1000	26.05	66.1	HVDC	€ 1,460,000.00
1	(4.919999999800325, 56.78000000029994)	terminal	1	2	1500	7.34	12.1	HVAC	€ 900,000.00
2	(5.118057, 56.7850253)	terminal	1	4	2100	14.42	34.4	HVAC	€ 3,010,000.00
3	(4.568783, 56.7804175)	terminal	1	3	4600	22.64	21.4	HVAC	€ 2,760,000.00
4	(4.7850087, 56.4794326)	terminal	3	10	7700	10.15	12.9	HVAC	€ 2,140,000.00
5	(3.141372, 57.7545173)	terminal	3	11	1000	0.93	3.1	HVAC	€ 190,000.00
6	(3.2291128, 57.3063843)	terminal	10	9	1000	11.3	41.3	HVDC	€ 910,000.00
7	(3.6686463, 57.0447216)	terminal	10	12	3500	1.01	1.6	HVAC	€ 180,000.00
8	(3.8106814, 56.3233705)	terminal	5	6	1000	13.85	50.1	HVDC	€ 1,100,000.00
9	(4.5640245, 57.2637125)	terminal	6	7	2500	24.39	39.3	HVAC	€ 3,750,000.00
10	(4.522535596108262, 56.89341006824362)	terminal	7	12	3500	48.04	53.3	HVDC	€ 2,020,000.00
11	(4.55439, 56.75334)	corner							
12	(4.51045, 56.90661)	corner							

Table G3.8. Final electricity network details Cluster 8.

Appendix H: Hydrogen Demand

In this Appendix, the hydrogen demand per entry point in the hydrogen backbone is detailed. The demand share per entry point is derived as explained in *5.5 Onshore Entry Points*. The total hydrogen production capacity in the system is equal to 93 GW. The resulting demand per entry point is found in Table H.1

ID	Entry point	Share (%)	Hydrogen demand (MW)
BE01	Zeebrugge	7.2%	6,671
DK01	Jutland	1.8%	1,668
FR01	Dunkerque	5.0%	4,670
DE01	Emden	2.2%	6,783
DE02	Dornum	7.3%	2,001
NL01	Maasvlakte	1.6%	1,445
NL02	IJmuiden	1.2%	1,112
NL03	Den Helder	7.2%	6,671
NL04	Eemshaven	2.2%	2,001
NO01	Karsto	2.5%	2,335
NO02	Sleipner	6.0%	5,560
NO03	Kollsnes	6.3%	5,893
UK01	Bacton	17.5%	16,234
UK02	Shetland	1.8%	1,668
UK03	St. Fergus	12.6%	11,675
UK04	Teeside	2.2%	2,001
UK05	Easington	10.2%	9,451
UK06	Theddlethorpe	5.4%	5,004

Table H.1. Hydrogen demand per entry point, based on current capacity of gas pipelines with diameter $\geq 20\ inch$ for each point. Except for IJmuiden, which is based on pipelines with diameter $< 20\ inch$.

After the rerouted segment analysis, the demand at Zeebrugge Maasvlakte, IJmuiden and Den Helder are updated. The update is shown in Table H.2. The values in Table H.2 are used instead of the values in Table H.1 for the final hydrogen backbone.

ID	Entry point	Share (%)	Hydrogen demand (MW)
BE01	Zeebrugge	0%	0
NL01	Maasvlakte	8.8%	8,116
NL02	IJmuiden	0%	0
NL03	Den Helder	8.4%	7,783

Table H.2. Updated hydrogen demand at Zeebrugge, Maasvlakte, IJmuiden and Den Helder.

Appendix I: Rerouting of Infeasible Backbone Segments

In this Appendix, the rerouting of infeasible segments is shown. First, relevant details are shared. Then, the results per segment are visualized.

I1. Rerouting Details of Infeasible Segments

In this section, the rerouting details of each infeasible segment is provided in Table I1.1. The capacity of Segments 3 and 8 is significantly higher than for the other segments. It entails that more capacity must be rerouted, which may be more challenging than for lower capacities.

Segment	Capacity to reroute (GW)
0	6.3
1	2.1
2	7.2
3	20.4
4	8.1
5	9.1
6	4.4
7	1.7
8	14.1
9	1.1
10	6.7
11	2.0

Table I1.1. Hydrogen capacity flow that must be rerouted per identified infeasible pipeline segment, in GW.

I2. Rerouting Results per Infeasible Segment

In this section, the results of the rerouting process are visualized in Figures I2.1 to I2.9. The results for Segments 4, 9 and 10 are shown in *6.3 Offshore Hydrogen Network*. The figures first show the segment that must be rerouted. In the second plot, the specification of supply and demand nodes for the rerouted segment is provided. Then, in the last plot, the result of the rerouting process is shown by visualizing the newly routed segment.

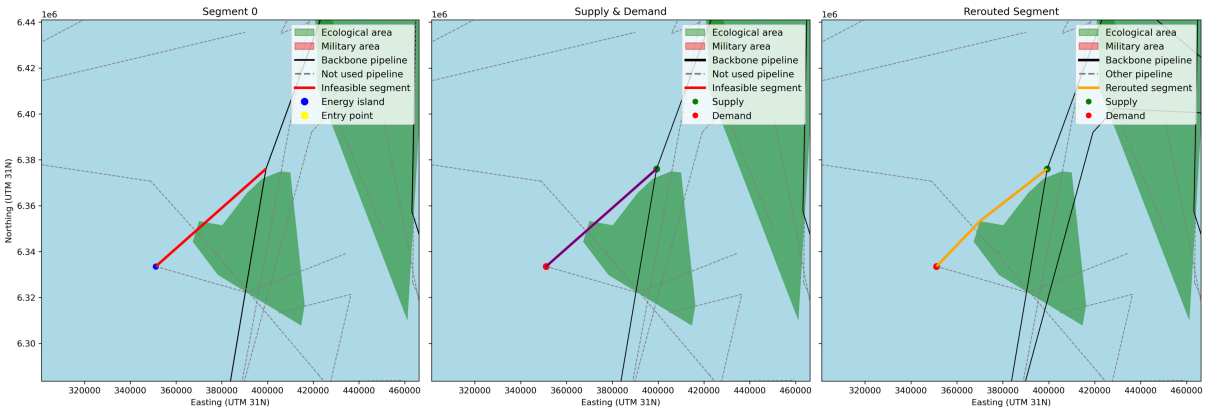

Figure I2.1. Rerouting steps for infeasible pipeline segment 0.

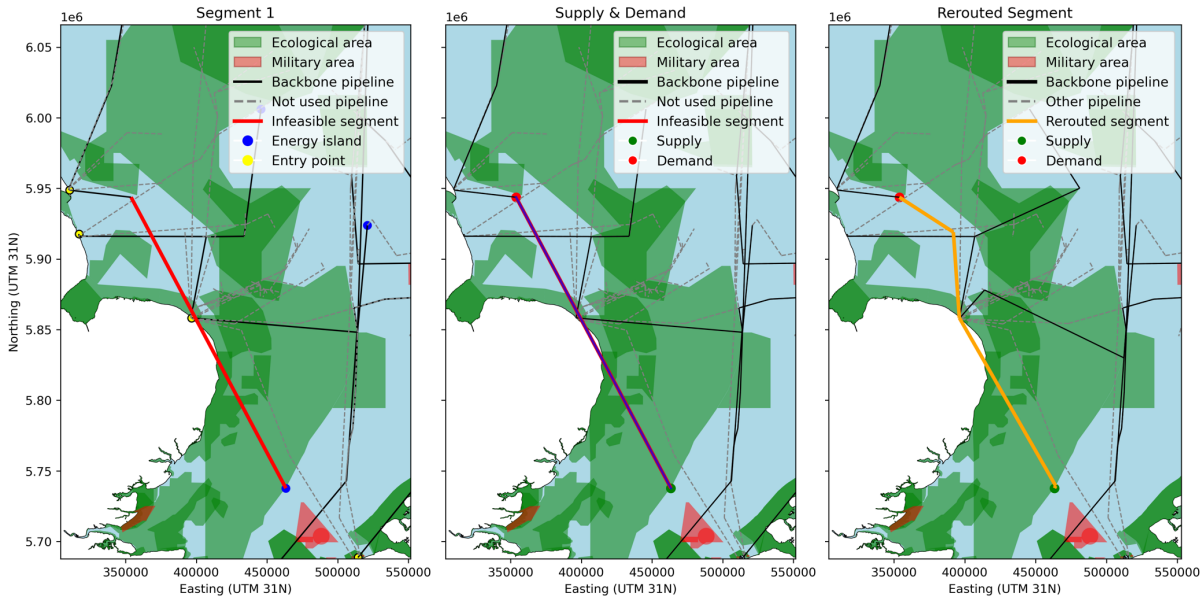

Figure I2.2. Rerouting steps for infeasible pipeline segment 1.

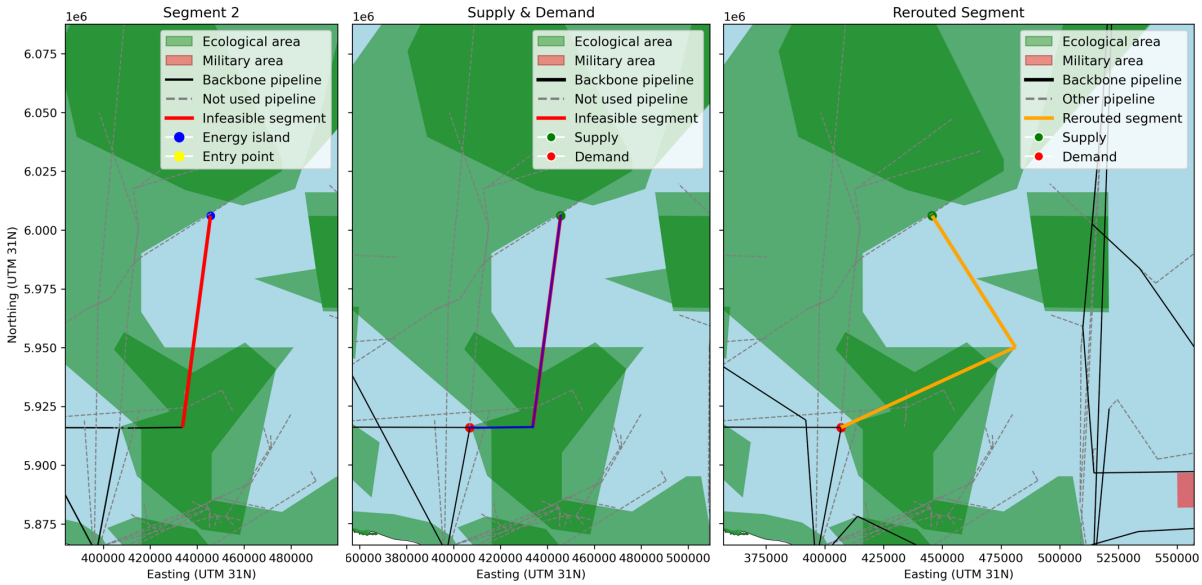

Figure I2.3. Rerouting steps for infeasible pipeline segment 2, for which the segment is extended to enable rerouting.

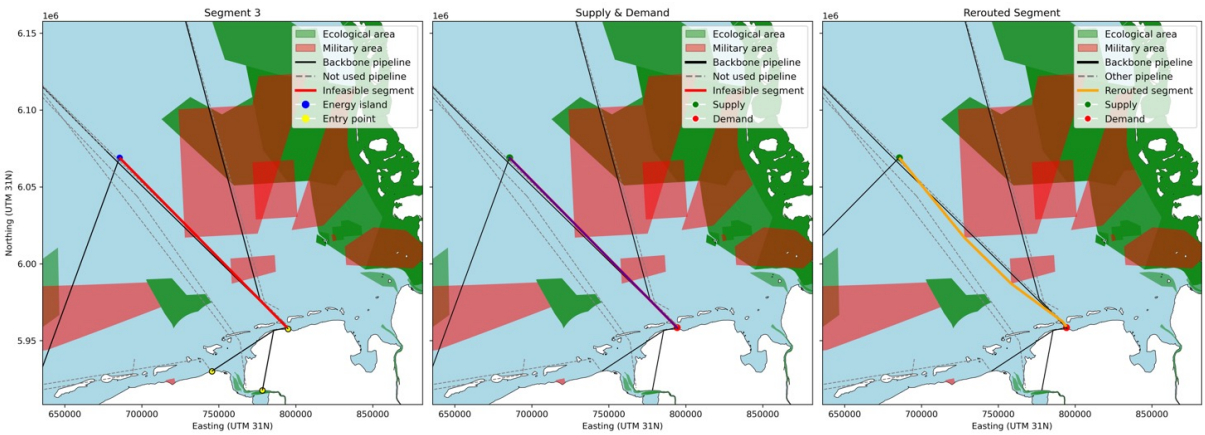

Figure I2.4. Rerouting steps for infeasible pipeline segment 3.

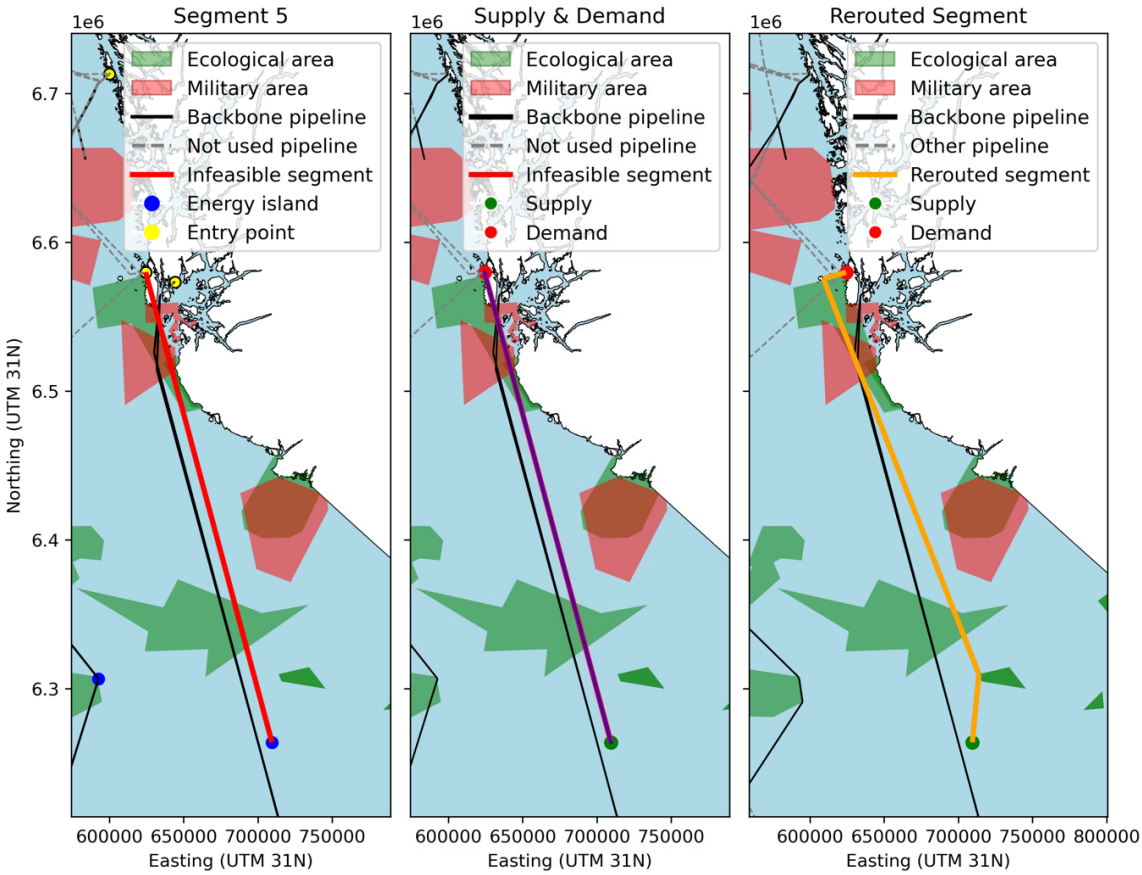

Figure I2.5. Rerouting steps for infeasible pipeline segment 5.

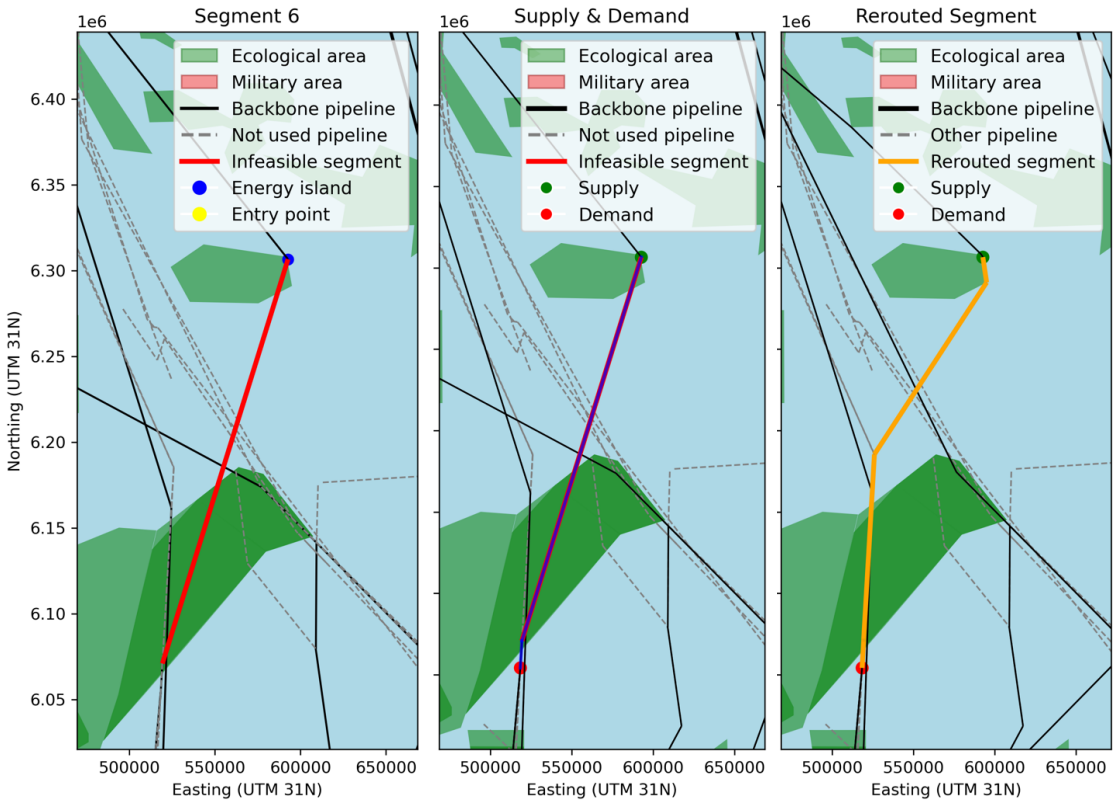

Figure I2.6. Rerouting steps for infeasible pipeline segment 6, for which the segment is extended to enable rerouting.

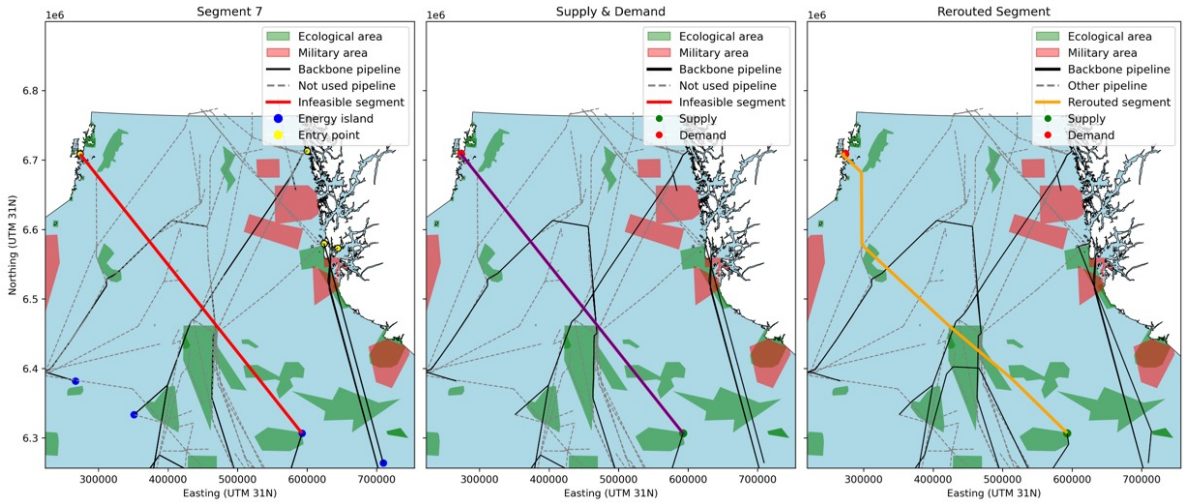

Figure I2.7. Rerouting steps for infeasible pipeline segment 7.

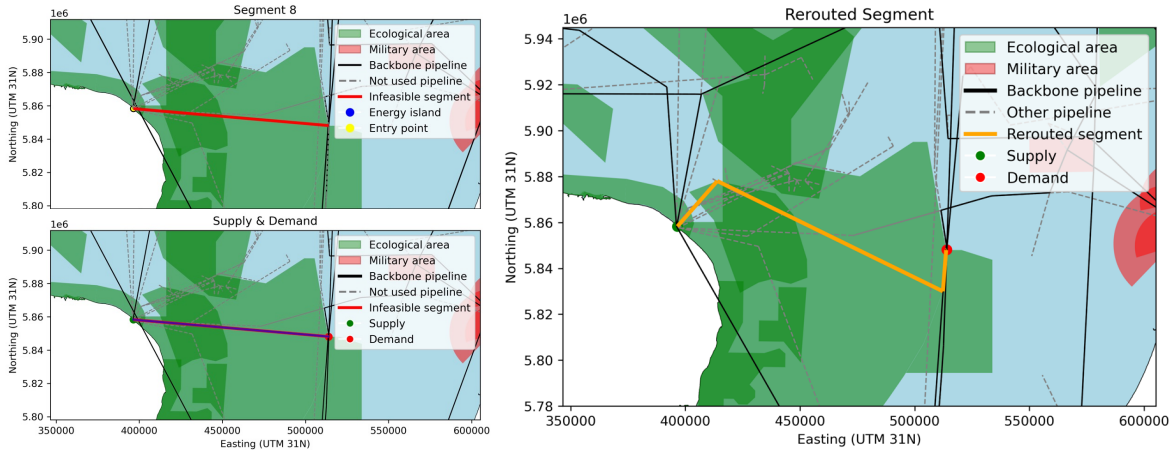

Figure I2.8. Rerouting steps for infeasible pipeline segment 8.

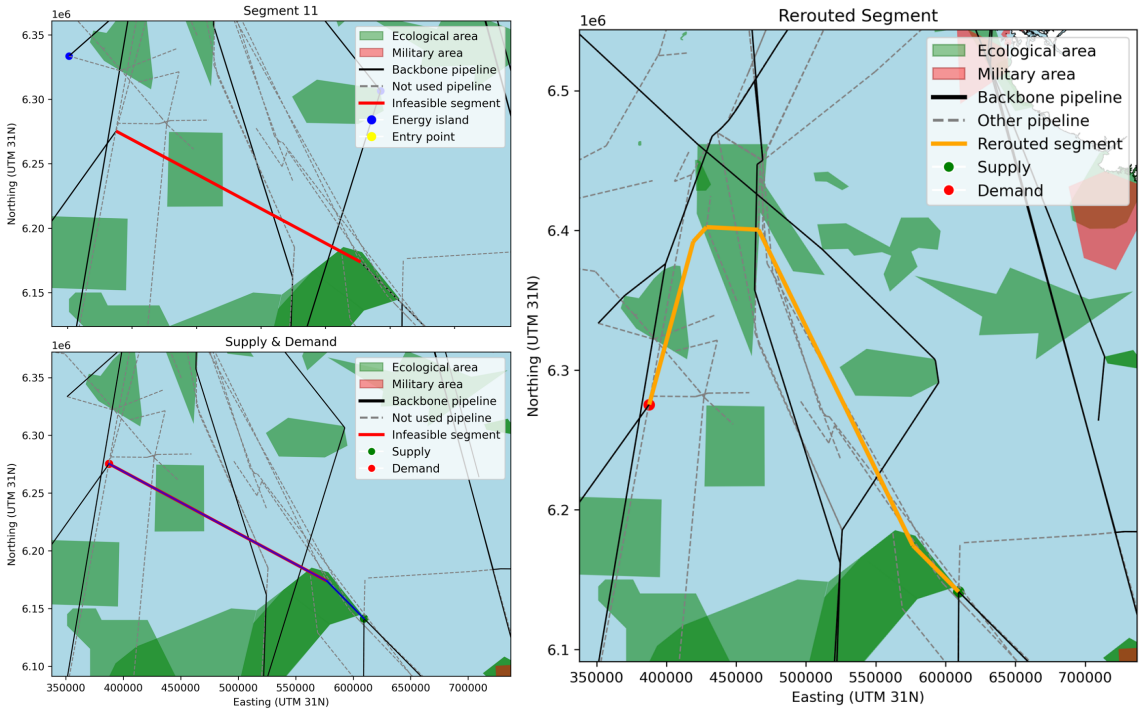

Figure I2.9. Rerouting steps for infeasible pipeline segment 11, for which the segment is extended to enable rerouting.

COLOPHON


TU Delft